1-1-1987

Studies of miscibility and phase behavior in blends of two random copolymers/

Heung Sup Kang
University of Massachusetts Amherst

STUDIES OF MISCIBILITY AND PHASE BEHAVIOR IN BLENDS OF TWO RANDOM COPOLYMERS

A Dissertation Presented

by

Heung Sup Kang

submitted to the Graduate School of the

University of Massachusetts in partial fulfillment

of the requirements for the degree of

DOCTOR OF PHILOSOPHY

September 1987

Department of Polymer Science and Engineering

STUDIES OF MISCIBILITY AND PHASE BEHAVIOR IN BLENDS OF TWO RANDOM COPOLYMERS

A Dissertation Presented

by

Heung Sup Kang

Approved as to style and content by:

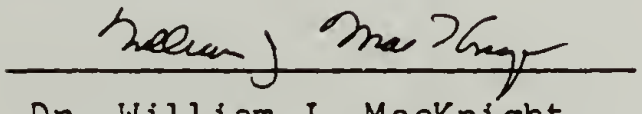

Dr. William J. MacKnight

Cochairperson of Committee

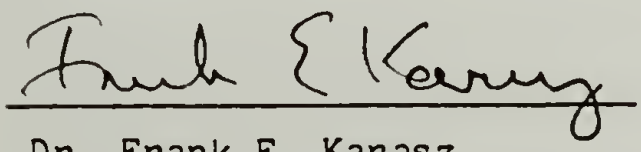

Dr. Frank E. Karasz

Cochairperson of Committee

Dr. Horst H. Winter, Member

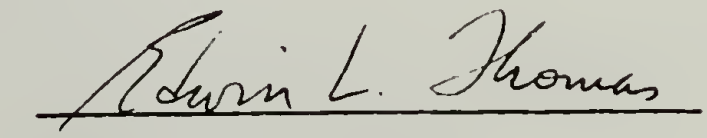

Dr. Edwin L. Thomas

Department Head

Polymer Science & Engineering

This thesis is dedicated to my wife, Kyung, and to my two sons, Jin and Hyun, for their understanding and patience during the course of this work.

ACKNOWLEDGEMENTS

I would like to express my sincere gratitude to my co-advisors, Professors William J. MacKnight and Frank E. Karasz for their valuable guidance and support throughout the course of this research. It has been a great pleasure to work closely with them. I would like to thank Professor Horst H. Winter for serving on my committee and the efforts of Professor David A. Tirrell are also appreciated.

I am grateful for discussions with Drs. R. Longworth and R. Koningsveld. It is a pleasure to acknowledge Drs. C.H. Lau, S. Choe, K. Levon and, in particular, Dr. C.K. Sham for their assistance and useful comments. Thanks are extended to my colleagues, John Connolly, Richard Brady, Sergio Rojstaczer and Jean-Philippe Autran.

Appreciation is also extended to Jane Tirrell, Becky Bland and Dr. Christina Sham for their fine editorial work and typing of manuscripts and thesis.

ABSTRACT

STUDIES OF MISCIBILITY AND PHASE BEHAVIOR IN BLENDS OF TWO RANDOM COPOLYMERS

September 1987

Heung Sup Kang

B.S., Seoul National University, Korea

M.S., Korea Advanced Institute of Science

Ph.D., University of Massachusetts

Directed by : Professors William J. MacKnight and Frank E. Karasz

Miscibility and phase behavior in blends of random copolymers have been studied primarily by differential scanning calorimetry (DSC), optical microscopy, dynamic mechanical measurements and temperature plane and frequency plane dielectric measurements. A series of random copolymers comprising phenylsulfonyl group substituted phenylene oxide repeat units (SPPO copolymers) was prepared by a Friedel-Crafts sulfonylation reaction of poly(2,6-dimethyl-1,4-phenylene oxide) (PPO) and characterized by elemental analysis, gel permeation chromatography, IR, ^{1}H-NMR, DSC, thermogravimetric analysis, dynamic mechanical and dielectric measurements.

The SPPO copolymers were blended with poly(styrene-co-acrylonitrile) (SAN), poly(styrene-co-p(o)-fluorostyrene) and poly(styrene-co-methyl acrylate) (SMA); all systems are of the type $(A_{1-x}B_x)_{n_1}/(C_{1-y}D_y)_{n_2}$. SMA copolymers were prepared by free radical solution polymerization. Monomer sequence distributions in SAN copolymers were studied by dielectric relaxation and T_g measurements. The copolymers exhibited similar dielectric relaxation spectra reflecting small differences in the conformational characteristics and random natures of the copolymers.

Miscibility regimes for each system have been determined at 290°C and displayed in a Cartesian coordinate system and all segmental interaction parameters (χ_{ij}'s) involved have been estimated using a mean field treatment. All the blend systems except those containing SMA copolymers display wide miscible regions even though all the χ_{ij}'s are positive except $\chi_{st,po}$. The experimental miscibility-immiscibility boundaries have been analyzed geometrically and are in reasonably good agreement with calculated boundaries.

Normalized dielectric loss curves of the blends containing SAN copolymers, which were obtained from frequency plane dielectric relaxation measurements, are much broader than those of the pure SAN copolymer, indicating the occurence of composition fluctuations within the miscible blends. The role of repulsive interactions in

inducing miscibility in blends of poly(p-fluorostyrene) with SPPO copolymers without any specific interactions has been identified and all the critical phenomena observed in this work are of an LCST type.

TABLE OF CONTENTS

LIST OF TABLES

LIST OF FIGURES

CHAPTER I

INTRODUCTION

The study of miscibility in polymer blends has received extensive attention as a means of developing polymer systems with desired properties under proper processing conditions. In comparison with low molecular weight compounds, mixtures of high molecular weight components involve a nearly negligible combinatorial entropy of mixing. Thus, the negative exchange interaction was considered to be a prerequisite for the miscibility of binary mixtures of sufficiently high molecular weight.

However, some blend systems in which at least one of the components is a random copolymer have been found to be miscible for a particular range of the copolymer composition even though none of the binary combinations of the homopolymers is miscible. An increasing number of miscible copolymer blends without intermolecular interactions have been identified. Blends of poly(vinyl chloride)/poly(ethylene-co-vinyl acetate)[1], poly(vinyl chloride)/poly(butadiene-co-acrylonitrile)[2] and poly(methyl methacrylate)/poly(styrene-co-acrylonitrile)[3], systems of the type

$A_{n_1}/(C_{1-y}D_y)_{n_2}$, are among such cases. These findings reflect that specific interactions are not always necessary for miscibility and that, by the rational design of copolymers, new technologically important miscible systems can be engineered at reasonable cost.

Blends of a series of halogen containing styrenic copolymers with poly(2,6-dimethyl-1,4-phenylene oxide) (PPO), i.e., systems of the type $(A_{1-x}B_x)_{n_1}/C_{n_2}$, have been studied extensively[4-9] and blends of two random copolymers having a common monomer segment of the system of the type $(A_{1-x}B_x)_{n_1}/(C_{1-y}B_y)_{n_2}$ have been investigated[10-11]. However, no systematic experimental studies of miscibility behavior in blends of two random copolymers with four distinct repeat units of the type $(A_{1-x}B_x)_{n_1}/(C_{1-y}D_y)_{n_2}$ in which six segmental interaction parameters are required for a description of the miscibility behavior have been reported so far.

The main goal of this thesis is the extension of a mean field treatment to random copolymer blends of the type $(A_{1-x}B_x)_{n_1}/(C_{1-y}D_y)_{n_2}$ and the analysis of miscibility behavior in these blends. The phase stability above the glass transition temperature was explored. The monomer sequence distribution in the styrene-acrylonitrile copolymers employed in this work was also investigated.

In this chapter the general principles underlying polymer-polymer miscibility as a background to this thesis work will be discussed. In addition, a review of the literature on copolymer blend studies will be presented.

A. Theory of Polymer-Polymer Miscibility

The purpose of this section is to briefly review the thermodynamic theories dealing with polymer blends. The stability of any binary system requires that the Gibb's free energy of mixing be negative:

$$\Delta G_m = \Delta H_m - T\Delta S_m < 0 \qquad (1.1)$$

and that the second derivative of the free energy with respect to some composition variable, X, be positive[12]:

$$(\partial^2 \Delta G_m / \partial X_i^2)_{T,P} > 0 \qquad (1.2)$$

The inequality, Eqn. (1.2), requires that the energy-composition diagram be concave downward.

The boundary between the stable region and the metastable region where systems are stable to small perturbations but unstable

to large disturbances is termed the binodal. The boundary between the metastable and unstable region where the free energy-composition diagram is concave upward is termed the spinodal. The spinodal boundary is the inflection point of the free energy-composition diagram given as

$$(\partial^2 \Delta G_m / \partial X_i^2)_{T,P} = 0 \qquad (1.3)$$

The locus of the binodal is found by setting the chemical potentials of both homopolymers equal in the two coexisting phases.

Upon an increase in temperature, the binary system can phase separate. The temperature at which phase separation first appears is called an lower critical solution temperature (LCST). Analogously, phase separation upon a decrease in temperature is indicative of the existence of an upper critical solution temperature (UCST). The position of the critical solution temperatures can be calculated

$$(\partial^2 \Delta G_m / \partial X_i^2)_{T,P} = (\partial^3 \Delta G_m / \partial X_i^3)_{T,P} = 0 \qquad (1.4)$$

The first attempts at a description of polymer solution thermodynamics were performed by Flory[13,14] and Huggins[15,16]. The Flory-Huggins theory is based on a simple lattice representation for polymer solutions. The entropy of mixing is calculated on a

statistical basis. The polymer chain is divided into segments equal in size to the solvent molecules. Each segment and solvent molecule occupies a simple lattice site. The expression for the entropy of mixing for a binary mixture is :

$$\Delta S_m/R = (\phi_1/n_1)\ln\phi_1 + (\phi_2/n_2)\ln\phi_2 \qquad (1.5)$$

where ϕ_i is the volume fraction, and n_i is the number of segments per chain. The enthalpy of mixing is a van Larr-type energy term. This results in a free energy of mixing given by the following expression :

$$\Delta G_m/RT = (\phi_1/n_1)\ln\phi_1 + (\phi_2/n_2)\ln\phi_2 + \phi_1\phi_2\chi_{blend} \qquad (1.6)$$

The original Flory-Huggins theory ignores the equation of state parameters of the pure components and assumes no change in the volume of mixing. According to this theory, χ resulting only from contact energy dissimilarities between components 1 and 2, neglecting any specific interactions, is independent of concentration and molecular weight and decreases as the temperature increases. Thus, only UCST behavior can be predicted. The existence of an UCST is known to be fairly common for low molecular weight solutions. However, some polymer-polymer systems have been found to display LCST behavior.

Tompa[17] and Koningsveld[18] proposed the generalized Flory-Huggins theory in which they considered the interaction parameter to be dependent on temperature, molecular weight and composition. Koningsveld expressed the free enthalpy correction parameter g,

$$g = \Sigma\, g_k \phi^k \tag{1.7}$$

Assuming that the temperature and concentration dependence can be separated, one can write

$$g = g_{0,1} + g_{o,2}/T + g_{0,3}T + g_{0,4}\ln T \tag{1.8}$$

Thus, depending upon the sign of $g_{0,2}$ an LCST or UCST can be described. However, this is an empirical approach to describe the experimental data, and is lacking a molecular interpretation of the dependences of g on temperature, concentration and molecular weight.

Several theories[19-21] have been developed to explain the observed behavior on a more molecular level. These theories considered an additional contribution to the entropy of mixing, namely, the excess entropy of mixing resulting from volume changes on mixing, and such excess entropy effects are believed to play an important role in the overall thermodynamic behavior. Flory's equation of state theory[19] originated from Prigogine's assumption[22]

that the degrees of freedom of a molecule in a liquid can be separated into internal and external degrees of freedom. The external degrees of freedom per polymer segment are less than those for a similar small molecule and depend only on the intermolecular forces. The internal degrees of freedom depend on intramolecular chemical bond forces. Each pure component is characterized by three equation of state parameters : T^*, P^* and V^*_{sp} which are the characteristic temperature, pressure and specific volume, respectively. The three characteristic parameters, V^*, P^* and T^* can be determined from the experimental values of the thermal expansion coefficient α, the thermal pressure coefficient β, and the specific volume V_{sp}. The resulting equation of state is

$$\tilde{P}\tilde{V}/\tilde{T} = \tilde{V}^{\frac{1}{3}}/(\tilde{V}^{\frac{1}{3}} - 1) - (1/\tilde{V}\tilde{T}) \qquad (1.9)$$

where the tilde ($\tilde{}$) represents reduced parameters; $\tilde{P} = P/P^*$; $\tilde{V} = V/V^*$ and $\tilde{T} = T/T^*$.

According to the Prigogine-Flory theory[23], as reviewed by Patterson and Robard[24], the χ parameter consists of two contributions : an interactional term and a free volume term. The sign of the enthalpy of mixing is determined by the first derivative of the χ parameter[25]. That is,

$$\Delta H_m = -RT^2(\partial\chi/\partial T)\phi_2\phi_3 \qquad (1.10)$$

Figure 1.1 shows the possible temperature dependence of χ. Curve 1 shows the contribution to χ due to contact energy dissimilarities between component 1 and component 2. In the absence of specific interactions, curve 1 decreases with temperature. Curve 2 shows the contribution to χ due to the equation of state parameters for the two components. Curve 3 is the sum of these two contributions. Thus, the equation of state theory predicts that blends will show an LCST as the temperature increases and that an UCST will appear as the temperature decreases. However, two polymers with a specific interaction will exhibit only an LCST, in this case curve 1 will not be applicable. McMaster[26] evaluated the effect of molar mass, thermal expansion coefficient, thermal pressure coefficient and the entropic correction parameter on the basis of the equation of state theory and asserted that if the equation of state parameters for the two polymers are similar, the polymers have a better chance for miscibility.

Sanchez[27] proposed a lattice fluid theory based on similar reasoning to that of Flory's equation of state theory. For the pure components an equation of state is given by

$$\tilde{\rho}^2 + \tilde{\rho} + \tilde{T}[\ln(1 - \tilde{\rho}) + (1 - 1/n)\tilde{\rho}] = 0 \qquad (1.11)$$

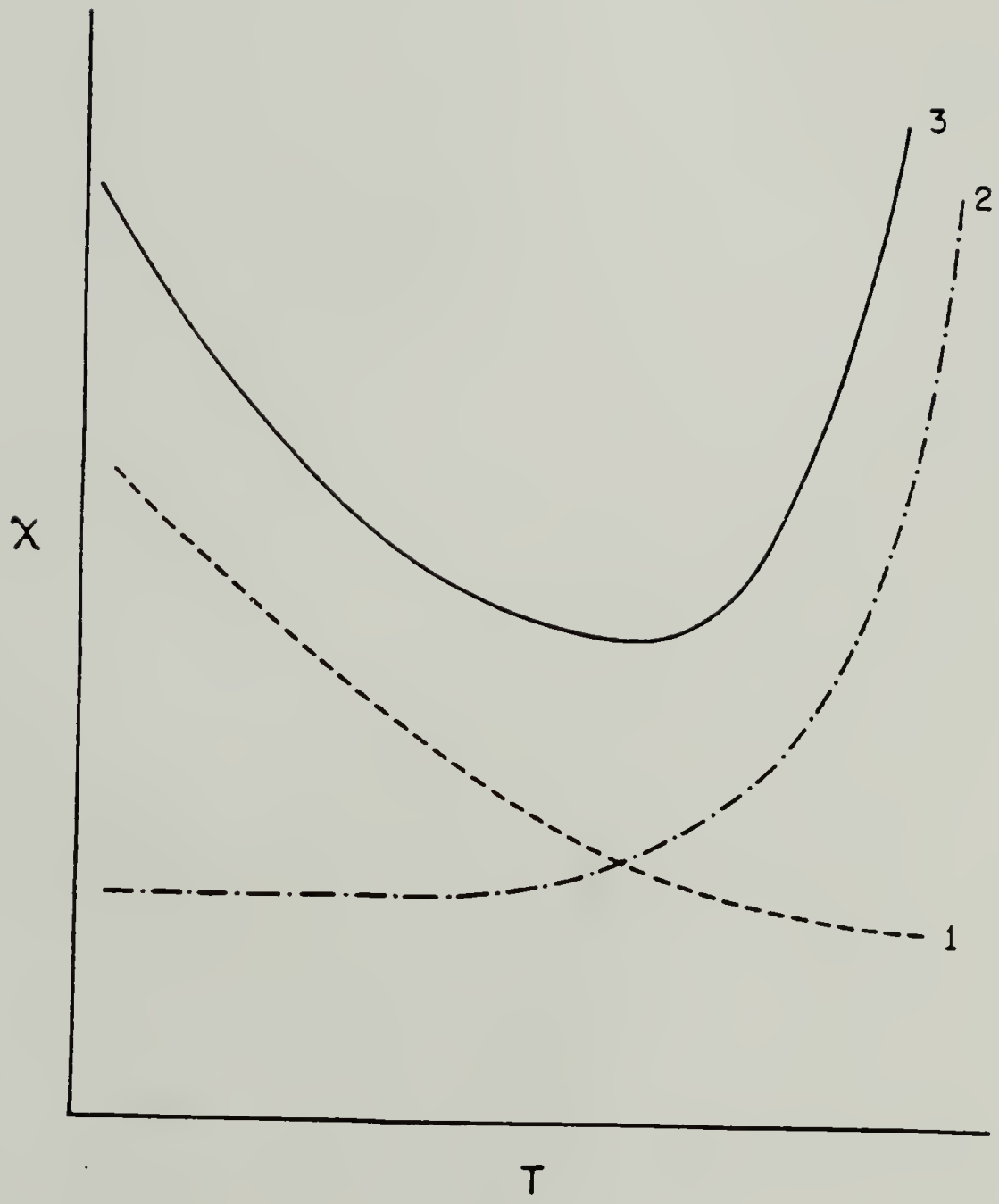

Figure 1.1. Temperature dependence of the interaction parameter

where $\tilde{\rho}$, $\tilde{P}$ and $\tilde{T}$ are the reduced density, pressure and temperature and "n" is the number of mers. The phase behavior of the polymer mixtures could be inferred by examination of the spinodal[28]. The condition for phase stability was derived as

$$\tilde{\rho}(2\chi + \tilde{T}\psi^2 P^* \beta) < (1/n_1\phi_1) + (1/n_2\phi_2) \qquad (1.12)$$

where ψ is a term containing volume parameters and ϕ_i the volume fractions. The right hand side of Eqn. (1.12) is a combinatorial entropy of mixing type expression. By analysis of the temperature dependences of the terms on the left hand side of Eqn. (1.12). the general features of the phase diagram could be ascertained. In all cases, LCST behavior was predicted.

According to the lattice fluid theory[27], the second derivative of the free energy of mixing is composed of incompressible and compressible contributions and for a binary mixture to be miscible, the Gibbs free energy at fixed temperature and pressure should be a convex function of the concentration and specific volume. That is,

$$\partial^2 G/\partial C^2 - \nu\beta(\partial^2 G/\partial C \partial \nu)^2 > 0 \qquad (1.13)$$

The second term is always negative, thus giving an unfavorable effect on mixing and since β increases with temperature, this term becomes pronounced at higher temperature, thus resulting in the destabilization of mixtures at elevated temperature indicative of LCST behavior.

B. Mean Field Treatment

To explain a range of miscibility phenomena involving random copolymer blends, ten Brinke *et al*[29] proposed a mean field treatment which assumes χ_{ij} to be independent of composition and local environment. Then χ_{blend} in Eqn. (1.6) is, in the case of a blend of two copolymers of the type $(A_{1-x}B_x)_{n_1}/(C_{1-y}D_y)_{n_2}$, given by a linear combination of the respective segmental interaction parameters such that

$$\chi_{blend} = (1-x)(1-y)\chi_{AC} + y(1-x)\chi_{AD} + x(1-y)\chi_{BC} + xy\chi_{BD} - x(1-x)\chi_{AB} - y(1-y)\chi_{CD} \qquad (1.14)$$

where x and y denote the copolymer compositions expressed in volume fractions.

A critical point occurs at a temperature for which χ_{blend} equals χ_{blend}^{crit}, given by

$$\chi_{blend}^{crit} = \frac{1}{2}\left(n_1^{-1/2} + n_2^{-1/2}\right)^2 \qquad (1.15)$$

Thus, miscibility corresponds to $\chi_{blend} < \chi_{blend}^{crit}$ and immiscibility to $\chi_{blend} > \chi_{blend}^{crit}$.

If χ_{AB} and/or χ_{CD} are positive and large, i.e., of sufficiently large mutual repulsion between segments A and B, or C and D, then a region of miscibility may be predicted for a particular range of x and/or y, even if all χ_{ij}'s are positive. This "repulsion effect" can lead to the negative net interaction energy necessary to induce thermodynamic miscibility.

Paul et al[30] also proposed a binary interaction model which considers that an intermolecular interaction plays an important role in the polymer blend. A van Laar type of heat of mixing is given by

$$\Delta H_m/V = \sum_{i>j} B_{ij}\phi_i\phi_j \qquad (1.16)$$

where V is the total volume of mixture and B_{ij} is a binary interaction energy density between the components i and j and is related to the χ parameters such that

$$B/kT = \chi_A/V_A = \chi_B/V_B = \tilde{\chi}_{AB} \qquad (1.17)$$

where V_i is the molar volume of component i. The effective interaction energy density for the mixing of polymers A and B is given by

$$B = B_{13}\phi_1'\phi_3' + B_{14}\phi_1'\phi_4' + B_{23}\phi_2'\phi_3' + B_{24}\phi_2'\phi_4' - B_{12}\phi_1'\phi_2' - B_{34}\phi_3'\phi_4' \qquad (1.18)$$

where polymer A is comprised of monomers 1 and 2 with volume fractions of each denoted by ϕ_i' and polymer B is comprised of monomers 3 and 4. If B_{12} and/or B_{34} is positive and large enough, this repulsion makes B less than additive and favorable to mixing. Kambour et al[31] also proposed an analogous model which considers the local free energy of mixing to be related to χ.

The temperature dependence of χ_{blend} is[29], for blends involving copolymers,

$$\chi_{blend}^{crit}(T) = \{C/[V(T)T]\}\chi_{eff} \qquad (1.19)$$

where T is the temperature, C is a constant, V is the reduced volume of the mixture, χ_{eff} is the effective interaction parameter which is a function of copolymer composition and individual real interaction parameters. For $\chi_{eff} > 0$, χ_{blend}^{crit} decreases as a function of temperature whereas it increases as a function of temperature for $\chi_{eff} < 0$. For a particular copolymer composition either of these cases may occur. If χ_{eff} is positive, χ_{blend} is also positive and miscibility does not occur. If, on the other hand, χ_{eff} is negative, χ_{blend} increases as a function of temperature, resulting in an LCST behavior.

C. Experimental Methods for Probing Polymer-Polymer Miscibility

A variety of methods is available for investigating polymer blends. The experimental criteria for miscibility have been extensively reviewed[27,32-34]. This section will briefly discuss only those techniques which have been used in this work.

Optical Microscopy

The optical microscope has been extensively used to examine the morphology of rubber blends and of semi-crystalline polymers. It has a resolution down to about 0.2 μm if the contrast is sufficient. For binary combinations of rubbers there seems to be a crude correlation between domain size and the solubility parameter differences.

However, this method is subject to certain limitations. Mixtures of poly(styrene-co-butadiene) and polybutadiene have been described as either homogeneous[35] or heterogeneous[36]. These opposing results are due to poor phase contrast. Furthermore, if two component polymers have equal refractive indices or the dispersed phases have dimensions smaller than the resolution limit of the optical microscope, absolute judgement on the miscibility of the two polymers cannot be made.

Glass Transition Criterion

The examination of glass tansition behavior has largely prevailed as a diagnostic test of miscibility. A miscible polymer blend will exhibit a single glass transition temperature lying between the two glass transition temperatures of the pure components. A phase separated polymer blend will exhibit two T_g's. Polymers exhibiting a partial miscibility may show two T_g's, one representing

a phase rich in component 1, the other representing a phase rich in polymer 2.

The techniques by which the T_g's of polymers may be determined will be discussed.

Differential Scanning Calorimetry

This technique is useful because of small sample requirements, relatively rapid measurement capability and high sensitivity. But, T_g measurements are subject to some drawbacks. The T_g of a polymer is rate dependent, that is the T_g occurs over a time and temperature range. Thus, the T_g criterion cannot normally yield information about equilibrium states below the T_g. In addition, T_g measurements cannot be used to assess the miscibility of two polymers if their T_g's lie within 20°C or less of each other. In this case, the use of a derivative presentation, dC_p/dT vs. T, may somewhat alleviate this problem. If one component is present in low concentration, for example less than 10%, in the mixture, its T_g may not be detected because of the limits of the sensitivity of the technique. Crystallization of either or both constituents may also cause a problem since the sensitivity of the technique is reduced by the diminution of the amorphous phase concentration and since, in

some cases, the crystallization itself may make T_g determination obscure.

Dynamic Mechanical Spectroscopy

Examination of the loss angle, tan δ, or the loss modulus, E", can be used to assess miscibility. This can be done over a frequency range, typically two to four decades wide. The low-temperature secondary relaxations of the component polymers may also be studied to reveal the extent of mixing between the different polymer molecules. However, if the size of the phase domain is small, the magnitude of the loss peak will be reduced, and may not be detected.

Dielectric Relaxation Spectroscopy

This technique is very powerful in the assessment of the miscibility of blends involving electrically dipolar groups. Although it is similar in many respects to its mechanical analogue, a much wider frequency range, usually six or more decades, is available, which makes the presentation of a time-temperature superposition possible. These measurements can provide information about the intra- and intermolecular interaction and the conformational effect in the blends. This technique is useful for studying the relaxational characteristics at equilibrium from the

frequency plane measurements. It can also yield information about the microstructure (i.e., the monomer level) of the mixture such as phase separation on a microscale in the blends. However, if one component has traces of ionic impurities, then a DC conductivity effect will take place, which makes the definite assessment of miscibility of blends difficult.

D. Review of Previous Studies of Copolymer Blends

The studies of copolymer blend systems analyzed by a mean field treatment will be listed in this section. The miscibility of PPO with random copolymers of poly(o-fluorostyrene-co-p(o)-chlorostyrene)[37-39], poly(o-fluorostyrene-co-p-fluorostyrene)[7,38,40], poly(o-chlorostyrene-co-p-chlorostyrene)[41,42], poly(o-bromostyrene-co-p-bromostyrene)[40], poly(o-fluorostyrene-p(o)-bromostyrene)[43], and poly(p-fluorostyrene-co-p(o)-bromostyrene)[43] has been studied. Copolymers of o-fluorostyrene with p-chlorostyrene containing 15-62 mole% p-ClS are miscible with PPO in all proportions[9,37-39]. Blends of this copolymer with 74 mole% p-ClS showed phase separation at 250°C. Miscibility in the PPO/poly(o-fluorostyrene-co-o-chlorostyrene) system was observed for copolymers containing between 15 and 36 mole % o-chlorostyrene and phase separation was observed after annealing to a temperature of 230°C[9,37-39].

Blends of PPO with copolymers of poly(p-fluorostyrene-co-o-fluorostyrene) containing from 10 to 38 % p-fluorostyrene were miscible in all proportions and showed LCST behavior[7,38,40]. Blends of PPO with copolymers of poly(p-chlorostyrene-co-o-chlorostyrene) with the p-chlorostyrene content from 23 to 64 % were miscible in all proportions and exhibited phase separation upon annealing at elevated temperatures indicative of an LCST[41,42]. The LCST was around 220°C when the copolymer composition was 0.23 or 0.65 mole fraction p-ClS and rose to 300°C at about 0.40 mole fraction p-ClS content. The copolymer of poly(o-fluorostyrene-co-p-bromostyrene) only with 11-73 mole % p-bromostyrene was miscible with PPO[43].

Miscibility of PPO with random copolymers of poly(styrene-co-p(o)-bromostyrene)[40,44], poly(styrene-co-p(o)-fluorostyrene)[5,8], and poly(styrene-co-p(o)-chlorostyrene)[40,42,45] has been studied. The blends of PPO with random copolymers of poly(styrene-co-p-bromostyrene) with a p-bromostyrene content of less than 60 mole % were miscible after annealing up to 200°C and showed an LCST at elevated temperature[40,44]. The blends of PPO with poly(styrene-co-o-bromostyrene) with an o-bromostyrene content of less than 40 mole % showed similar behavior[40,44].

The blends of PPO with poly(styrene-co-p-fluorostyrene) copolymers of p-fluorostyrene content less than 56 mole % were

miscible in all proportions and the same blends with copolymers containing 46-56 % p-fluorostyrene showed phase separation at elevated temperature[5,8]. Copolymers of poly(styrene-co-o-fluorostyrene) with less than 82 % o-fluorostyrene blended with PPO do not show any phase separation[5,8]. In the case of the blends of PPO with poly(styrene-co-o(p)- chlorostyrene), the LCST dropped sharply for the copolymer composition range of 60-75 mole % p-chlorostyrene and the blends of PPO with poly(styrene-co-p-chlorostyrene) with 67 mole % or less p-ClS were miscible[40,42,45].

Miscibility of polystyrene with random copolymers of poly(o-fluorostyrene-co-p-fluorostyrene)[7,40], poly(styrene-co-p(o)-fluorostyrene[5], poly(styrene-co-p-bromostyrene)[40], and poly(o-chlorostyrene-co-p-chlorostyrene)[6,46] has been studied. The blend of polystyrene with poly(o-chlorostyrene-co-p-chlorostyrene) showed a great sensitivity to the degree of polymerization of either or both components which could be a result of the very low positive value of the interaction parameter between styrene and o-chlorostyrene[6,46].

The blend of polystyrene with poly(styrene-co-o-fluorostyrene) was miscible and the blend of polystyrene with poly(styrene-co-p-fluorostyrene) with 46 mole% of p-fluorostyrene showed a single T_g, but additional proof is needed to verify

miscibility[5]. In the case of the blend of polystyrene with poly(o-chlorostyrene-co-p-chlorostyrene), a miscibility window was found for a copolymer composition of about 68 to 98 mole % o-chlorostyrene at 150 °C[6,46]. The maximum in the miscibility window occurred at a composition of 83 mole % o-chlorostyrene. The temperature dependence of χ in this blend was also studied by using polystyrene samples of varying molecular weights.

In the case of the blend of polystyrene with poly(styrene-co-p(o)-bromostyrene), the copolymers of o-bromostyrene and styrene with over 40 mole % o-bromostyrene exhibited two distinct T_g's[40]. The copolymer with 20 mole % o-bromostyrene appeared to exhibit a single T_g. The copolymers of p-bromostyrene and styrene with p-bromostyrene content of over 50 mole % p-bromostyrene were immiscible with polystyrene.

Kambour *et al*[31] calculated $\chi_{po,p\text{-}BrS}$ to be 0.22 at about 120 °C based on a study of PPO/poly(styrene-co-p-bromostyrene) blends; these workers also studied the blend of polystyrene with brominated PPO. Paul *et al*[30] studied blends of polyesters which may be considered to be random copolymers of CH_x and COO units.

The blends of syndiotactic PMMA with random copolymers of isotactic poly(methyl/ethyl methacrylate) have been studied[47]. Only the copolymers with an ethyl methacrylate content below 45 % were miscible with syndiotactic PMMA.

Shiomi *et al*[11,48] studied blends of chlorinated PVC(CPVC)/poly(ethylene-co-vinyl acetate), CPVC/poly(vinyl chloride-co-vinyl acetate), poly(vinyl chloride-co-vinyl acetate)/poly(ethylene-co-vinyl acetate), and poly(styrene-co-maleic anhydride)/poly(styrene-co-acrylonitrile). Ueda *et al*[49] studied the miscibility behavior in blends of chlorinated polyethylene which might be treated as random copolymers of CH_2 and CHCl segments and found that these blends exhibited an LCST or UCST depending upon the degree of chlorination and the nominal χ between CH_2 and CHCl was also shown to be dependent upon the mean degree of chlorination.

REFERENCES

1. C.F. Hammer, Macromolecules, 4, 69 (1971).
2. G.A. Zakrzewski, Polymer, 14, 347 (1973).
3. L.P. McMaster, Adv. Chem. Ser., No. 142, 43 (1975).
4. P.R. Alexandrovich, F.E. Karasz, W.J. MacKnight, Polymer, 18, 1022 (1977).
5. R. Vukovic, F.E. Karasz, W.J. MacKnight, J. Appl. Polym. Sci., 28, 219 (1983).
6. G. ten Brinke, E. Rubinstein, F.E. Karasz, W.J. MacKnight, R. Vukovic, J. Appl. Phys., 56(9), 2440 (1984).
7. R. Vukovic, F.E. Karasz, W.J. MacKnight, Polymer, 24, 529 (1983).
8. R. Vukovic, V. Kuresevic, F.E. Karasz, W.J. MacKnight, Thermochimica Acta, 54, 349 (1982).
9. R. Vukovic, V. Kuresevic, F.E. Karasz, W.J. MacKnight, J. Appl. Polym. Sci., 30, 317 (1985).
10. W.J. Hall, R.L.Cruse, R.A. Mendelson, Q.A. Trementozzi, ACS Div. Org. Plast. Chem. Prep., 47, 298 (1982).
11. T. Shiomi, F.E. Karasz, W.J. MacKnight, Macromolecules, 19, 2274 (1986).
12. J.H. Gibbs, Collected Works, Vol. I, Longmans, Green : New York, 1928.
13. P.J. Flory, J. Chem. Phys., 9, 660 (1941).
14. P.J. Flory, J. Chem. Phys., 10, 51 (1942).
15. M.L. Huggins, J. Chem. Phys., 9, 440 (1941).

16. M.L. Huggins, J. Phys. Chem., 46, 151 (1942).

17. H. Tompa, Polymer Solutions, Butterworth, London, 1956.

18. R.Koningsveld, L.A. Kleintjens, J. Polym. Sci., Polym. Sym., C61, 221 (1977).

19. P. J. Flory, J. Amer. Chem. Soc., 86, 1883 (1965).

20. R.H. Lacombe and I.C. Sanchez, J. Phys. Chem., 80, 2352 (1976).

21. M.L. Huggins, J. Phys. Chem., 74, 371 (1970); 75, 1255 (1971); 80, 1317 (1976).

22. I. Prigogine, The Molecular Theory of Solutions, North-Holland Pub., Amsterdam, 1957.

23. P.J. Flory, Discuss. Faraday Soc., 49, 7 (1970).

24. D.Patterson and A. Robard, Macromolecules, 11(4), 690 (1978).

25. I. Prigogine and R. Defay, Chemical Thermodynamics, Longmans, Green : London, 1952.

26. L.P. McMaster, Macromolecules, 6, 760 (1973).

27. I. C. Sanchez, Polymer Compatibility and Incompatibility, Principle and Practice, K. Solc, Ed.; Harwood, New York, 1982; MMI Symp. Ser., Vol. 3.

28. R.H. Lacombe, I.C. Sanchez, J. Phys. Chem., 80, 2568, (1976).

29. G. ten Brinke, F.E. Karasz, W.J. MacKnight, Macromolecules, 16, 1827 (1983).

30. D.R. Paul, J.W. Barlow, Polymer, 25, 487 (1984).

31. R.P. Kambour, J.T. Bendler, R.C. Bopp, Macromolecules, 16, 753 (1983).

32. D.R. Paul, S. Newman, eds., Polymer Blends, Vol. 1, Academic Press, New York, 1978.

33. O. Olabishi, L.M. Robeson, M.T. Shaw, Polymer-Polymer Miscibility, Academic Press, New York, 1979.

34. D.J. Walsh, J.S. Higgins, A. Maconnachie, eds., Polymer Blends and Mixtures, Martinus Nijhoff Publishers, Dordrecht, 1985.

35. P.A. Marsh, A. Voet, L.D. Price, T.J. Mullens, Rubber Chem. Technol., 41, 344 (1968).

36. J.E. Callan, W.M. Hess, C.E. Scott, Rubber Chem. Technol., 44, 814 (1971).

37. R. Vukovic, V. Kuresevic, N. Segudovic, F.E. Karasz, W.J. MacKnight, J. Appl. Polym. Sci., 28, 1379 (1983).

38. R. Vukovic, V, Kuresevic, F.E. Karasz, W.J. MacKnight, G.E. Gajnos, J. Polym. Alloys, in press.

39. R. Vukovic, V. Kuresevic, N. Segudovic, F.E. Karasz, W.J. MacKnight, J. Appl. Polym. Sci., 28, 3079 (1983).

40. C.L. Ryan, Ph.D. Thesis, Univ. of Mass., 1979.

41. P.R. Alexandrovich, F.E. Karasz, W.J. MacKnight, Polymer, 18, 1022 (1979).

42. P.R. Alexandrovich, Ph.D. Thesis, Univ. of Mass., 1978.

43. R. Vukovic, G. Bogdanic, V. Kuresevic, F.E. Karasz, W.J. MacKnight, to be summitted.

44. R. Vukovic, V. Kuresevic, C.L. Ryan, F.E. Karasz, W.J. MacKnight, Thermochemica Acta, 85, 383 (1985).

45. J.R. Fried, W.J. MacKnight, F.E. Karasz, J. Appl. Phys., 50(10), 6052 (1979).

46. S. Cimmino, F.E. Karasz, W.J. MacKnight, to be submitted.

47. J.A. Schroeder, F.E. Karasz, W.J. MacKnight, Polymer, 26, 1795

(1985).

48. T. Shiomi, F.E. Karasz, W.J. MacKnight, Macromolecules, 19, 2644 (1986).

49. H. Ueda, F.E. Karasz, Macromolecules, 18, 2719 (1985).

CHAPTER II

PREPARATION AND PROPERTIES OF SULFONYLATED POLY(2,6-DIMETHYL-1,4-PHENYLENE OXIDE) COPOLYMERS

The preparation and properties of a series of novel thermally stable random copolymers of sulfonylated poly(2,6-dimethyl-1,4-phenylene oxide) (SPPO) copolymers starting from poly(2,6-dimethyl-1,4-phenylene oxide) (PPO) were explored. The resulting copolymers blended with styrenic copolymers are represented as $(C_{1-y}D_y)_{n_2}$ in this work.

Polymer modifications by means of chemical, radiative or mechanochemical methods have received much attention recently. These modifications result in structurally well-defined polymers and copolymers and provide changes in solubility characteristics, surface properties, catalytic activities, increased thermal stability and tailored miscibility.

Several modification reactions of PPO such as bromination[1-3], carboxylation[4,5], sulfonation[6,7], phosphorylation[2,3,8] and vinylation[9] have been reported. These

modification reactions usually yield products with lower thermal stability than that of unmodified PPO.

Friedel-Crafts acylation or sulfonylation reactions have been used to make high performance polymers such as poly(arylene ether sulfones)[10] and poly(arylene ether ketones)[11]. In this chapter the preparation and properties of SPPO copolymers obtained by a Friedel-Crafts sulfonylation of PPO are presented.

A. Experimental Section

Materials and Reactions

PPO from General Electric Co., was purified by precipitation in excess methanol from 5% toluene solution and then dried in a vacuum oven at 100°C. The measured intrinsic viscosity was 0.52 dl/g ($CHCl_3$, 25°C).

Nitrobenzene was distilled and the middle fraction (b.p. 86°/10 mm Hg) was collected. Anhydrous aluminum chloride (Fisher Scientific) and benzenesulfonyl chloride (Eastman Organic Chemicals) were used as received.

A series of SPPO copolymers was prepared by varying the ratios of benzenesulfonyl chloride to PPO. The reaction scheme is depicted in Figure 2.1.

A typical run for a theoretical degree of sulfonylation of 45 mole % degree of sulfonylation, was as follows :

In a four neck flask was dissolved 10.0 g of PPO in 120 ml of nitrobenzene and 5.5 g of $AlCl_3$ was added. After the catalyst was dissolved, 6.6 g of benzenesulfonyl chloride was added gradually and the temperature was kept at 45°C ± 1°. After 27 hours the aluminum chloride complex was destroyed by adding the reaction mixture dropwise to methanol acidified with 4 volume % of HCl. The precipitated polymer was filtered and washed with additional acidified methanol and water and dried.

The product was finally reprecipitated into methanol from THF solution and then redried in a vacuum oven. A control sample was prepared in the same manner for 60 hours without adding benzenesulfonyl chloride, except that chloroform was used as a solvent during the reprecipitation process.

Characterization. The degree of sulfonylation was determined from the sulfur to carbon ratio based on elemental analyses performed by the University of Massachusetts Microanalysis Laboratory.

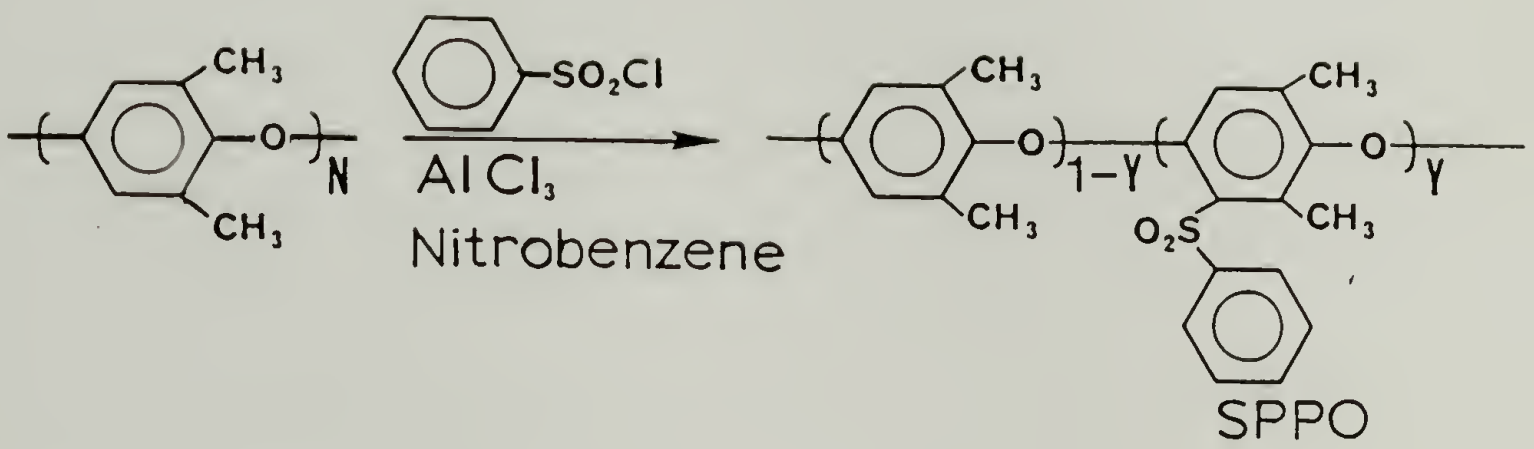

Figure 2.1. Schematic diagram of the modification reaction of PPO

Molecular weights, based on calibration with monodisperse polystyrene standards (Polymer Laboratories), were determined on a Waters Associate 150-C ALC/GPC interfaced with a Data Module. The eluant for SPPO was THF delivered at 1.0 ml min^{-1} at ambient conditions.

Densities of the copolymers in the form of cast films were measured at 23°C using a density gradient column. The linear gradient column was prepared from a solvent mixture of carbon tetrachloride and heptane and calibrated over a range of densities from 1.02 to 1.26 g cm^{-3} with calibrated glass beads.

Infrared spectra were obtained using KBr pellets in a Perkin-Elmer 1320 infrared spectrophotometer.

^{1}H-NMR spectra were recorded on a Varian XL-300 NMR spectrometer with tetramethyl silane as an internal standard. All samples were examined in $CDCl_3$ solutions.

DSC measurements were performed on a Perkin-Elmer DSC 7 microcalorimeter controlled by a Perkin-Elmer 7500 computer at a heating rate of 20°C/min under nitrogen and indium was used as a standard. T_g was taken as the inflection point of the ΔC_p, the specific heat increment at the glass transition. ΔC_p's were averaged for at least two runs.

Thermogravimetric measurements of the powdered samples were made using a Perkin-Elmer TGS-2 thermobalance with a heating rate of 10 °C/min under nitrogen. The samples were predried at 200 °C for 20 min in the TGA furnace to remove any absorbed water.

Dynamic mechanical measurements were carried out with a Polymer Laboratories DMTA operated in the three point bending mode with a strain amplitude of 60μm. The SPPO copolymer films, which were cast from chlorobenzene solution and dried in a vacuum oven, were annealed above T_g in the DMTA furnace to remove any residual solvent and analyzed over the frequency range 0.1 Hz to 30 Hz under a nitrogen atmosphere. Measurements were carried out in the temperature range -140 °C to 280 °C at a heating rate of 1.5 °C/min. After completion of dynamic mechanical measurements on a dried sample with a degree of sulfonylation of 38.8 wt%, the sample was immersed in distilled water at room temperature for 7 days. The wet sample was removed, and the excess water was wiped off with filter paper. The water uptake was determined to be 0.25 % by weighing.

PPO powders were compression molded into films at 280 °C under nitrogen and annealed above T_g in the DMTA furnace before dynamic mechanical measurements.

Dielectric measurements for the SPPO copolymer samples (degree of sulfonylation 38.8 wt%), which were obtained as described

above, were carried out with a General Radio model 1689M RLC Digibridge at 50 KHz over a temperature range from -155° to 280°C with a nitrogen purge. The temperature was raised at a rate of 2.0°C/min. Samples approximately 0.1 mm in thickness were employed with an active electrode cell diameter of 3.3 cm.

B. Results and Discussion

Figure 2.2 shows the degree of sulfonylation determined by elemental analysis versus the theoretical degree of sulfonylation given by the molar ratio of benzenesulfonyl chloride to PPO. As the degree of substitution increases, it is more difficult to reach higher conversion since unreacted sites for further reaction are screened by the neighboring reacted units. Thus, longer reaction times and increased amounts of benzenesulfonyl chloride were required for higher degrees of sulfonylation.

Table 2.1 shows the molecular weight characteristics of PPO and a series of SPPO copolymers. The weight average molecular weight of SPPO copolymers increases with the degree of sulfonylation.

SPPO 90, the copolymer with the highest degree of sulfonylation , is soluble in a variety of organic solvents. At a solution concentration of 5 wt% it is soluble in THF, chlorobenzene,

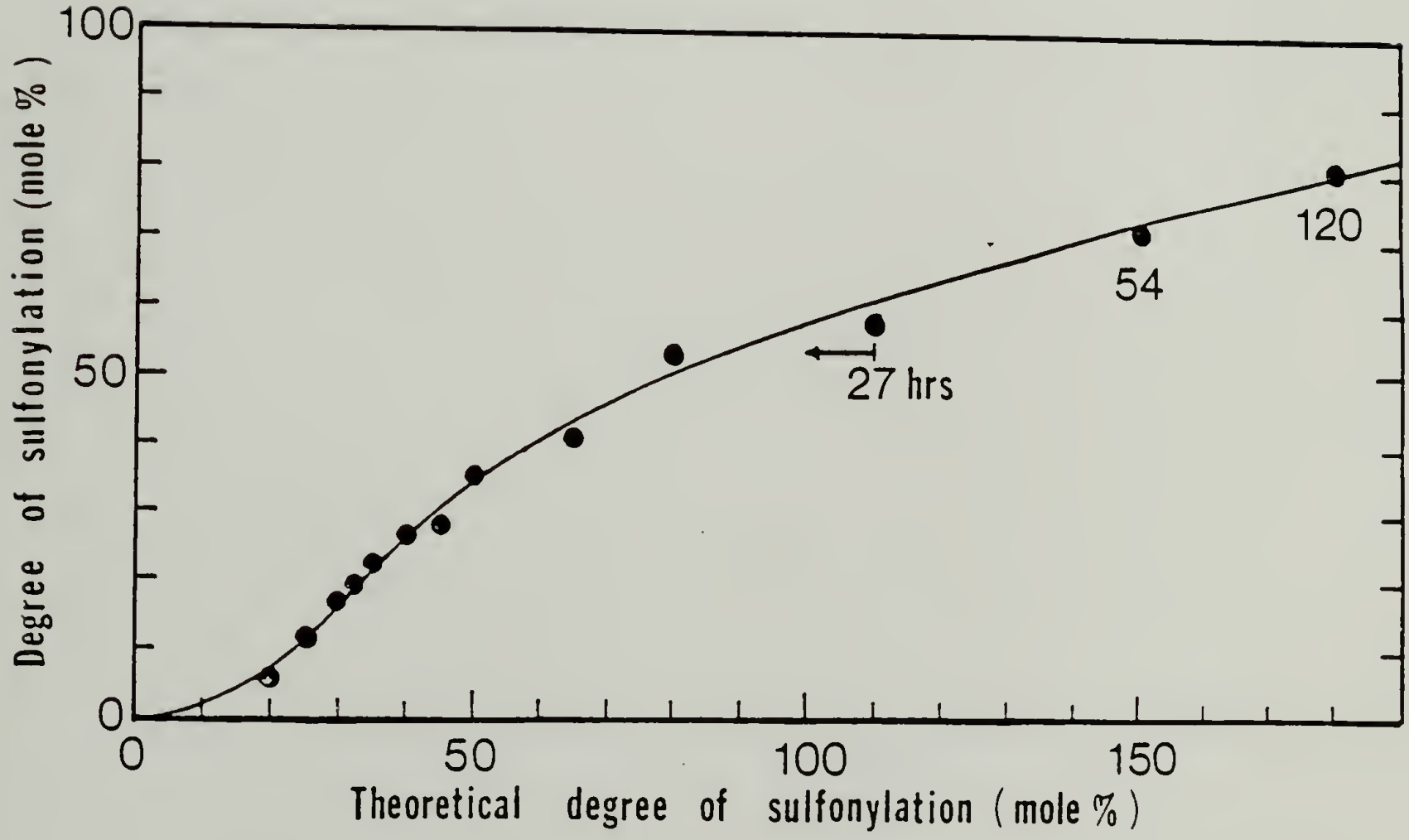

Figure 2.2. Degree of sulfonylation vs. theoretical degree of sulfonylation. The numbers 27, 54 and 120 indicate reaction times in hours

Table 2.1

Molecular Weights of Sulfonylated
Poly(2,6-dimethyl-1,4-phenylene oxide) Copolymers

	$\overline{M}_n \times 10^{-4}$	$\overline{M}_w \times 10^{-4}$	$\overline{M}_w/\overline{M}_n$
PPO[a)]	1.72	3.50	2.03
SPPO 12	1.83	4.21	2.30
SPPO 24	1.73	4.85	2.80
SPPO 30	1.58	4.42	2.80
SPPO 34	1.60	4.40	2.75
SPPO 39	1.51	4.85	3.21
SPPO 44	1.65	5.49	3.33
SPPO 47	1.99	5.80	2.91
SPPO 54	2.60	6.24	2.40
SPPO 55	2.52	6.08	2.41
SPPO 60	2.44	7.81	3.20
SPPO 72	2.56	8.07	3.15
SPPO 75	2.50	7.33	2.93
SPPO 85	2.48	8.72	3.52
SPPO 90	2.79	8.81	3.16

a) Toluene was used as an eluant.

nitrobenzene, chloroform, N,N-dimethyl acetamide, dimethyl sulfoxide, and N-methylpyrrolidone but is insoluble in acetone, toluene, and carbon tetrachloride at room temperature.

Figure 2.3 shows the variation of the density of SPPO as a function of the degree of sulfonylation. No evidence of swelling or dissolution of samples in mixed solvents was observed even after a month of immersion. The densities of the SPPO copolymers increase linearly with the degree of sulfonylation. By extrapolation the density of a completely sulfonylated homopolymer is estimated to be 1.26 g $cm^{-3} \pm 0.005$. The density of PPO (1.09 g cm^{-3}) compares well with the value of 1.066 g cm^{-3} determined by Fried[12].

The structure of these modified materials was confirmed by infrared and ^{1}H-NMR spectra. Figure 2.4 shows the infrared spectra of unmodified PPO and one of its sulfonylated derivatives. Only the region ranging from 600-1600 cm^{-1} is shown for clarity of display since little change could be seen in other regions. The SPPO copolymer exhibits new $-SO_2-$ absorption peaks at 1150 cm^{-1}.

Figures 2.5, 2.6 and 2.7 show ^{1}H-NMR spectra of PPO and some SPPO copolymers. Based on a series of spectra, chemical shift assignments have been made and are shown in Figure 2.6. In comparison to the starting PPO, pendant aromatic protons located at

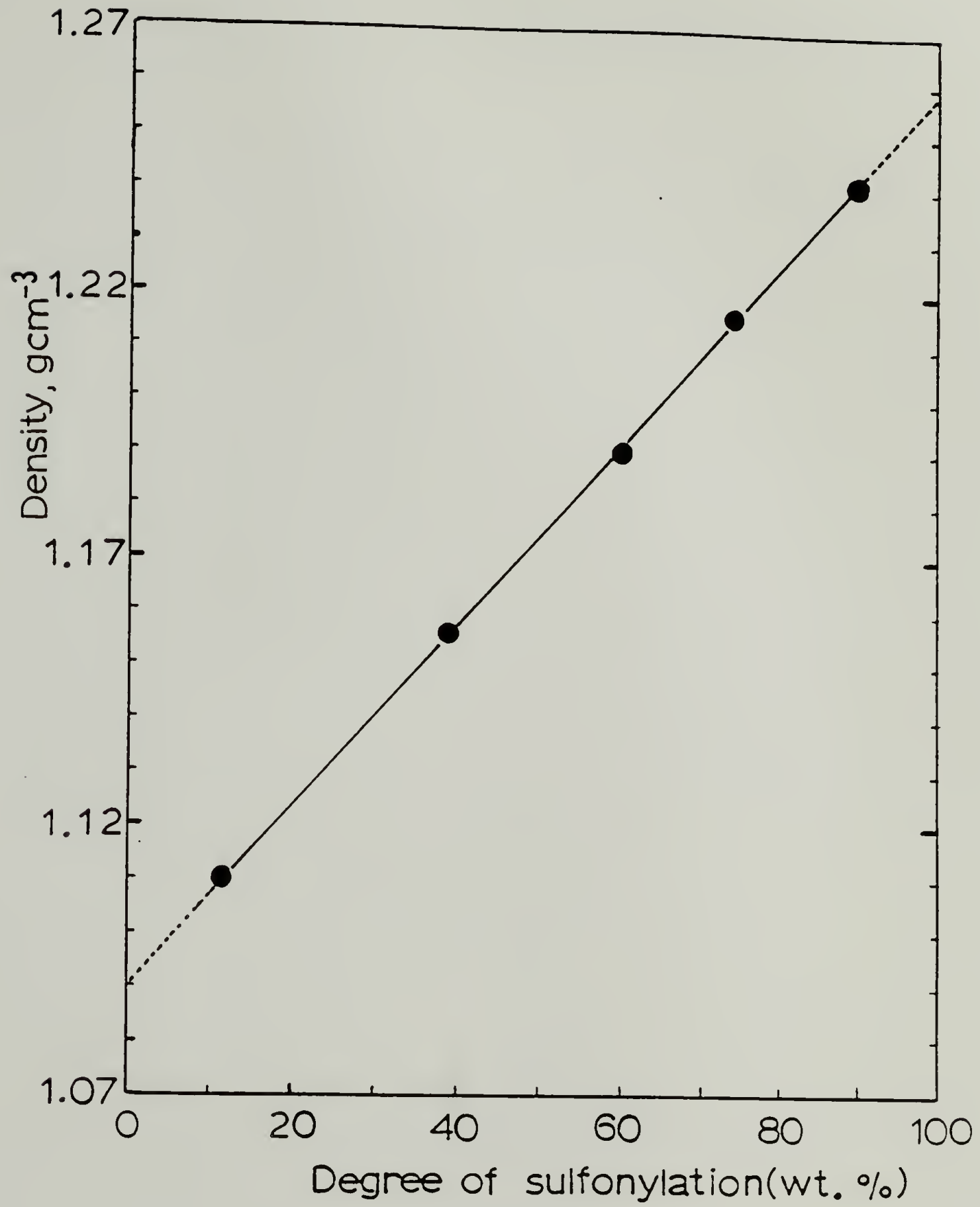

Figure 2.3. Density of SPPO copolymers vs. degree of sulfonylation

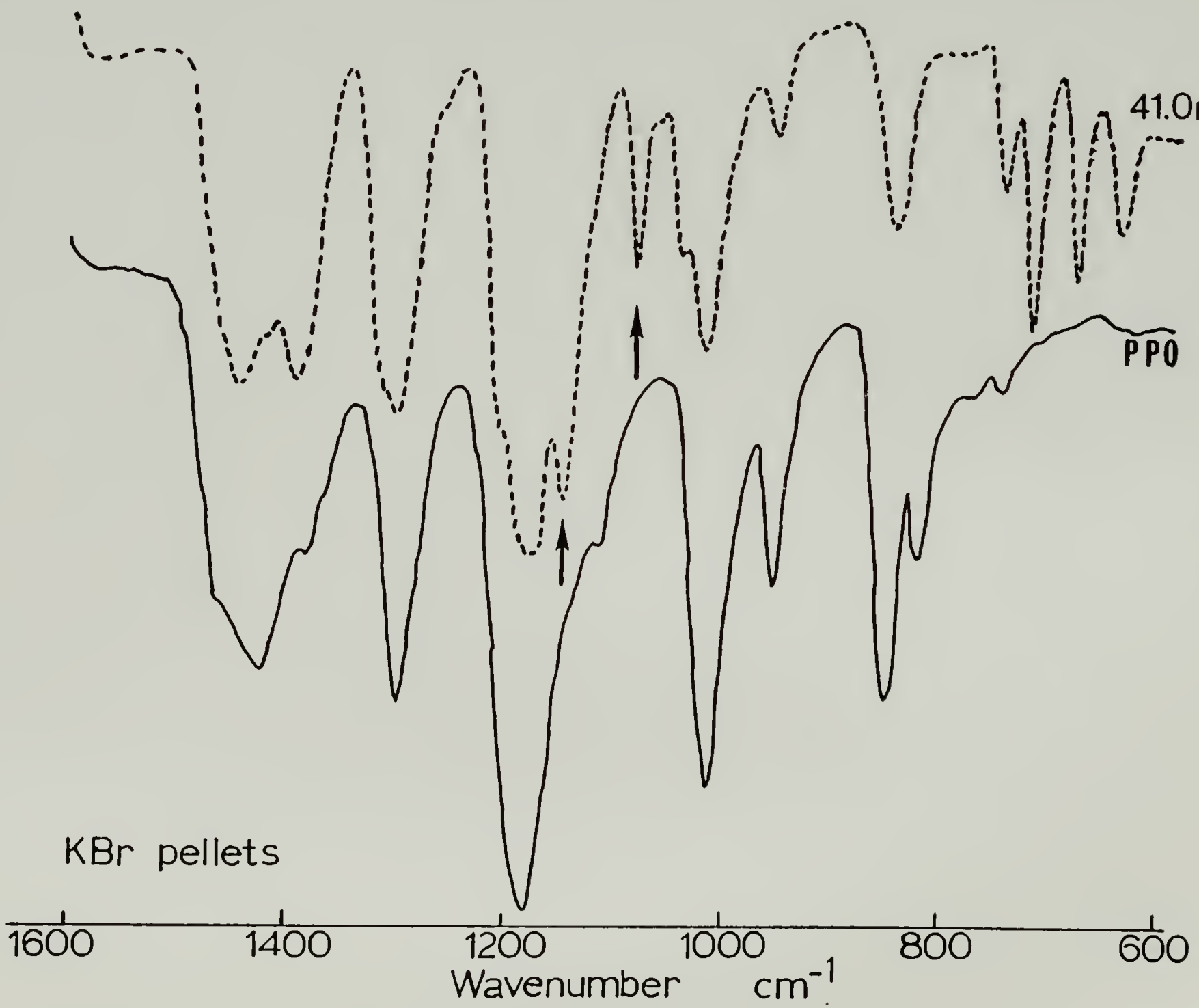

Figure 2.4. IR spectra of PPO (solid line) and sulfonylated PPO, degree of sulfonylation: 41.0 mole% (broken line)

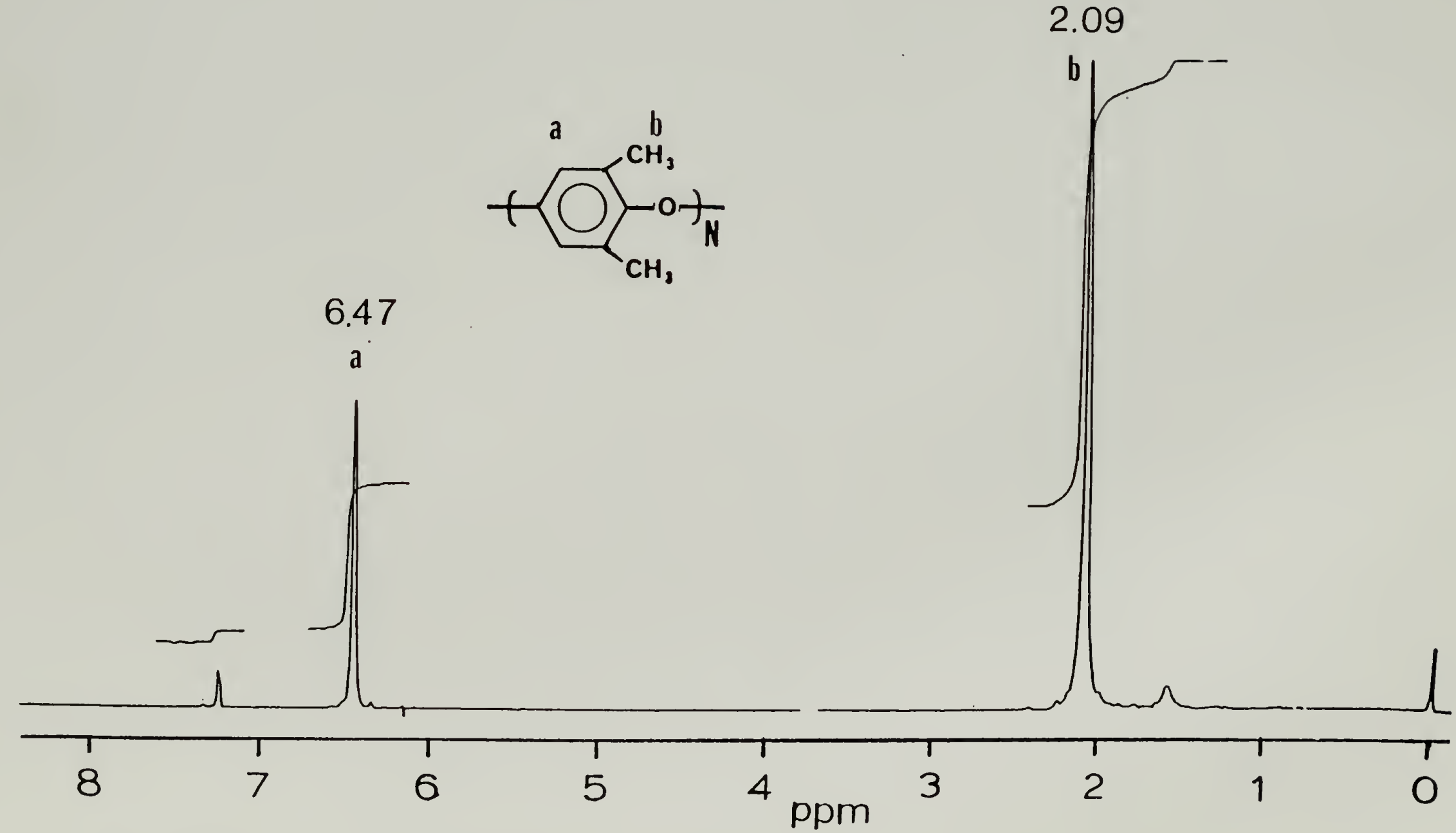

Figure 2.5. ^{1}H-NMR spectrum of PPO

35.2 mol %

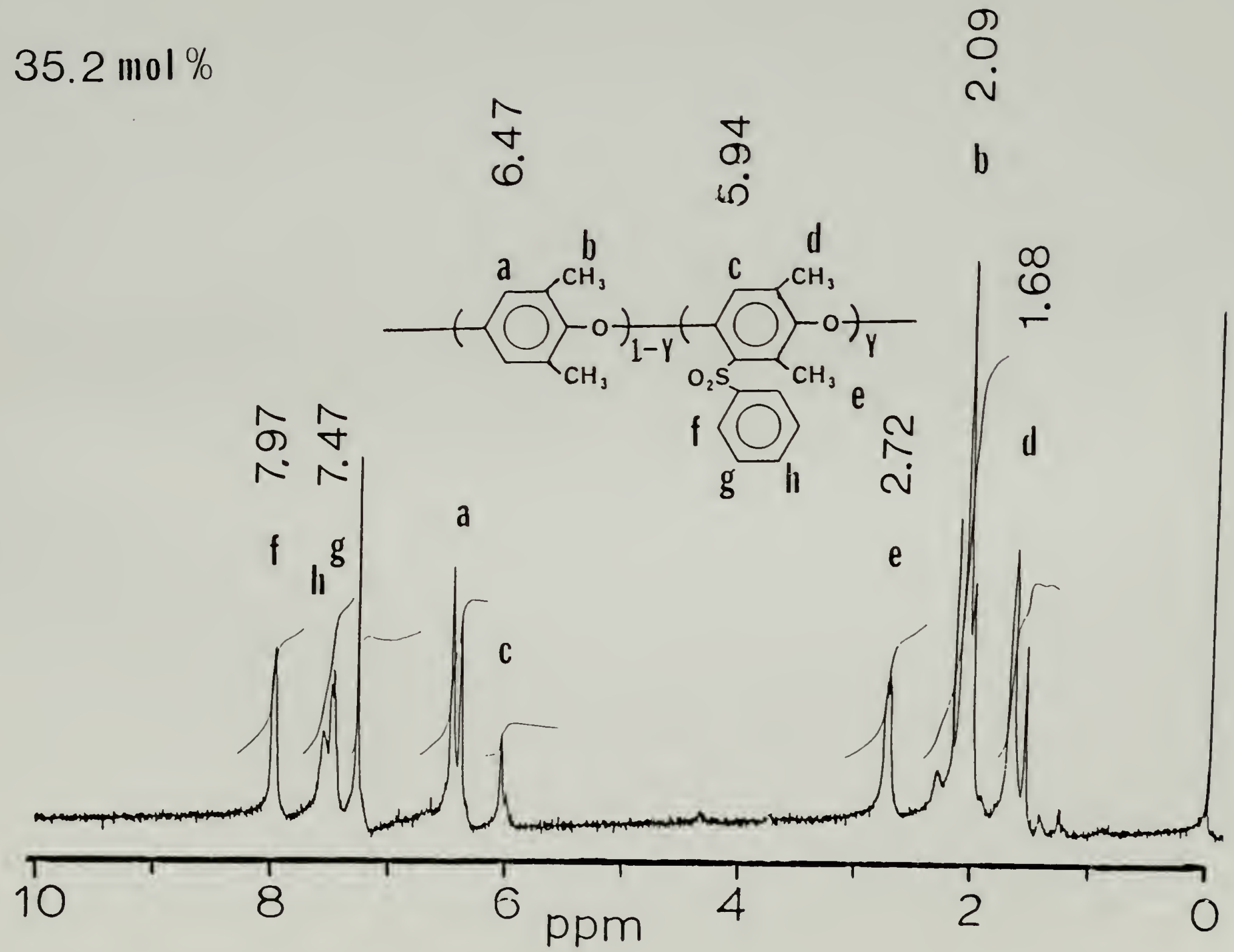

Figure 2.6. ^{1}H-NMR spectrum of sulfonylated PPO; degree of sulfonylation: 35.2 mole%

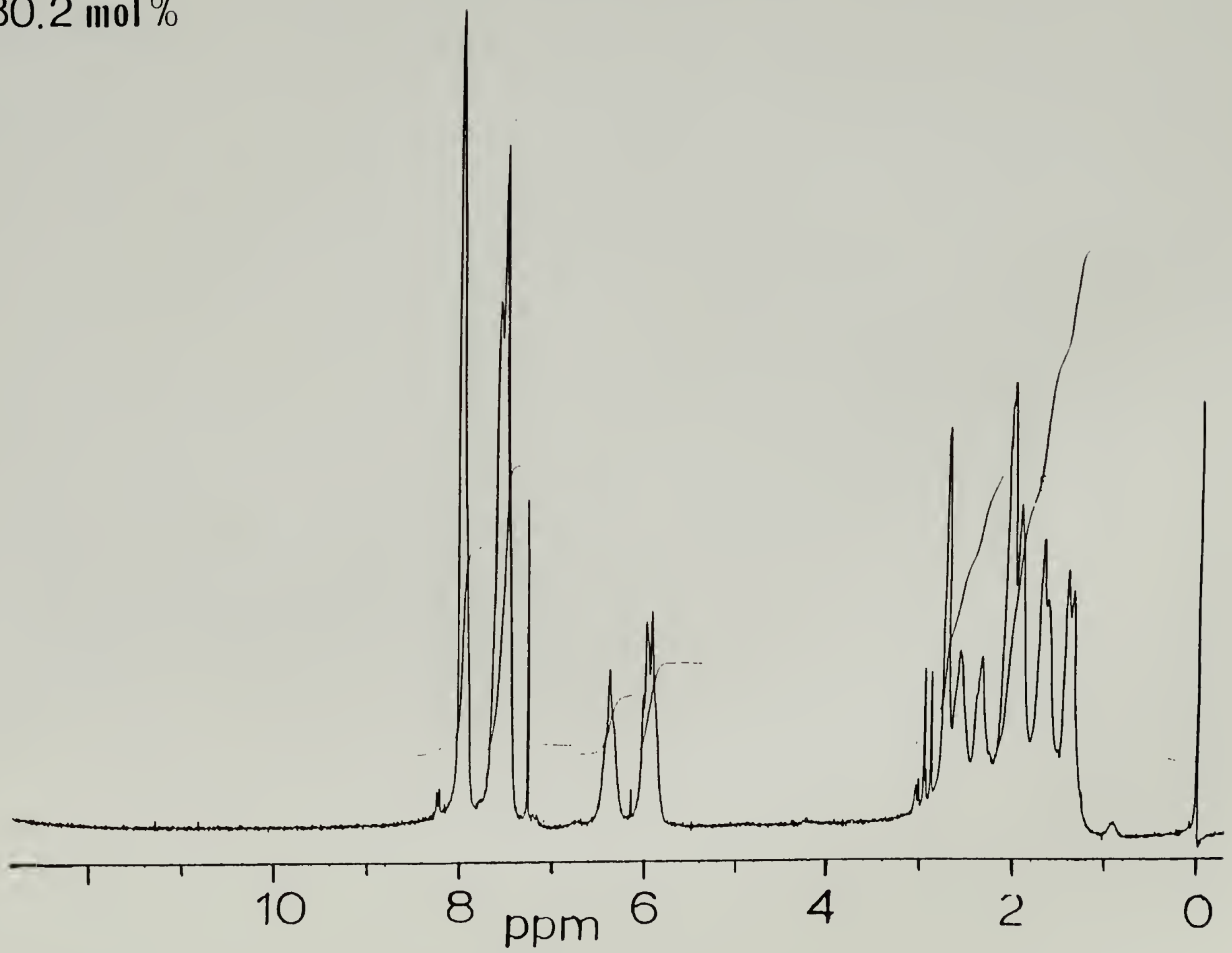

Figure 2.7. ^{1}H-NMR spectrum of sulfonylated PPO; degree of sulfonylation: 80.2 mole%

ortho, meta and para positions to the electron withdrawing sulfone group in the SPPO copolymer are resolved at 7.97, 7.47 and 7.60 ppm, respectively.

Some of the physical properties of a series of SPPO copolymers are tabulated in Table 2.2, where the range of error in the measurement of ΔC_p is estimated to be less than 10 %. Figure 2.8 shows that the glass transition temperature (T_g) increases linearly with the weight percent of sulfonylation. The control sample exhibited the same T_g and infrared spectrum as those of PPO itself, which implies that no competing side reactions or chain degradation take place.

Many attempts[13-15], mostly empirical in nature, have been made to predict the effect of composition on the T_g's of random amorphous copolymers. Assuming that copolymers behave like solutions of small molecules with regard to packing behavior and that the relationship of ideal volume-additivity of the repeating units in the copolymers holds and taking into account the thermal expansion in the glassy and rubbery states, Gordon and Taylor[13] derived the relation.

$$T_g = [T_{g_1} + (kT_{g_2} - T_{g_1})W_2]/[1 + (k - 1)W_2] \qquad (2.1)$$

Table 2.2

Properties of Sulfonylated Poly(2,6-dimethyl-1,4-phenylene oxide) Copolymers

Sample	Degree of Sulfonylation		T_g	ΔC_p	Transition	Density
	Mole %	Wt %	°C	J/g/deg	Width[a] °C	g cm^{-3}
PPO	0	0	218	0.217	7.4	
SPPO 12	5.8	11.8	227	0.187	7.8	1.110
SPPO 24	12.4	23.5	234	0.172	12.0	
SPPO 30	16.8	30.4	244	0.162	8.6	
SPPO 34	19.2	34.0	247	0.159	9.6	
SPPO 39	22.6	38.8	251	0.153	12.6	1.156
SPPO 44	26.2	43.5	255	0.150	11.8	
SPPO 47	28.7	46.6	257	0.141	9.2	
SPPO 54	35.2	54.1	259	0.138	9.2	
SPPO 55	35.6	54.5	261	0.134	9.8	
SPPO 60	41.0	60.1	266	0.129	11.8	1.190
SPPO 72	53.6	71.5	272	0.110	11.6	
SPPO 75	57.6	74.6	279	0.104	11.0	1.216
SPPO 85	71.6	84.5	287	0.095	10.4	
SPPO 90	80.2	89.8	293	0.070	14.0	1.241

a) Transition width was determined from twice the difference, $T_g - T_{g,onset}$.

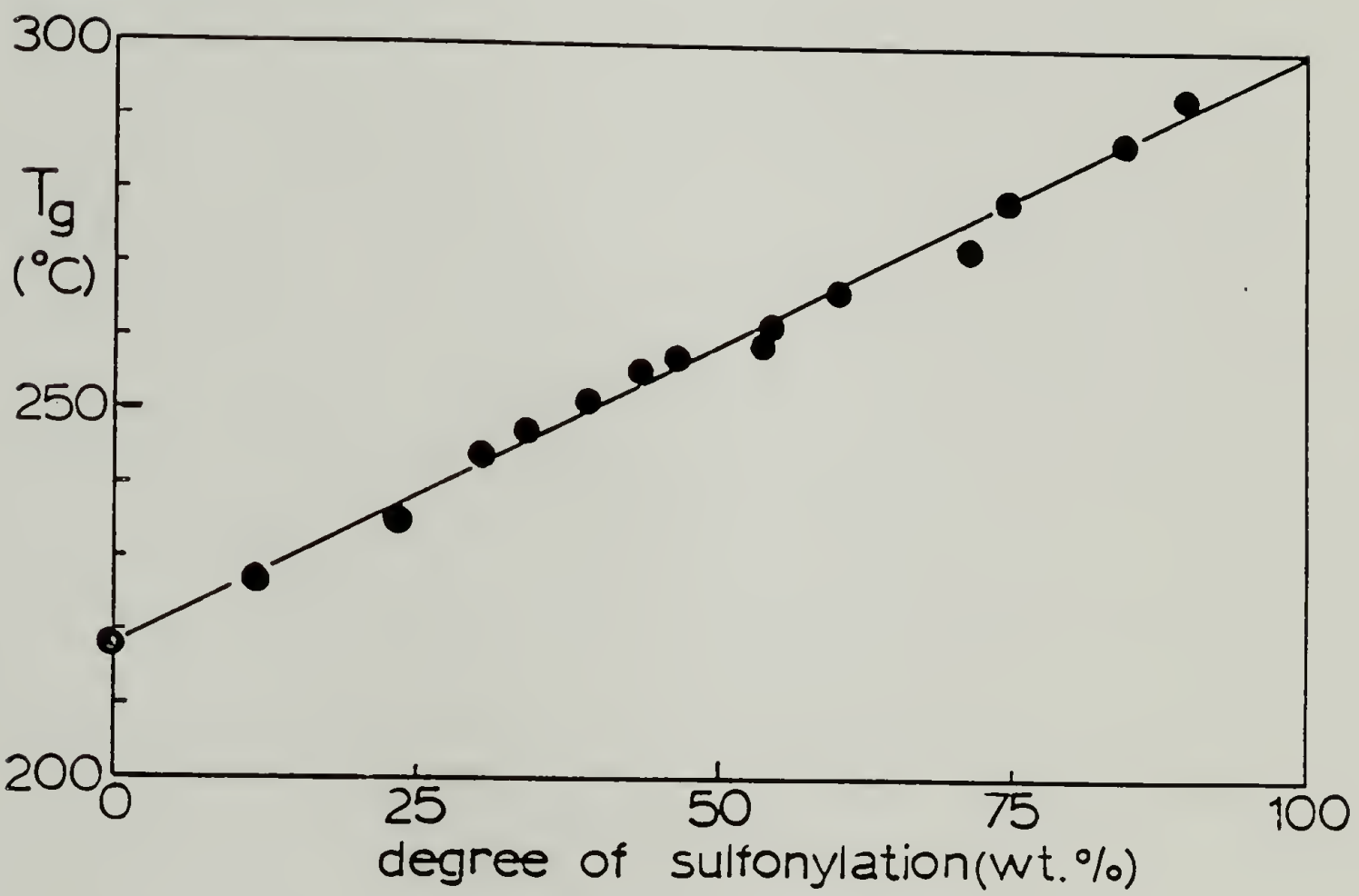

Figure 2.8. Glass transition temperature vs. degree of sulfonylation

where k is an empirical constant and W_2 is the weight fraction of component 2. As can be seen in Figure 2.8, the best fit of the experimental results is given by the Gordon-Taylor equation with k=1. The extrapolated T_g of a completely sulfonylated homopolymer is seen to be 300 ℃. PPO itself obeys freely rotating chain statistics on an intramolecular basis i.e., there is little hindrance to rotation about the oxygen ether bonds in the main chain. Dielectric relaxation studies by Karasz et al[16] and conformational energy calculations by Tonelli[17] confirm this concept of free rotation in PPO.

The intermolecular forces and the chain packing play a decisive role in affecting the molecular motion in the glassy state[2]. In the case of the SPPO copolymers, it is reasonable to assume that the bulky and very polar phenyl sulfone group attached to the phenylene oxide unit has the effect of increasing the T_g of the SPPO copolymer by raising the intermolecular and steric barrier to the rotation of monomer units.

ΔC_p, the specific heat increment at T_g per unit mass, decreases linearly with the degree of sulfonylation, as shown in Figure 2.9. This behavior has also been reported for random

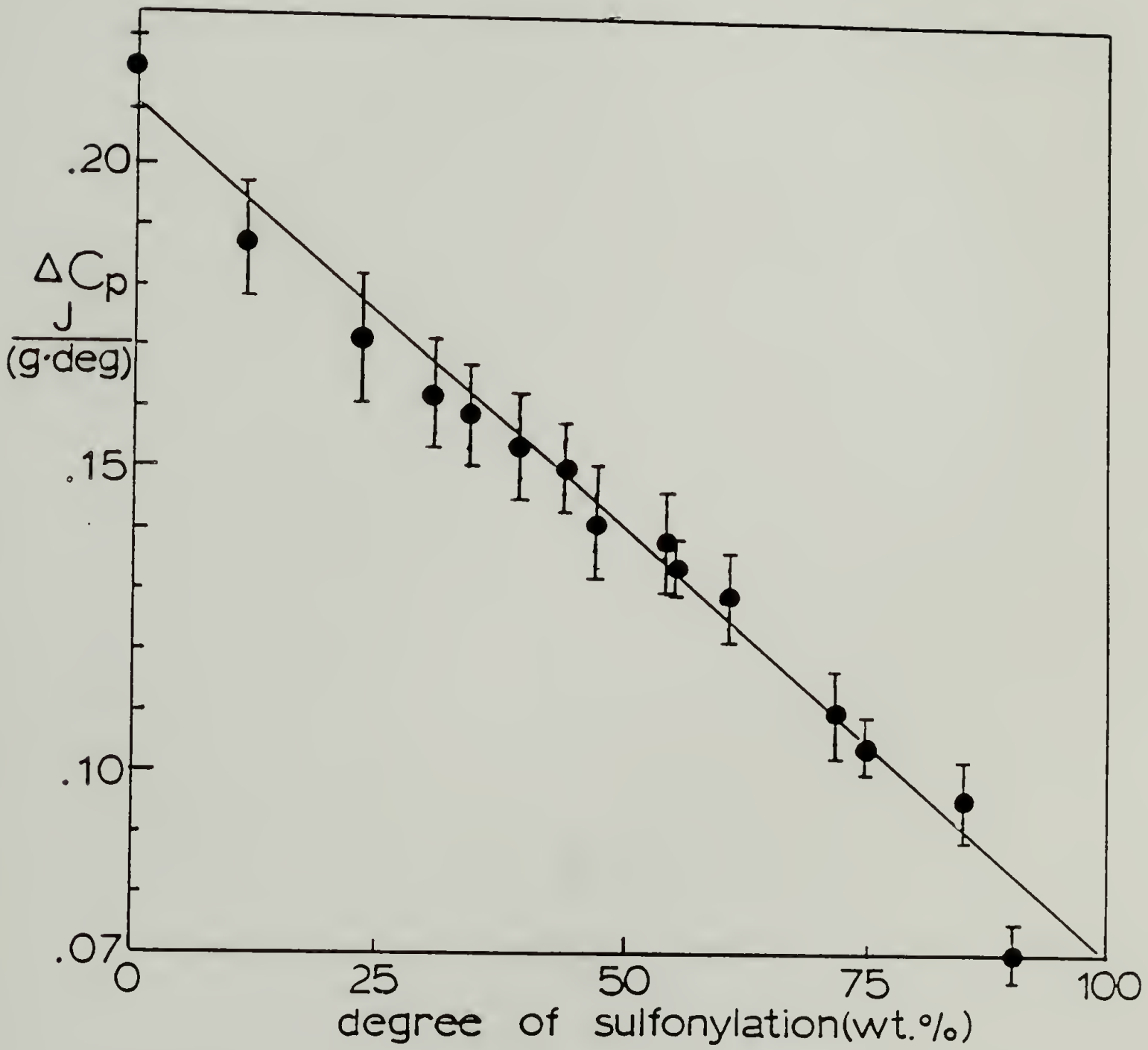

Figure 2.9. ΔC_p's of SPPO copolymers vs. degree of sulfonylation

copolymers of poly(o-fluorostyrene-co-p-fluorostyrene)[18] and also for some miscible blends[12,18]. i.e.,

$$\Delta C_p = W_1 \Delta C_{p_1} + W_2 \Delta C_{p_2} \qquad (2.2)$$

where W_i is the weight fraction of component i.

Figure 2.10 compares TGA traces of PPO and some modified PPO's. The data for phosphorylated PPO were cited from ref. 19. The thermal stability of PPO has been found not to decrease upon sulfonylation. SPPO copolymers with the degree of sulfonylation of 71.5 wt% start to lose weight at 370°C and experience a 10 % weight loss when a temperature of 470°C is reached. Figure 2.11 shows the temperatures of indicated weight loss for a series of the SPPO copolymers. These temperatures appear to be nearly independent of the degree of sulfonylation, which is unusual in the light of previous results on other derivatives which showed that substitution onto PPO decreased both thermal and oxidative stability[20].

The temperature dependences of the storage moduli (E'), loss moduli (E"), and loss factor (tan δ) at 10 Hz for PPO, dry and wet samples of SPPO copolymer (both with a degree of sulfonylation of 38.8 wt%) are shown in Figures 2.12, 2.13 and 2.14, respectively.

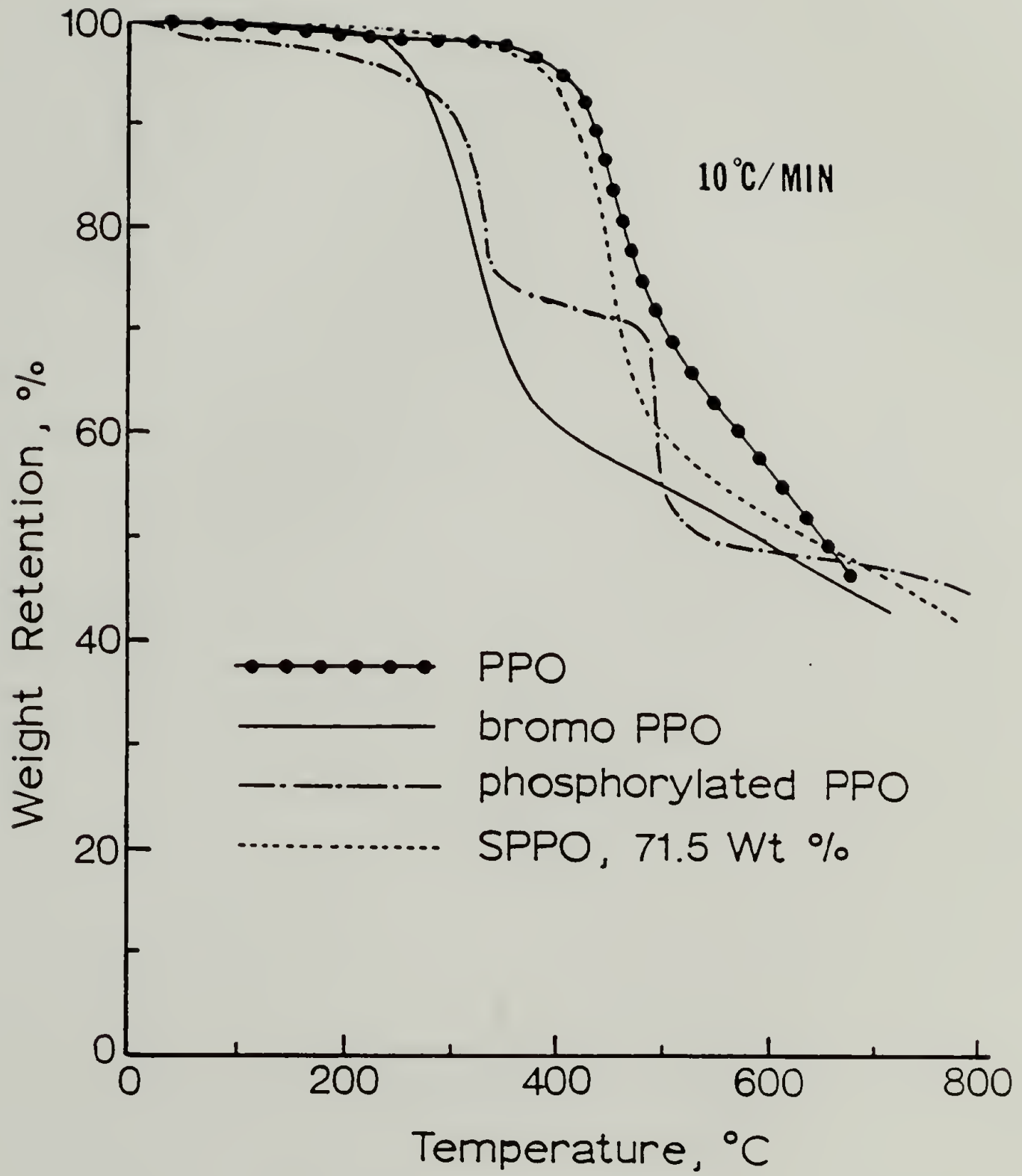

Figure 2.10. Thermogravimetric analysis of PPO and some modified PPO's

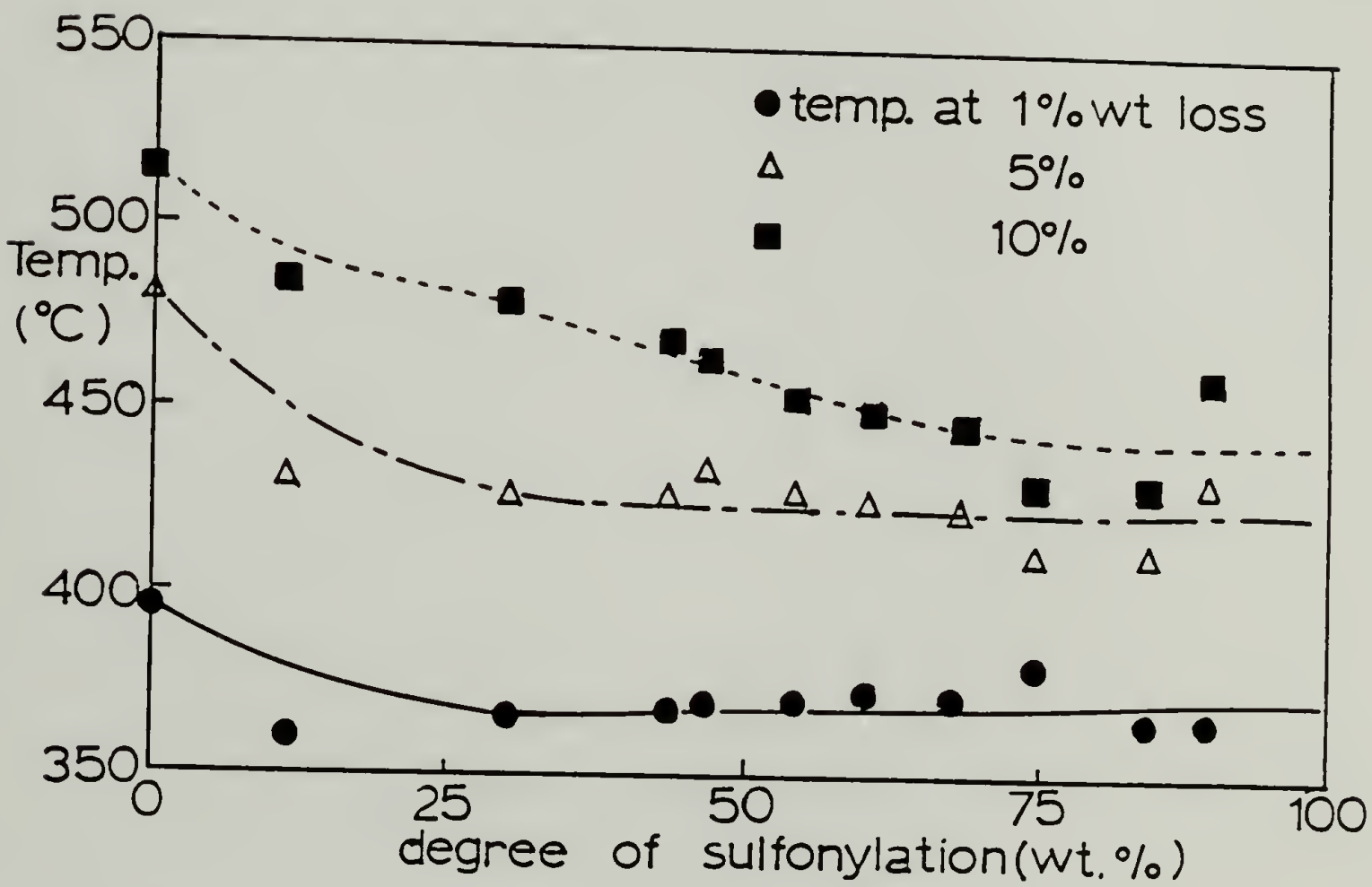

Figure 2.11. Temperatures of indicated weight loss in sulfonylated PPO during heating at 10 °C min^{-1}

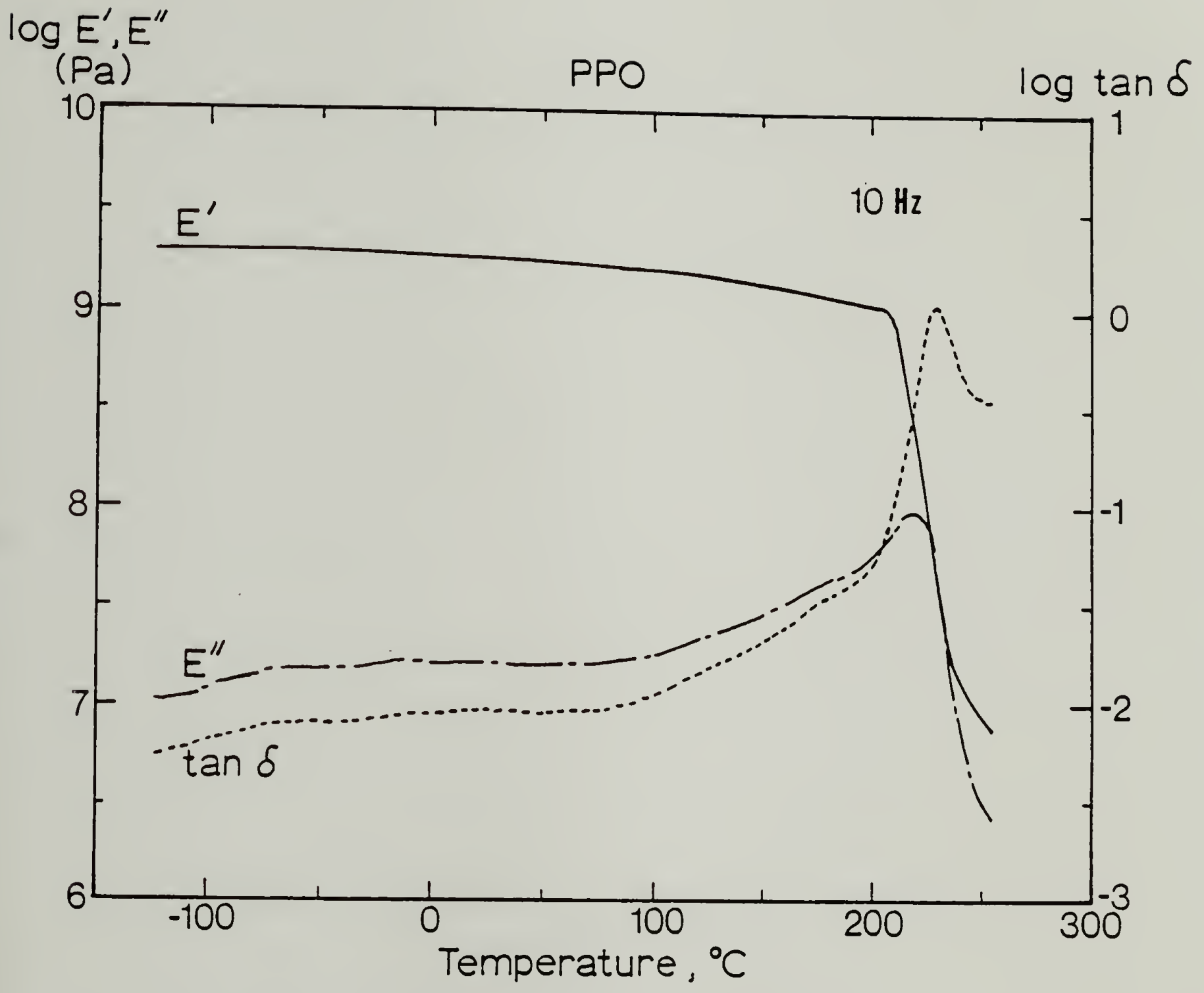

Figure 2.12. Temperature dependences of mechanical E', E" and tan δ for PPO at 10 Hz

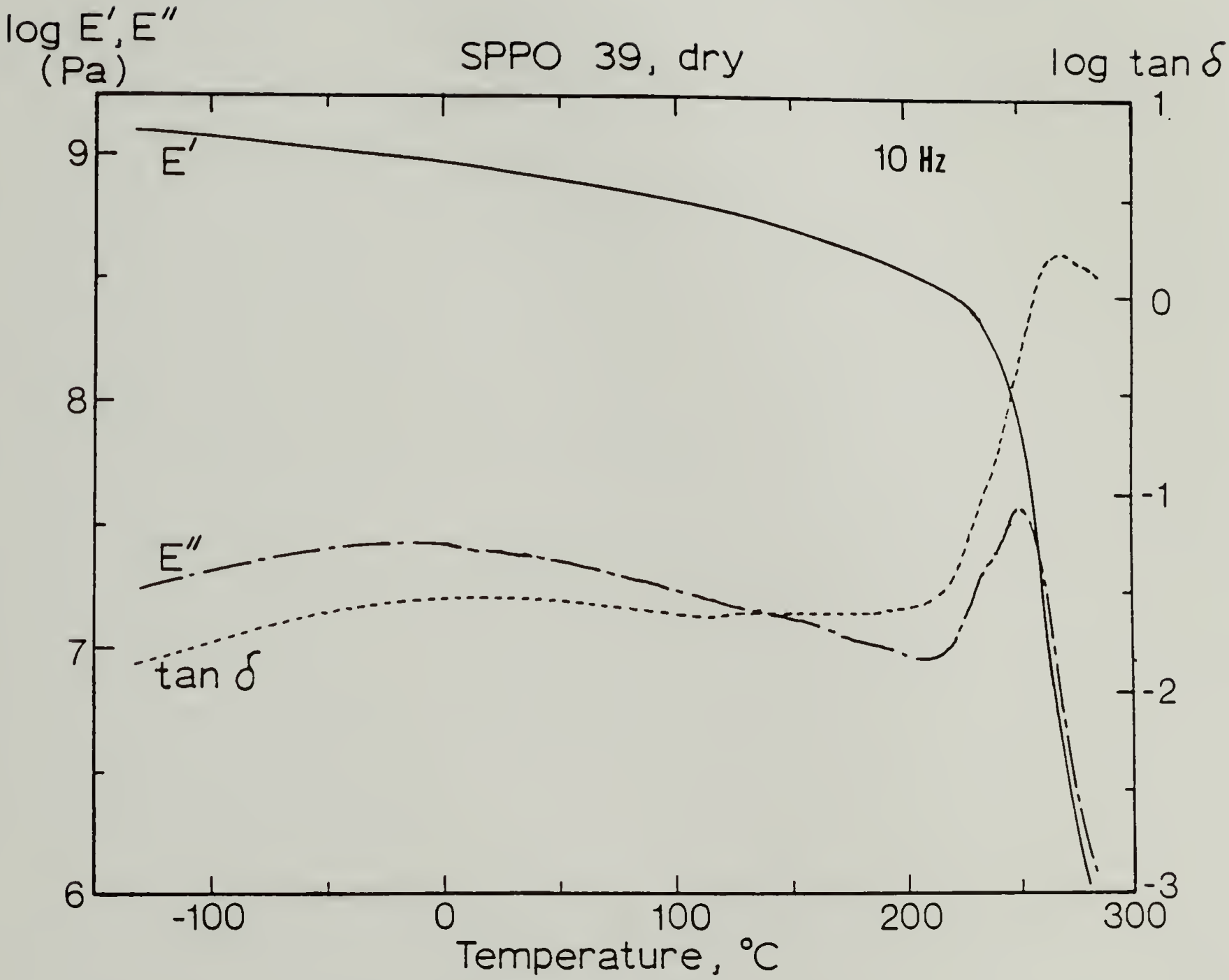

Figure 2.13. Temperature dependences of mechanical E', E" and tan δ for dry SPPO 39 at 10 Hz

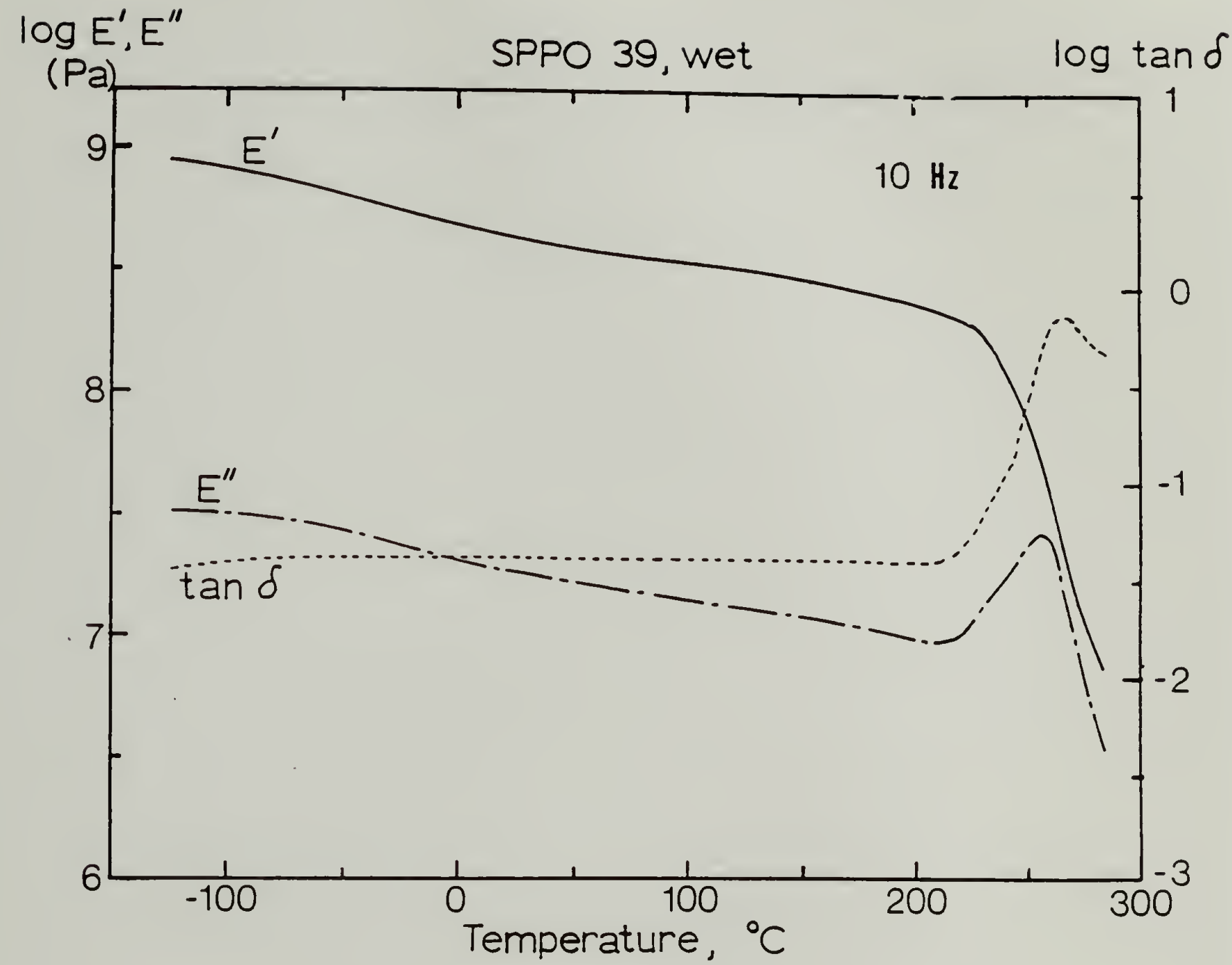

Figure 2.14. Temperature dependences of mechanical E', E" and tan δ for wet SPPO 39 at 10 Hz

In contrast to previous results[21-24] which showed that PPO exhibited three mechanical relaxations, in the temperature range employed in the current study, only one α-relaxation associated with the glass-rubber transition around 230°C was observed as shown in Figure 2.12. The storage moduli for the three samples decrease with increasing temperature and show a marked decrease around T_g. In addition, a slight decrease of the storage modulus for the SPPO copolymer can be observable in the presence of water. The tan δ peak maximum for the SPPO copolymer around 260°C is indicative of the α-relaxation process associated with the glass transition involving the onset of long-range segmental motions of the main chain. This temperature compares well with the T_g (251°) measured by DSC if frequency differences are taken into account.

The very broad low-temperature β-relaxation, which is spread over several decades of temperature centered around -10°C, is readily observed for the dry SPPO copolymer, as shown in Figure 2.13. However, the β-relaxation for the wet sample, as seen in Figure 2.14, is not observed. The α-relaxation peak position for the wet sample decreased only slightly (2°C) compared with that of the dry sample owing to gradual redrying during the measurements. However, the removal of water by annealing in the DMTA furnace regenerated a distinct broad β-relaxation.

Any motion of the polymer segment in a localized lattice, absorbed species, impurities or structural irregularities are known to be associated with low temperature relaxation[25]. In the case of the poly(arylene ether sulfones) the amplitude of β-relaxation was found to increase as the water content increased[26] probably because of the participation of absorbed water in hydrogen bonds to polar groups.

In contrast to poly(arylene ethers) bearing polar groups on the main chain, rather peculiar behavior was observed for the SPPO copolymer. In particular, the secondary β-relaxation disappeared in the presence of water. The association of water with the pendant sulfone group may cause either average motion of the phenyl sulfone group to become slower by structure tightening, or a hindrance of the local motion which gives rise to the β-relaxation.

It has been reported that the addition of water and methanol to nylon decreases the amplitude of the γ-relaxation and shifts it to slightly lower temperature[27]. This effect was ascribed to the formation of mechanically stable bridges between amide groups in adjacent chains and water acting as an antiplasticizer.

The decrease in the amplitude of the β-relaxation has been observed in bisphenol A-polysulfone by the addition of 4,4'-dichlorodiphenyl sulfone[28-30], which is known to act as an

antiplasticizer of the polysulfone. The similar suppression of the β-relaxations of bisphenol A-polycarbonate with added antiplasticizer has also been observed[31]. However, there are not enough data at present to suggest that water acts as an antiplasticizer in the SPPO copolymer.

For the SPPO copolymer, there are several possible local motions which could be responsible for the β-relaxation. First, there may be local motion of the pendant phenyl sulfone groups. Second, a local twisting motion of the ether group proposed by Yamafuji *et al*[32] may occur. Third, methyl group motion may cause a local mode process.

According to Schaefer *et al*[33] a ring flip process is not permitted for the stiffer PPO main chain. Broad line NMR studies on PPO[34] revealed that the methyl groups are in motion at -180°C. Thus, local motions of the phenyl sulfone groups appear to be the source of the very broad β-relaxation at -10°C. In addition, this motion is considered not to be entirely intramolecular since it depends on the surroundings of the sulfone group.

The temperature dependence of dielectric ε" for the SPPO copolymer with a degree of sulfonylation of 38.8 wt%, as shown in Figure 2.15, supports this hypothesis, although dc conductive loss[35]

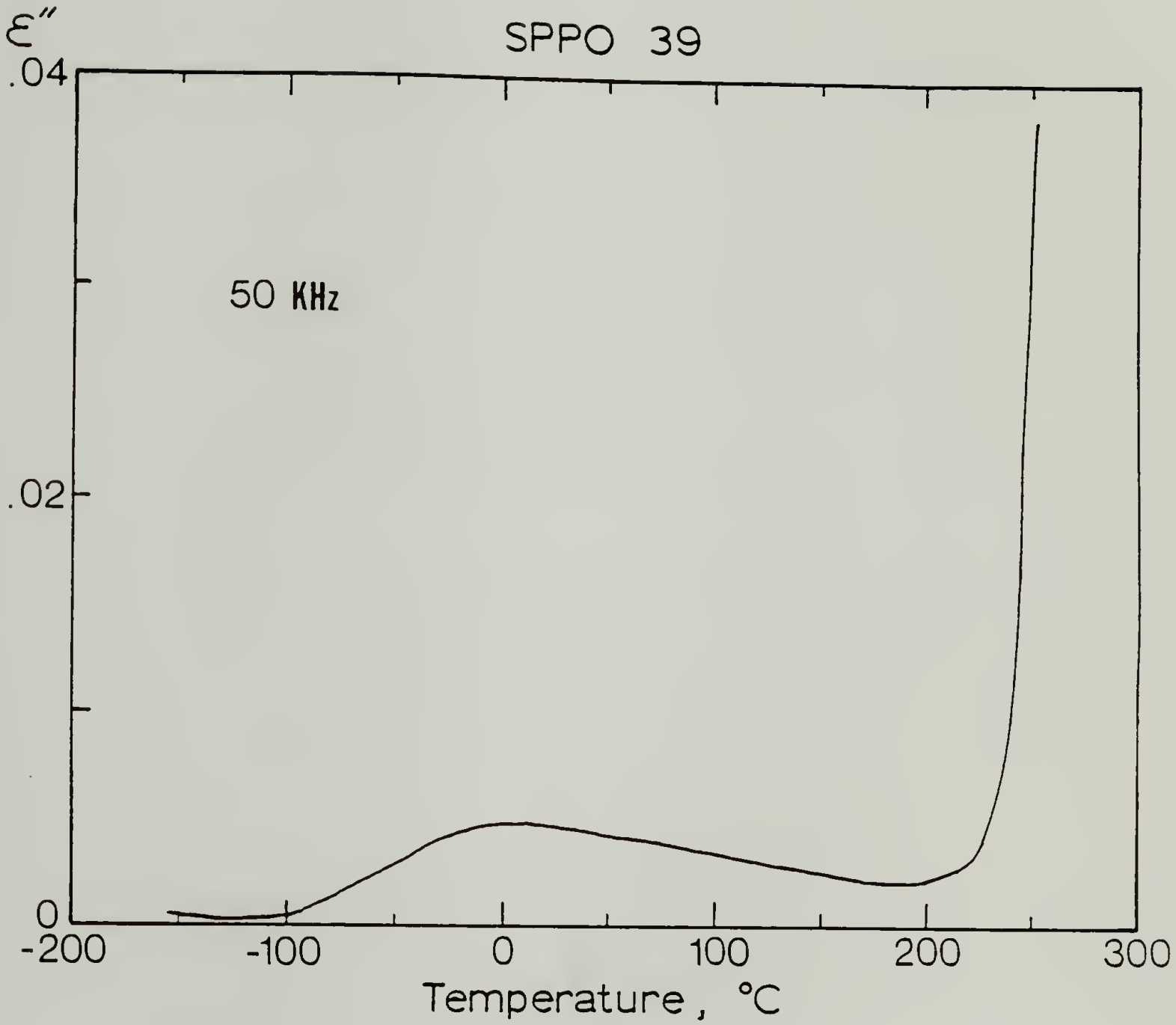

Figure 2.15. Temperature dependences of dielectric ε" for dry SPPO 39 at 50 KHz

is seen to be significant at higher temperatures. The broad secondary β-relaxation at 0°C can be clearly seen. The height of the dielectric ε" peak is on the order of 10^{-2}. It is noted that the amplitude of the β-relaxation of SPPO is quite large compared to that of PPO, which may be due to the contribution of the dielectrically active sulfone group.

In the case of PPO low-temperature dielectric relaxation was reported to appear at -100°C, and its molecular origin is uncertain[16]. The height of the dielectric ε" for γ-relaxation is only 3×10^{-3}; the low intensity of the relaxations is ascribed to the relatively nonpolar nature of PPO.

Accordingly, a localized mode of the dipolar sulfone group appears to be responsible for the β-relaxation of the SPPO copolymer at 0°C. The temperature shift of the dielectric β-relaxation compared with the dynamic mechanical β-relaxation can be understood by taking into account the frequency difference or the differing relative contribution of dipolar and mechanical motions of the pendant tetrahedral sulfone group, whose exact nature of motion is unknown.

The activation energies for the mechanical α-relaxation of the PPO and SPPO copolymer were compared from the multiple frequency run using the relation :

$$-E_a/2.3R = d\ \log f/d(1/T) \qquad (2.3)$$

In the case of the SPPO copolymer with a degree of sulfonylation of 38.8 wt% the mechanical tan δ peak temperatures observed for 0.1, 1, 3 and 30 Hz are 251°C, 256°C, 258°C and 263°C, respectively, as shown in Figure 2.16. Figure 2.17 shows an Arrhenius plot of the frequencies as a function of the reciprocal temperature for the peak maxima. The SPPO copolymr of higher degree of sulfonylation has the larger activation energy, reflecting the increased intermolecular and steric barrier to long-range segmental motion by the sulfonylation reaction of PPO.

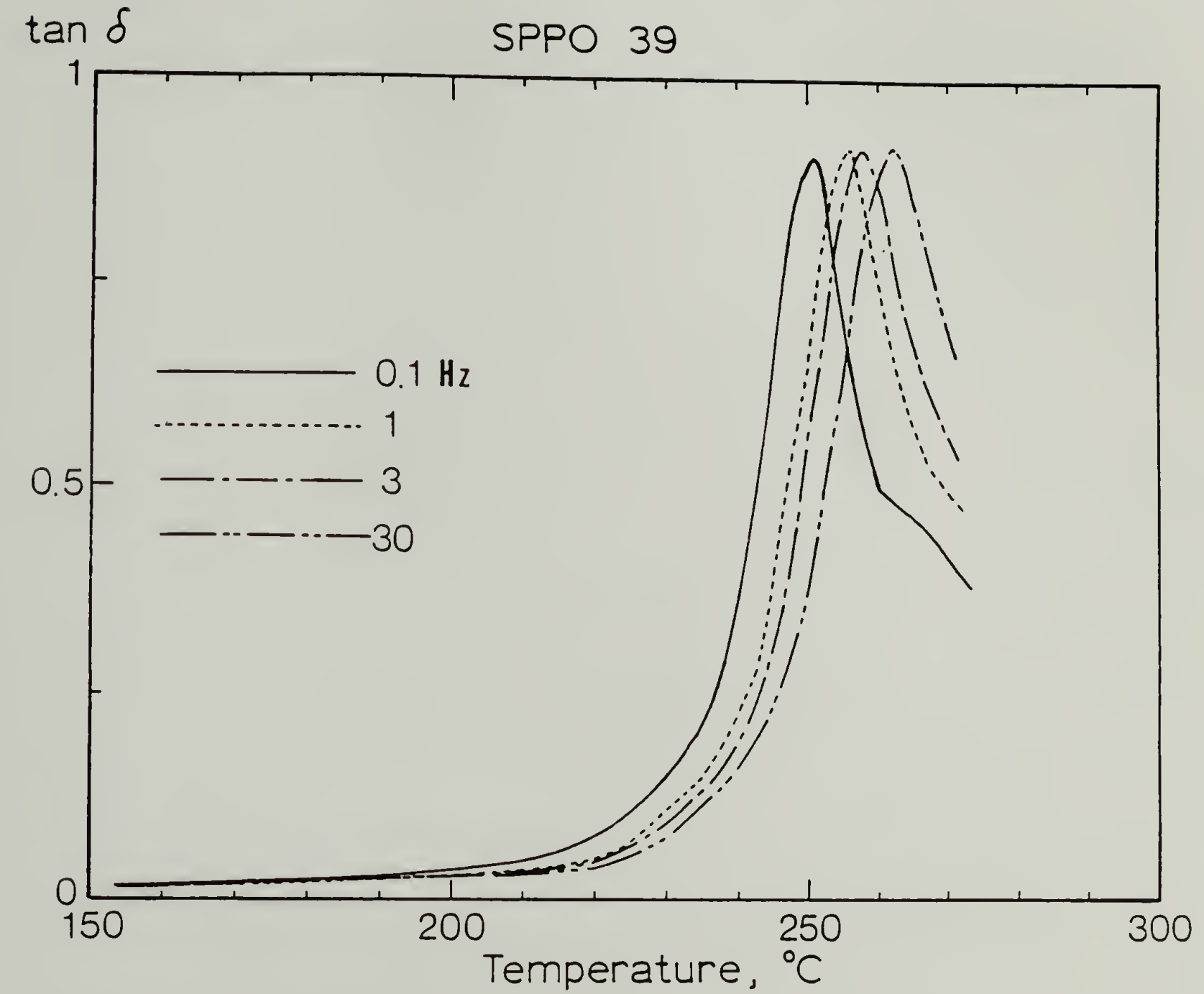

Figure 2.16. Frequency dependences of mechanical tan δ curves for dry SPPO 39

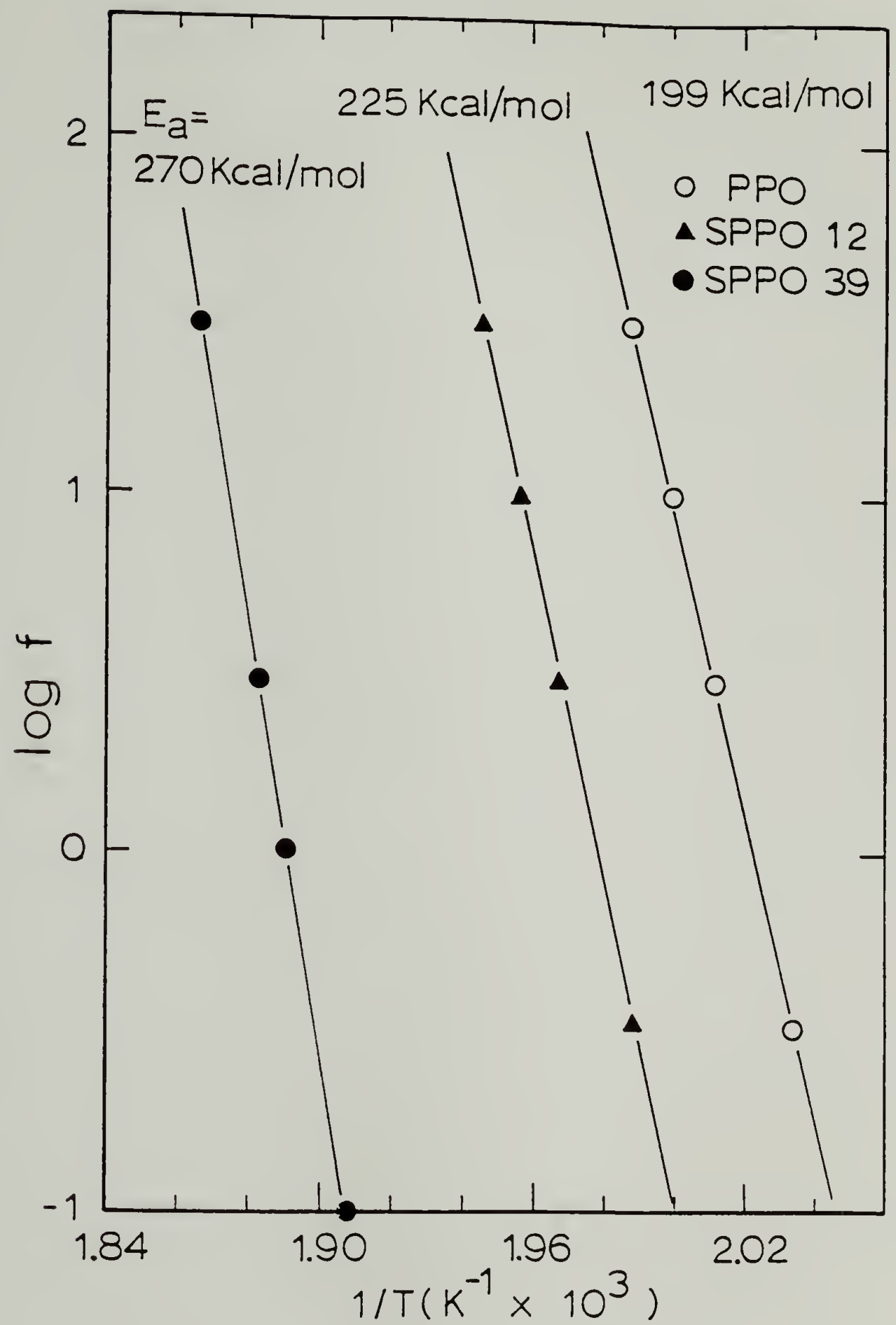

Figure 2.17. Arrhenius plot of relaxation maxima vs. frequency for PPO, SPPO 12 and SPPO 39

REFERENCES

1. R.C. Bopp, U. Gaur, R.P. Kambour, B. Wunderlich, J. Therm. Anal., 25(2), 243 (1982).
2. T.P. Jauhiainen, Angew. Makromol. Chem., 104, 117 (1982).
3. I. Cabasso, J. Jagur-Grodzinski, D. Vofsi, J. Appl. Polym. Sci., 18, 1969 (1974).
4. A.J. Chalk, A.S. Hay, J. Polym. Sci., A1(7), 691 (1968).
5. S. Xie, W.J. MacKnight, F.E. Karasz, J. Appl. Polym. Sci., 29(8), 2679 (1984).
6. R.Y.M. Huang, J.J. Kim, J. Appl. Polym. Sci., 29(12), Pt. 1, 4017 (1984).
7. P.J. Chludzinski, J.F. Austin, J.F. Enos, Office of Saline Water Research and Development Progress Report No. 697, General Electric Co., Lynn, Mass, 1971.
8. K. Chander, R.C. Anand, I.K. Varma, Angew. Makromol. Chem., 127, 137 (1984).
9. V. Percec, B.C. Auman, Makromol. Chem., 185(11), 2319 (1984).
10. J.B. Rose, Polymer, 15, 456 (1974).
11. T.E. Attwood, P.C. Dawson, J.L. Freeman, L.R.J. Hoy, J.B. Rose, P.A. Staniland, ACS, Polymer Preprints, 20(1), 191 (1979).
12. J.R. Fried, Ph.D. Thesis, University of Massachusetts, 1976.
13. M. Gordon, J.S. Taylor, J. Appl. Chem., 2, 493 (1952).
14. L.A. Wood, J. Polym. Sci., 28, 319 (1958).
15. F.N. Kelley, F. Bueche, J. Polym. Sci., 50, 549 (1961).

16. F.E. Karasz, W.J. MacKnight, J. Stoelting, J. Appl. Phys., 41, 4357 (1970).

17. A.E. Tonelli, Macromolecules, 6, 503 (1973).

18. C.L. Ryan, Ph.D. Thesis, University of Massachusetts, 1979.

19. K. Chander, R.C. Anand, I.K. Varma, J. Macromol. Sci. Chem., A20(7), 697 (1983).

20. G.F.L. Ehlers, "Structure Stability Relationships of Polymers Based on Thermogravimetric Analysis Data, Pt. 1", AFML-TR-74-177.

21. J. Stoelting, F.E. Karasz, W.J. MacKnight, Polym. Eng. Sci., 10, 133 (1970).

22. T. Lim, V. Frosini, V. Zaleckas, D. Morrow, J.A. Sauer, Polym. Eng. Sci., 13, 51 (1973).

23. A.F. Yee, Polym. Eng. Sci., 17, 213 (1977).

24. J.R. Fried, G.A. Hanna, Polym. Eng. Sci., 22, 705 (1982).

25. R.D. McCammon, R.G. Saba, R.N. Work, J. Polym. Sci., A7, 1721 (1969).

26. G. Allen, J. McAinsh, G.M. Jeffs, Polymer, 12, 85 (1971).

27. H.W. Starkweather, ACS Symp. Ser., No. 127, 433 (1980).

28. M.K. Gupta, J.A. Ripmeester, D.J. Carlsson, D.M. Wiles, J. Polym. Sci., Polym. Lett. Ed., 21, 211 (1983).

29. S.E.B. Petris, R.S. Moore, J.R. Flick, J. Appl. Phys., 43, 4318 (1972).

30. J.J. Dumais, A.L. Cholli, L.W. Jelinski, J.L. Hedrick, J.E. McGrath, Macromolecules, 19, 1884 (1986).

31. W.J. Jackson Jr., J.R. Caldwell, Adv. Chem. Ser., 48, 185(1965).

32. K. Yamafuji, Y. Ishida, Kolloid-Z., 183, 15 (1962).

33. J. Schaefer, E.O. Stejskal, D. Perchak, J. Skolnick, R. Yaris, Macromolecules, 18, 368 (1985).

34. W.G. Gall, N.G. McCrum, J. Polym. Sci., 50, 489 (1961).

35. N.G. McCrum, B.E. Read, G. Williams, Anelastic and Dielectric Effects in Polymeric Solids, John Wiley and Sons, London, 1967.

CHAPTER III

MISCIBILITY IN BLENDS OF SULFONYLATED POLY(2,6-DIMETHYL-1,4-PHENYLENE OXIDE) (SPPO) COPOLYMERS AND IN BLENDS OF POLYSTYRENE/SPPO COPOLYMERS

This chapter is divided into two parts. The first part describes the miscibility behavior in blends of SPPO copolymers differing only in copolymer composition, systems of the type $(C_{1-x}D_x)_{n_1}/(C_{1-y}D_y)_{n_2}$ where C and D refer to unsulfonylated phenylene oxide and sulfonylated phenylene oxide units, respectively. The segmental interaction parameter between unsulfonylated and sulfonylated unit in SPPO copolymers (χ_{CD}) is determined from the critical composition difference for miscibility. This determination is based on Scott's prediction[1] and is made using a mean field treatment, as discussed in Chapter I.

Scott predicted that copolymers with a certain degree of heterogeneity in chemical compositions would be thermodynamically unstable. Namely, two random copolymers differing only in composition are not necessarily miscible in all proportions. Accordingly, there is a tolerable difference in copolymer composition

above which the blends are immiscible. This prediction has been corroborated for several copolymer blend systems[2-7]. The tolerable difference in copolymer composition for the blends of SPPO copolymers was determined by DSC and optical microscopy.

The second part describes miscibility behavior and phase stability in blends of polystyrene with SPPO copolymers, systems of the type $A_{n_1}/(C_{1-y}D_y)_{n_2}$ where A refers to the styrene unit. Based on the χ_{CD} determined in the first part, χ_{AD} is determined by employing a mean field treatment. From the temperature induced phase separation study LCST behavior was observed and interphase mixing in the two phase blend is also discussed on the basis of the glass transition width.

A. Experimental Section

The sulfonylation procedure and the characterization of a series of SPPO copolymers were described in Chapter II. Polystyrene samples (Mw = 13,000, 68,000 and 115,000) were purchased from Polymer Laboratories and used as received. All the samples had $\bar{M}w/\bar{M}n < 1.05$. The numeral following polystyrene represents its molecular weight, thus the polystyrene sample with $\bar{M}w$ of 115,000 is designated as PS-115.

Blends (50/50 wt%) were prepared by casting films from 2 wt% THF solutions. The solvent was allowed to evaporate slowly at ambient conditions for at least four days and the resulting films were placed in a vacuum oven at 140°C for 96 hr to completely remove residual solvent.

Glass transition temperatures were measured in the same way as described in Chapter II. Due to the proximity of the T_g's of the constituents in some blends, first derivative DSC thermograms were also recorded. T_g measurements to assess the miscibility of two polymers are suitable only if their T_g's are sufficiently far apart from each other. Thus, if the differences in the glass transition temperatures of each constituent were greater than 15°C, then DSC and optical microscopy were employed to determine miscibility. Otherwise, only the latter was used.

Optical micrographs were taken on a Leitz optical microscope with cross-polarizers at a magnification of 100X. Solutions of 50/50 wt% blend mixtures in THF were cast onto microscope slides. After drying at ambient conditions, these were further dried under vacuum and annealed at 290°C for 15 min followed by rapid quenching into liquid N_2.

The temperature induced phase separation study in the blends of polystyrene with SPPO copolymers was done by heating the samples

to 290°C and maintaining them for 20 min followed by rapid cooling (-320 K/min) to room temperature and subsequent scanning at 20°C/min, unless otherwise noted.

B. Results and Discussion

i). Blends of SPPO Copolymers

Figures 3.1-3 show typical DSC thermograms with their first derivative curves. One can see clearly that the blends exhibit two distinct T_g's for each constituent with slight inward shift of T_g of each component indicative of some partial miscibility. Figure 3.4 displays a DSC thermogram for the blend of PPO with SPPO 24, implying its two phase nature. However, the blends at Δ wt% = 18.3 and 20.5, as seen in Figures 3.5 and 3.6, show a single T_g between those of the pure constituents.

To verify that the single T_g observed in the blend is not due to an experimental artifact concerned with the sensitivity of DSC, samples of pure SPPO 72 and SPPO 90 were separated in a DSC sample pan by a thin aluminum foil barrier to prevent mixing, as similarly done by Ueda[8]. The resulting DSC thermogram is also

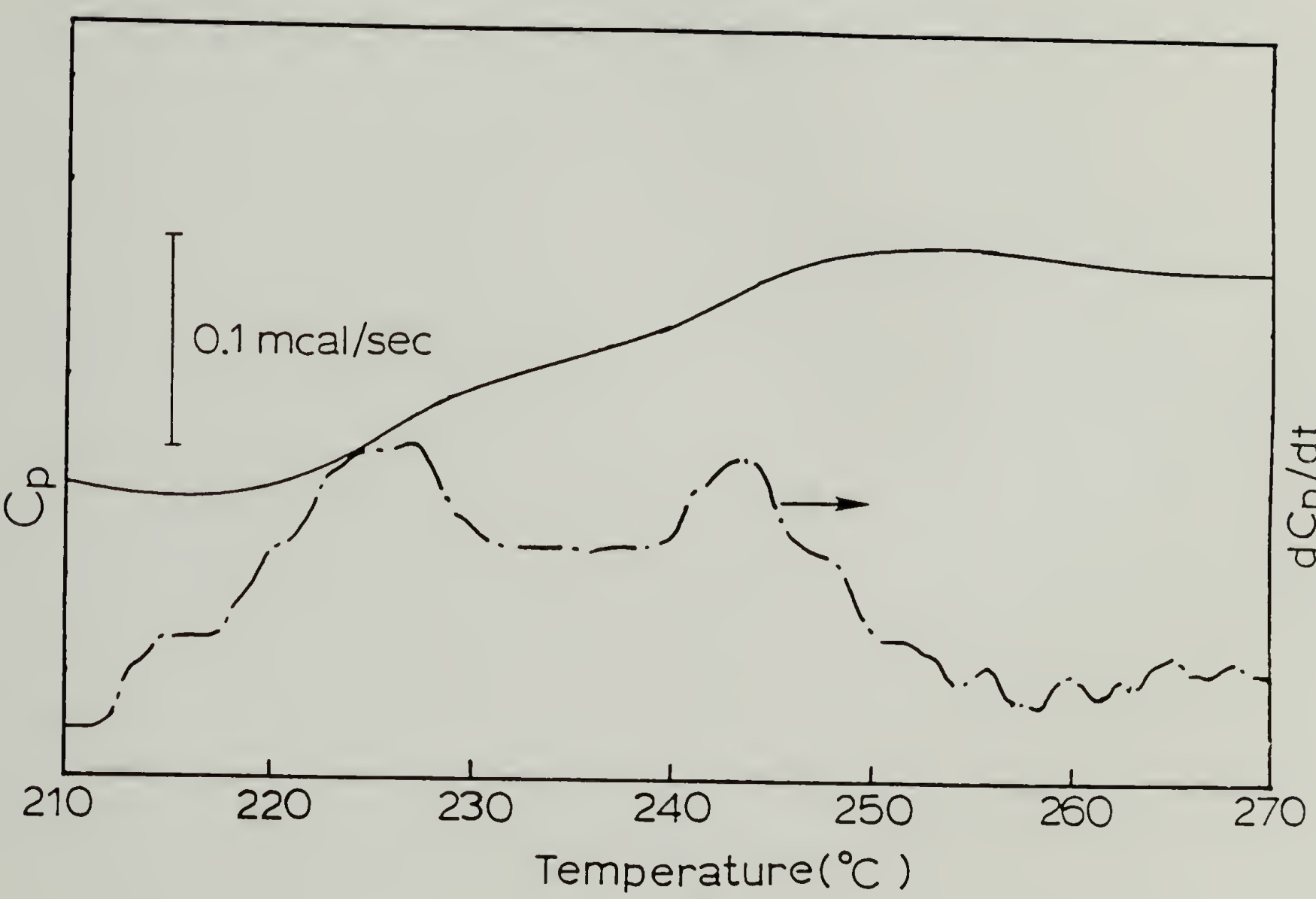

Figure 3.1. DSC thermogram for SPPO 12/34 (50/50 wt% blend)

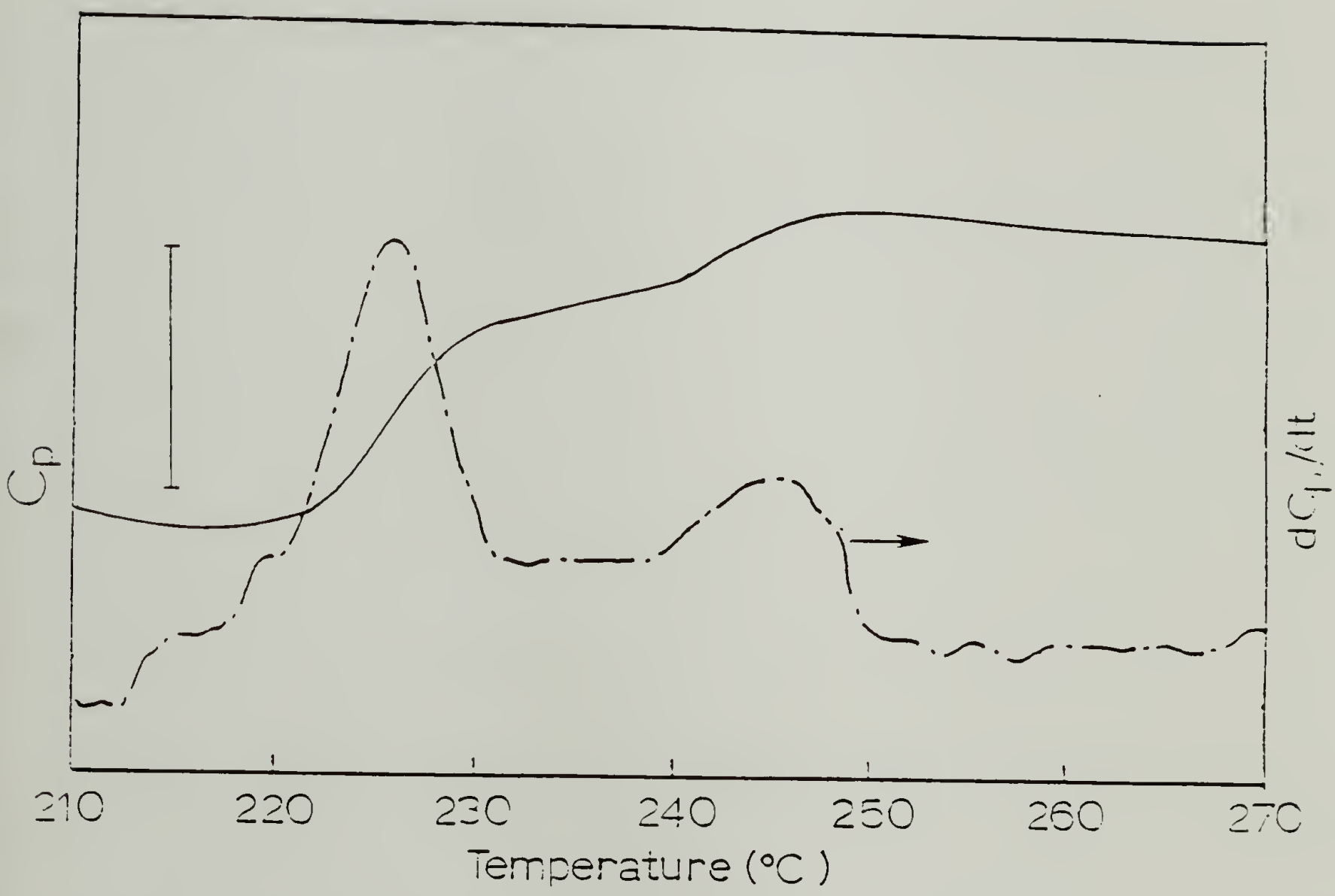

Figure 3.2. DSC thermogram for OPPO 12/39 (50/50 wt% blend)

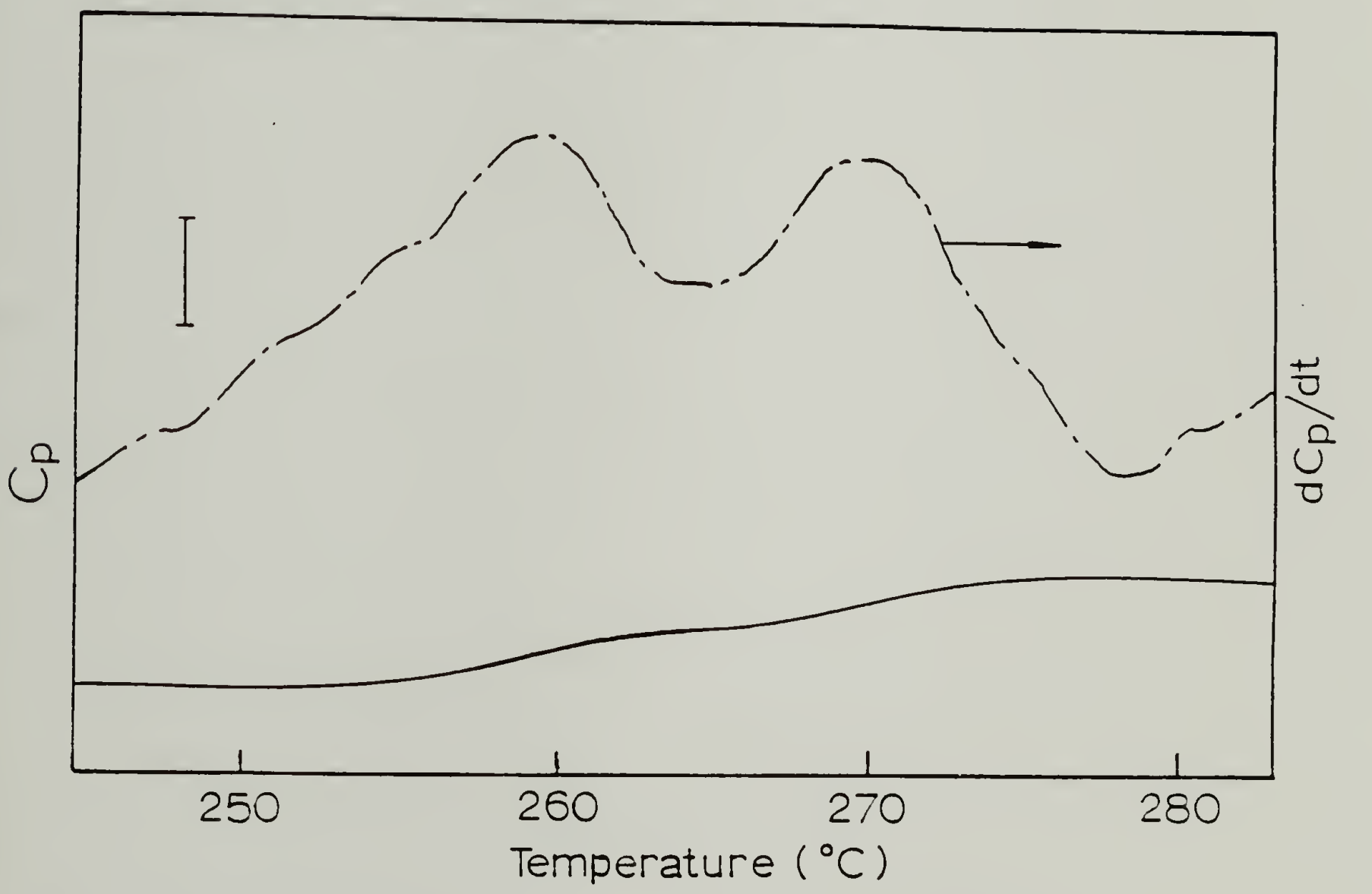

Figure 3.3. DSC thermogram for SPPO 47/75 (50/50 wt% blend)

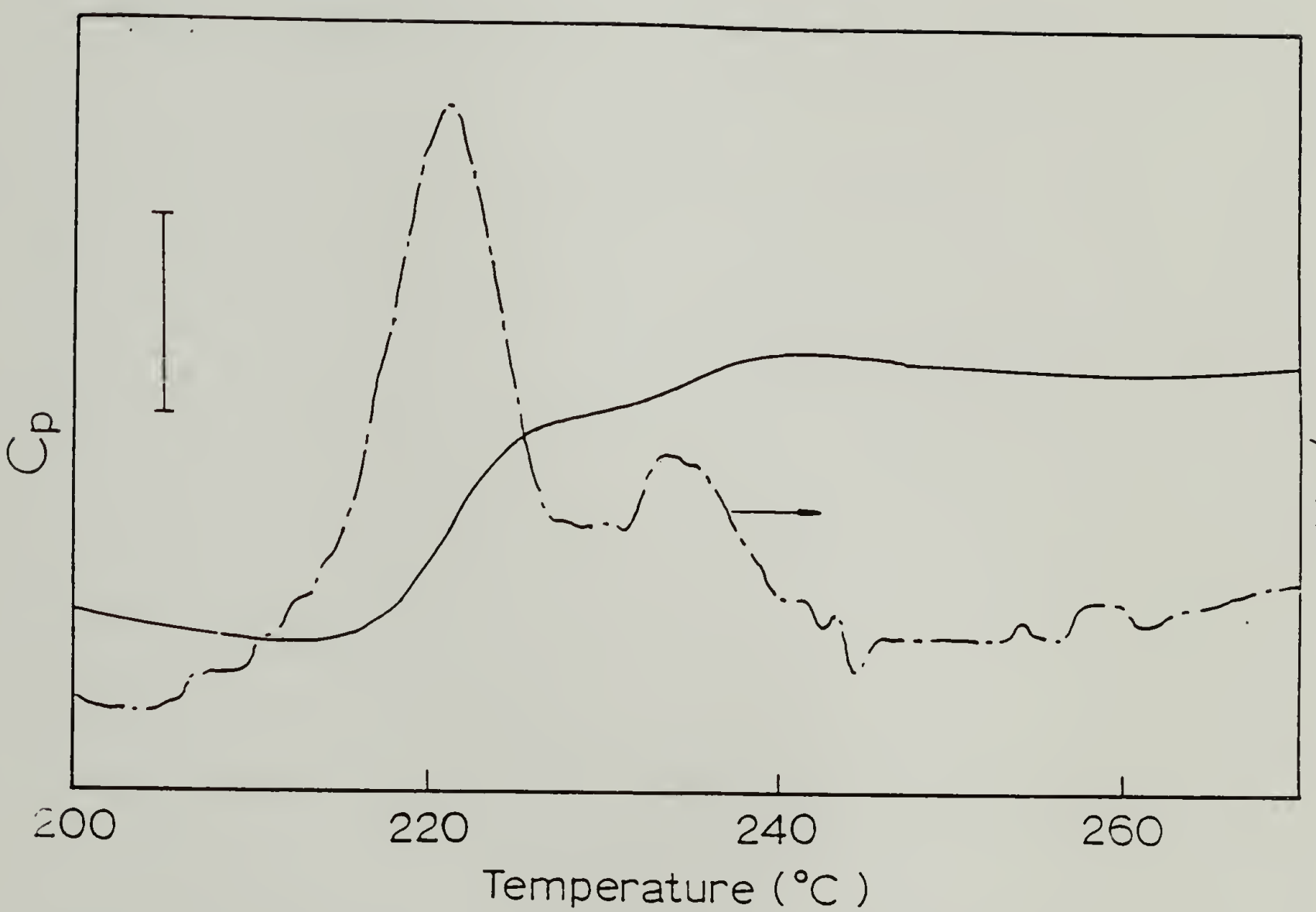

Figure 3.4. DSC thermogram for PPO/SPPO 24 (50/50 wt% blend)

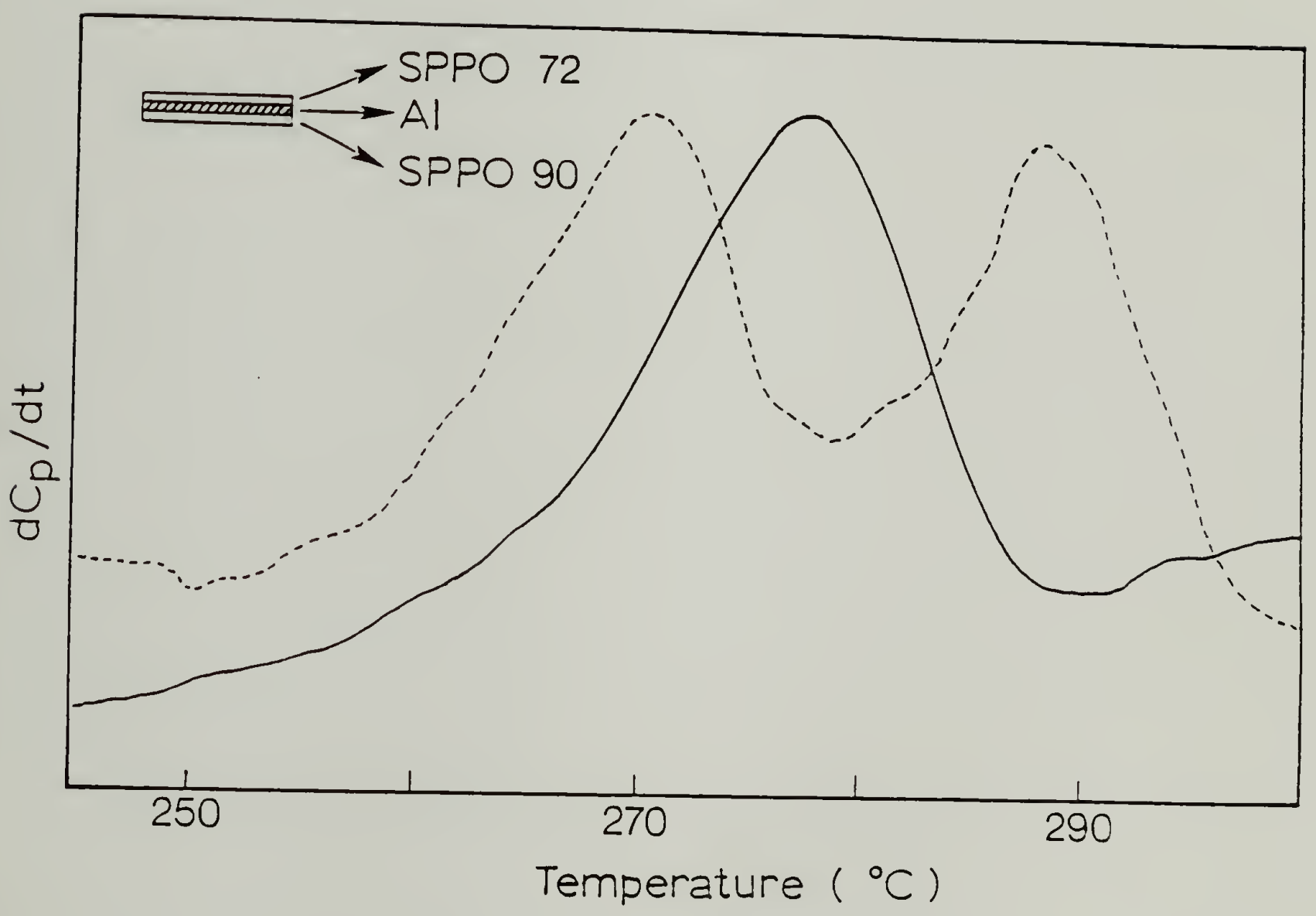

Figure 3.5. DSC thermogram for SPPO 72/90 (50/50 wt% blend). Dotted line indicates pure constituents separated by aluminum foil.

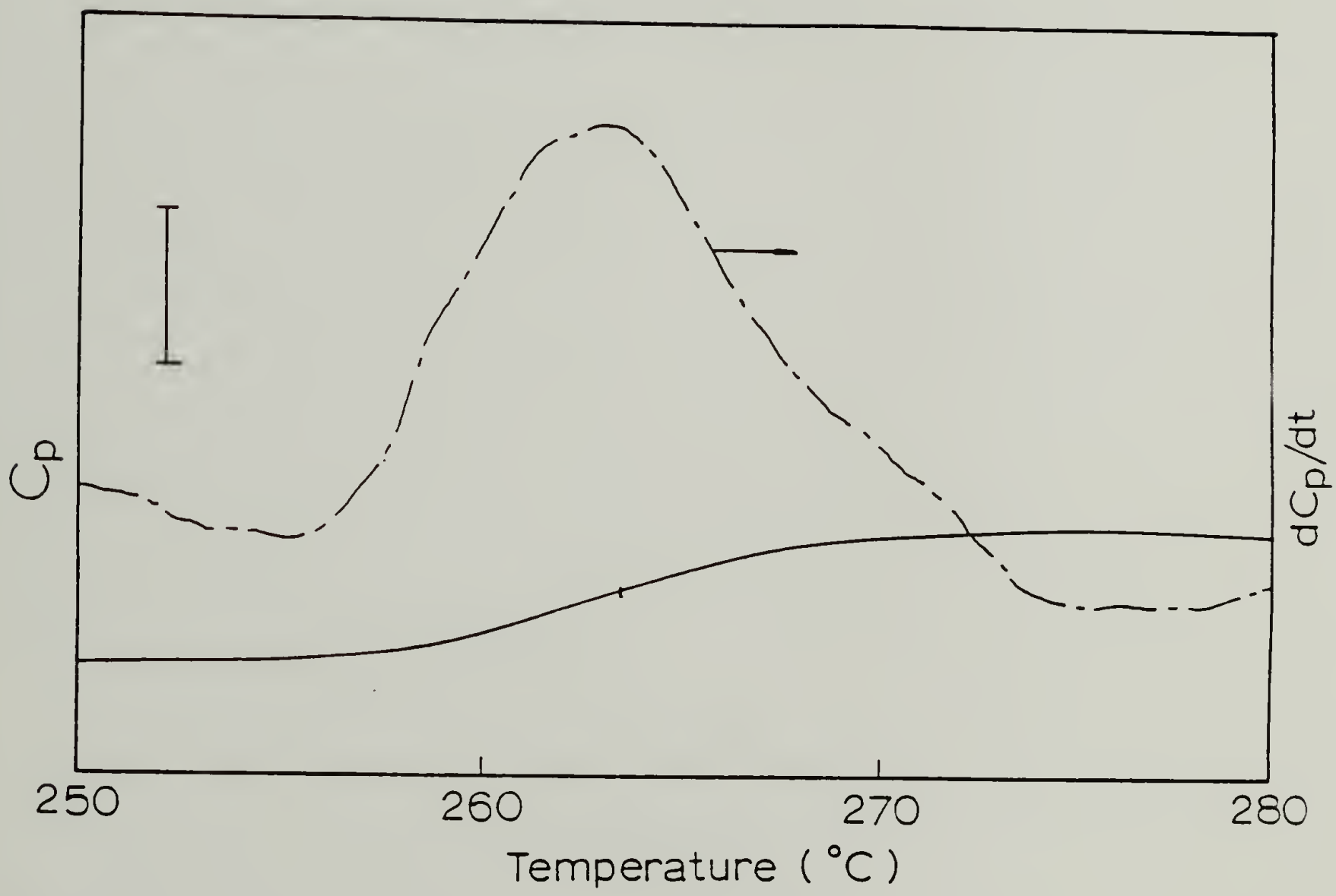

Figure 3.6. DSC thermogram for SPPO 54/75 (50/50 wt% blend)

displayed in Figure 3.5, and shows two T_g's for each component, thus reflecting clearly that the single T_g observed for the blend of SPPO 72/90 is due to a homogenization of the two blend constituents.

Figure 3.7 shows optical micrographs in which phase separation is observed at Δ wt% equal to or greater than 22.2. The kinetics of phase separation in blends depends on the viscosity of the medium and the thermodynamic driving force[9]. Thus, it is necessary to keep equal degrees of superheating for each blend in comparing the growth of the segregated domains. Although the phase boundary remains undetermined at present, it can be seen qualitatively that the domains of the phase separated blend become larger as Δ wt% increases. However, no evidence of phase separation in the blend at Δ wt% below 18.6 was observed.

Two techniques employed in the current study are considered to be supplementary based on the summary of results illustrated in Figure 3.8. However, it should be pointed out that two experimental probing techniques of miscibility reflect different length scales. That is, the DSC has a length scale of several hundreds angstroms, while the optical microscope has a maximum resolution down to about 0.2 μm.

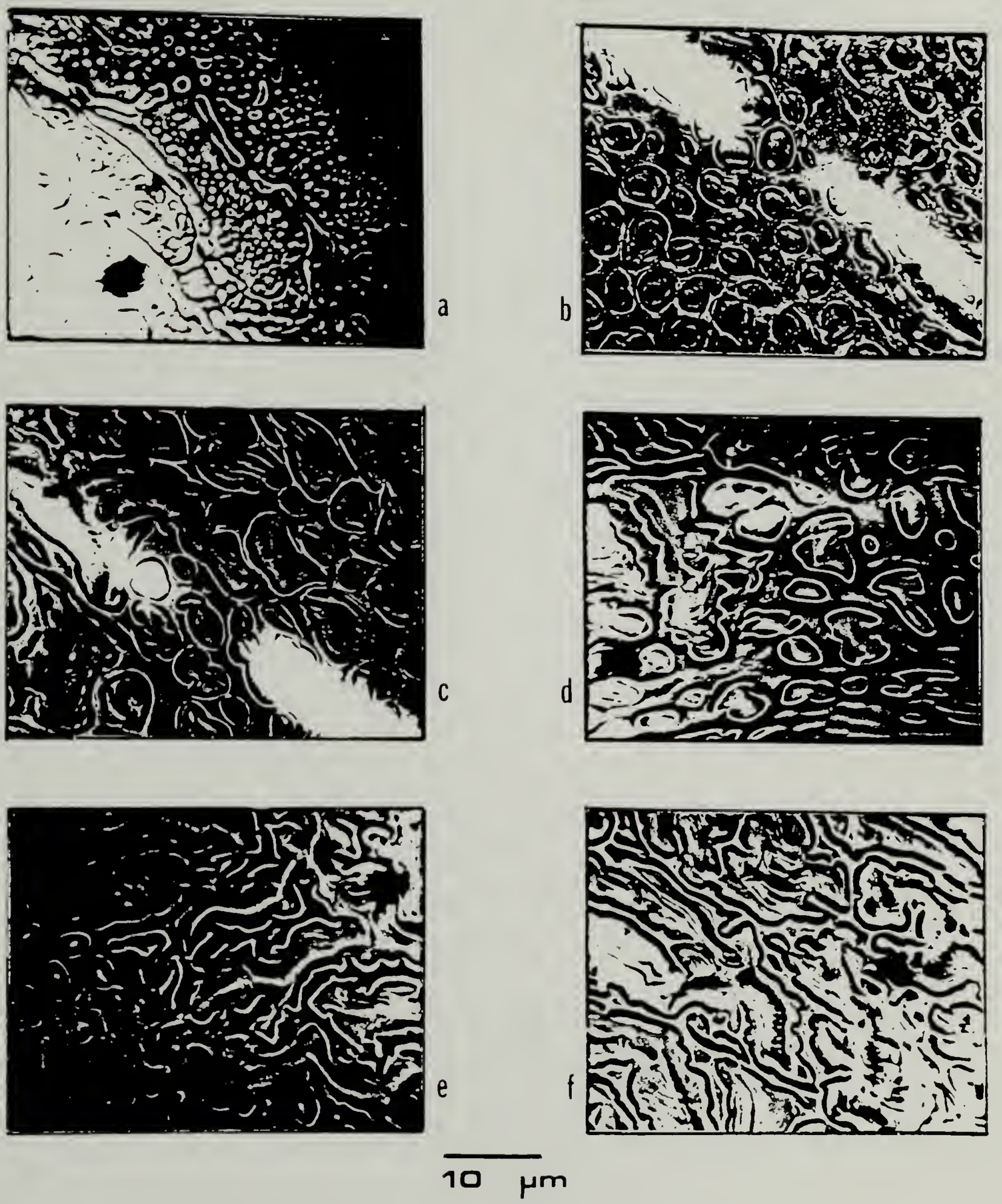

Figure 3.7. Optical micrographs for 50/50 wt% blends :

(a) SPPO 12/34; (b) SPPO 30/54; (c) SPPO 30/55;

(d) SPPO 12/39; (e) SPPO 47/75; (f) SPPO 12/44

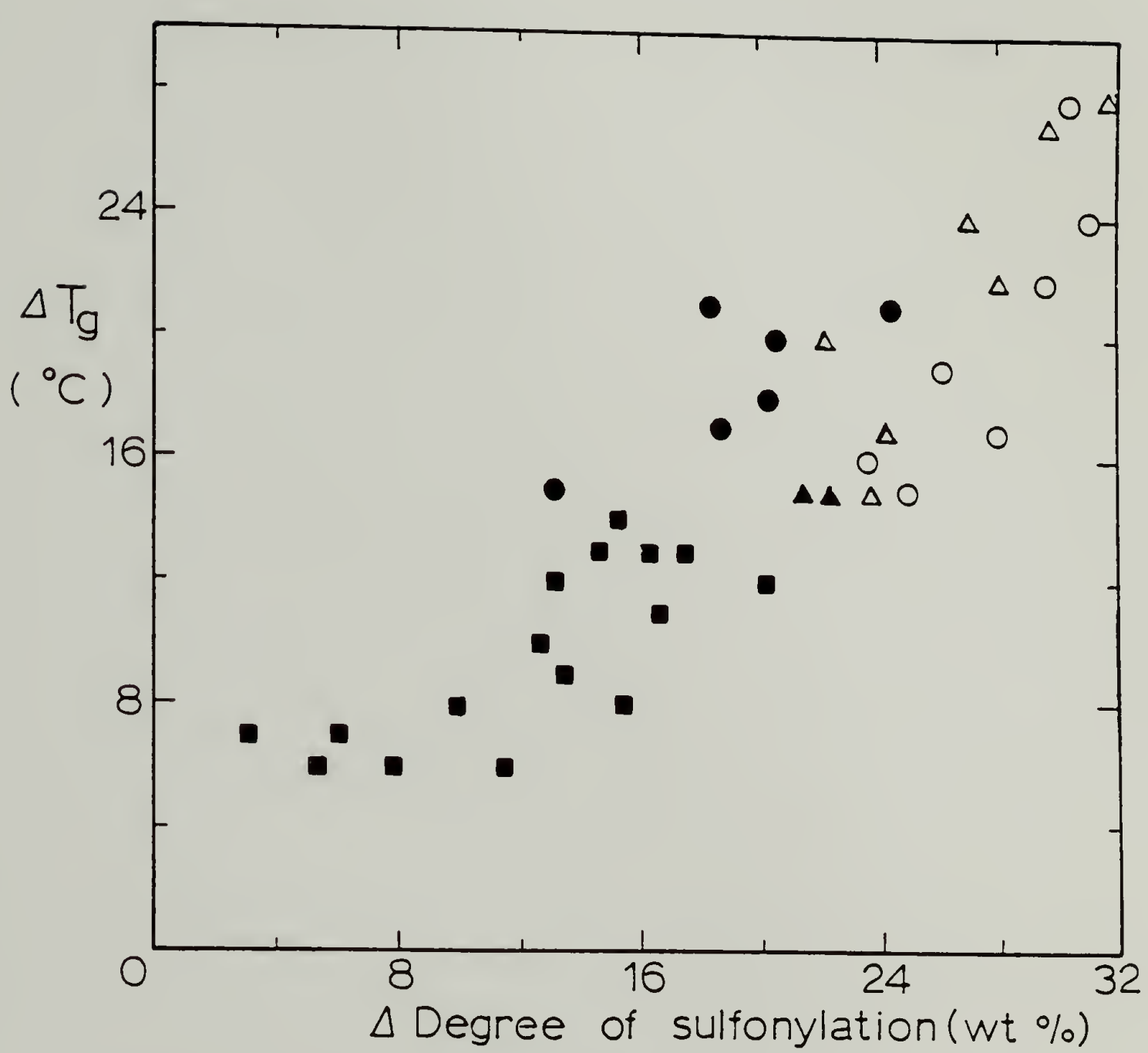

Figure 3.8 ΔT_g vs. Δ degree of sulfonylation. Filled and open symbols represent one phase and two phase systems, respectively. The data represented by triangles were obtained by DSC and optical microscopy. The data represented by circles were obtained by DSC only. The data represented by squares were obtained by optical microscopy only.

For a mixture of two copolymers which differ only in copolymer composition, i.e., A = C and B = D, in the blend system of $(A_{1-x}B_x)_{n_1}/(C_{1-y}D_y)_{n_2}$, Eqn. (1.14) reduces to :

$$\chi_{blend} = (x - y)^2 \chi_{CD} \qquad (3.1)$$

At a critical point one can write, from Eqn. (1.15) and Eqn. (3.1),

$$\frac{1}{2}(n_1^{-\frac{1}{2}} + n_2^{-\frac{1}{2}})^2 = (x - y)^2 \chi_{CD} \qquad (3.2)$$

Figure 3.9 shows an isothermal miscibility diagram of 50/50 wt% blends of SPPO copolymers. The critical composition difference $|x-y|_{crit}$ in the blend for phase separation varies from 0.20 at the lower degree of sulfonylation to 0.26 at the higher degree of sulfonylation.

Based on the Flory-Huggins lattice treatment of binary mixtures, Koningsveld[10] proposed an expression which takes into account the disparity between the relative sizes of the monomer units. This disparity gives rise to differing numbers of nearest-neighbor contacts, provided that the number of nearest-neighbor contacts is proportional to the interacting surface areas.

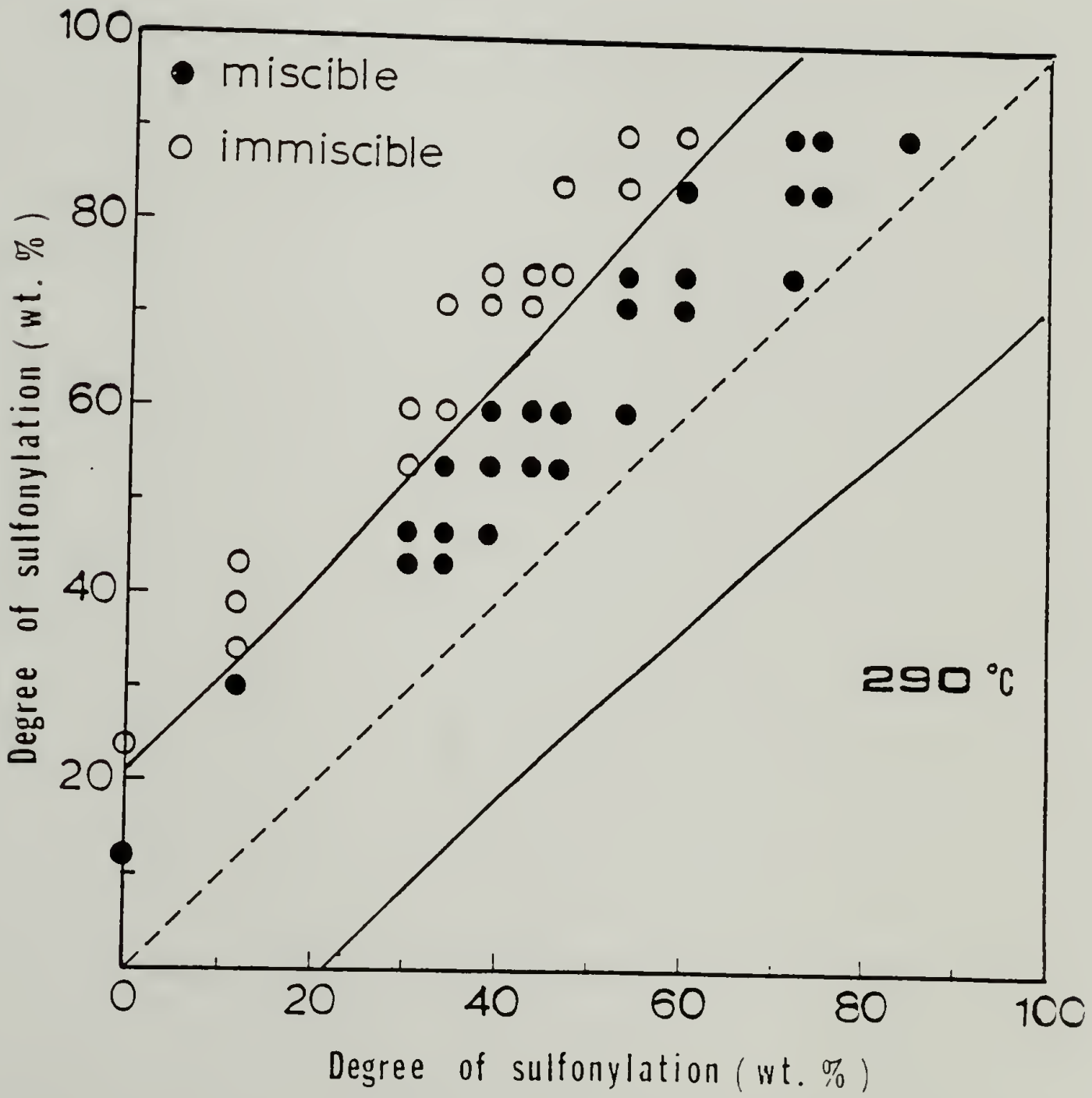

Figure 3.9. Isothermal miscibility diagram of 50/50 wt% blends of SPPO

In the case of blends of acrylic or methacrylic copolymers[4,6], the disparity of monomer size has been found to affect miscibility behavior significantly. As the content of a monomer of larger surface area increases, the critical composition difference increases, i.e., the respective copolymer blends tend to be much more miscible.

The phenylene oxide unit (C) and the sulfonylated phenylene oxide unit (D) in the present system have, from the calculation of Bondi's group contribution[11], surface areas of 68×10^{-9} cm^2/mole and 115×10^{-9} cm^2/mole, respectively, which are greatly different from each other. The slight increase in the critical difference in degree of sulfonylation for miscibility at higher degree of sulfonylation may be due to an increasing interacting surface area.

Table 3.1 shows $|x-y|_{crit}$ and the effective degree of polymerization, N, which is equal to the weight-average molar mass of the copolymer divided by the mass of PPO repeat unit. By introducing $|x-y|_{crit}$ and N into Eqn. (3.2) we determine χ_{CD}, the segmental interaction parameter between unsulfonylated and sulfonylated repeat units in the SPPO copolymer, to be 0.15-0.06 at 290°C. Figure 3.10 displays the composition (mean degree of sulfonylation) dependence of χ_{CD} which decreases with increasing degree of sulfonylation,

Table 3.1

Mean Degree of Sulfonylation Dependence of χ_{CD}

Mean Degree of Sulfonylation %	n	$\lvert x-y \rvert_{crit}$	$\chi_{CD,\ 290°C}$
10	330	0.20	0.15
20	360	0.21	0.13
30	390	0.22	0.11
50	470	0.24	0.07
70	590	0.26	0.05

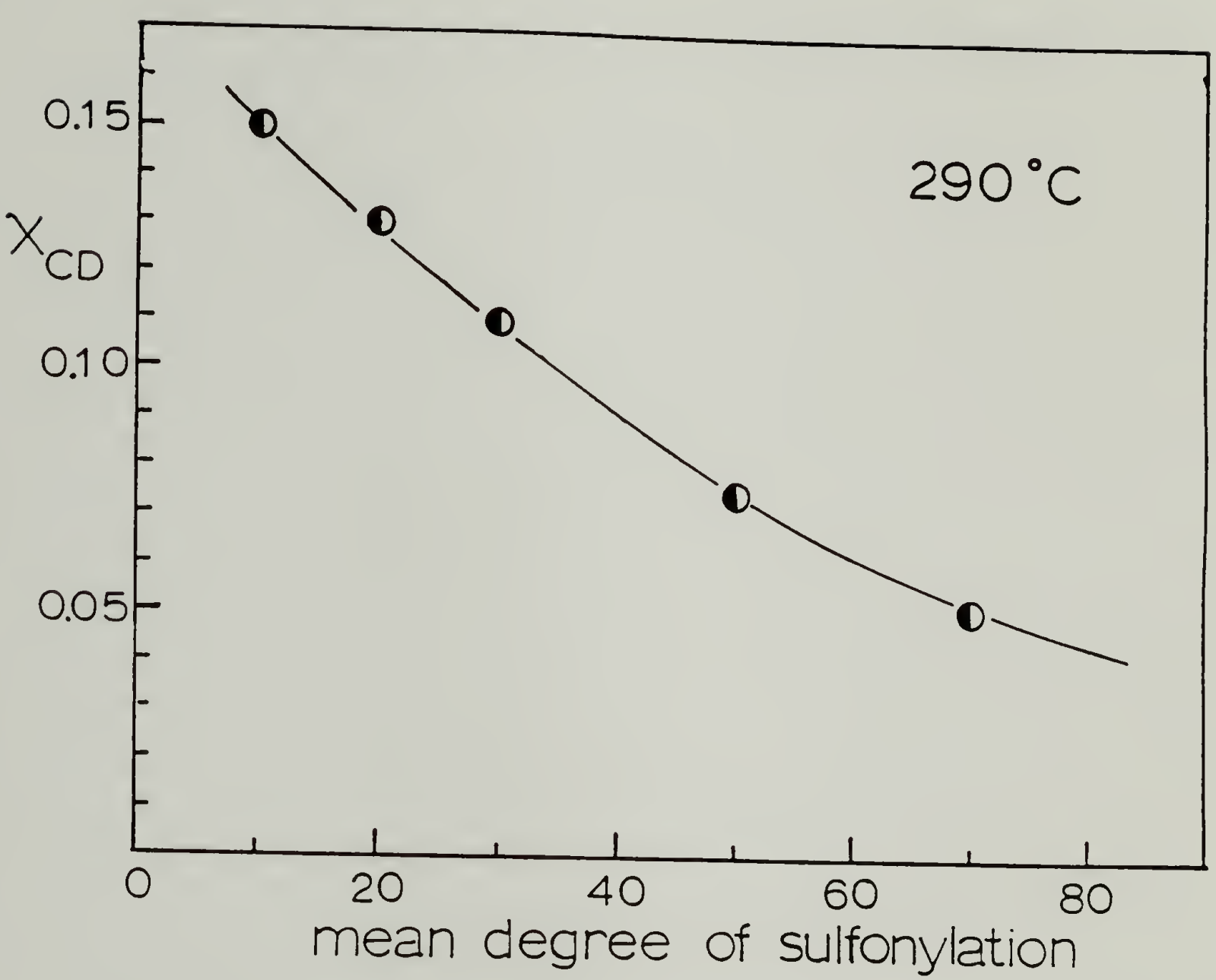

Figure 3.10. Mean degree of sulfonylation dependence of χ_{CD} at 290 °C

indicating that the van Laar type exchange interaction energy decreases with increasing degree of sulfonylation.

To determine the critical phenomena in the present system, sample annealing up to 360°C, above which significant degradation of polymers appears to occur, has been attempted. However, the phase separation of miscible blends or the homogenization of immiscible blends could not be induced by annealing, implying either that χ_{CD} is very temperature-insensitive or that phase boundary on the temperature plane is very stiff.

ii). Blends of Polystyrene with SPPO Copolymers

Blends of SPPO with the degree of sulfonylation equal to or less than 23.5 wt% were miscible with PS-115 using a miscibility criterion of a single, composition-dependent glass transition. Blends of PS-115/SPPO with the degree of sulfonylation of 30.4 wt% didn't show a single intermediate T_g over the whole range of blend compositions but exhibited a single T_g at the blend composition of 50/50 wt% and thus, are regarded as being miscible in this work.

In contrast, SPPO with the degree of sulfonylation equal to or greater than 34.0 wt% was found to be immiscible with PS-115. The two T_g values observed didn't correspond to those of the pure

components, indicating a separation into mixed phases. As will be discussed later, this partial miscibility increases as the degree of sulfonylation of SPPO approaches the critical degree of sulfonylation (31 wt%) for phase separation in these blends.

Figure 3.11 displays the DSC thermograms (normalized to the weight of the sample) of SPPO 12/PS-115 blends. Figure 3.12 shows the composition dependences of the T_g's of these blends and a comparison of the compositional variation of T_g to the thermodynamic or empirical expressions. Based on the entropy of mixing of two polymers and assuming temperature independent heat capacity increments, Couchman[12] derived the relation

$$\ln T_g = (W_1 \Delta C_{p_1} \ln T_{g_1} + W_2 \Delta C_{p_2} \ln T_{g_2}) / (W_1 \Delta C_{p_1} + W_2 \Delta C_{p_2}) \quad (3.3)$$

where W_1 and W_2 refer to the weight fractions of the blend constituents, T_{g_1} and T_{g_2} are the T_g's of the pure components and ΔC_{p_1} and ΔC_{p_2} are the heat capacity increments at T_g for each constituent.

Fox equation[13] is given by

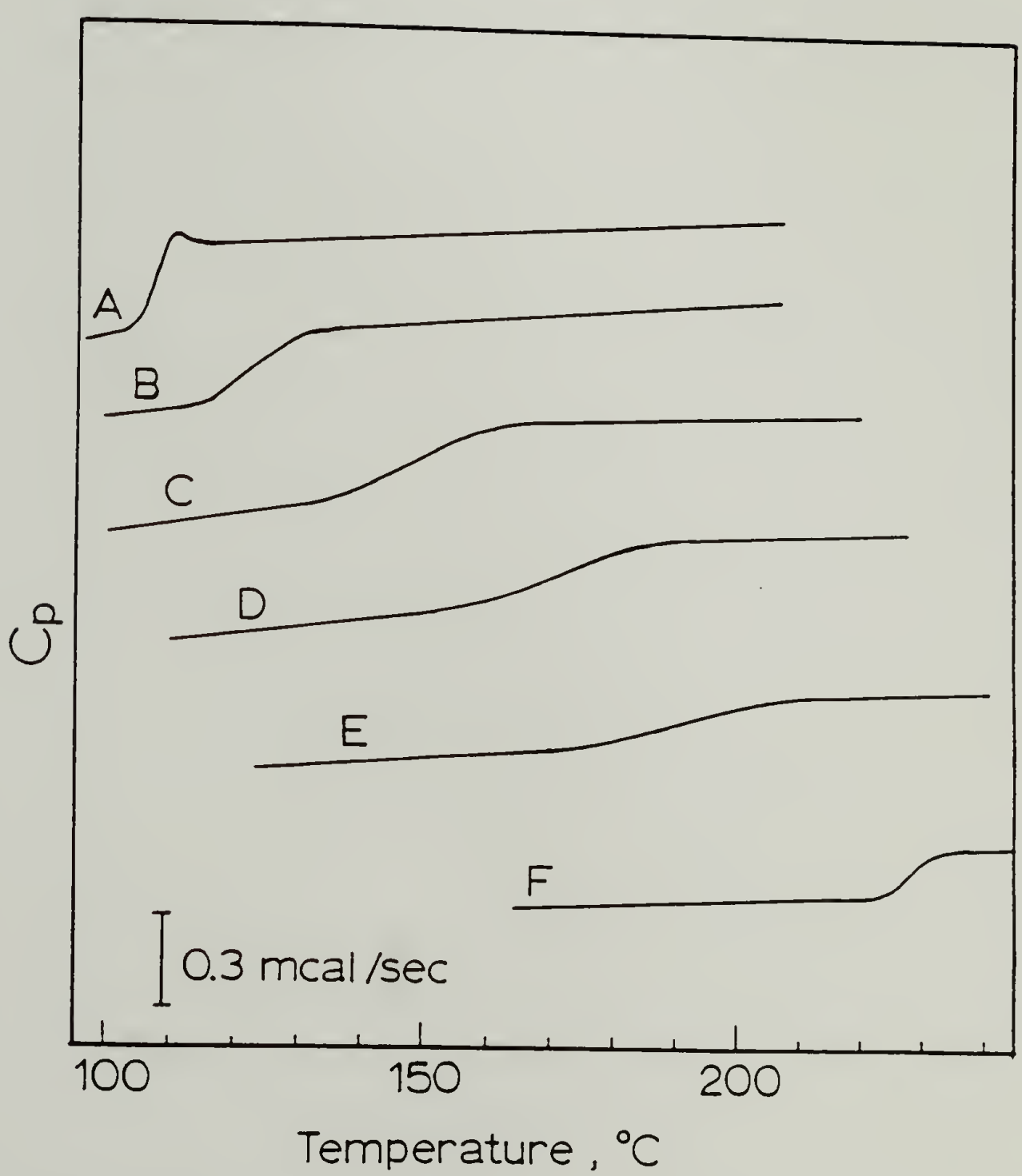

Figure 3.11. DSC thermograms of PS-115, SPPO 12 and blends :

(A) pure PS-115; (B) 25 wt% SPPO 12; (C) 50 wt% SPPO 12;

(D) 70 wt% SPPO 12; (E) 85 wt% SPPO 12; (F) pure SPPO 12

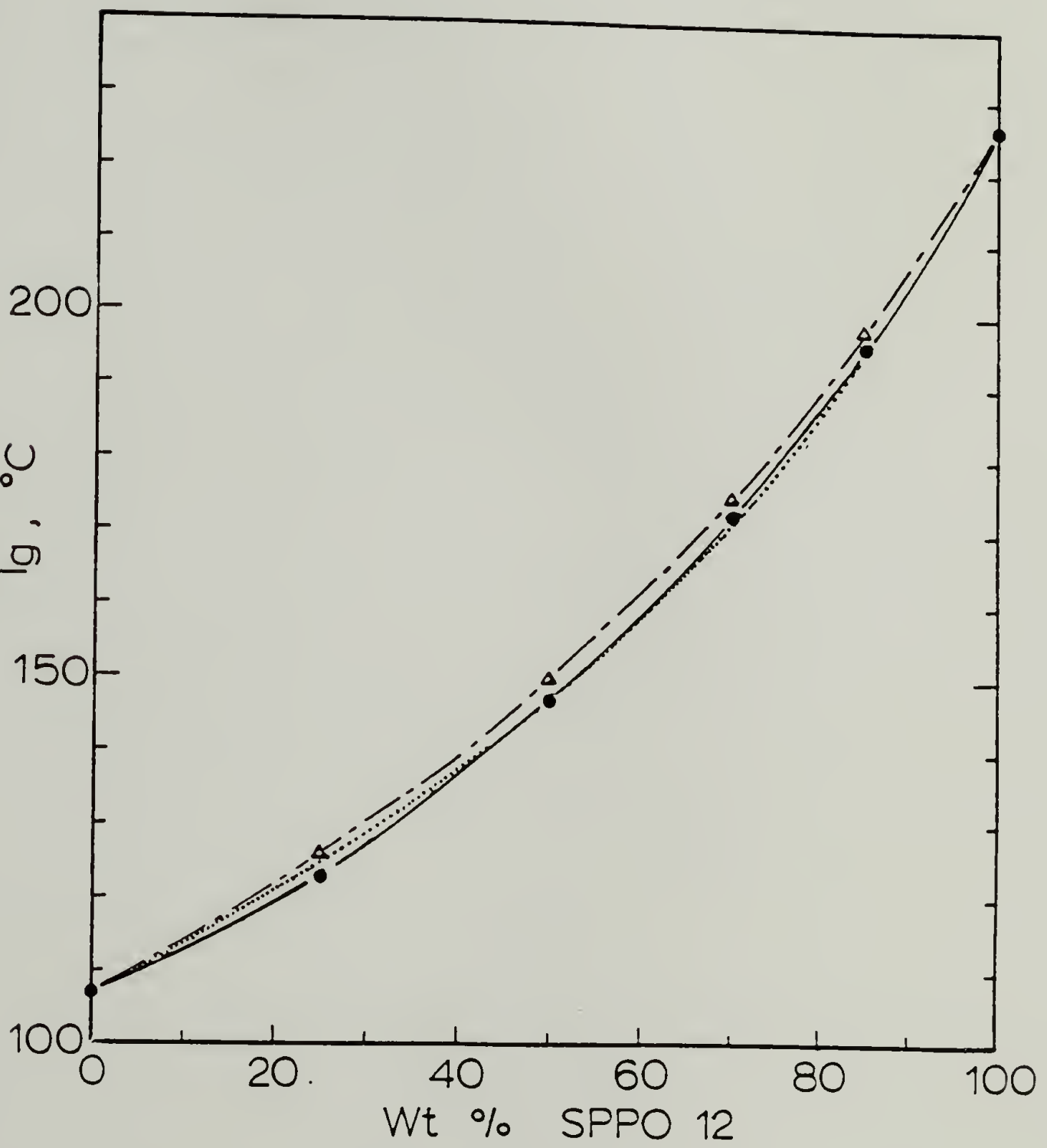

Figure 3.12. Dependence of T_g's on the weight fraction of SPPO 12 for the PS-115/SPPO 12 blends. Dashed lines represent the Couchman equation, and dotted lines represent the Fox equation with k=0.66.

$$(W_1 + kW_2)/T_g = W_1/T_{g_1} + kW_2/T_{g_2} \qquad (3.4)$$

The T_g values calculated using Couchman equation and Fox equation with k = 0.66 are in good agreement with the experimental values. The pertinent parameters used in the calculation are ΔC_p(PS) = 0.28 J/g.deg and ΔC_p(SPPO 12) = 0.18 J/g.deg.

Transition width of the blend, ΔT_g as defined by $2(T_g - T_g$, onset), is plotted as a function of the weight fraction of SPPO 12 in Figure 3.13. The ΔT_g's of the blends are much broader than those of the pure components as noted previously for the blend of polystyrene with PPO[14]. This feature may be due to local compositional fluctuation still present within the miscible blend. A maximum width of the glass transition region of the blends around 80 wt% of SPPO 12 can be ascribed to a much larger fluctuation in local composition resulting from a skewed phase diagram toward the low molecular weight component, SPPO 12, as discussed by Koningsveld[15]. The driving force for phase segregation will be maximum at the blend composition corresponding to the critical point, which is predicted to exist above the decomposition temperature of each constituent. These blends exhibit LCST behavior, as discussed later.

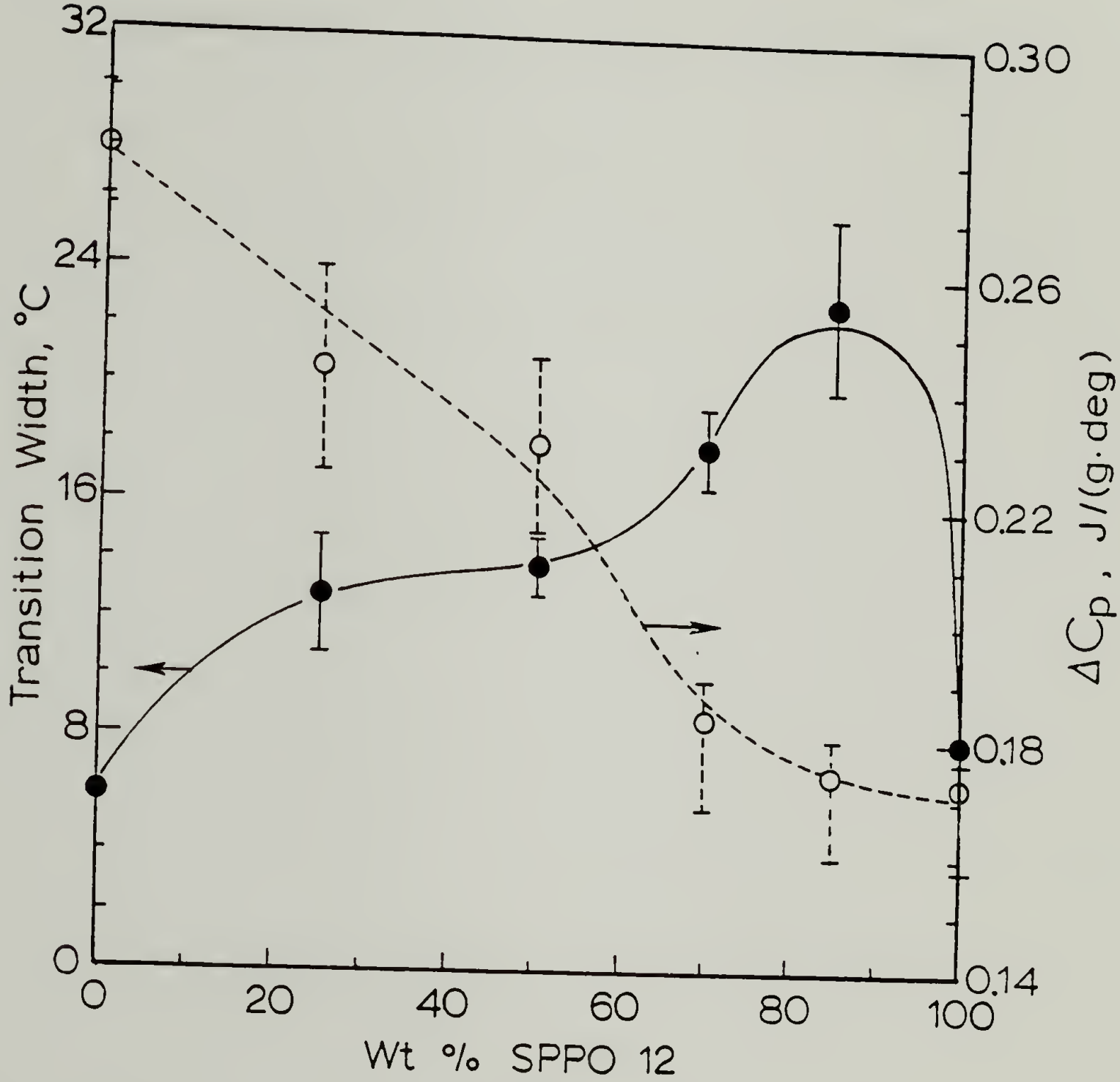

Figure 3.13. Width of the glass transition and ΔC_p's for the PS-115/ SPPO 12 blends as a function of blend composition

Taking the polydispersities in chain length into account, Koningsveld[16] derived an expression relating the composition at the critical point, i.e.,

$$\Phi_{2_C} = 1/[1 + (N_{w_2} a_1 / N_{w_1} a_2)^{\frac{1}{2}}] \qquad (3.5)$$

where $a_i = N_{z_i}/N_{w_i}$ and N_{w_i} and N_{z_i} refer to the degree of polymerization based on the weight average molecular weight and on the z-average molecular weight, respectively. The critical point in the current blends is calculated to be at 74 wt% of SPPO 12 by employing $N_{w_1} = 1150$, $a_1 = 1$, $N_{w_2} = 350$ and $N_{z_2} = 700$ (determined from GPC measurements). This calculation compares well with the observed maximum ΔT_g around 80 wt% of SPPO 12.

Figure 3.13 also shows the blend composition dependence of the transition intensity (ΔC_p) i.e., the specific heat increment at T_g. The ΔC_p's of the blends decrease sigmoidally or almost linearly with the addition of SPPO 12. The latter case follows the relation found for some miscible blends[17] such that

$$\Delta C_p = W_1 \Delta C_{p_1} + W_2 \Delta C_{p_2} \qquad (3.6)$$

In these blends of the type, $A_{n_1}/(C_{1-y}D_y)_{n_2}$, three segmental interaction parameters are involved and χ_{blend} is, according to the mean field treatment[18], given by

$$\chi_{blend} = (1 - y)\chi_{AC} + y\chi_{AD} - y(1 - y)\chi_{CD} \qquad (3.7)$$

At the critical condition, χ_{blend} equals χ_{blend}^{crit} given as follows :

$$\chi_{blend}^{crit} = \frac{1}{2}(n_1^{-\frac{1}{2}} + n_2^{-\frac{1}{2}})^2 \qquad (3.8)$$

The experimental results reflect that the critical degree of sulfonylation of SPPO above which the copolymers are immiscible with PS-115 is 31 wt% at 290°C. Here, we employ $\chi_{AC} = -0.043$, recently recalculated from the miscibility study[19] of blends of PPO with poly(o-chlorostyrene-co-p-chlorostyrene). (Maconnachie et al[20] reported, by the small angle neutron scattering study of blends of deuterated PPO with polystyrene, $\chi_{AC} = -0.033 \sim -0.021$ over a temperature range of 104 to 273°C). Thus, equating χ_{blend} with χ_{blend}^{crit} of 0.0035 and using χ_{CD} of 0.15, as determined in the first part of this chapter, χ_{AD}, the segmental interaction parameter between styrene and sulfonylated phenylene oxide unit, is determined

to be 0.20. It should be noted that the use of 50/50 wt% blends, rather than those compositions corresponding to the critical solution temperatures may induce some errors in the estimation of χ. However, it is particularly interesting that χ_{AD} and χ_{CD} are of similar values. Accordingly, phenylene oxide and styrene unit in this system may be considered as equivalent units, thus these blends may be represented as $A_{n_1}/(A'_{1-y}D_y)_{n_2}$.

Figure 3.14 displays transition width of 50/50 wt% blends of PS-115/SPPO as a function of the degree of sulfonylation. The data represent the transition widths of single T_g's in miscible blends, provided the degrees of sulfonylation are equal to or less than 30.4 wt%. The left extreme of the abscissa in Figure 3.14 represents the blend of PS with PPO. Transition widths of two phase blends with degrees of sulfonylation greater than 31 wt% are indicated for the PS rich phase and an inward shift in T_g indicates the difference between the T_g of the PS rich phase and that of pure PS. Some remarks should be mentioned here. First, the transition width of miscible blends slightly increases, reflecting a larger fluctuation in local composition, namely, an apparent decrease in the miscibility of the mixtures as the degree of sulfonylation increases. Second, the two phase blends form mixed phases and this partial miscibility decreases as the degree of sulfonylation deviates from the critical degree of sulfonylation, as expected. In addition, despite the fact that there

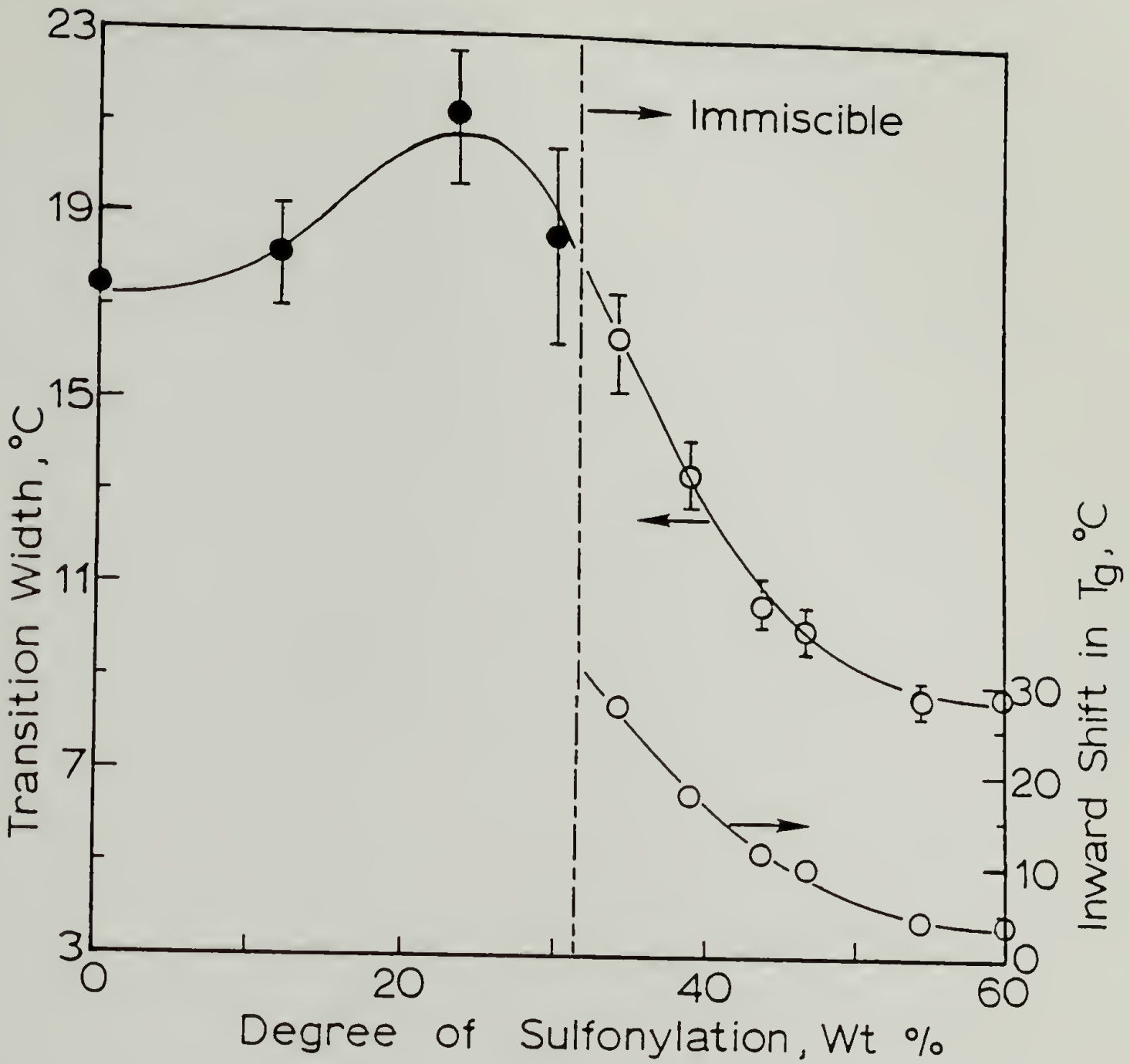

Figure 3.14. Width of the glass transition and inward shift in T_g for PS-115/SPPO blends vs. degree of sulfonylation. Widths and inward shifts of the two phase blends are indicated for the PS rich phase.

are no chemical constraint between the two constituents which may result in macrophase separation, the T_g of the PS rich phase in the blend of PS-115/SPPO with the degree of sulfonylation of 34 wt% shifts inward by 27°C. If we assume that the simple Fox equation[13] (with k = 1) in Eqn. (3.4) is valid to predict the T_g of the mixed phase, then the PS rich phase is composed of 75 wt% PS and 25 wt% SPPO. Third, as the degree of sulfonylation deviates from the critical degree of sulfonylation, the transition width decreases indicative of a smaller composition fluctuation resulting from decreased interphase mixing. Namely, the segregated phase region is much purer, as the degree of sulfonylation increases. In this context, employing the values of χ_{blend} which were calculated from Eqn. (3.7) and summarized in Table 3.2, one can get an initial slope of -1/3 from the log(transition width) - log(χ_{blend}) plot, as seen in Figure 3.15. It seems likely that the increased χ_{blend} which requires an increased van Laar type exchange interaction involved on mixing of the two constituents, makes the interphase mixing less significant, provided that the contribution of compressibility of the mixture involving SPPO with differing degrees of sulfonylation is assumed to be negligible at the sample annealing temperature of 290°C.

To investigate the critical phenomena of these blends, thermally induced phase separation study by using PS with varying

Table 3.2

Transition Width and Calculated χ_{blend} Values

Degree of Sulfonylation, wt%	Transition Width, °C	$\chi_{blend} \times 10^3$
30.4		-1.60
34.0	17.0	5.96*
38.8	13.5	15.67
43.5	10.7	25.80
46.6	10.0	32.90
54.1	9.0	51.20
60.0	9.0	66.80

* It is to be noted that $\chi_{blend}^{crit} = 3.50 \times 10^{-3}$

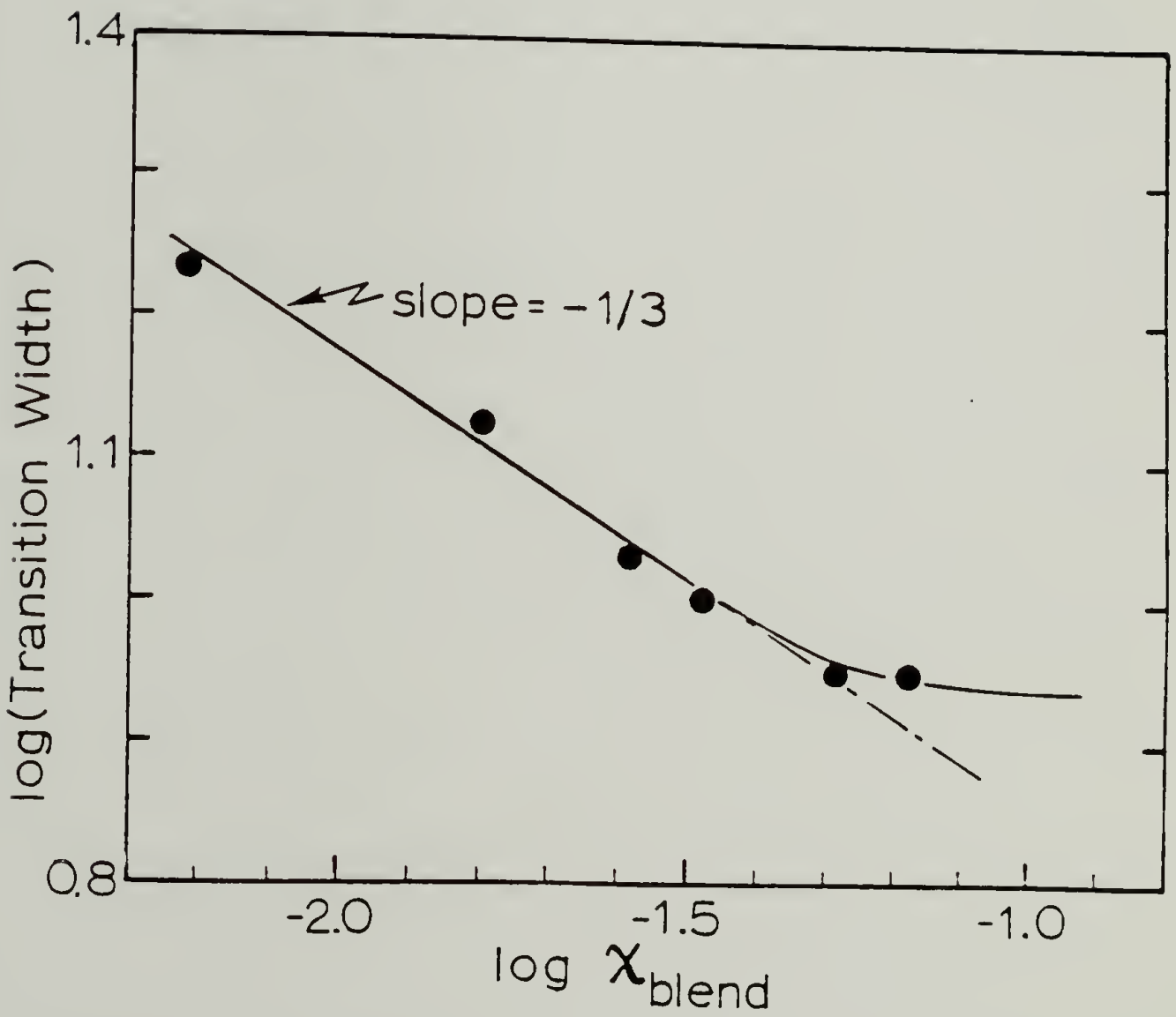

Figure 3.15. Width of the glass transition for PS-115/SPPO blends vs. χ_{blend}

molecular weights was carried out. Figure 3.16 shows the DSC thermograms for 40/60 wt% of PS-13 (and PS-68)/SPPO 34 blends. The samples annealed at lower temperature show a single T_g. However, at higher temperatures they exhibit two distinct T_g's indicative of a separation into mixed phases. From a series of DSC studies the phase diagram seen in Figure 3.17 was constructed, which represents the existence of an LCST behavior.

The equation of state theory[21] and the lattice fluid theory[22] predict that polymer-polymer mixtures which are miscible at lower temperatures tend to exhibit phase separation at higher temperatures in contrast to the predictions of the classical Flory-Huggins theory[23]. For binary mixtures to be miscible the second derivative of the free energy of mixing (at fixed temperature and pressure) which is composed of incompressible and compressible contributions should satisfy the relation[24]

$$\partial^2 G/\partial C^2 - \nu\beta(\partial^2 G/\partial C \partial \nu)^2 > 0 \qquad (3.9)$$

where G, C, ν and β refer to the molar Gibbs free energy, concentration, specific volume and the compressibility of the mixture, respectively. The second term in Eqn. (3.9) is always negative, thus giving an unfavorable effect on mixing. Since β increases with temperature, this term becomes more pronounced at

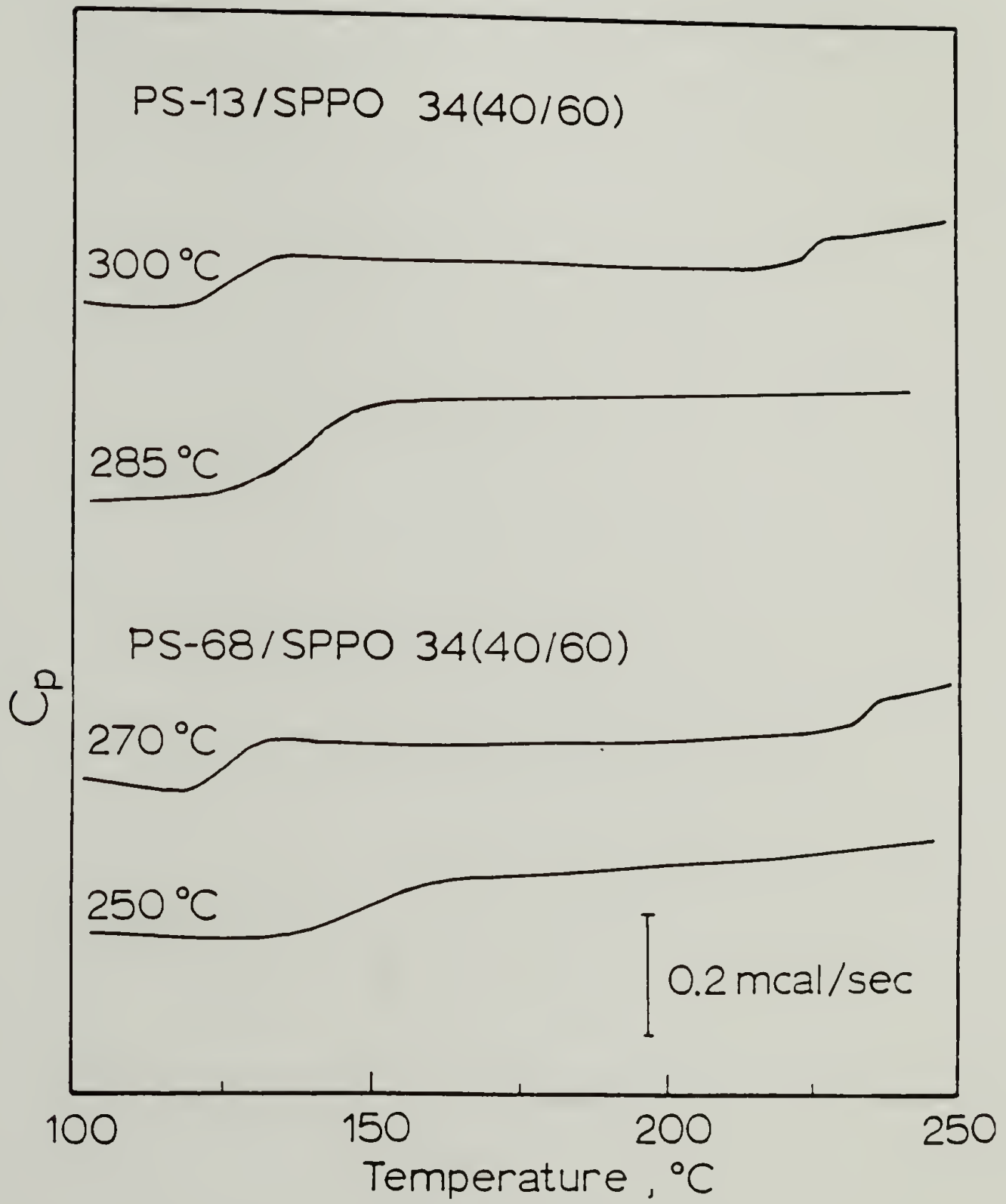

Figure 3.16. DSC thermograms of blends of SPPO 34 and PS of different molecular weights annealed at the indicated temperatures

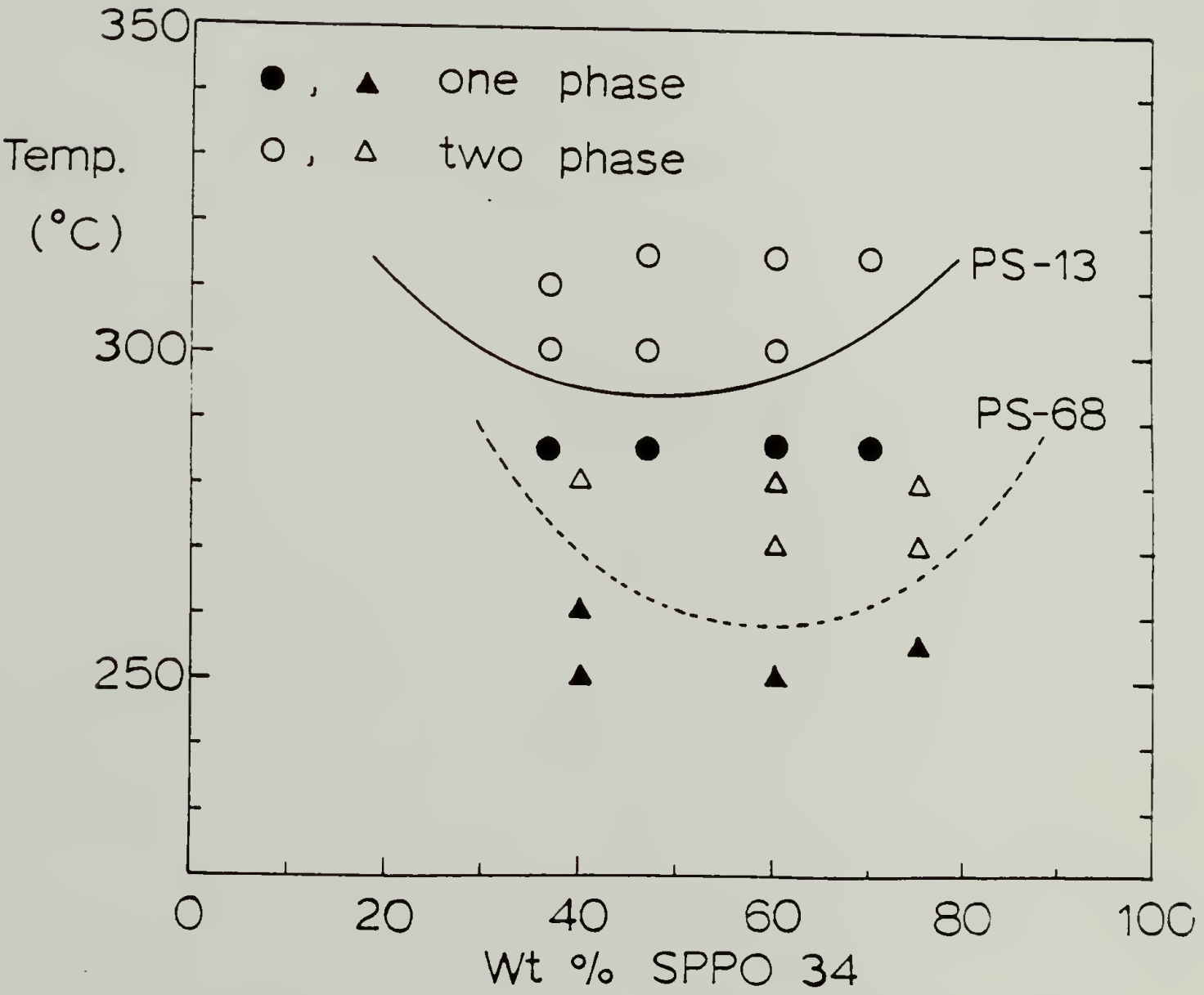

Figure 3.17. Phase diagram for blends of PS/SPPO 34

higher temperature, thus resulting in the destabilization of the mixture at high temperature. In this system a weak intermolecular interaction (which is directionally dependent in nature[25]) between PS and PPO segments is also involved. Thus, at higher temperature this interaction will be diluted by randomization by which the combinatorial entropy of mixing will be regained more or less. It should be noted that this orientational effect was neglected in the original equation of state theory. However, the unfavorable compressibility contributions appear more dominant than the entropy regain, thus explaining the occurence of phase separation at elevated temperature.

REFERENCES

1. R.L. Scott, J. Polym. Sci., 9, 423 (1952).
2. V. Landi, Rubber Chem. Technology, 45, 222 (1972).
3. G.M. Bartenev, G.S. Kongarov, Rubber Chem. Technology, 36, 668 (1963).
4. F. Kollinsky, G. Markert, Makromol. Chem., 121, 117 (1969).
5. E. Jenckel, H.U. Herwig, Kolloid-Z., 148, 57 (1956).
6. D.I. Livingston, R.L. Rongone, Proc. Int. Rubber Conf., 5th, p. 337 (1968).
7. G.E. Molau, J. Polym. Sci., Polym. Lett. Ed., 3, 1007 (1965).
8. H. Ueda, F.E. Karasz, Macromolecules, 18, 2719 (1985).
9. D.R. Paul, S. Newman (eds.), Polymer Blends, Vol. I, Chapter 4, Academic Press, New York (1978).
10. R. Koningsveld, L. Kleintjens, Macromolecules, 18, 243 (1985).
11. A. Bondi, J. Phys. Chem., 68(2), 441 (1964).
12. P.R. Couchman, Macromolecules, 11, 6 (1978).
13. T.G. Fox, Bull. Amer. Phy. Soc., 1, 123 (1956).
14. J.R. Fried, F.E. Karasz, W.J. MacKnight, Macromolecules, 11, 150 (1978).
15. R. Koningsveld, Chem. Z., 26, 263(1972).
16. R. Koningsveld, a lecture note on " Polymer Phase Diagram" held in Univ. of Mass., Amherst, September, 1985.
17. C.L. Ryan, Ph.D. Thesis, University of Massachusetts, 1979.
18. G. ten Brinke, F.E. Karasz, W.J. MacKnight, Macromolecules, 16,

1827 (1983).

19. G. ten Brinke, E. Rubinstein, F. E. Karasz, W.J. MacKnight, R. Vukovic, J. Appl. Phys., 56 (9), 2440 (1984).

20. A. Maconnachie, R.P. Kambour, D.M. White, S. Rostami, D.J. Walsh, Macromolecules, 17, 2645 (1984).

21. P.J. Flory, R. Orwell, A. Vrij, J. Amer. Chem. Soc., 86, 3507 (1964).

22. I.C. Sanchez, R.H. Lacombe, J. Phys. Chem., 80, 2352 (1976).

23. P.J. Flory, Principles of Polymer Chemistry, Cornell University : Ithaca, NY, 1953.

24. K.Solc (ed.), Polymer Compatibility and Incompatibility : Principles and Practice, MMI Press, 1982, p. 59.

25. G. ten Brinke, F.E. Karasz, Macromolecules, 17, 815 (1984).

CHAPTER IV

MONOMER SEQUENCE DISTRIBUTIONS IN POLY(STYRENE-CO-ACRYLONITRILE)

A microstructure of copolymer, more specifically, a comonomer sequence distribution is known to affect miscibility behavior by varying intrachain interactions. A model to take into account that effect on the miscibility behavior has been proposed by Balazs *et al*[1].

styrene[1]-acrylonitrile[2] (SAN) copolymers, unless special processes are employed, tend to have an alternating sequences during copolymerization because a product of the monomer reactivity ratio, $r_1 r_2$, is much smaller than unity ($r_1 = 0.52$, $r_2 = 0.03$)[2]. Accordingly, studies of comonomer sequence distribution in SAN copolymers employed in this work were carried out by dielectric relaxation and T_g measurements to see if these copolymers are of quite random in nature, and are presented in this chapter.

A comparison of experimentally determined dipole moments with those calculated on the basis of the rotational isomeric state

model[3] can provide information on the microstructures of vinyl polymers or copolymers such as the degree of stereoregularity, tacticity or monomer sequence distribution[4-8]. The dielectric properties of the copolymers obtained by frequency plane measurements are correlated with considerations of dyad distributions calculated from monomer reactivity ratios, which allows us to deduce information on intra- and intermolecular interaction in copolymers[9]. T_g measurements are interpreted on the basis of an expression proposed by Johnston[10] which considers the effect of monomer sequence distribution on the T_g of copolymers.

A. Experimental Section

The SAN copolymers (SAN 5 - SAN 48) were obtained from Dow Chemical Co., courtesy of Dr. Sue McKinley; SAN 76 was supplied by Du Pont Co., Courtesy of Dr. R. Saxton. Polymer compositions were determined by nitrogen analysis.

Molecular weights and densities of molded films were determined as described in Chapter II. The molecular weight of SAN 76 could not be measured because of its insolubility in THF. The inherent viscosity of SAN 76 at the concentration of 0.5 g/dl was 0.63 dl/g in r-butyrolactone at 35°C. T_g measurements were performed

similarly as described in Chapter II. Samples of monodisperse polystyrene (Polymer Laboratories, $\bar{M}w$ = 115,000) and samples of polyacrylonitrile (Polysciences, Inc.) were also subjected to T_g measurements. All characterization details are listed in Table 4.1.

Dielectric measurements for the SAN copolymer samples, which were obtained by compression molding into films, were carried out isothermally at 56 discrete frequencies in the range of 20 Hz to 100 KHz with a General Radio model 1689M RLC Digibridge. Samples approximately 0.3 mm thick were employed with an active electrode cell diameter of 3.3 cm. The temperature of the sample assembly was maintained within ±0.2°C with a thermocouple in contact with the sample disc in the Polymer Laboratories DETA head. At least 1 hr was required for the temperature to reach equilibrium between measurements. Temperature scan modes at 1, 10, 50 KHz over a temperature range from -155 to 170°C were also used. The temperature was raised at a rate of 2.0°C/min.

B. Results and Discussion

Figure 4.1 and 4.2 display ε' and ε'' for SAN 32 on the frequency plane, respectively; Figure 4.3 shows the Argand diagram (Cole-Cole plot) for SAN 32. Good superposition over a range of

Table 4.1

Compositions and Properties of Poly(styrene-co-acrylonitrile)

Sample	AN Mole %	AN Wt %	$\bar{\bar{M}}n \times 10^{-5}$	$\bar{\bar{M}}w \times 10^{-5}$	T_g (°C)
SAN 5	11.5	5.4	1.18	3.34	109
SAN 18	33.4	18.0	1.24	2.10	111
SAN 21	38.1	21.2	0.92	1.59	113.7
SAN 26	44.8	26.2	1.34	2.23	112.5
SAN 32	52.0	32.1	1.56	2.80	111.6
SAN 48	67.6	47.7	1.09	2.28	113.7
SAN 76	86.0	76.0	a)		108.0

a) see text.

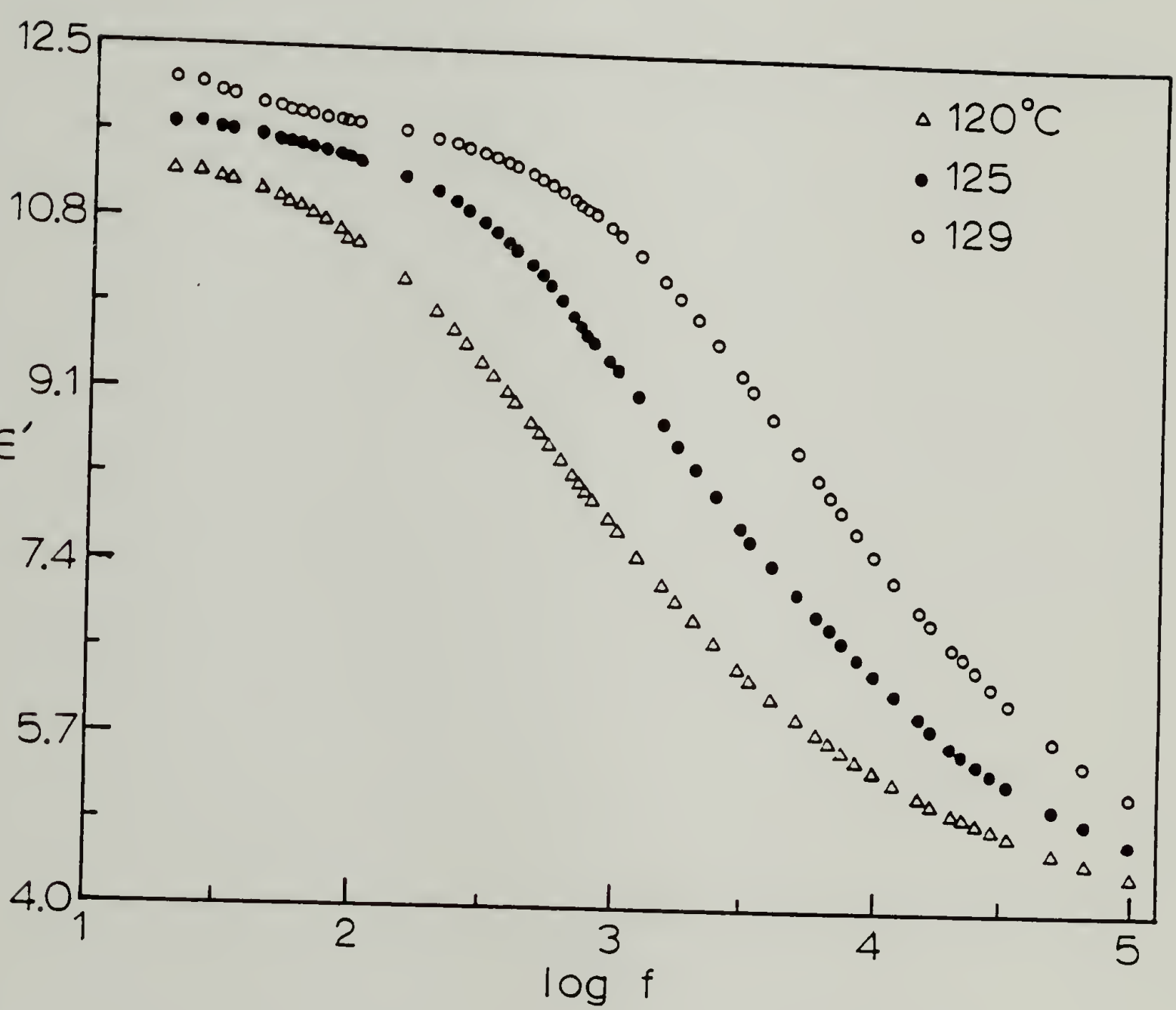

Figure 4.1. Frequency dependence of dielectric constant, ε', for SAN 32

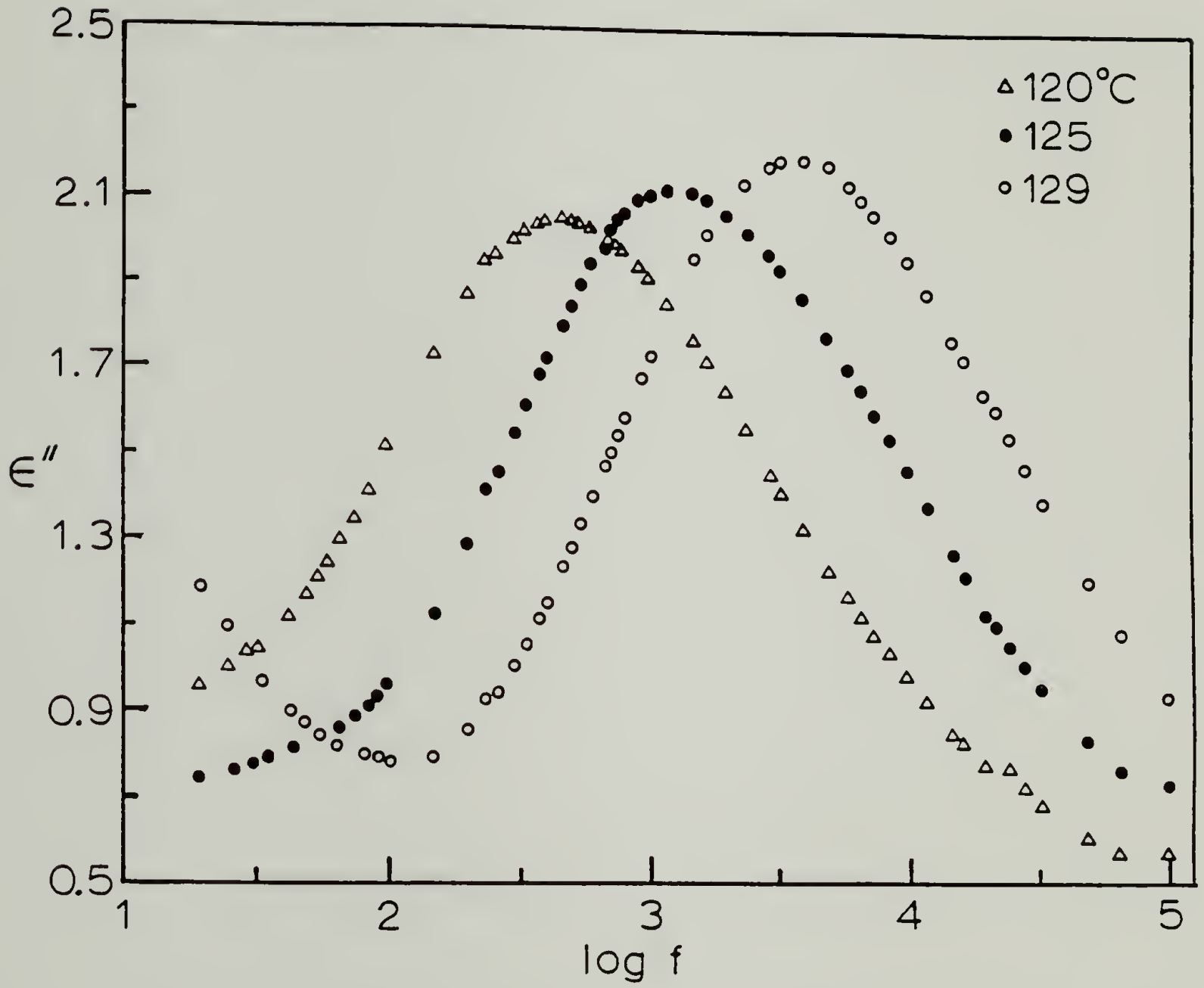

Figure 4.2. Frequency dependence of dielectric loss factor, ε",
for SAN 32

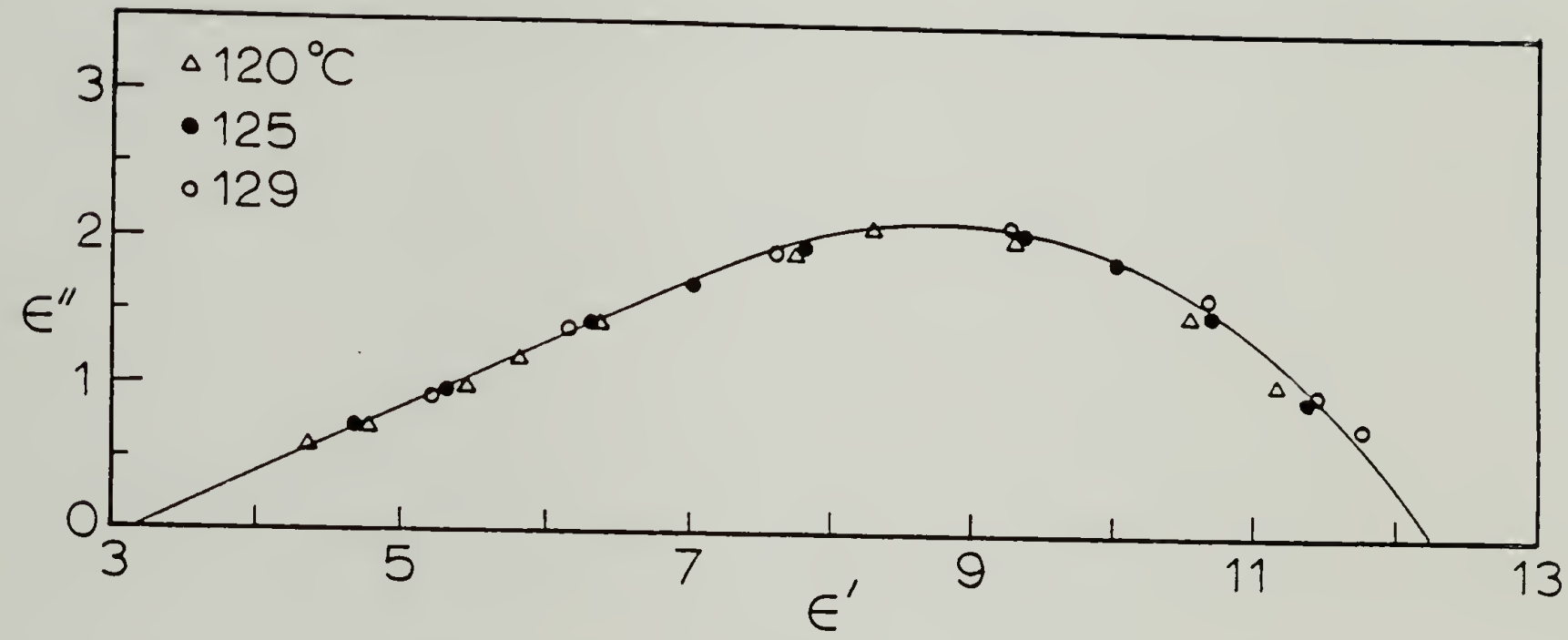

Figure 4.3. Argand diagram for SAN 32 in the α relaxation region

temperatures is observed. The limiting low frequency (ε_R) and high frequency (ε_u) dielectric constants were obtained from Figure 4.3.

Considering only long-range dipolar interactions, Onsager[11] derived the relation which predicts the effective dipole moments per repeat unit (μ_e) :

$$\mu_e^2 = [9kT(2\varepsilon_R + \varepsilon_u)(\varepsilon_R - \varepsilon_u)]/[4\pi N\varepsilon_R(\varepsilon_u + 2)^2] \qquad (4.1)$$

where k is the Boltzman constant, T is the absolute temperature, and N is the number of monomer units per unit volume which is calculated by

$$N = A\rho/(X_1M_1 + X_2M_2) \qquad (4.2)$$

where A is Avogadro's number, X_i is the mole fraction and M_i is the comonomer repeat unit molecular weight. The room temperature density values (ρ), as displayed in Figure 4.4, and a temperature of 400K were employed throughout all calculations.

The dielectric relaxation strength, $\varepsilon_R - \varepsilon_u$, and μ_e^2 are listed in Table 4.2. Figure 4.5 shows the dipole moments of the copolymers as a function of composition. Data shown by open circles

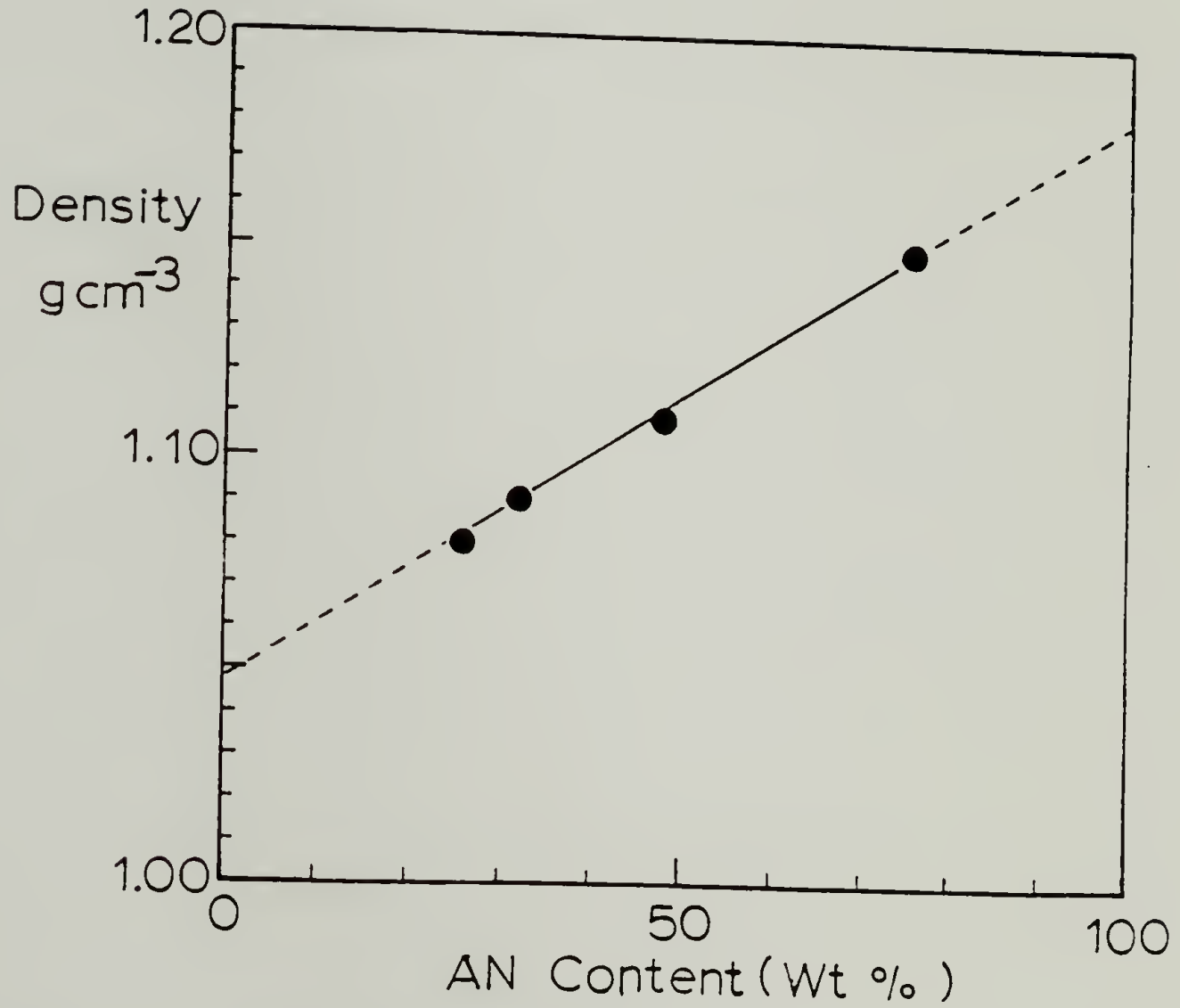

Figure 4.4. Density of copolymers as a function of AN content

Table 4.2

Dielectric Parameters for Poly(styrene-co-acrylonitrile)

Sample	$\varepsilon_R - \varepsilon_u$	μe^2	g	α	$\Delta H/\Delta L$	y	Width (Decades in Frequency) 0.5	0.75
SAN 5	1.45	0.85	0.62	0.42	1.42	0.64	2.18	1.36
SAN 18	3.75	1.96	0.52	0.34	1.30	0.52	2.30	1.40
SAN 21	4.85	2.15	0.50	0.36	1.38	0.50	2.14	1.30
SAN 26	6.15	2.85	0.56	0.32	1.24	0.56	2.24	1.43
SAN 32	9.10	3.55	0.61	0.30	1.24	0.62	2.24	1.37
SAN 48	9.10	3.40	0.45	0.31	1.45	0.30	2.45	1.44
SAN 76	19.9	5.61	0.58	0.40	-	0.55	-	2.04

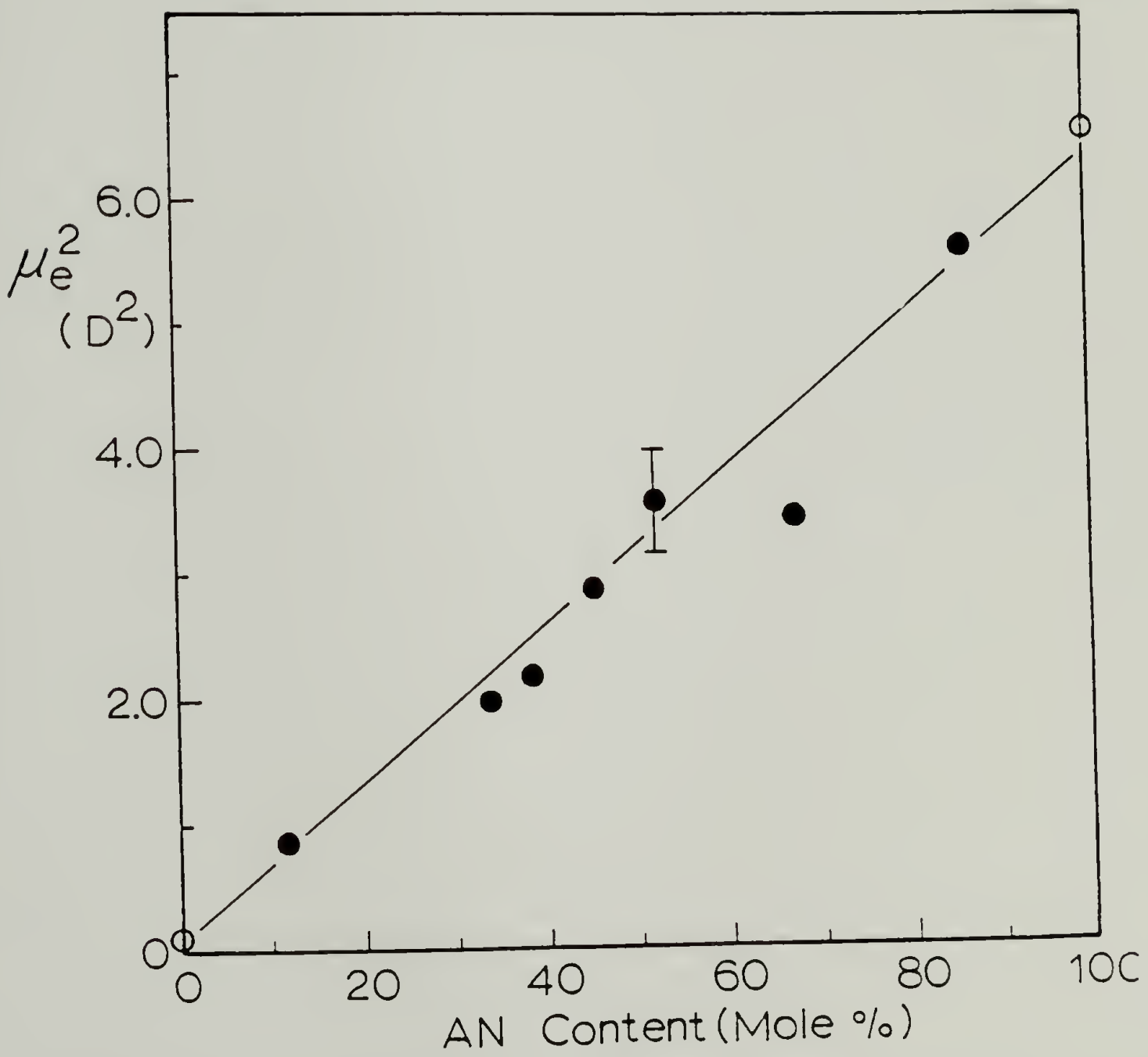

Figure 4.5. Effective dipole moments of copolymers

were obtained from refs. 17 and 18. It can be seen that SAN 48 exhibits a somewhat lower dipole moment; possible explanations will be discussed later.

Kirkwood-Frohlich [12] introduced the orientation correlation function, g, which takes into account short-range intrachain interactions between a reference molecule and its nearest neighbors. g is defined by

$$g = \mu_e^2/\mu_o^2 \tag{4.3}$$

where μ_o^2 is the square of the dipole moment of an isolated monomer unit. For copolymers

$$\mu_o^2 = X_1(\mu_{1,0})^2 + X_2(\mu_{2,0})^2 \tag{4.4}$$

where $\mu_{1,0}$ and $\mu_{2,0}$ are the dipole moments of model compounds 1 and 2, respectively. $\mu_{1,0} = 0.36D$[13] (dipole moment of toluene) and $\mu_{2,0} = 3.34D$[13] (dipole moment of propionitrile) were used in the calculation. The g values thus obtained are plotted as a function of AN content in Figure 4.6 and are observed to increase slightly with decreased AN content because of dilution of the nitrile group through copolymerization which results in reduced barriers to internal

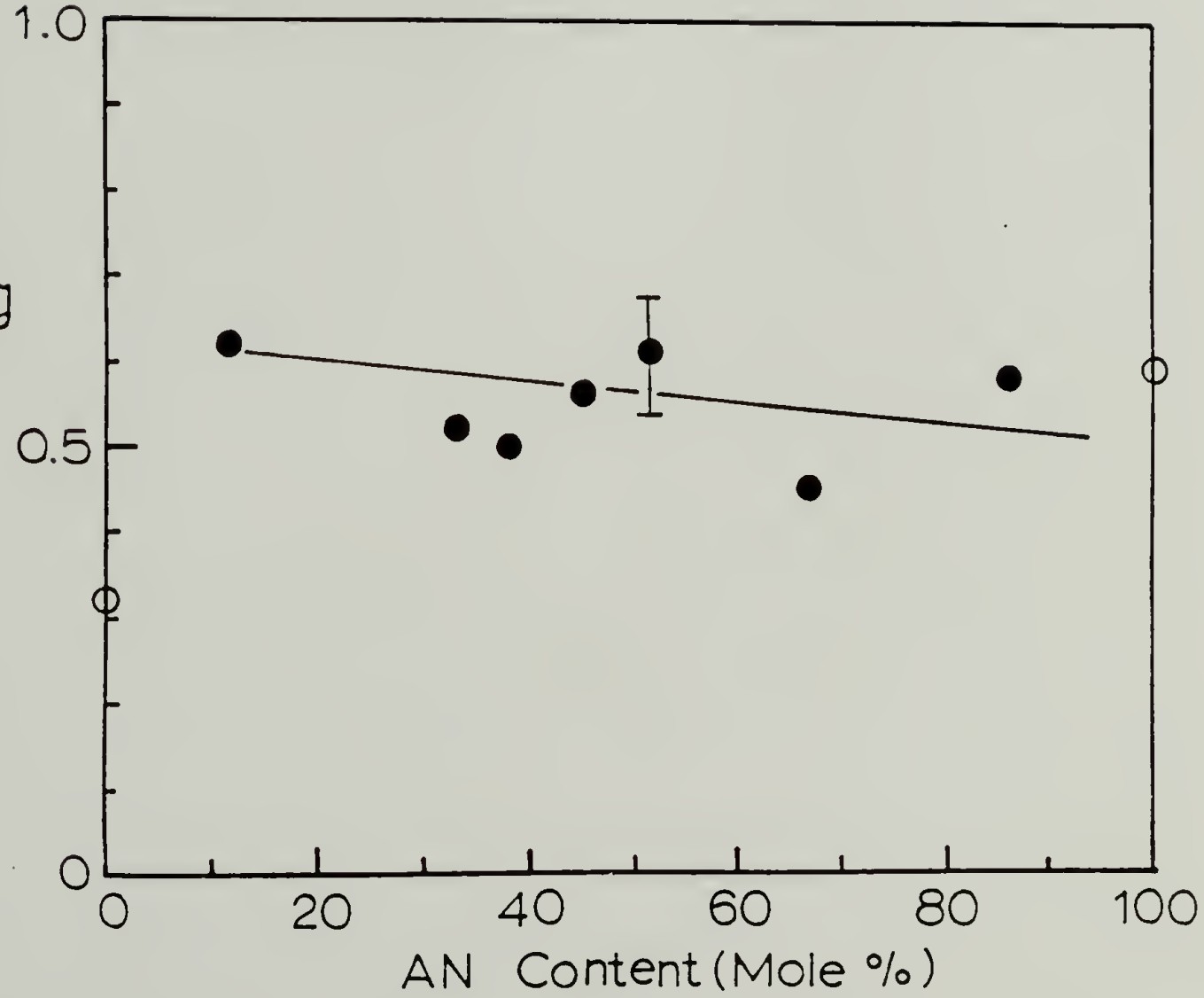

Figure 4.6. Composition dependence of the correlation parameter, g, for SAN copolymers

rotation. Nevertheless, the hindrance to internal rotation appears to be not much different for all the copolymers.

$(\varepsilon_R - \varepsilon_u)$, which is a measure of the orientation polarization, can be calculated from the area under an ε'' versus $1/T$ curve according to the relation[14]

$$(\varepsilon_R - \varepsilon_u) = (2E/\pi R)\int_{-\infty}^{\infty} \varepsilon'' \, d(1/T) \qquad (4.5)$$

where E is the activation energy. For SAN 76 the variations of ε'' with temperature at three frequencies are shown in Figure 4.7, in which two relaxation regions are observed similarly to the results of Cook et al[15] for SAN copolymers with 25% AN content. The high temperature α process is related to the large scale Brownian motion of the dipoles. The lower temperature β process around -25°C is due to limited motions of dipoles in the glassy state. Due to the presence of DC conductivity effects[14] in the data at lower frequencies, the data at 50 KHz were used in the calculation. The areas under the ε'' vs $1/T$ plots were determined after symmetric extrapolation of the loss peaks, as seen in Figure 4.8. By using the activation energy (E = 80 kcal/mole) calculated from the slope of the linear portions of Arrhenius plots, $(\varepsilon_R - \varepsilon_u)$ was calculated to be 20.7, which is consistent with the value obtained from the Argand diagram for SAN 76.

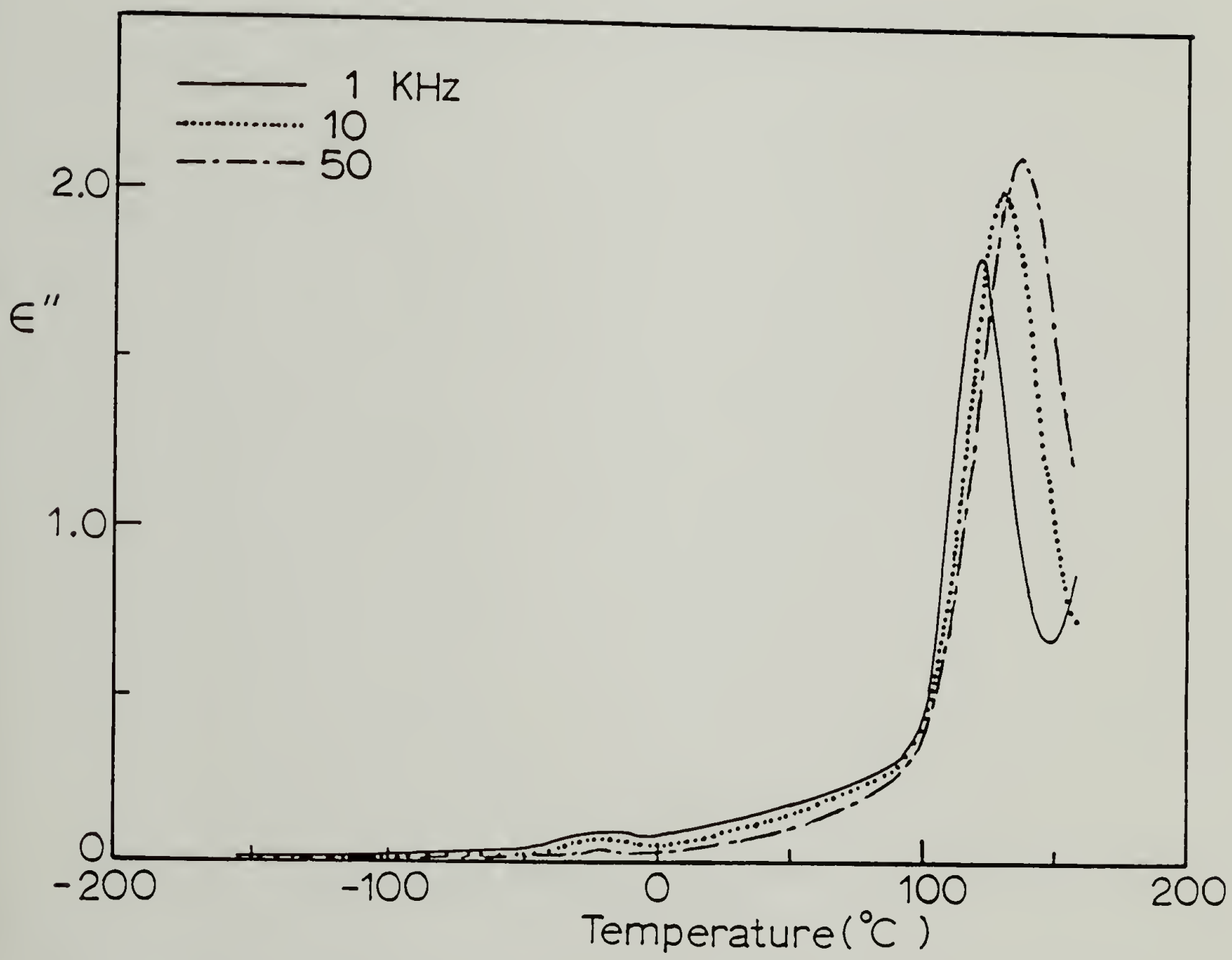

Figure 4.7. Temperature dependence of dielectric loss factor, ε", for SAN 76

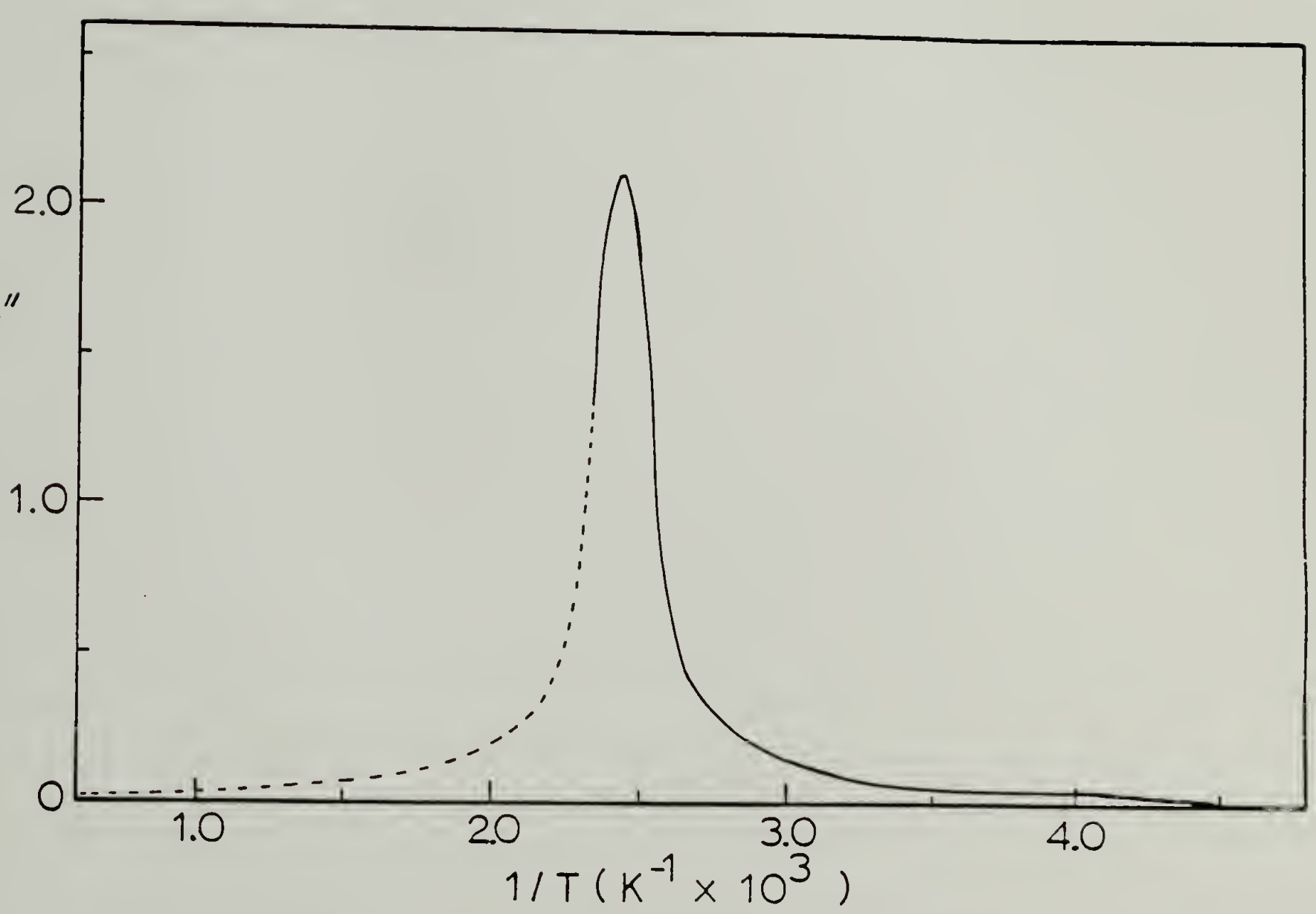

Figure 4.8. Dielectric loss factor ε" as a function of reciprocal temperature at 50 KHz for SAN 76

Figure 4.9 shows the frequency dependence of the normalized dielectric loss of SAN 32, which indicates that the temperature-frequency superposition is applicable over the temperature range studied. Table 4.2 also lists the loss half widths which are the distances in decades of frequency between the right and left hand branches of normalized curves at half-height. The half widths span the range of 2.1 to 2.5. These values are similar to those obtained by Williams et al for SAN copolymers[15] (25 and 32.5 wt% AN) and other amorphous polymers[16]. The normalized loss widths are plotted as a function of composition in Figure 4.10. It is noted that the width of the loss curves remains essentially constant except for copolymer SAN 76, which exhibits a far broader relaxation than the other copolymers. However, its g value is not significantly different from those of the others.

The ratios $\Delta H/\Delta L$ representing the ratio of the distance of the high frequency branch at half-height from $\log (f/f_m) = 0$ to that of the low frequency branch at half-height from $\log (f/f_m) = 0$ (thus reflecting the asymmetry of the dispersion curve) are collected in Table 4.2. Table 4.2 also lists the Cole-Cole parameter α, which is obtained from the linear portion of a plot of ε'' versus ε' at high frequencies at an angle of $\alpha\pi/2$ with the ε' axis, whose magnitude is inversely related to the departure from a single relaxation time associated with semi-circular arc in the Argand diagram.

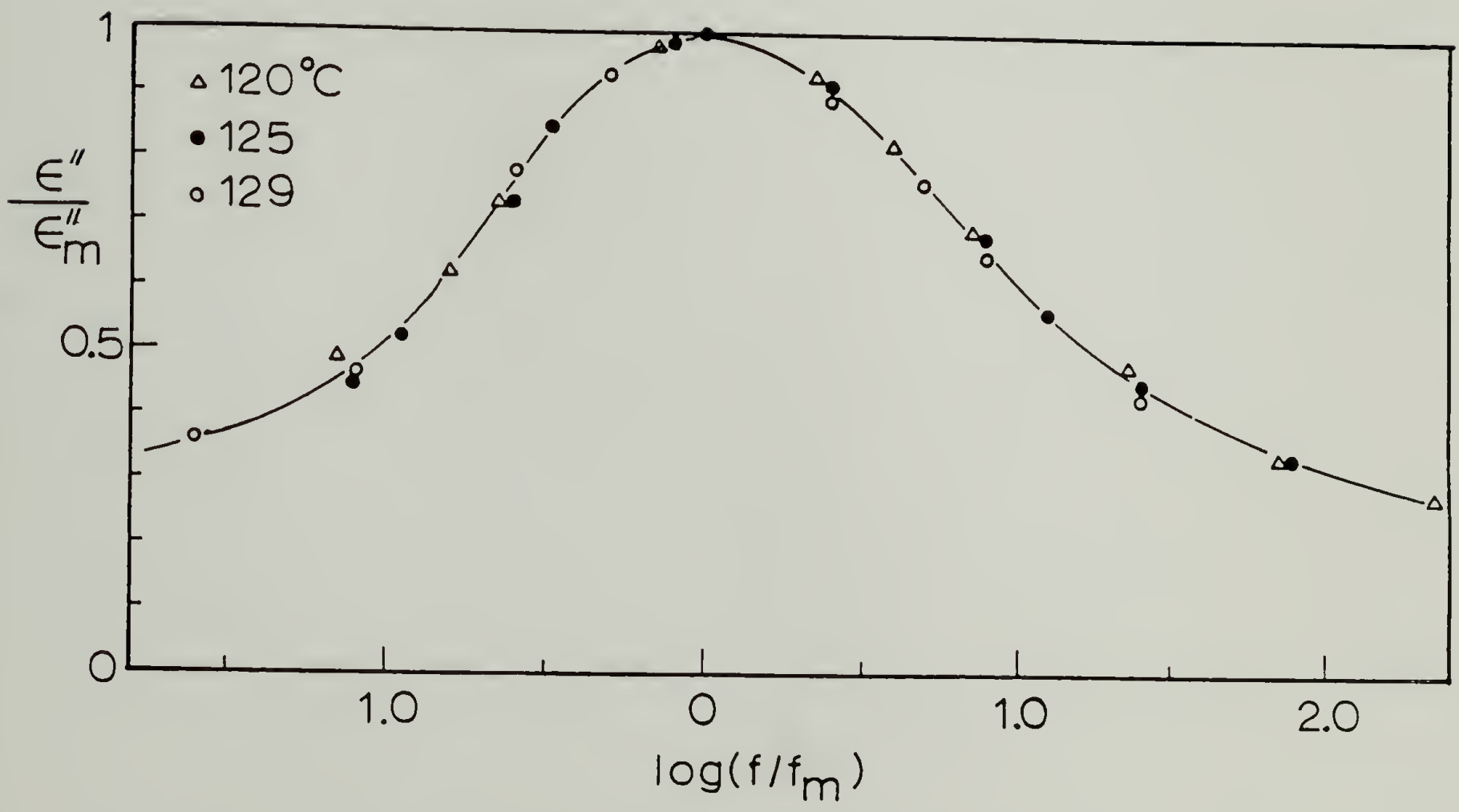

Figure 4.9. Frequency dependence of the normalized dielectric loss for SAN 32

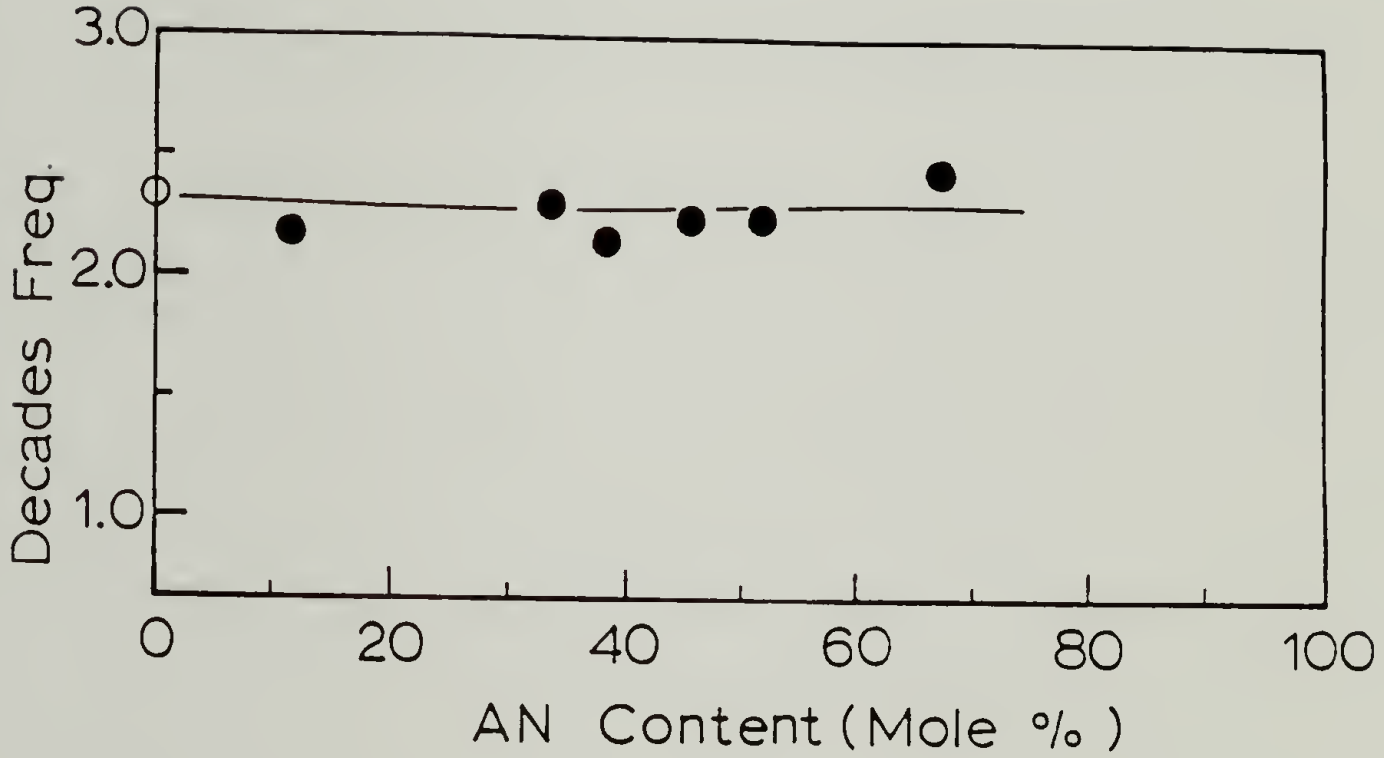

Figure 4.10. Composition dependence of the half width of the dielectric loss for SAN copolymers. The point shown by the open circle was obtained from ref. 17

It can be seen that all the shape parameters of the relaxation spectra collected in Table 4.2 are similar, indicating small differences in the conformational characteristics of the relaxing chains and the random nature of the copolymers. Although information on the details of polymerization for each copolymer is not available at present, it appears likely that an addition of a more reactive styrene monomer is continued throughout the polymerization at a rate designed to maintain a constant ratio of styrene to acrylonitrile monomers thus resulting in random SAN copolymers with less compositional heterogeneity.

The composition dependence of g i.e., the angular correlations between comonomer units in these copolymers can be correlated with a very simple model in which dipolar cancelling is assumed to arise from the geometry of dyads alone[9,17]. The dyad fractions, F_{11}, F_{22}, and F_{12} can be determined for random copolymers from the conditional probability P_{ij} (the probability that the given unit "i" is followed by unit "j"), which is calculated from copolymer compositions and reactivity ratios. As described thoroughly by Alexandrovich[9], the instantaneous copolymerization equation is given by :

$$n = (r_1 N + 1)/(r_2/N + 1) \qquad (4.6)$$

$n = X_i/X_j$ = copolymer monomer ratio

$N = X_I/X_J$ = feed monomer ratio

The conditional probability, P_{ij}, is given by :

$$P_{ij} = 1/(r_1N + 1) = 1 - P_{ii} \qquad (4.7)$$

Combination of Eqn. (4.6) and (4.7) leads to the following relation for P_{ii}, in terms of the known copolymer composition, n, and the reactivity ratio product $R = r_1r_2$.

$$[n(1 - R)]P_{ii}^2 + [1 + n(2R - 1)]P_{ii} - nR = 0 \qquad (4.8)$$

If P_{ii} is determined for a given copolymer, the other conditional probabilities can be obtained from the copolymer compositions in terms of mole fractions X_i and X_j ;

$$P_{ij} = 1 - P_{ii}$$

$$P_{ji} = 1 - P_{jj}$$

$$X_iP_{ij} = X_jP_{ji} \qquad (4.9)$$

Dyad fractions F_{ii}, F_{jj} and $F_{ij} = F_{ji}$ can be calculated :

$$F_{ii} = X_i P_{ii}$$

$$F_{ij} = X_i P_{ij}$$

$$F_{jj} = X_j P_{jj}$$

$$F_{ji} = X_j P_{ji}$$

$$F_{ii} + F_{jj} + 2F_{ij} = 1 \qquad (4.10)$$

The reactivity ratios, $r_1 = 0.52$ and $r_2 = 0.03$[2] were used in the calculations.

The dipole moments are then calculated from the expression[9]

$$\mu_e^2 = g_1 F_{11} (\mu_{1,0})^2 + g_2 F_{22} (\mu_{2,0})^2 + y2F_{12}\{[(\mu_{1,0})^2/2] + [(\mu_{2,0})^2/2]\} \qquad (4.11)$$

where g_1, g_2 refer to the appropriate homopolymer values and y is the correlation factor for the mixed dyad. In the calculation g_1 =

0.32[17] and g_2 = 0.59 were employed. The latter was calculated using Eqn. (4.1) - (4.4) from the dielectric relaxation strength ($\varepsilon_R - \varepsilon_u$ = 32)[18] and the density of 1.18 g/cm^3 for the polyacrylonitrile homopolymer. Table 4.2 also lists the y values thus determined which are consistent with Kirkwood-Frohlich orientation correlation function g. However, SAN 48 may contain some alternating sequences as indicated by the T_g measurements.

Considering the effect of adjacent dissimilar monomer units on steric and intramolecular interactions in the copolymer backbone, Johnston[10] reported a relation predicting the copolymer glass transitions from the conditional probability P_{ij} which takes into account the copolymer sequence distribution.

$$1/T_{gp} = (W_i P_{ii}/T_{gii}) + [(W_i P_{ij} + W_j P_{ji})/T_{gij}] + (W_j P_{jj}/T_{gjj}) \qquad (4.12)$$

where T_{gp} is the T_g of a copolymer containing weight fraction W_i and W_j of two monomer units i and j which have the conditional probabilities P_{ii}, P_{ij}, P_{ji}, and P_{jj} of having various linkages contributing the T_g's of T_{gii}, $T_{gij} = T_{gji}$, and T_{gjj} to the copolymer. Here, T_{gii} and T_{gjj} can be regarded as the T_g's of

polystyrene and polyacrylonitrile, respectively and T_{gij} is taken as the T_g of SAN alternating copolymers. The T_g of polystyrene measured in this work is 107°C, which is higher than that reported in the literature[10]. The T_g of polyacrylonitrile is determined to be 105°C. The experimentally determined T_g's of the copolymers and the T_g's predicted by employing either 111.5°C[10] or 117°C[19] as T_{gij} taken from different sources are plotted as a function of AN content in Figure 4.11 where the calculated fraction of S-AN dyads is also displayed. These data exhibit positive deviation from those predicted using the Fox equation and the deviation increases as the fraction of S-AN dyads increases as noted by Johnston[10]. This is ascribed, on the basis of Tonelli's calculation[20] of the conformational entropies of the various dyads in the SAN copolymer, to the fact that the conformational entropy of an S-AN dyad is smaller than half the sum of the entropies of S-S and AN-AN dyads if we assume that the T_g of a polymer is inversely related to the intramolecular equilibrium flexibility of a polymer chain.

The experimentally measured T_g's are higher than those determined by Johnston[10]. However, the T_g's fall between two predicted curves; a higher T_g was noted for SAN 48 which may be due to a large fraction of S-AN dyads resulting from a slightly higher

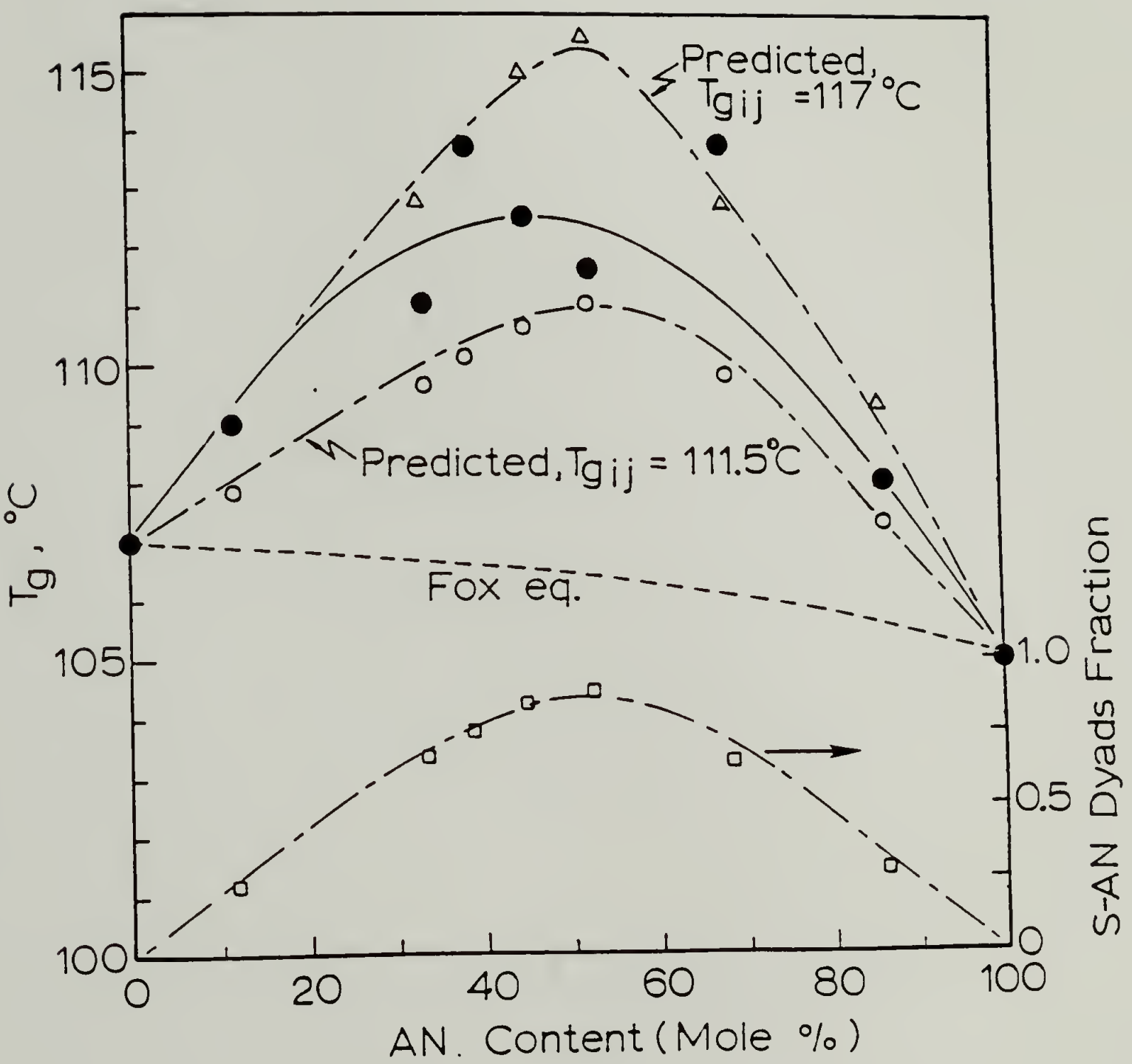

Figure 4.11. T_g's determined experimentally and predicted by considering sequence distribution and the fraction of S-AN dyads calculated vs. mole% AN content

degree of alternating sequences than are present in the other copolymers.

REFERENCES

1. A.C. Balazs, I.C. Sanchez, I.R. Epstein, F.E. Karasz, W.J. MacKnight, Macromolecules, 18, 2188 (1985).
2. R.G. Fordyce, J. Amer. Chem. Soc., 69, 1903 (1947).
3. P.J. Flory, "Statistical Mechanics of Chain Molecules", Interscience, New York, 1969.
4. J.E. Mark, J. Amer. Chem. Soc., 94, 6645 (1972).
5. J.E. Mark, J. Chem. Phys., 56(1), 451 (1972).
6. E. Saiz, J.E. Mark, P.J. Flory, Macromolecules, 10(5), 967 (1977).
7. A.E. Tonelli, Macromolecules, 10(1), 153 (1977).
8. G. Khanarian, R.E. Cais, J.M. Kometani, A.E. Tonelli, Macromolecules, 15(3), 866 (1982).
9. P.S. Alexandrovich, Ph.D. Thesis, University of Mass., 1978.
10. N.W. Johnston, J. Macromol. Sci-Rev. Macromol. Chem., C14(2), 215 (1976).
11. L.Onsager, J. Amer. Chem. Soc., 58, 1486 (1936).
12. H. Frohlich, "Theory of Dielectrics", Oxford University Press, London, 1958.
13. C.P. Smyth, "Dielectric Behavior and Structure", McGraw-Hill, New york, 1955.
14. N.G. McCrum, B.E. Read, G.Williams, "Anelastic and Dielectric Effects in Polymeric Solids", John Wiley and Sons, London, 1967.

15. M. Cook, G. Williams, T.T. Jones, Polymer, 16(11), 835 (1975).

16. G. Williams, D.C. Watts, S.B. Dev, A.M. North, Trans. Far. Soc., 67, 1323 (1971).

17. P.S. Alexandrovich, F.E. Karasz, W.J. MacKnight, Polymer, 21, 488 (1980).

18. A.K. Gupta, N. Chand, R. Singh, A. Mansingh, Europ. Polym. J., 15, 129 (1979).

19. M. Hirooka, T.Kato, J. Polym. Sci., Polym. Lett. Ed., 12(1), 31 (1974).

20. A.E. Tonelli, Macromolecules, 7(5), 632 (1974).

CHAPTER V

MISCIBILITY IN BLENDS OF POLY(STYRENE-CO-ACRYLONITRILE) WITH SPPO COPOLYMERS

This chapter describes studies of miscibility behavior in blends of poly(styrene-co-acrylonitrile) (SAN) with sulfonylated poly(2,6-dimethyl-1,4-phenylene oxide) (SPPO) copolymers, namely, blends of two random copolymers with four distinct repeat units. The isothermal composition-composition diagram displaying the miscibility-immiscibility boundary represented in Cartesian coordinates is interpreted on the basis of a mean field theory through which all the χ_{ij}'s are determined. The primary experimental techniques employed to probe miscibility are DSC, dynamic mechanical spectroscopy and density measurements. Dielectric relaxation spectroscopy was also employed to explore the extent of miscibility on the basis of normalized dielectric loss spectra obtained from frequency plane measurements.

A. Experimental Section

Materials The preparation and properties of SPPO copolymers were described in Chapter II. The compositions and properties of SAN copolymers can be found in Chapter IV. The numerals following SPPO and SAN indicate its degree of sulfonylation by weight % and its AN content by weight %, respectively.

Blends involving SPPO copolymer for T_g measurements were prepared by dissolving the components in THF in the desired proportions and then casting in aluminum dishes. The solvent was allowed to evaporate slowly at ambient conditions for at least four days and the resulting films were further dried in a vacuum oven at 120°C for 72 hr to completely remove residual solvent. Blends of PPO with SAN copolymers were prepared by casting films from chloroform solutions.

For dynamic mechanical and dielectric measurements pellets of SAN copolymers were compression molded into films at 200°C under nitrogen and annealed above T_g in the DMTA or DETA furnace. The films of SPPO copolymers and their blends with either SAN 5 or SAN 18 were cast from chlorobenzene solution and dried in a vacuum oven followed by annealing above T_g in the DMTA or DETA furnace to remove residual solvent.

T_g Measurements T_g measurements were performed similarly as described in Chapter II. All the samples were annealed in the DSC

pan at 290°C for 20 min before T_g measurements, unless otherwise noted.

Density Measurements Densities of cast films of blend samples were measured as described in Chapter II.

Dynamic Mechanical Measurements Dynamic mechanical measurements were carried out as described in Chapter II. The samples were measured under nitrogen at 1 Hz. The temperature range was from -150°C to 280°C at a heating rate of 4°C/min.

Dielectric Measurements Dielectric measurements were carried out with a General Radio model 1689M RLC Digibridge at 0.1, 1 and 10 KHz over a temperature range from -155°C to 280°C with a nitrogen purge. The temperature was raised at a rate of 2.0°C/min. Samples approximately 0.2 mm thick were employed with an active electrode cell diameter of 3.3 cm. Frequency plane measurements were also carried out as described in Chapter IV.

B. Results and Discussion

Miscibility Map Figure 5.1 illustrates the DSC thermograms of SAN 26/SPPO 54 blends. The composition dependences of the T_g's of these

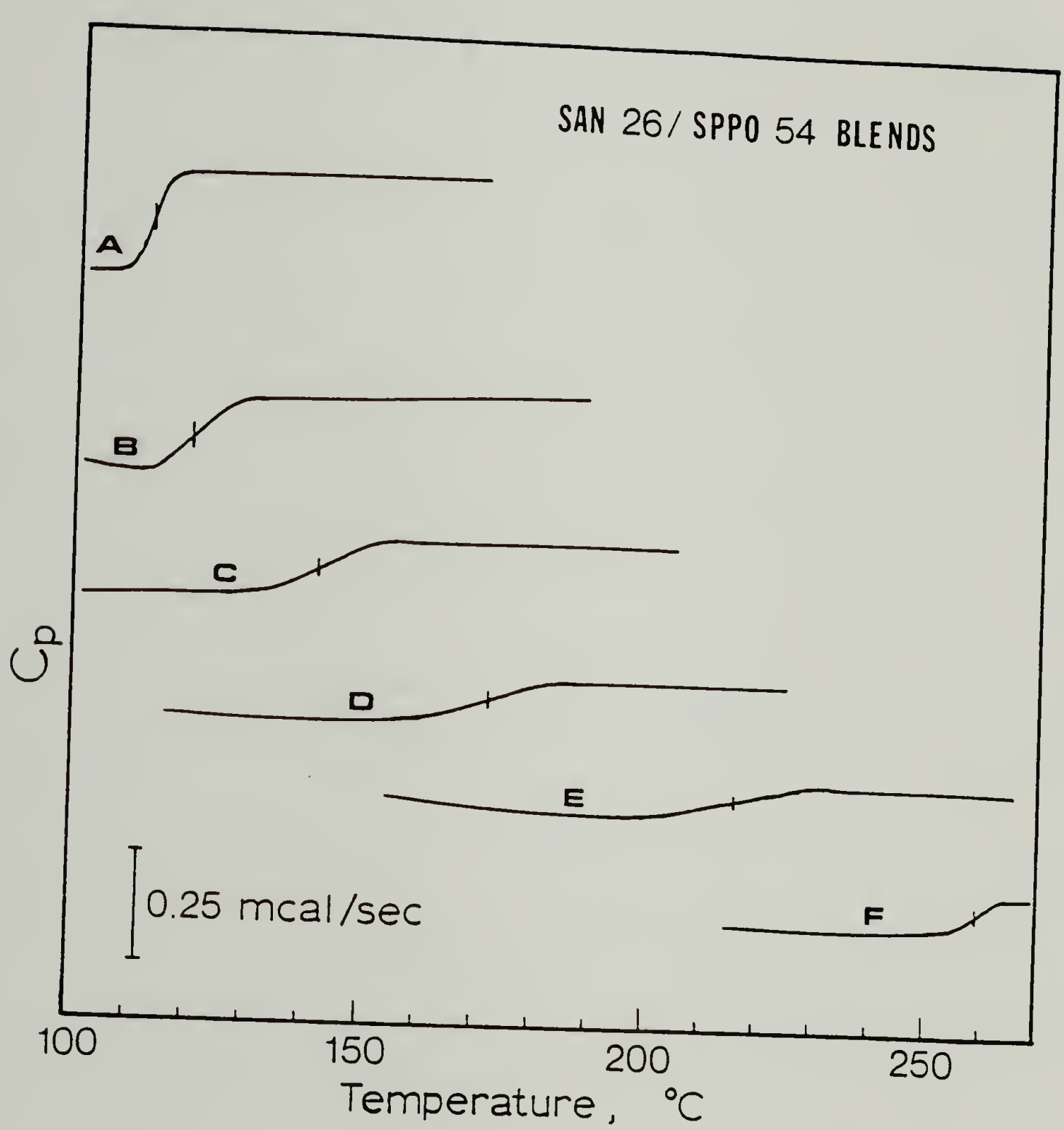

Figure 5.1. DSC thermograms of SAN 26, SPPO 54 and blends :
(A) Pure SAN 26; (B) 25% SPPO 54; (C) 50% SPPO 54;
(D) 70% SPPO 54; (E) 85% SPPO 54; (F) Pure SPPO 54.

blends and a comparison to the T_g's calculated using the Fox (k=0.4) and Couchman equation[1] are shown in Figure 5.2. The pertinent parameters used in the calculation are ΔC_p(SAN 26) = 0.32 J/g/deg and ΔC_p(SPPO 54) = 0.14 J/g/deg (refer to Chapter II). The experimental T_g's are in reasonably good agreement with the values calculated. Figure 5.3 displays the composition dependences of the T_g's of SAN 5/SPPO 12 blends.

On the basis of a series of DSC analyses and by using the miscibility criterion of a single glass transition, the composition-composition diagram ("C-C plots") displaying the miscibility-immiscibility boundary for 50/50 wt% blends at 290°C was constructed and is shown in Figure 5.4.

Estimation of χ_{ij}'s The blends of the type, $(A_{1-x}B_x)_{n_1}/(C_{1-y}D_y)_{n_2}$, involve six segmental interaction parameters where A, B, C and D refer to styrene, acrylonitrile, unsulfonylated phenylene oxide and sulfonylated phenylene oxide units, respectively. The χ_{AC}[2], χ_{AD} and χ_{CD} (refer to Chapter III) have been determined on the basis of a mean field treatment.

From the studies of Molau[3] on binary mixtures of SAN copolymers which differ only in chemical composition, the tolerable

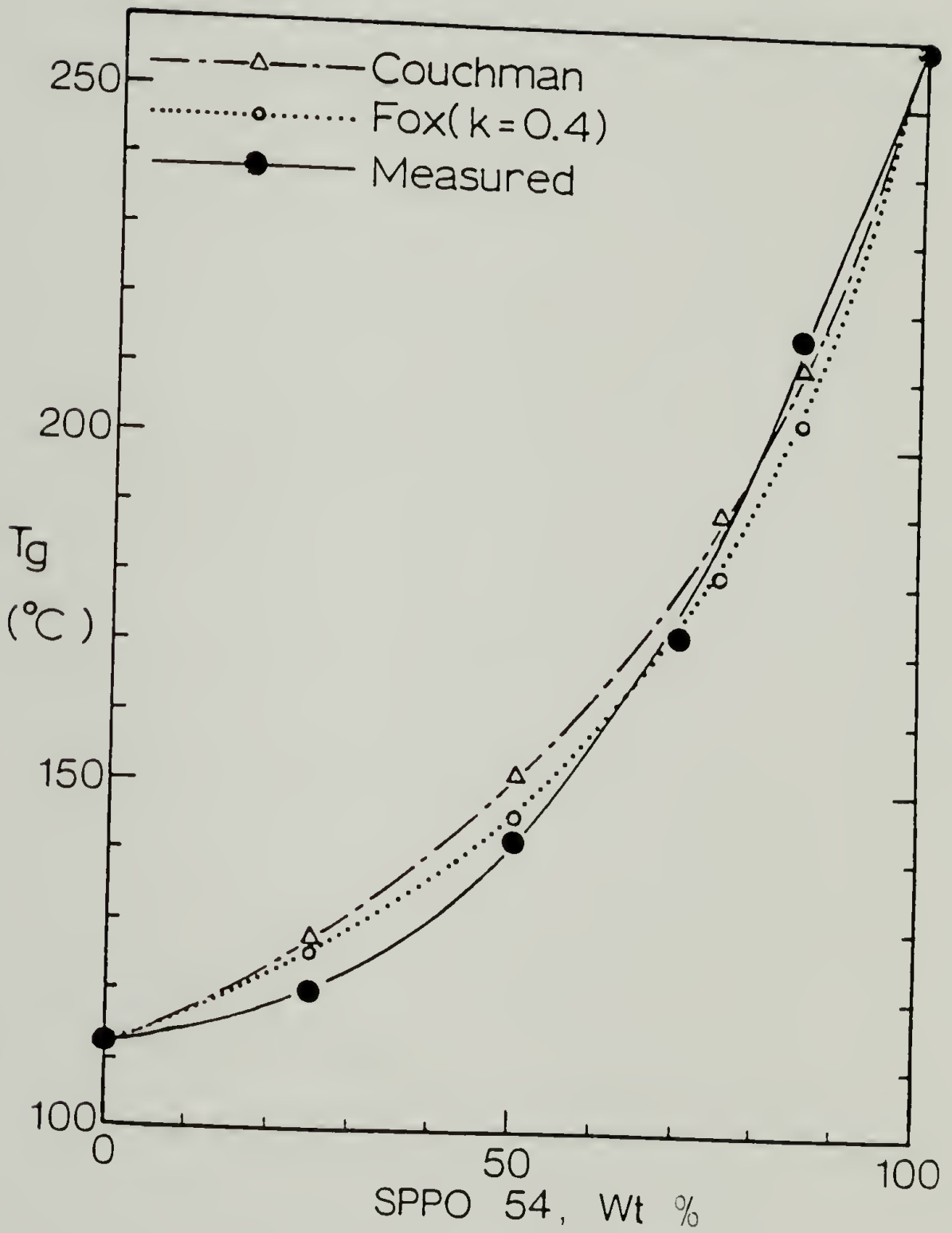

Figure 5.2. T_g's vs. composition for SAN 26/SPPO 54 blends.

Dashed lines represent the Couchman equation and dotted lines represent the Fox equation with k=0.4.

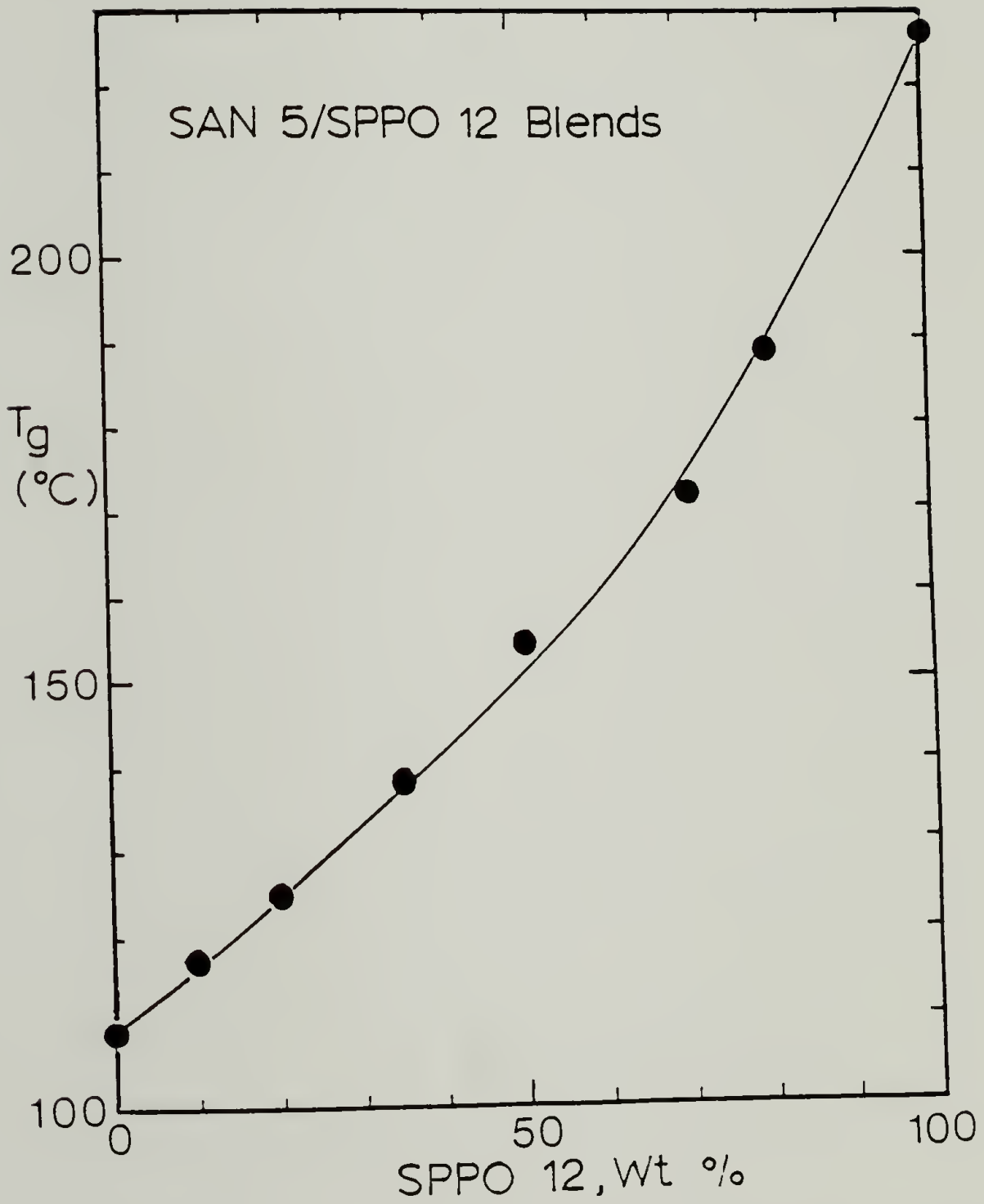

Figure 5.3. T_g's vs. composition for SAN 5/SPPO 12 blends

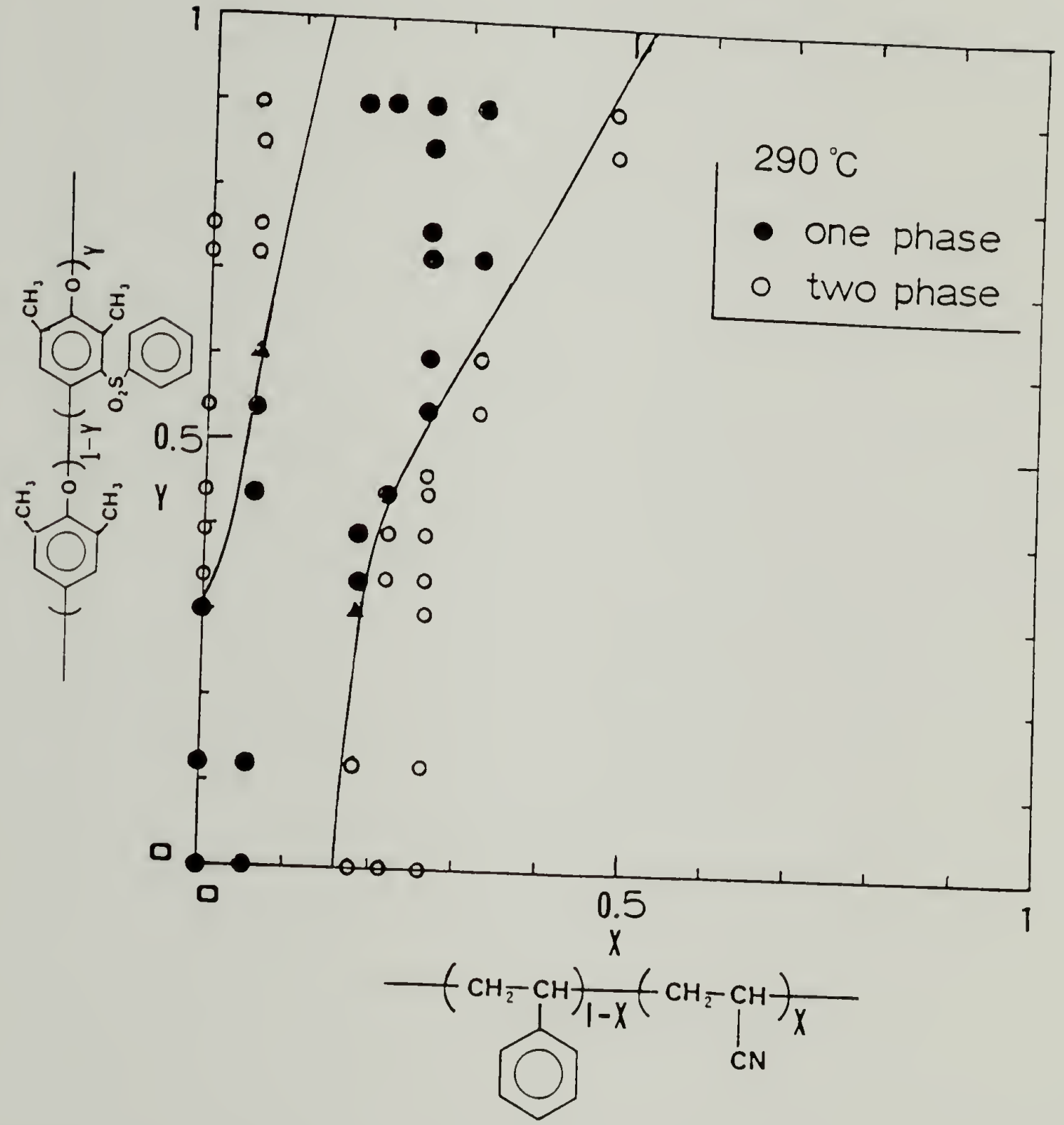

Figure 5.4. Miscibility domain for 50/50 wt% blends of SAN copolymers with SPPO copolymers at 290°C

difference in AN content (Δ) for miscibility was found to be 4%. On the basis of a mean field treatment, as described in Chapter I, the critical condition for these mixtures obeys the relation :

$$1/2(n_1^{-1/2} + n_2^{-1/2})^2 = \Delta^2 \chi_{AB} \qquad (5.1)$$

From the Eqn. (5.1) and using $n_1 = n_2 = 1800^3$ χ_{AB} is estimated to be 0.70.

Figure 5.4 indicates that the critical AN content for miscibility in blends of SAN copolymers with the PPO homopolymer is 17 wt%. The critical condition for these blends of the type, $(A_{1-x}B_x)_{n_1}/C_{n_2}$, holds the relation :

$$\chi_{blend}^{crit} = 1/2(n_1^{-1/2} + n_2^{-1/2})^2 = (1-x)\chi_{AC} + x\chi_{BC} - x(1-x)\chi_{AB} \qquad (5.2)$$

For the present system, n_1 = 2800 (from Chapter IV) and n_2 = 290, which yields χ_{blend}^{crit} of 0.003. From the Eqn. (5.2) χ_{BC} is determined to be 0.80.

By extrapolation, Figure 5.4 also indicates the presence of a "window of miscibility" for blends of SAN copolymers with the fully sulfonylated PPO homopolymer. The window of miscibility is found

over the AN content of 13-52 wt%. χ_{BD} is estimated to be 0.14 by a procedure similar to that described above to determine χ_{BC} except that blends of the type, $(A_{1-x}B_x)_{n_1}/D_{n_2}$, are considered.

It should be noted that the window of miscibility may be observed because of the very large intramolecular repulsive interaction between styrene and acrylonitrile segments comprising the copolymer, even though χ_{AB}, χ_{AD}, and χ_{BD} are all positive.

Volume of Mixing For immiscible blends the density is equal to or lower than the values calculated from the additivity relationship[4]:

$$\rho = \phi_1\rho_1 + \phi_2\rho_2$$

or

$$1/\rho = W_1/\rho_1 + W_2/\rho_2 \qquad (5.3)$$

where W_i and ρ_i are the weight fraction and the density of the ith component, respectively. A negative volume change on mixing has been observed for several miscible blends[5-7].

Figure 5.5 displays the blend composition dependence of the specific volume of SAN 26/SPPO 54 (miscible) blends and SAN 26/SPPO 44 (immiscible) blends. Since the densities have been measured below

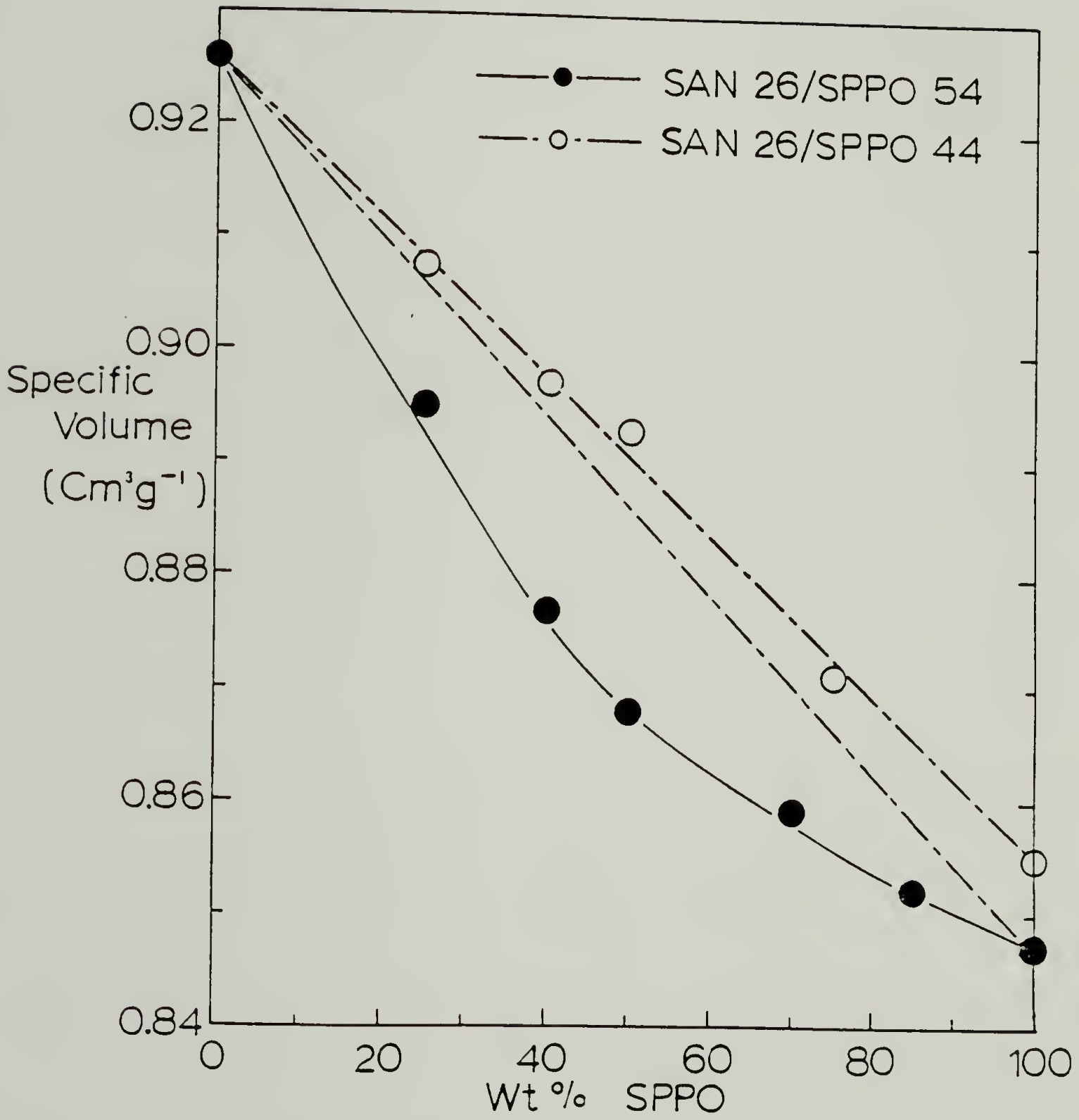

Figure 5.5. Specific volume vs. blend composition expressed as weight fraction SPPO. Dashed lines indicate specific volume calculated from the additivity relationship.

the T_g's of each component and the blends, there may be a contribution to the specific volume associated with the excess free volume during solvent casting and drying[7]. The immiscible blends are seen to obey the additivity relationship, while the miscible blends exhibit a negative volume change on mixing of about 2% at 50/50 wt% composition, which infers that the miscible region shown in the "C-C plots" (Figure 5.4) involves better packing on mixing, even though all χ_{ij}'s are positive except χ_{AC}.

Dynamic Mechanical Measurements Temperature dependences of tan δ for SAN 18, SPPO 39 and their 50/50 wt% blends, which are found to be miscible based on a single calorimetric glass transition temperature, are shown in Figure 5.6. The 50/50 wt% blend exhibits a single, well-defined mechanical loss peak with no apparent shoulder occurring at a temperature between the transitions of the pure components. However, peak broadening is noticeable because of a fluctuation in local composition within the blend.

Dielectric Measurements Dielectric relaxation measurements of blends involving polymers with permanent dipole moments are suitable for probing the molecular environment, or more specifically, intramolecular and intermolecular interactions. And the wide range of frequency and time available allows us to conduct the representation on the basis of time-temperature superposition.

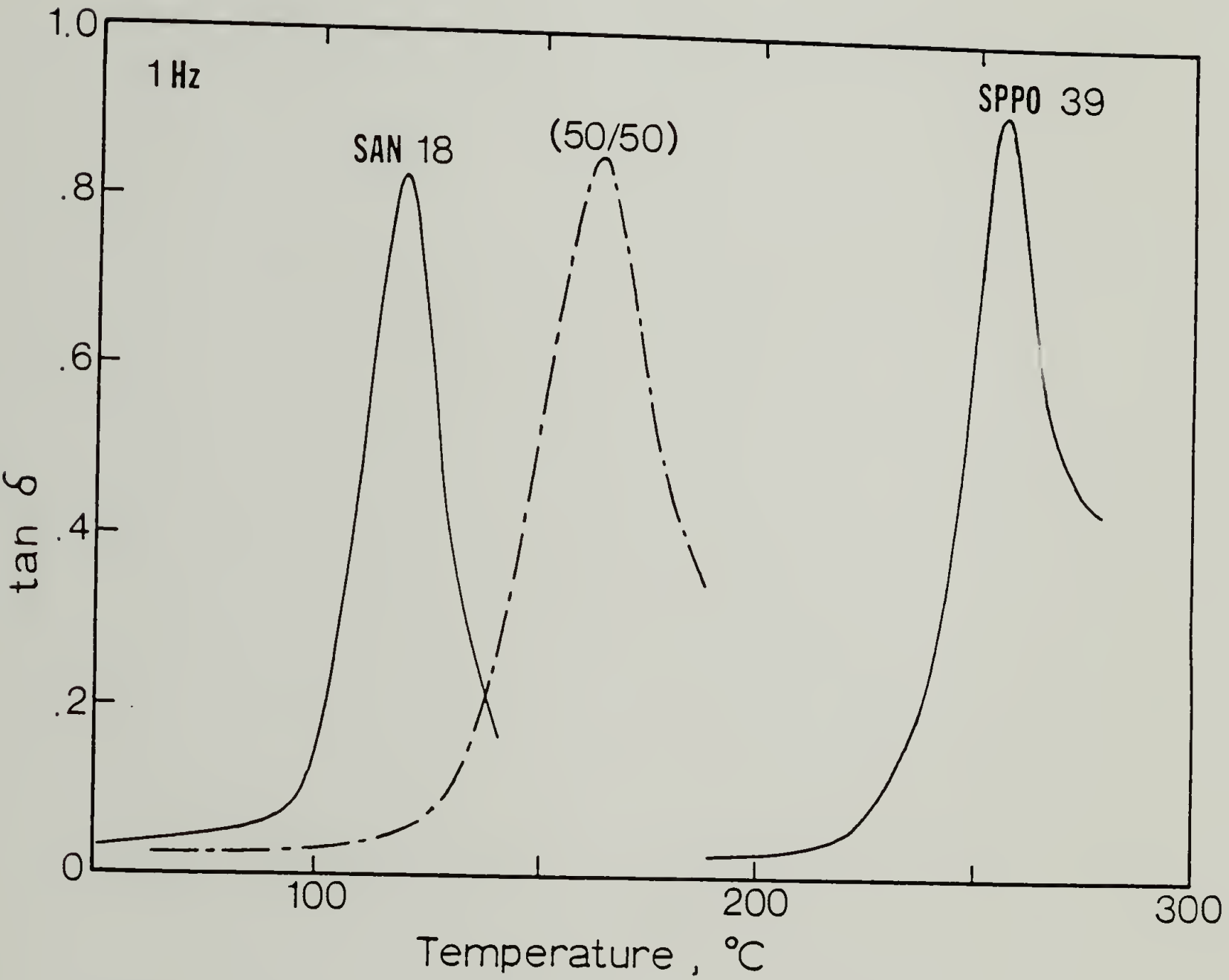

Figure 5.6. Dynamic mechanical tanδ as a function of temperature for SAN 18, SPPO 39 and 50/50 wt% SAN 18/SPPO 39 blends at 1 Hz

Temperature Plane Measurements The loss curves of SAN 5, SPPO 12 and their blends are plotted as a function of temperature in Figure 5.7. The 50/50 wt% blend exhibits a single, broadened dielectric α-relaxation with no evidence of shoulders between the transitions of the pure components. An ionic conduction[8] can be seen from the sharp upturn in tan δ above the loss peak temperatures, particularly at lower frequencies. However, since the ionic conduction of pure SAN 5 appears to be almost negligible, it is assumed that impurities in SAN 5 cause little change in the high temperature loss peak of the 50/50 wt% blend even above the T_g of SAN 5. The charge carriers in the blend seem to originate mainly from SPPO 12. In the SPPO copolymer a trace of residual catalyst, even after a careful purification of the copolymer, is regarded as the primary source of the ionic conduction.

Frequency Plane Measurements Temperature plane dynamic mechanical or dielectric relaxation measurements cannot provide information on phase equilibrium at a certain temperature because of the possible "freezing in" of a nonequilibrium structure and of their insensitivity to detect the very small dispersed phase[9], if any. Thus, to investigate the nature of the molecular interactions, conformational states in the system and the extent of miscibility within the miscible blend, frequency plane measurements of blends of SAN 5/SPPO 12 were carried out isothermally. The blend compositions were limited to those with higher SAN 5 content since SPPO 12 exhibits significant ionic transport losses.

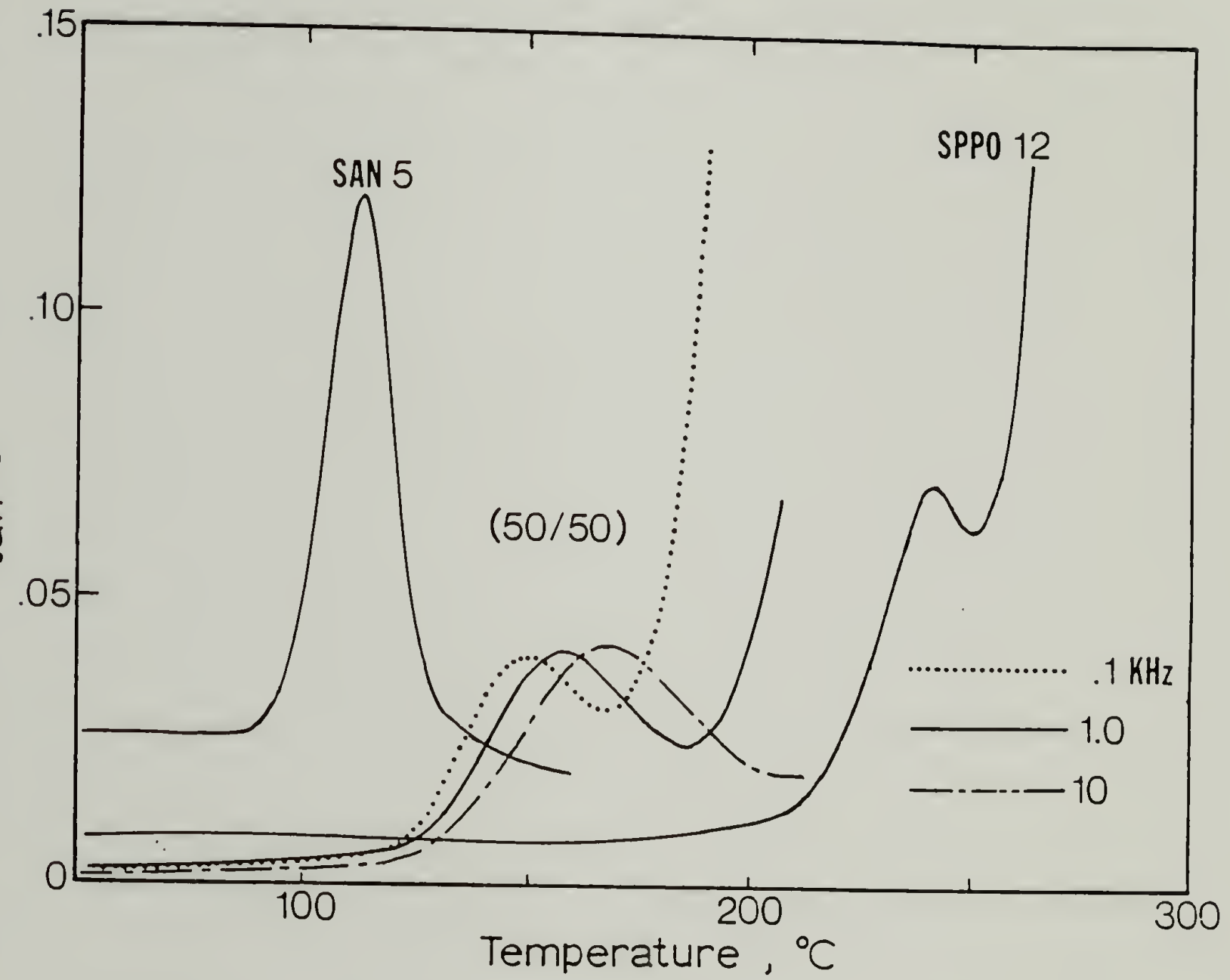

Figure 5.7. Dielectric tan δ as a function of temperature for SAN 5, SPPO 12 and 50/50 wt% SAN 5/SPPO 12 blends

Dielectric constants (ε') and losses (ε'') for SAN 5 and its blends with SPPO 12 of varying compositions are displayed in the frequency plane in Figures 5.8 (a)-(h). Figures 5.9 (a)-(b) are the corresponding Argand diagrams. Good superposition over a range of temperatures can be seen.

Figure 5.10 shows the normalized dielectric loss curves, which indicates that the temperature-frequency superposition is applicable and that the shape parameters change negligibly over the temperature ranges studied. Table 5.1 summarizes the loss half widths, three-quarter widths, $\Delta H/\Delta L$, representing the ratio of the distance of the high frequency branch at half-height from $\log(f/f_m) =$ 0 to that of the low frequency branch at half-height from $\log(f/f_m) =$ 0 (thus, indicating the asymmetry of the dispersion curve), and the Cole-Cole parameter, α, whose magnitude is inversely related to the departure from a single relaxation time.

As seen both from Figure 5.10 and Table 5.1, the blends exhibit a significant broadening in the dielectric loss spectra with increasing SPPO content compared with pure SAN 5 copolymer, reflecting the differences in local environments as a consequence of the cooperative nature of the relaxation as suggested by Glarum[10]. This broadening of relaxation spectra is ascribed to local concentration fluctuations which persist for longer times than those required for dipolar polarization. In other words, this would imply

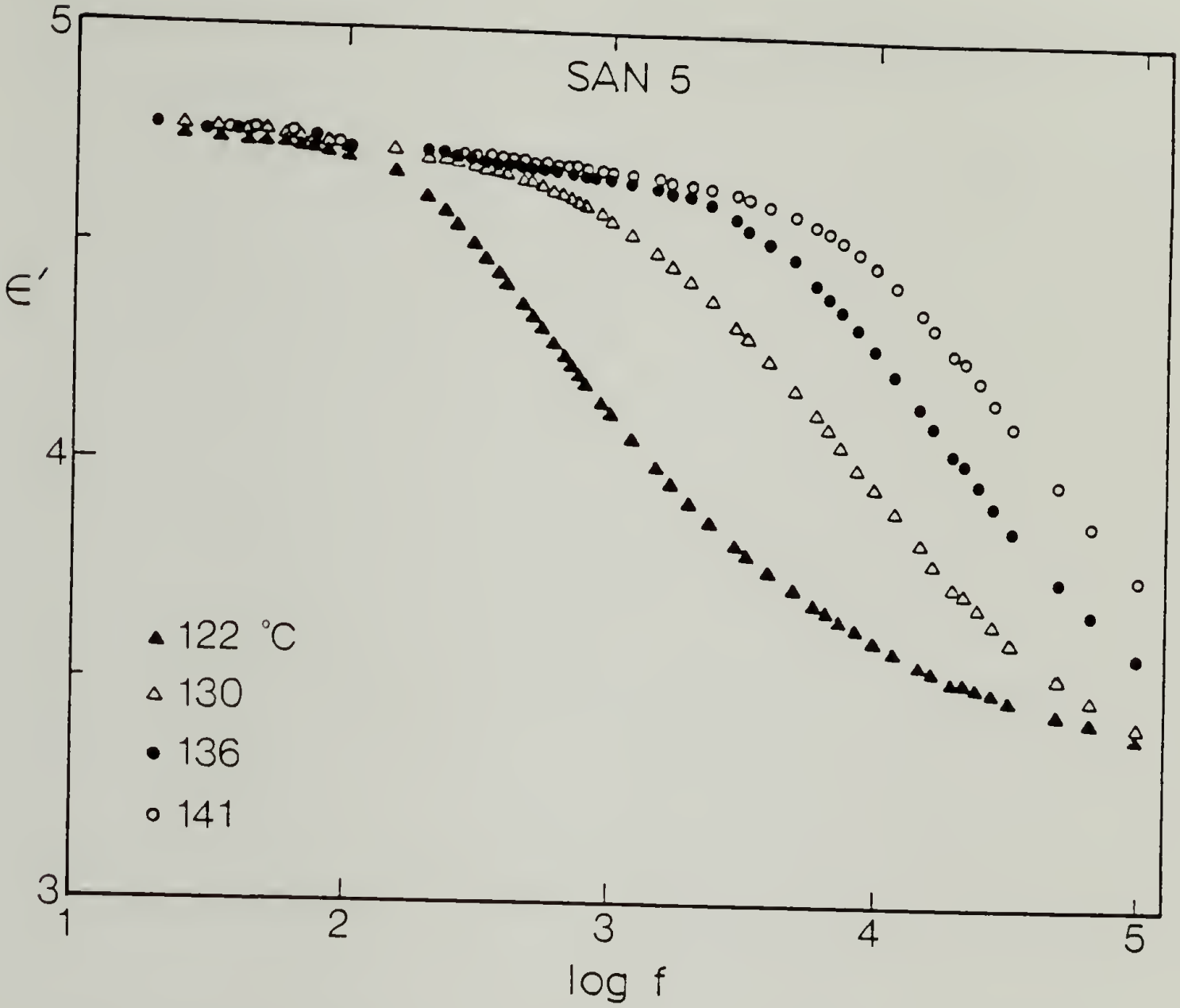

Figure 5.8. (a) Dielectric constant vs. frequency for SAN 5 (b) loss factor for SAN 5; (c) Dielectric constant vs. frequency for 90/10 wt% SAN 5/SPPO 12 blends; (d) Loss factor for 90/10 wt% SAN 5/SPPO 12 blends; (e) Dielectric constant vs. frequency for 80/20 wt% SAN 5/SPPO 12 blends; (f) Loss factor for 80/20 wt% SAN 5/SPPO 12 blends; (g) Dielectric constant vs. frequency for 65/35 wt% SAN 5/SPPO 12 blends; (h) Loss factor for 65/35 wt% SAN 5/SPPO 12 blends.

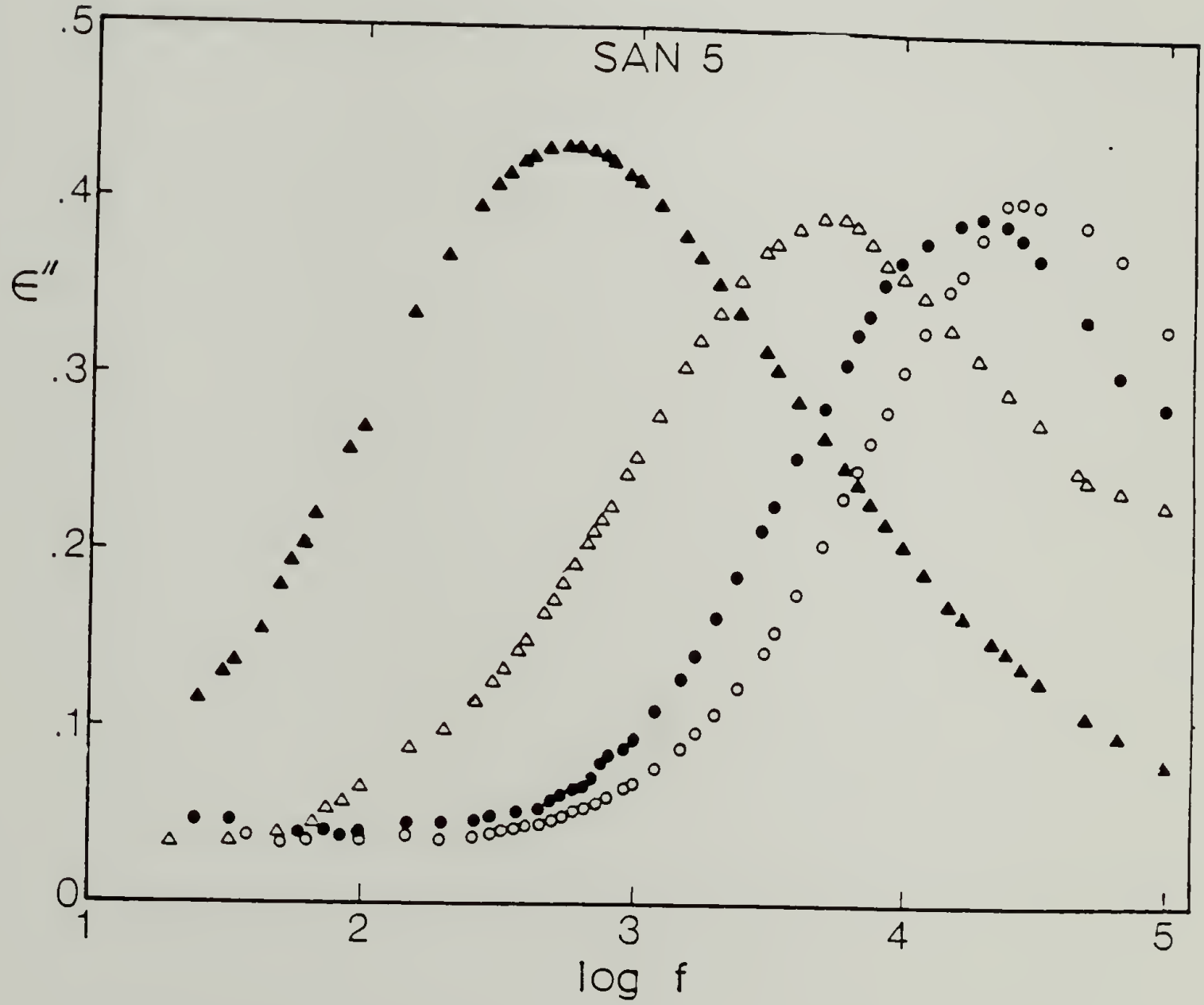

Figure 5.8. (b)

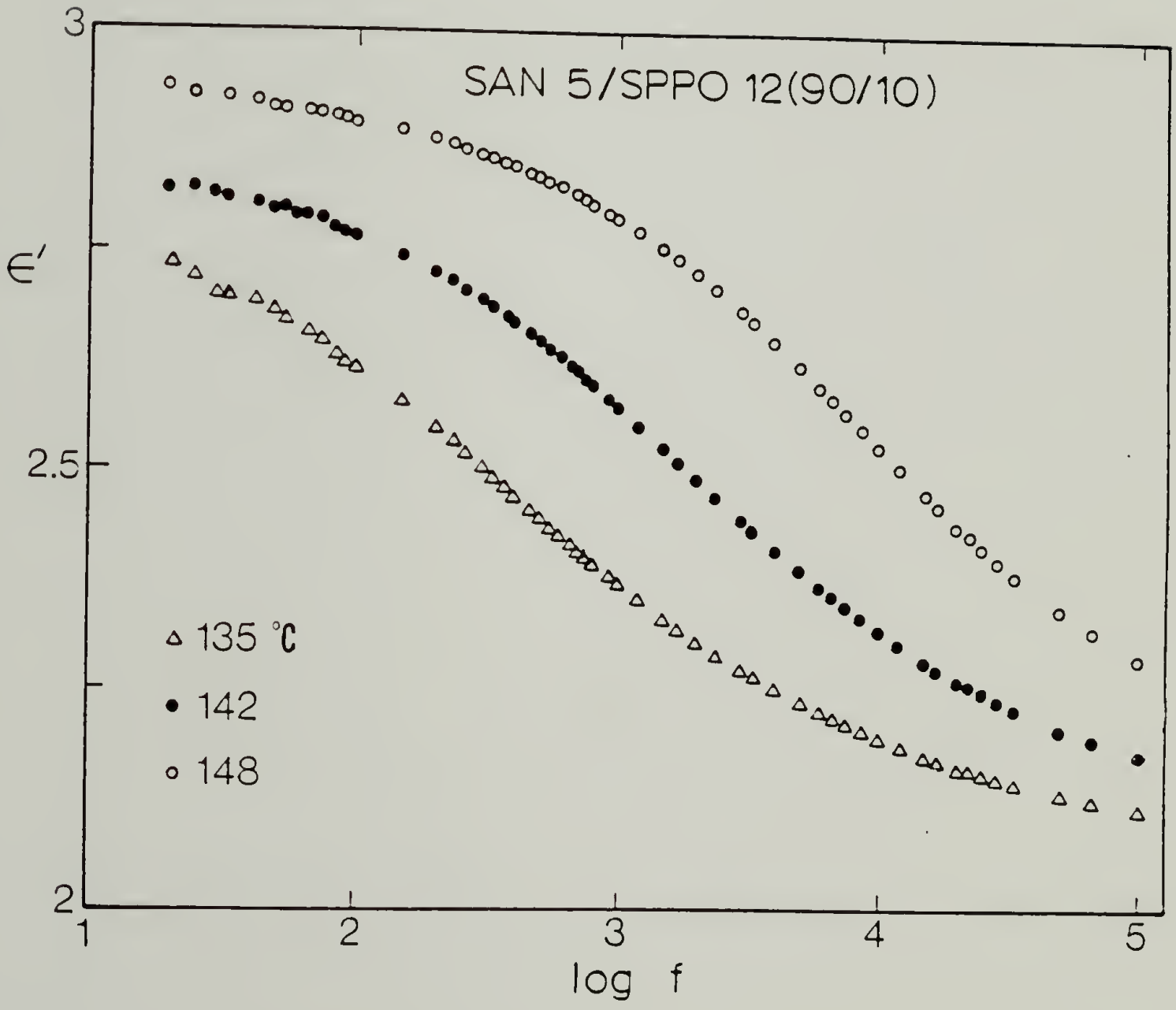

Figure 5.8. (c)

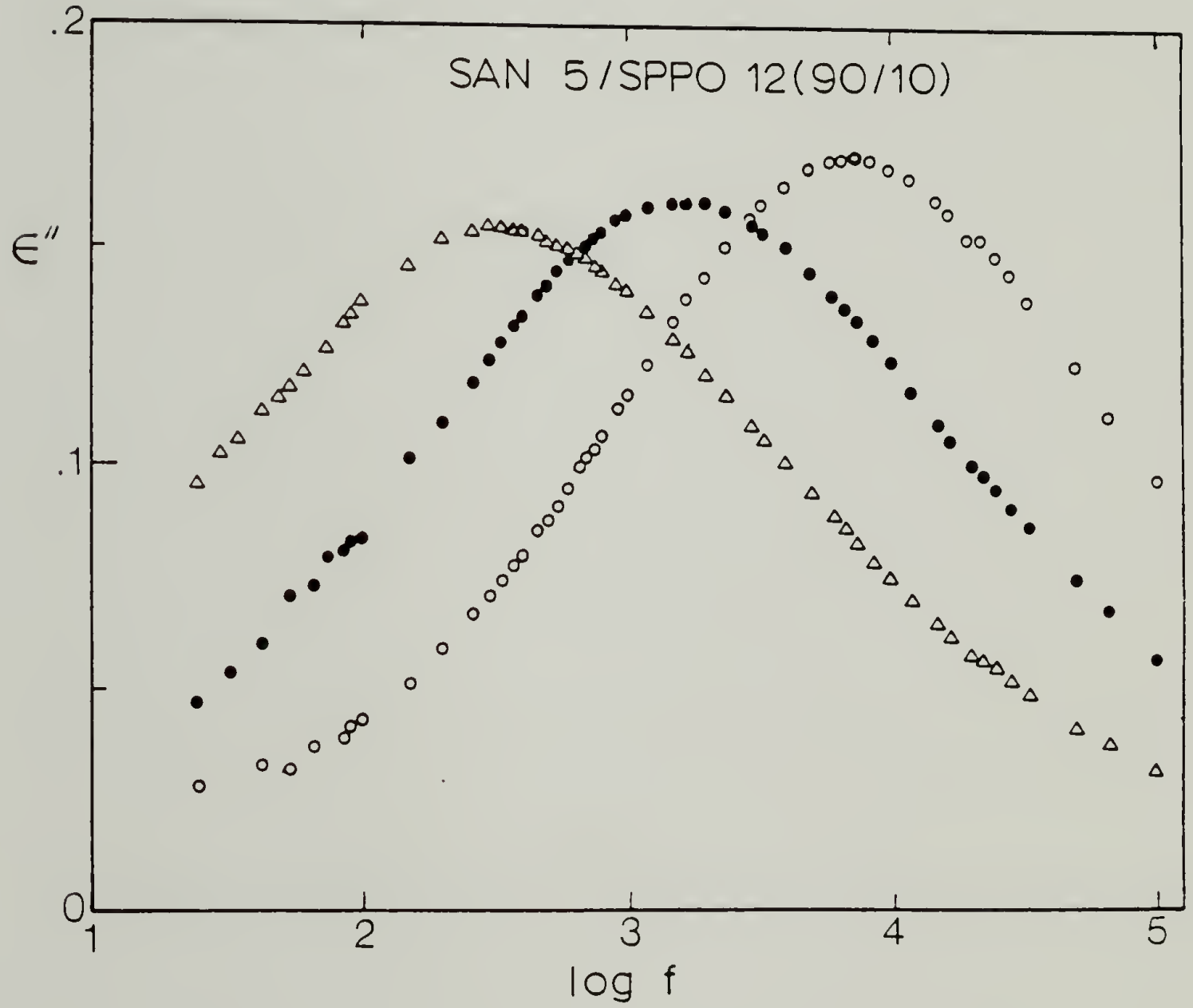

Figure 5.8. (d)

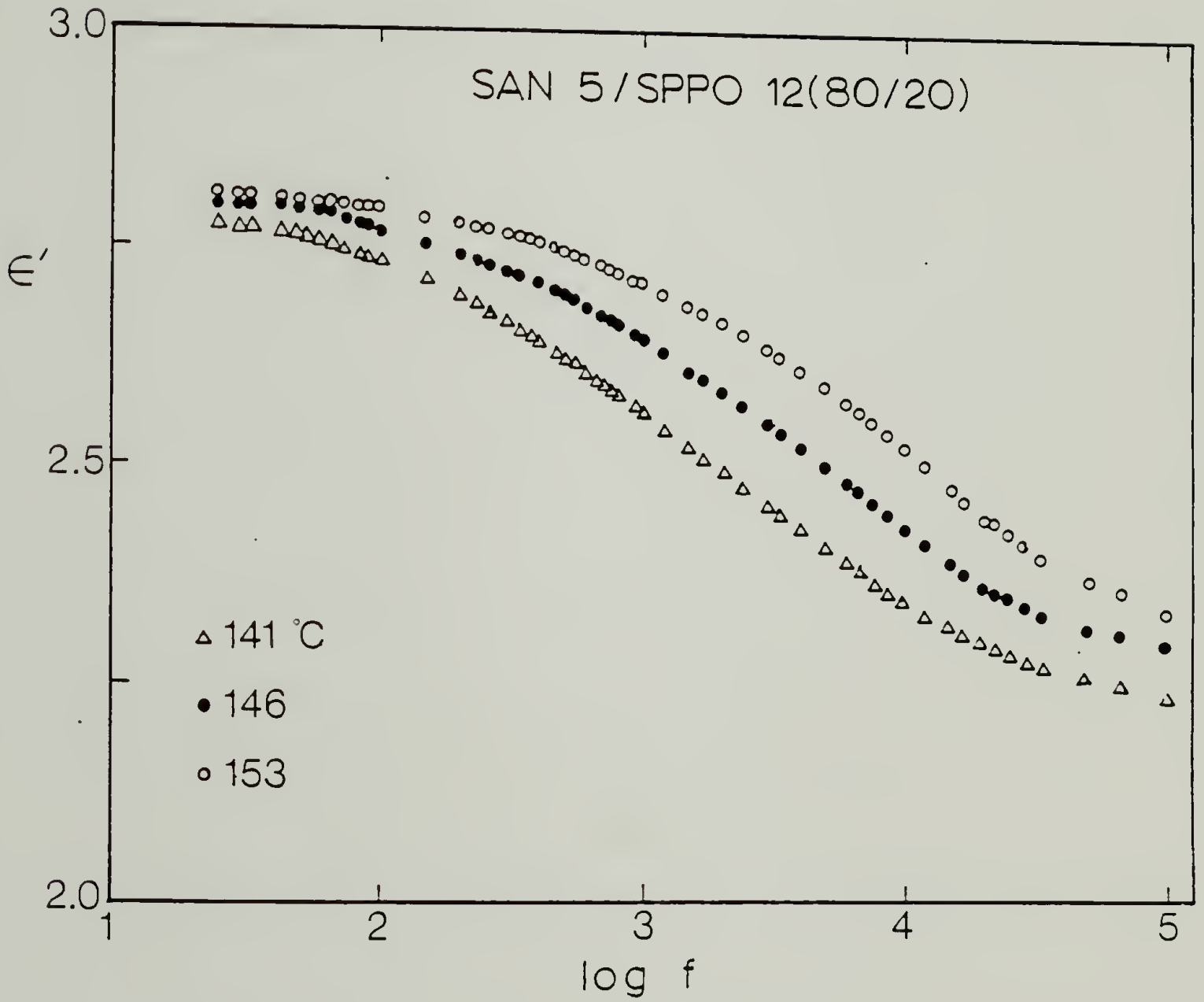

Figure 5.8. (e)

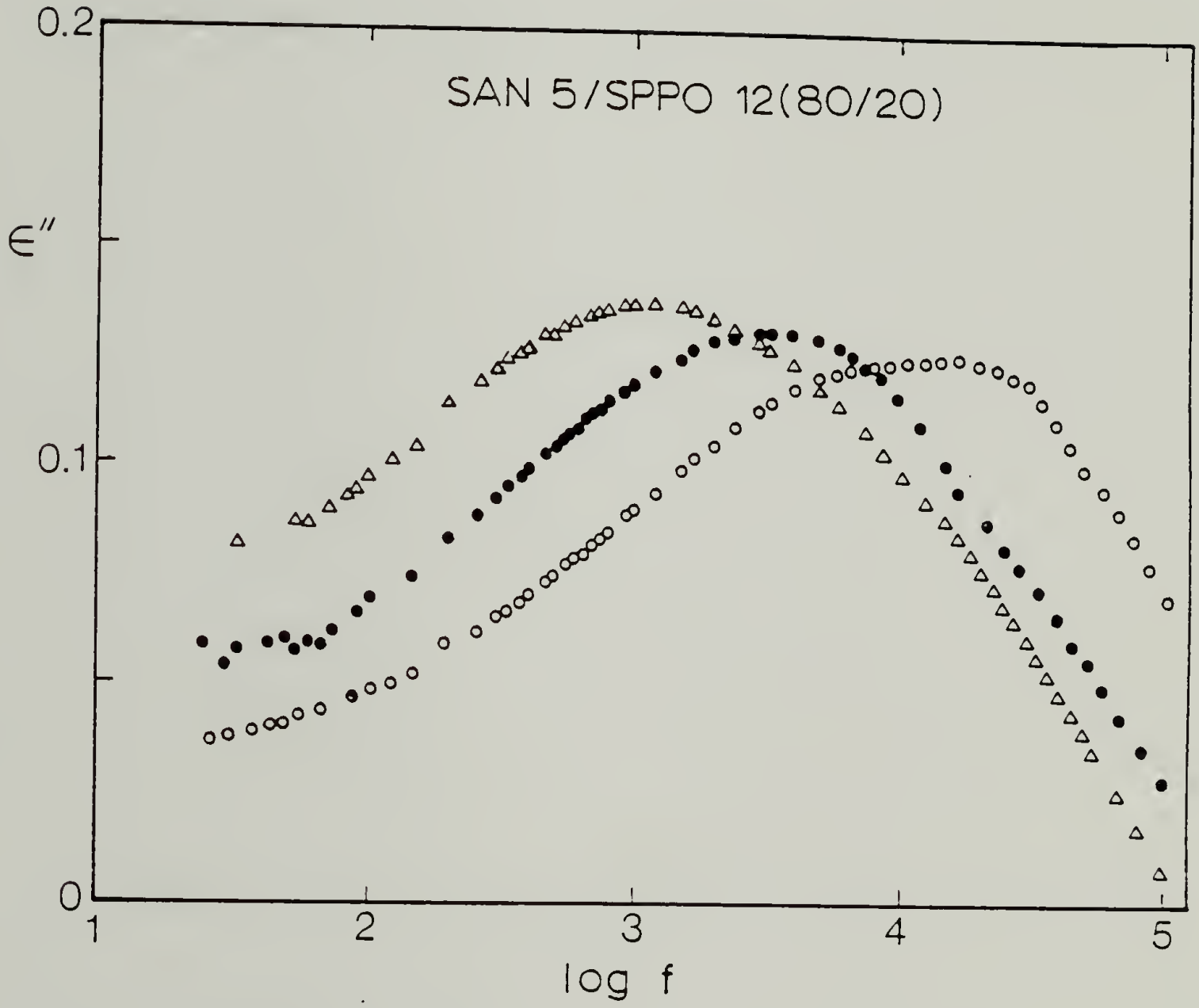

Figure 5.8. (f)

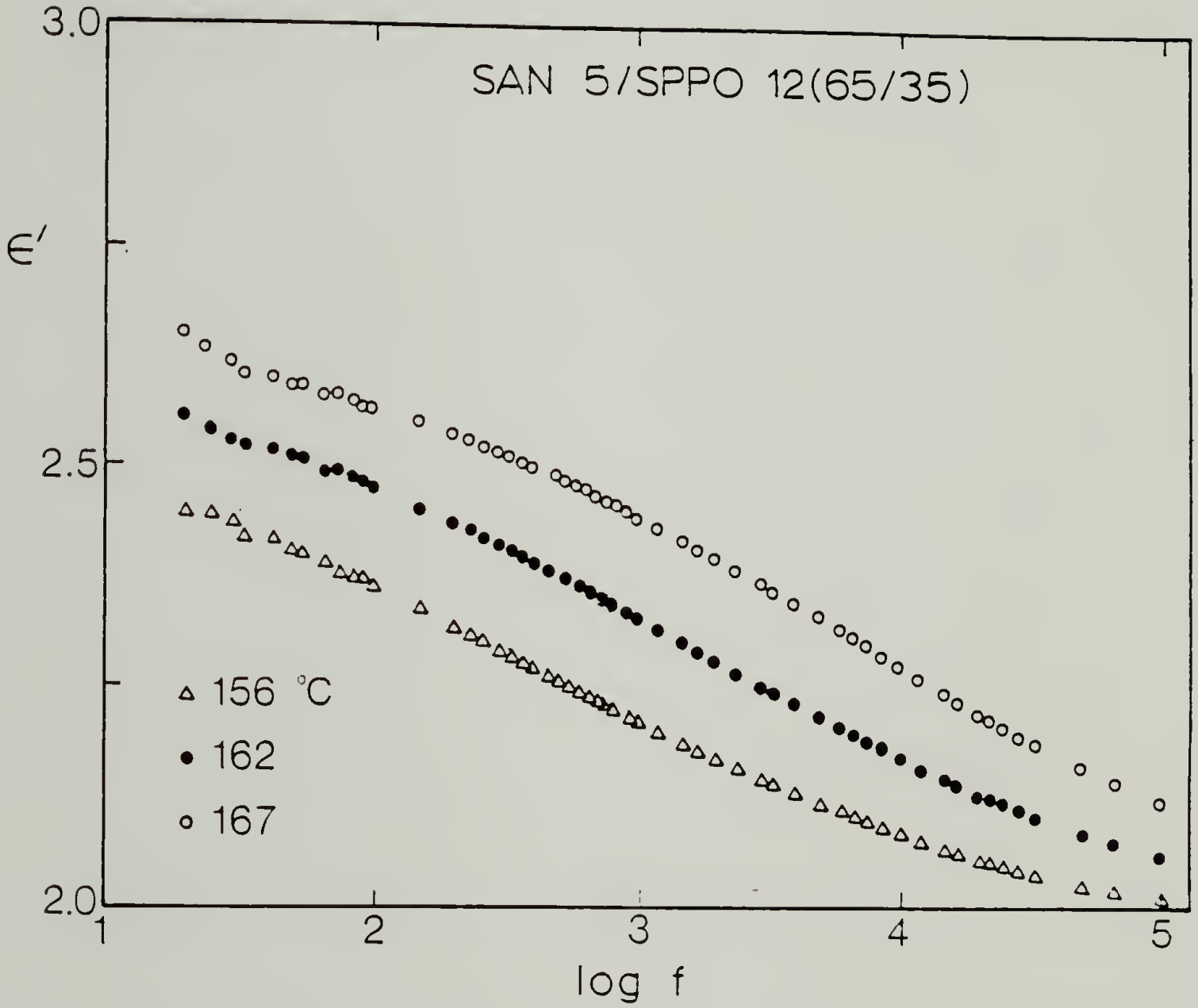

Figure 5.8. (g)

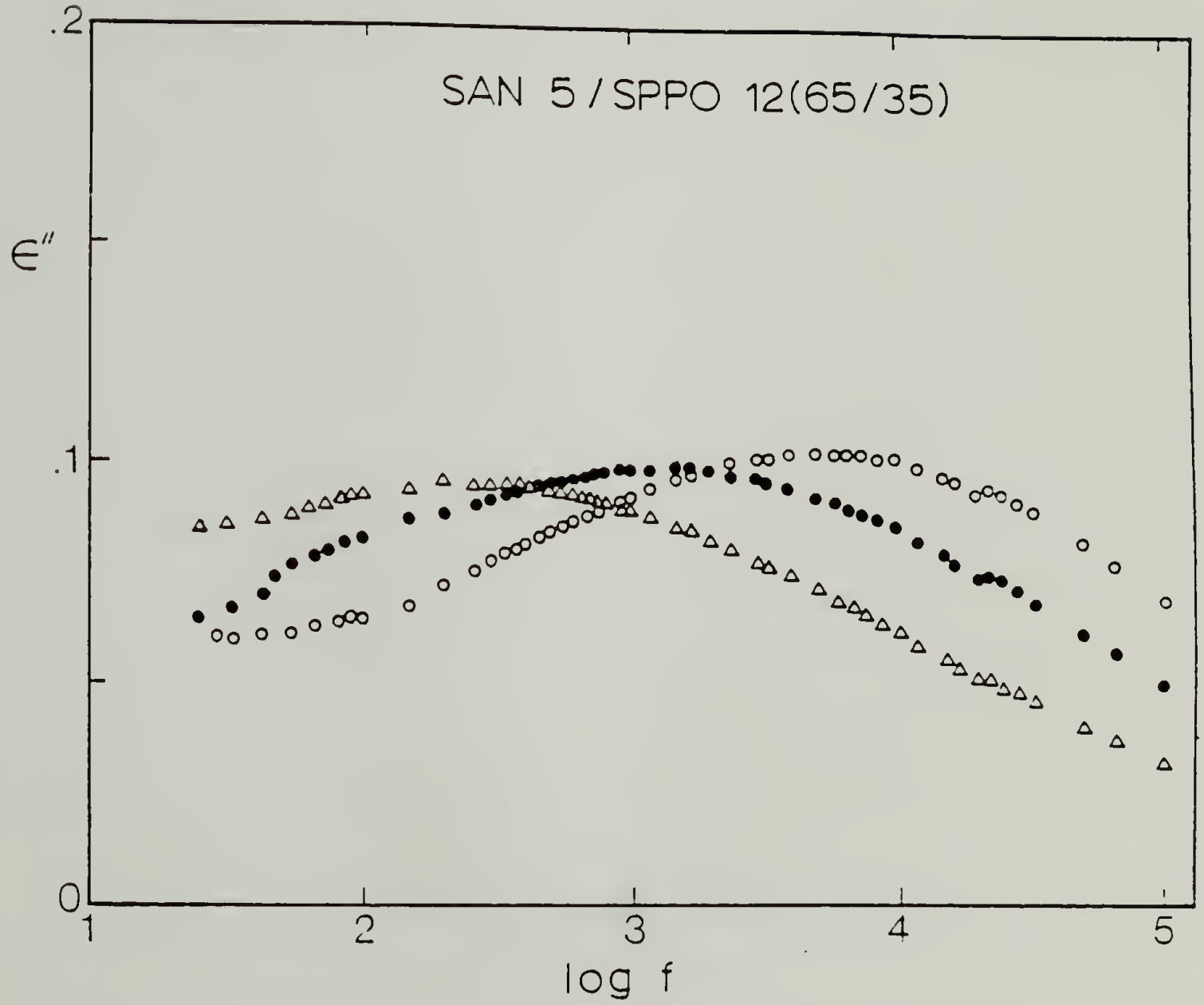

Figure 5.8. (h)

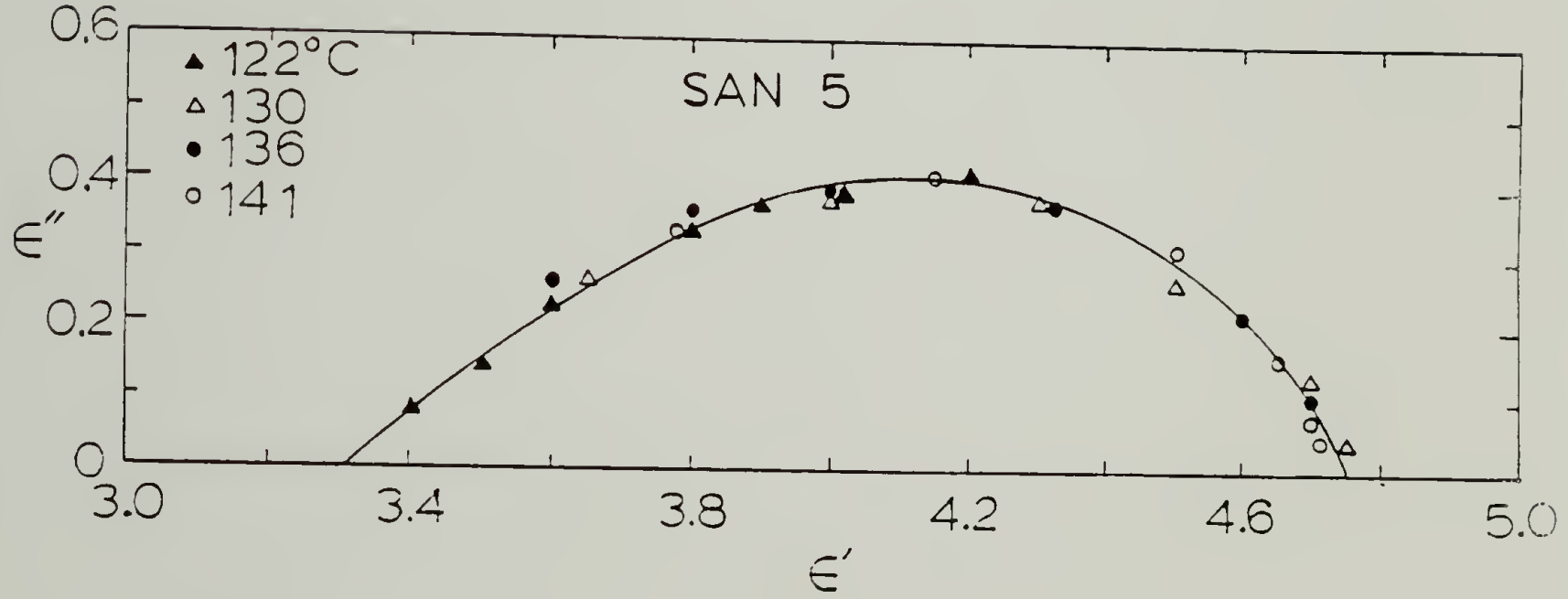

Figure 5.9. (a) Argand diagram for SAN 5; (b) Argand diagrams for the blends of SAN 5/SPPO 12 of varying compositions.

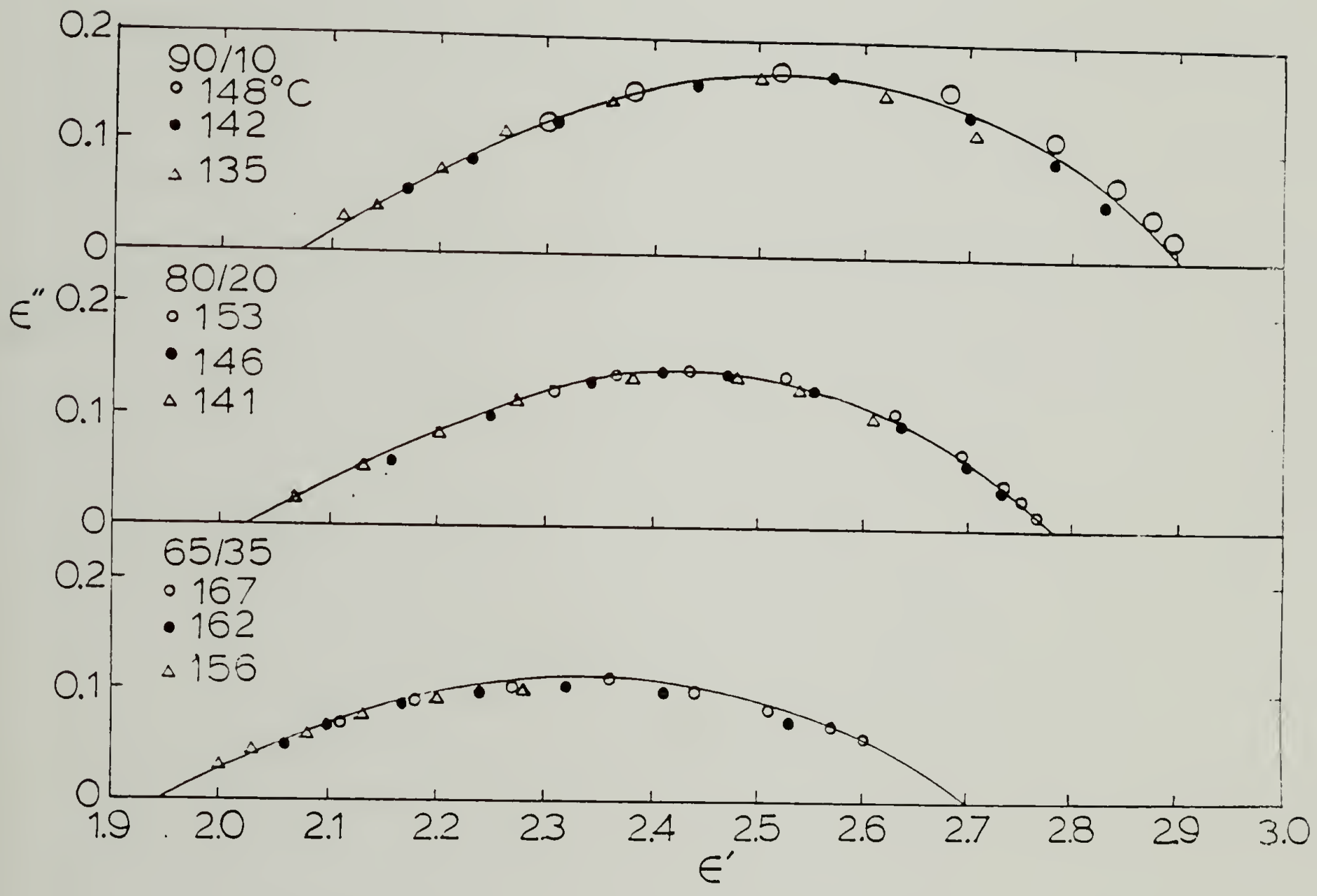
90/10
° 148°C
• 142
△ 135
80/20
° 153
• 146
△ 141
65/35
° 167
• 162
△ 156
0.2
0.1
0
ϵ″
1.9
2.0
2.1
2.2
2.3
2.4
2.5
2.6
2.7
2.8
2.9
3.0
ϵ′

Figure 5.9. (b)

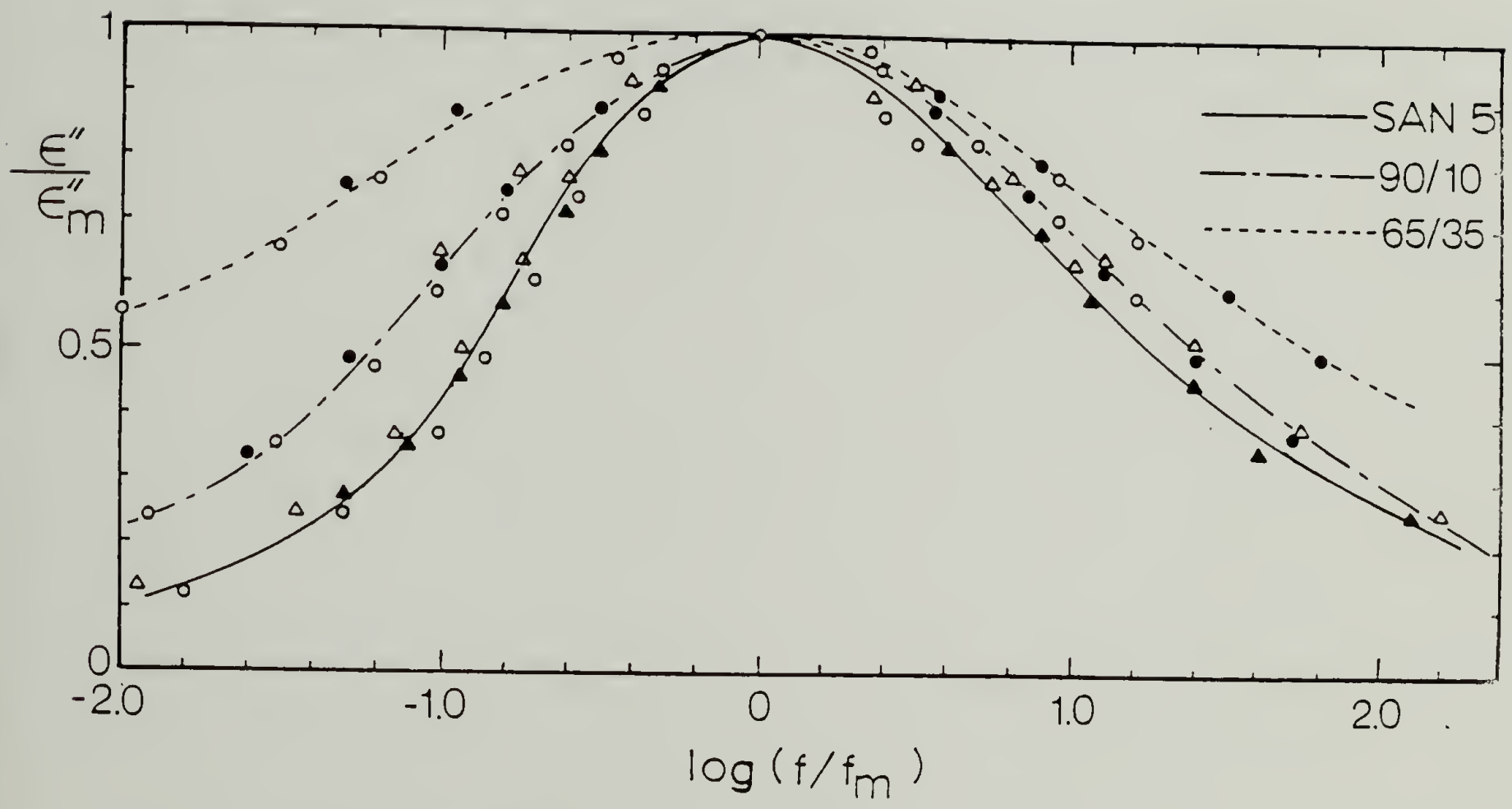

Figure 5.10. Normalized dielectric loss factor curves for SAN 5 and its blends

Table 5.1

Dielectric Parameters for SAN 5 and Its Blends with SPPO 12

Sample	ΔH/ΔL	α	0.5 Width (Decades Frequency)	0.75 Width
SAN 5	1.42	0.41	2.18	1.36
SAN 5/SPPO 12 (90/10)	1.18	0.33	2.62	1.64
SAN 5/SPPO 12 (65/35)	-	0.28	-	2.32

the presence of equilibrium conformational correlation lengths greater than or at least comparable to the dimension of the cooperative relaxing regions.

The Kirkwood-Frohlich correlation parameters [11] (g factors) can provide information on dipole-dipole interactions. Although calculation of g factors for these blends has not been attempted because the g factor for pure SPPO 12 copolymer is under question at present (more specifically, the dipole moment of the gas phase or its model compound of sulfonylated phenylene oxide unit is uncertain), dipole cancellation in the blend due either to the hindered rotation of a molecule relative to its neighbors or to the orientation correlations of the dipoles between polymer chains may be inferred qualitatively from the decreased dielectric strength $\varepsilon_r - \varepsilon_u$, as seen in Figures 5.9 (a)-(b), where ε_r and ε_u refer to the relaxed and unrelaxed dielectric constants corresponding to the low and high frequency limits, respectively. It should be noted that in FTIR spectra, no change in peak position at 2236.74 cm^{-1} corresponding to the absorption frequency of the nitrile group could be seen in SAN 5 and in the 50/50 wt% blend signifying that this dipolar correlation is of a different nature from the intermolecular interaction. Figure 5.11 and 5.12 display the Fourier transform infrared spectra of SAN 5 and its blends with SPPO 12, respectively. Plots of log f_{max} (for the peak in ε'') vs. the reciprocal temperature are displayed for SAN

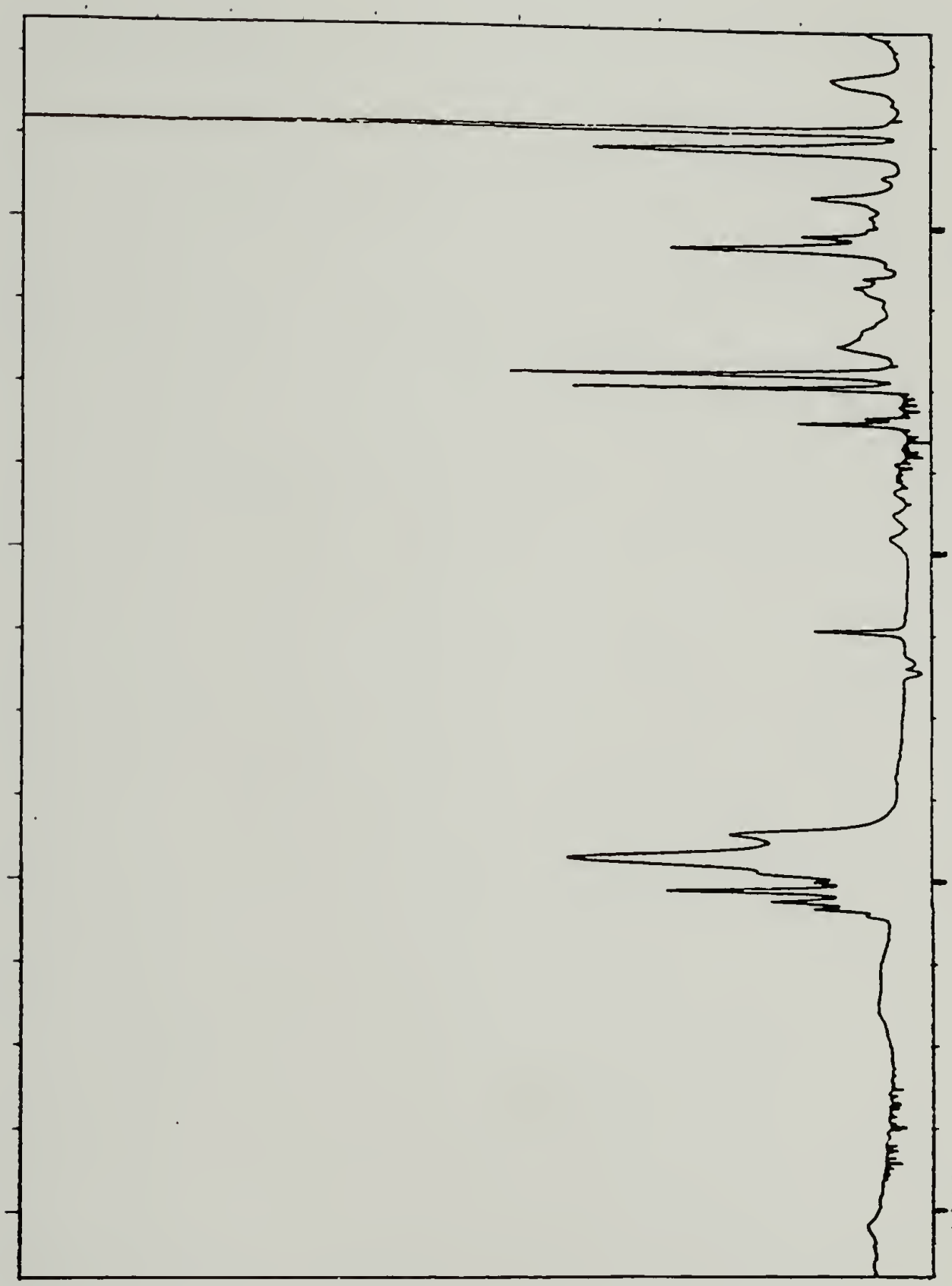

Figure 5.11. Fourier transform infrared spectrum of SAN 5

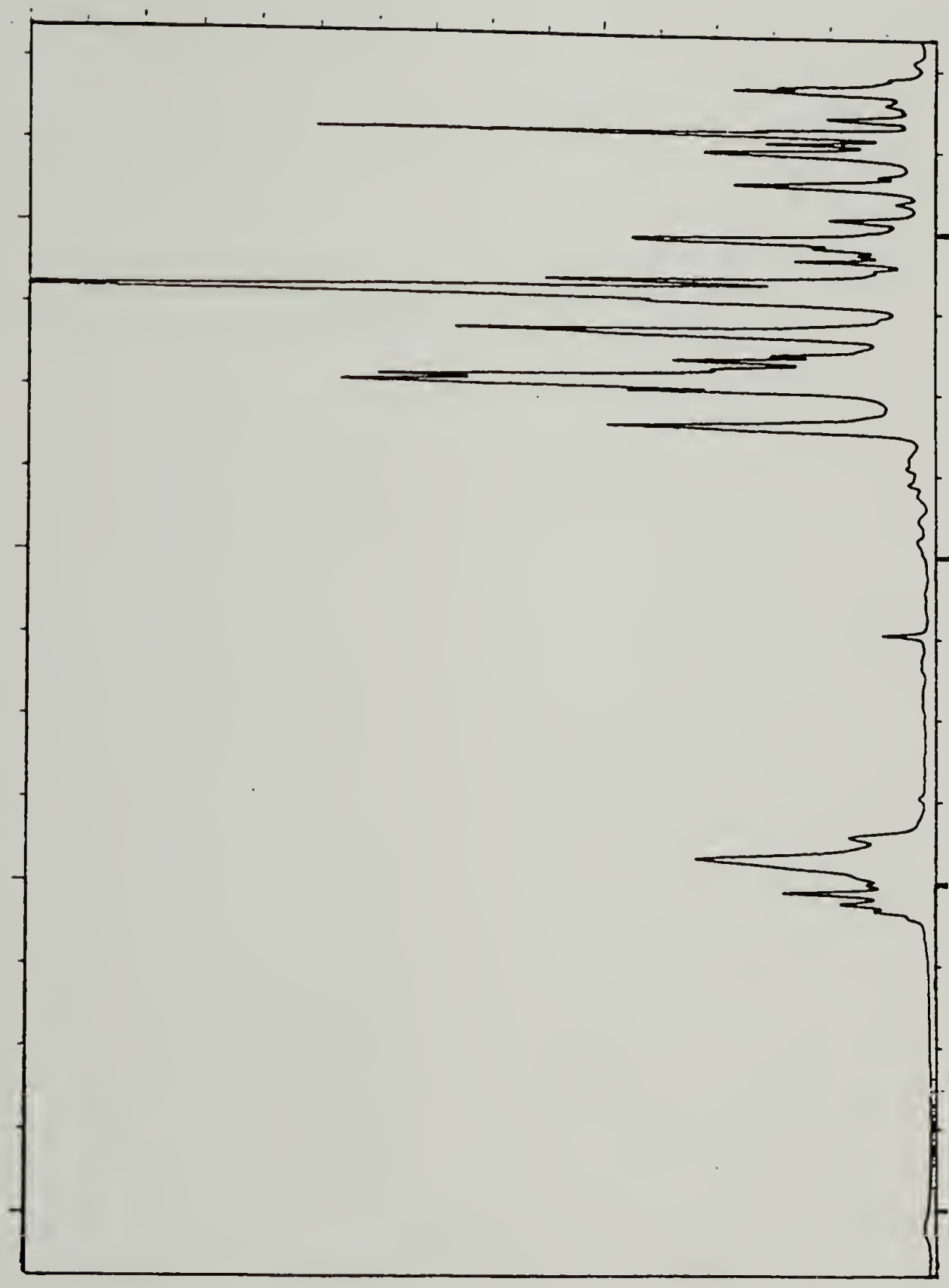

Figure 5.12. Fourier transform infrared spectrum of 50/50 wt% blend of SAN 5/SPPO 12

5 and its blends in Figure 5.13. The data can be represented by straight lines in this region giving higher activation energies with increasing SPPO 12.

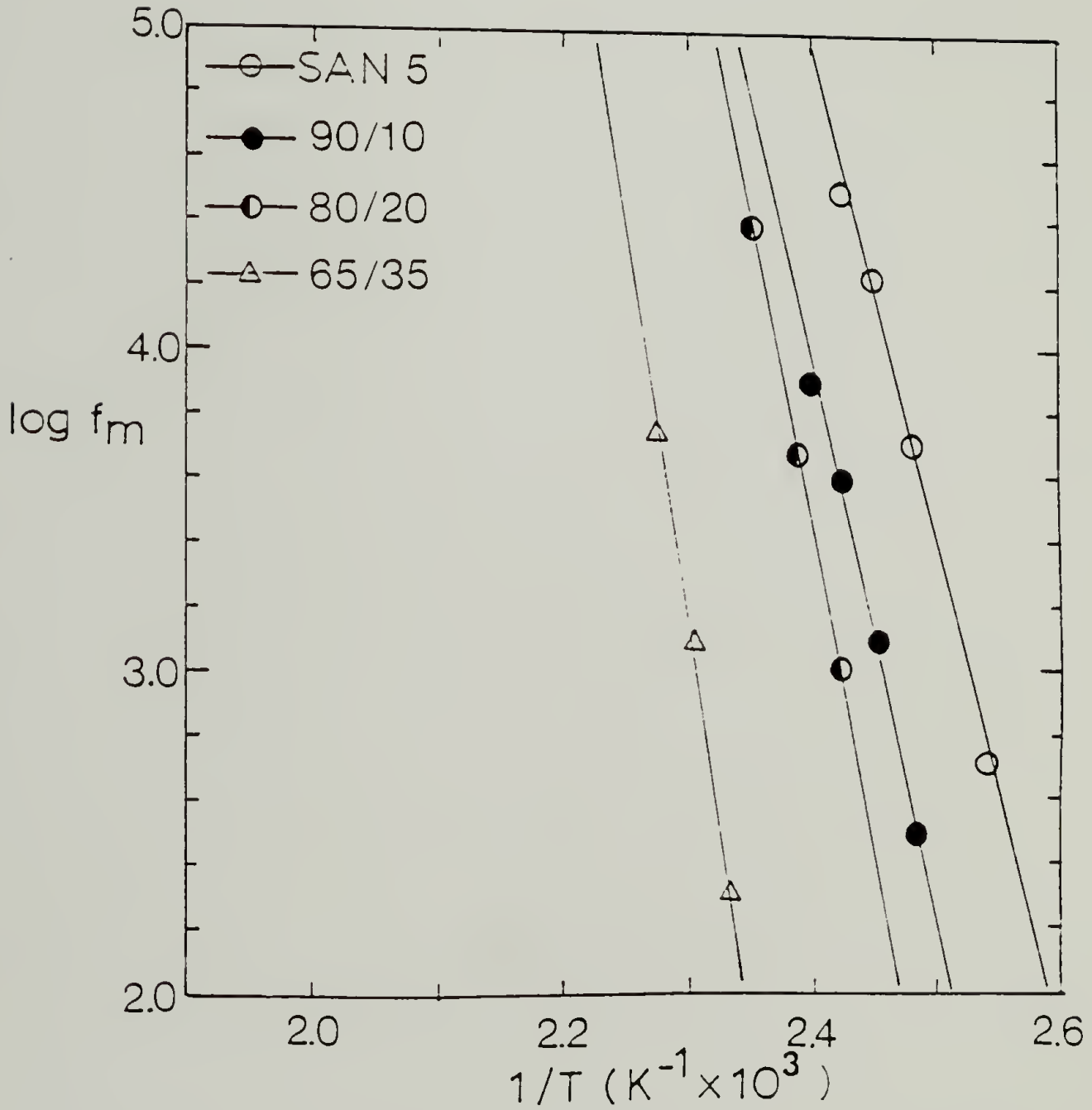

Figure 5.13. Arrhenius plots for SAN 5 and its blends

REFERENCES

1. P.R. Couchman, Macromolecules, 11, 6 (1978).
2. G. ten Brinke, E. Rubinstein, F.E. Karasz, W.J. MacKnight, R. Vukovic, J. Appl. Phys., 56 (9), 2440 (1984).
3. G.E. Molau, J. Polym. Sci., Polym. Lett. Ed., 3, 1007 (1965).
4. O.F. Noel, J.F. Carley, Polym. Eng. Sci., 15, 117 (1975).
5. T.K. Kwei, T. Nishi, R.F. Roberts, Macromolecules, 7, 667 (1974).
6. J.R. Fried, F.E. Karasz, W.J. MacKnight, Macromolecules, 11, 150 (1978).
7. H. Yang, M. Shibayama, R. Stein, N. Shimizu, T. Hashimoto, Macromolecules, 19, 1667 (1986).
8. N.G. McCrum, B.E. Read, G. Williams, "Anelastic and Dielectric Effects in Polymeric Solids", John Wiley and Sons, London, 1967.
9. R.E. Wetton, W.J. MacKnight, J.R. Fried, F.E. Karasz, Macromolecules, 11, 158 (1978).
10. S. Glarum, J. Chem. Phys., 33, 639 (1960).
11. H. Frohlich, Theory of Dielectrics", Oxford University Press, London, 1958.

CHAPTER VI

MISCIBILITY IN BLENDS OF POLY(STYRENE-CO-P(O)-FLUOROSTYRENE) AND POLY(STYRENE-CO-METHYL ACRYLATE) WITH SPPO COPOLYMERS

This chapter describes the studies of miscibility and phase behavior in blends of poly(styrene-co-p(o)-fluorostyrene) and poly(styrene-co-methyl acrylate) with sulfonylated poly(2,6-dimethyl-1,4-phenylene oxide) (SPPO) copolymers, i.e., the blends of the type, $(A_{1-x}B_x)_{n_1}/(C_{1-y}D_y)_{n_2}$. The isothermal composition-composition diagram displaying the miscibility-immiscibility boundary in Cartesian coordinates is interpreted on the basis of a mean field theory, as discussed in Chapter I, through which all χ_{ij}'s are determined. The role of intramolecular interactions in inducing miscibility in copolymer blends without attractive interactions is reemphasized from the discovery of new systems which are miscible because of purely "repulsive interaction".

A. Experimental Section

Materials The preparation and properties of SPPO copolymers were described in Chapter II. Poly(p-fluorostyrene), poly(o-fluorostyrene) and a series of poly(styrene-co-p(o)-fluorostyrene) copolymers with differing compositions were synthesized by Vukovic[1,2] via a free radical polymerization technique. The polymer molecular weights and compositions, cited from this work, are listed in Table 6.1.

A series of poly(styrene-co-methyl acrylate) copolymers was prepared by free radical polymerization in toluene at 60°C, using azobisisobutyronitrile (AIBN) (0.3% based on total monomer weight) as the initiating species. Styrene and methyl acrylate monomers were purified by washing with 10% aqueous solution of sodium hydroxide and then distilled under vacuum. The initiator was purified by recrystallization from methanol. Spectral grade toluene was used without further purification.

The polymerization was stopped at a conversion of ~40% to prevent copolymer composition drift. To terminate polymerization the reaction mixtures were precipitated into a large excess of methanol. The samples were then dried under vacuum at 80°C to constant weight.

Molecular weights were obtained by GPC as described in Chapter II. The polymer compositions were determined by oxygen elemental analysis. T_g determinations were also performed as

Table 6.1

Molecular Weights of Poly(styrene-co-p(o)-fluorostyrene)

Polymer	$\bar{\bar{M}}n(x10^{-5})$	$\bar{\bar{M}}w(x10^{-5})$	$\bar{\bar{M}}w/\bar{\bar{M}}n$
PoFS	0.44	0.84	1.9
P(S-oFS,18*)	0.53	0.95	1.8
P(S-oFS,40)	0.65	1.24	1.9
P(S-oFS,68)	0.68	1.35	2.0
P(S-oFS,77)	0.71	1.39	2.0
PpFS	0.67	1.27	1.9
P(S-pFS,8)	0.54	0.97	1.8
P(S-pFS,16)	0.56	0.99	2.0
P(S-pFS,25)	0.51	0.97	1.9
P(S-pFS,46)	0.52	1.00	1.9
P(S-pFS,55)	0.51	1.04	1.95
P(S-pFS,67)	0.53	1.04	2.0
P(S-pFS,77)	0.50	1.00	2.0

* Numerals represent mole percent of fluorostyrene.

described in Chapter II. Table 6.2 summarizes the relevant data for the copolymers used in this work.

Preparation of blend samples and measurements of glass transition temperatures were carried out as described in Chapter II, except that, in case of the blend of the PPO homopolymer with poly(o-fluorostyrene), blends were prepared by casting films from 2 wt% chloroform solutions. All blend samples were annealed at 290°C in the DSC pan, unless otherwise noted. The critical composition differences in blends of poly(styrene-co-methyl acrylate) which differ only in composition were determined using an optical microscope attached with hot stage (Mettler FP2) and DSC.

B. Results and Discussion

i). Blends of Poly(styrene-co-p-fluorostyrene) with SPPO Copolymers

These systems are of the type $(A_{1-x}B_x)_{n_1}/(C_{1-y}D_y)_{n_2}$ in which A, B, C and D represent styrene, p-fluorostyrene, unsulfonylated phenylene oxide and sulfonylated phenylene oxide units, respectively. Figure 6.1 shows DSC thermograms of blends of poly(styrene-co-p-fluorostyrene, 77) with SPPO 34. A single composition dependent T_g is observed. T_g's of these blends are plotted as a function of blend

Table 6.2

Compositions and Molecular Weights of
Poly(styrene-co-methyl acrylate) Samples

Sample	Monomer feed Methyl Acryl.	Copolymer Composition Methyl Acrylate		$\bar{M}n$	$\bar{M}w$	T_g
	Mole %	Mole %	Wt%	(x 10^{-4})		°C
SMA 15	16.3	17.0	14.5	3.77	7.03	91
SMA 19	25.7	22.2	19.1	3.74	7.30	85
SMA 25	34.7	29.0	25.3	3.95	6.52	80
SMA 31	43.5	34.8	30.7	3.97	7.10	75
SMA 34	50.0	38.2	33.9	4.26	6.90	70

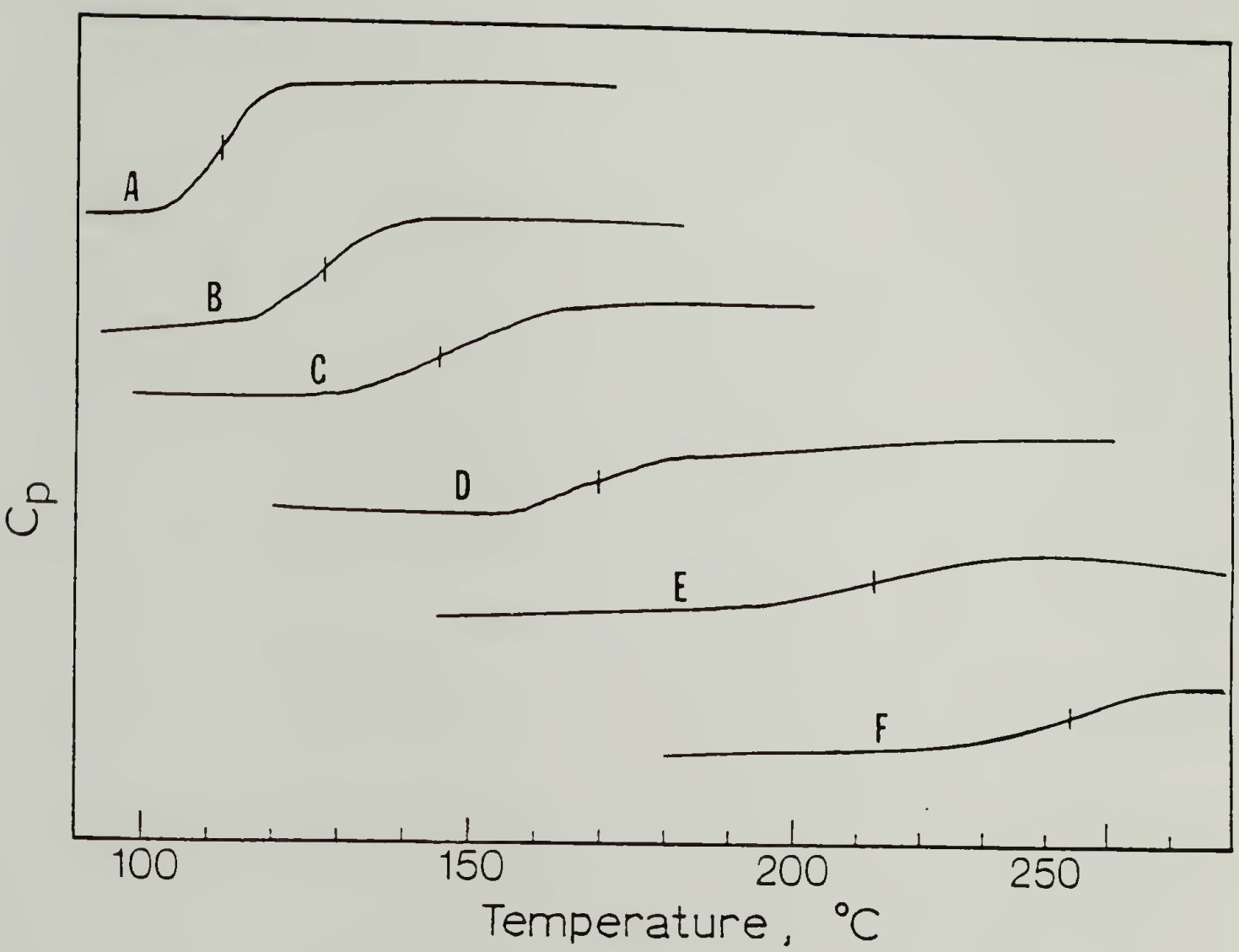

Figure 6.1. DSC thermograms of P(S-pFS, 77), SPPO 34 and blends :
(A) pure P(S-pFS, 77); (B) 25 wt% SPPO 34;
(C) 50 wt% SPPO 34; (D) 70 wt% SPPO 34;
(D) 85 wt% SPPO 34; (F) pure SPPO 34.

composition in Figure 6.2 and fit the predicted values from the Couchman equation[3] reasonably well. The relevant parameters are $\Delta C_p[p(S\text{-}pFS, 77)]=0.26$ J $g^{-1}deg^{-1}$, $T_g=112°C$. The parameters for SPPO 34 were taken from Table 2.2.

Figure 6.3 shows the dependence of T_g on the degree of sulfonylation in 50/50 wt% blends of SPPO with varying degree of sulfonylation with poly(styrene-co-p-fluorostyrene, 77). As seen in Figure 6.3, poly(styrene-co-p-fluorostyrene, 77) copolymers are miscible with SPPO copolymers containing from 20 to 64 wt% sulfonylated units. In all cases the two T_g values observed do not correspond to those of the pure components indicating a separation into mixed phases.

Figure 6.4 shows the experimental isothermal composition-composition diagram displaying the miscibility-immiscibility boundary. In this diagram, the far right abscissa represents the blend of the poly(p-fluorostyrene) homopolymer with SPPO copolymers, a blend of the type $B_{n_1}/(C_{1-y}D_y)_{n_2}$. Setting $\chi_{BC} = 0.055$ and $\chi_{CD} = 0.15$ and by employing an analogous procedure as for the blend system of polystyrene with SPPO copolymers, as discussed in chapter III, χ_{BD} was determined to be 0.02. In this system, even though all three χ_{ij}'s are positive, since $\chi_{CD} >> \chi_{BC}$ and/or χ_{BD}, the blends may have a

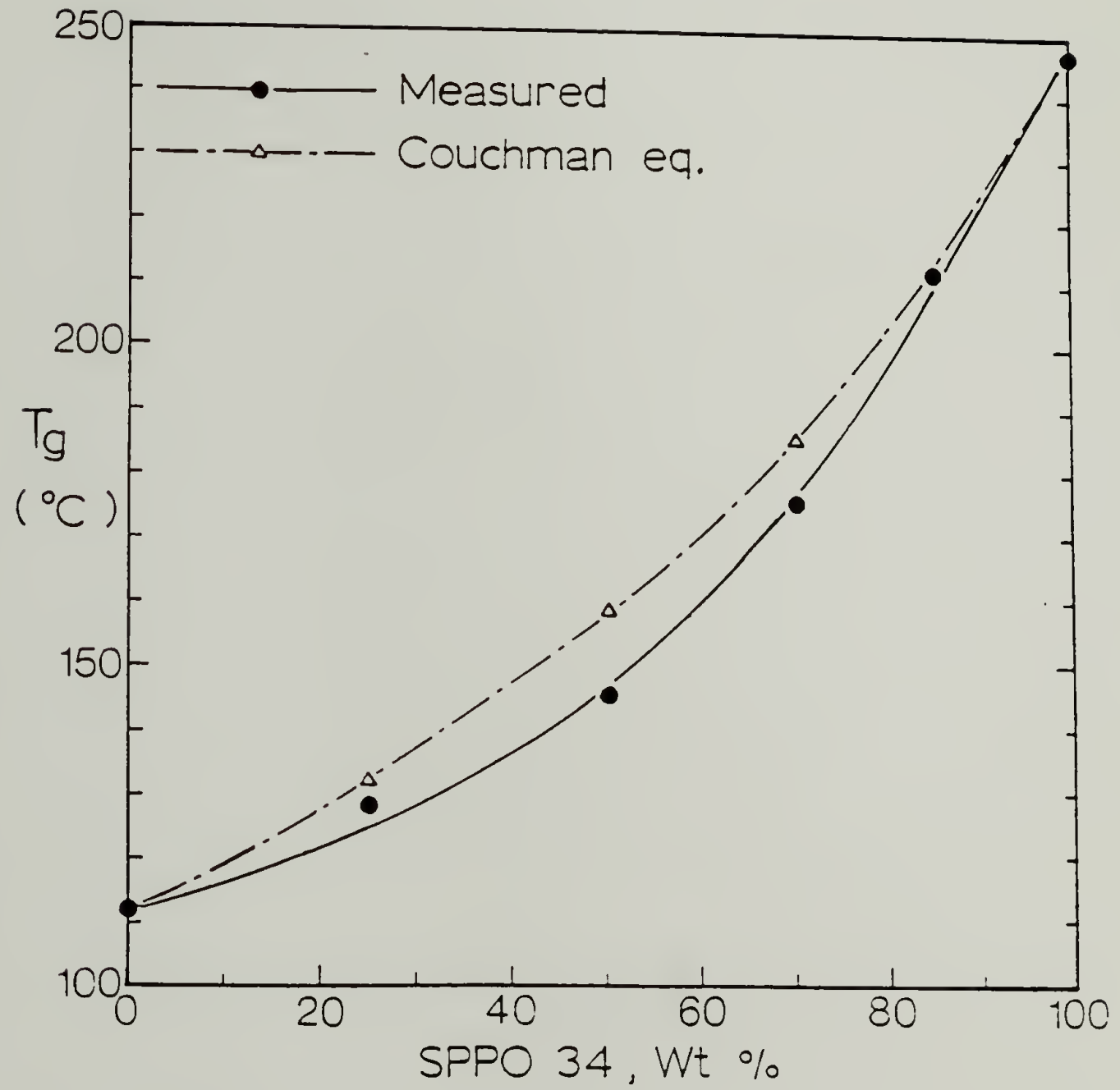

Figure 6.2. Composition dependences of T_g's for the P(S-pFS, 77)/ SPPO 34 blends

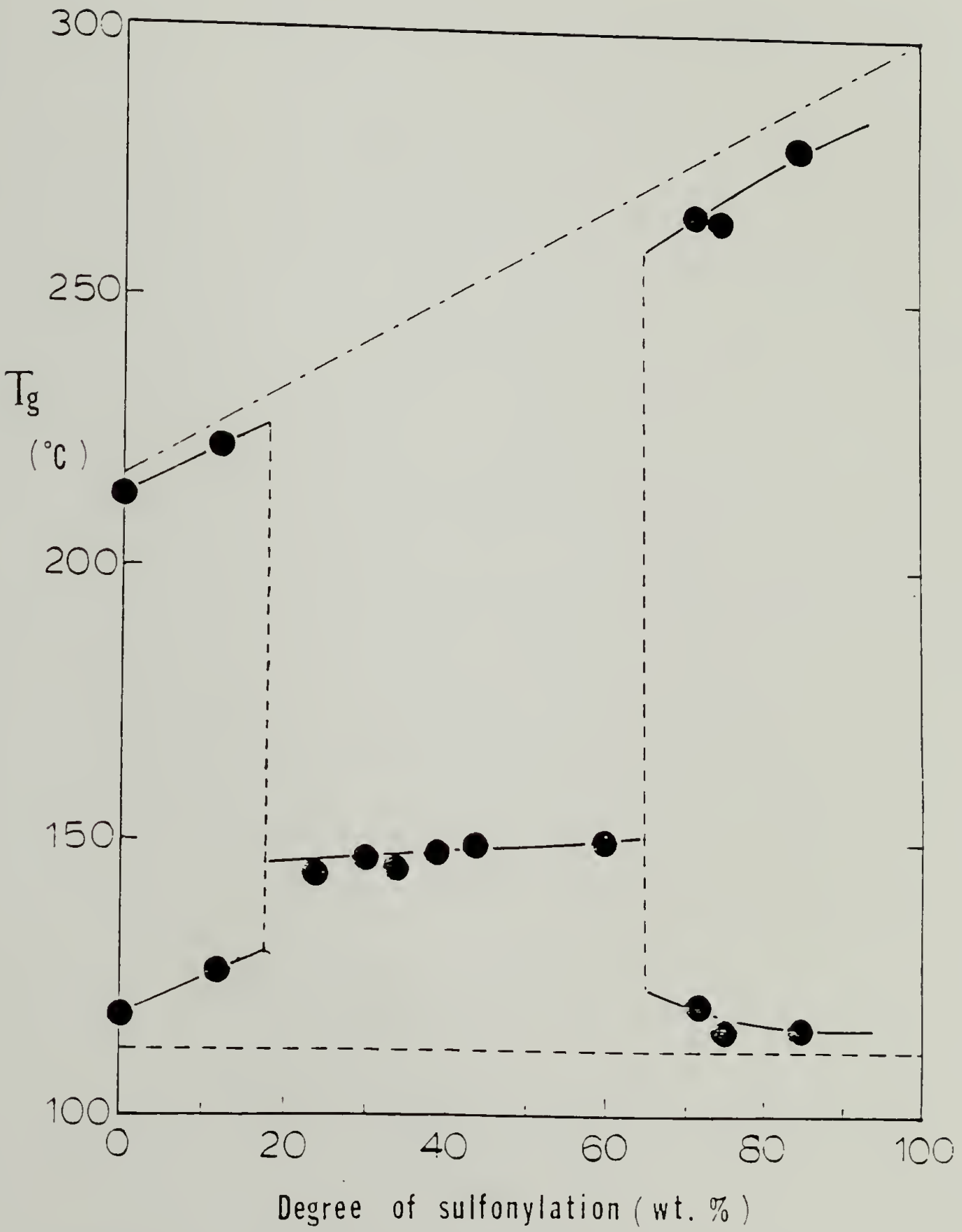

Figure 6.3. T_g's for blends of P(S-pFS, 77)/SPPO copolymers

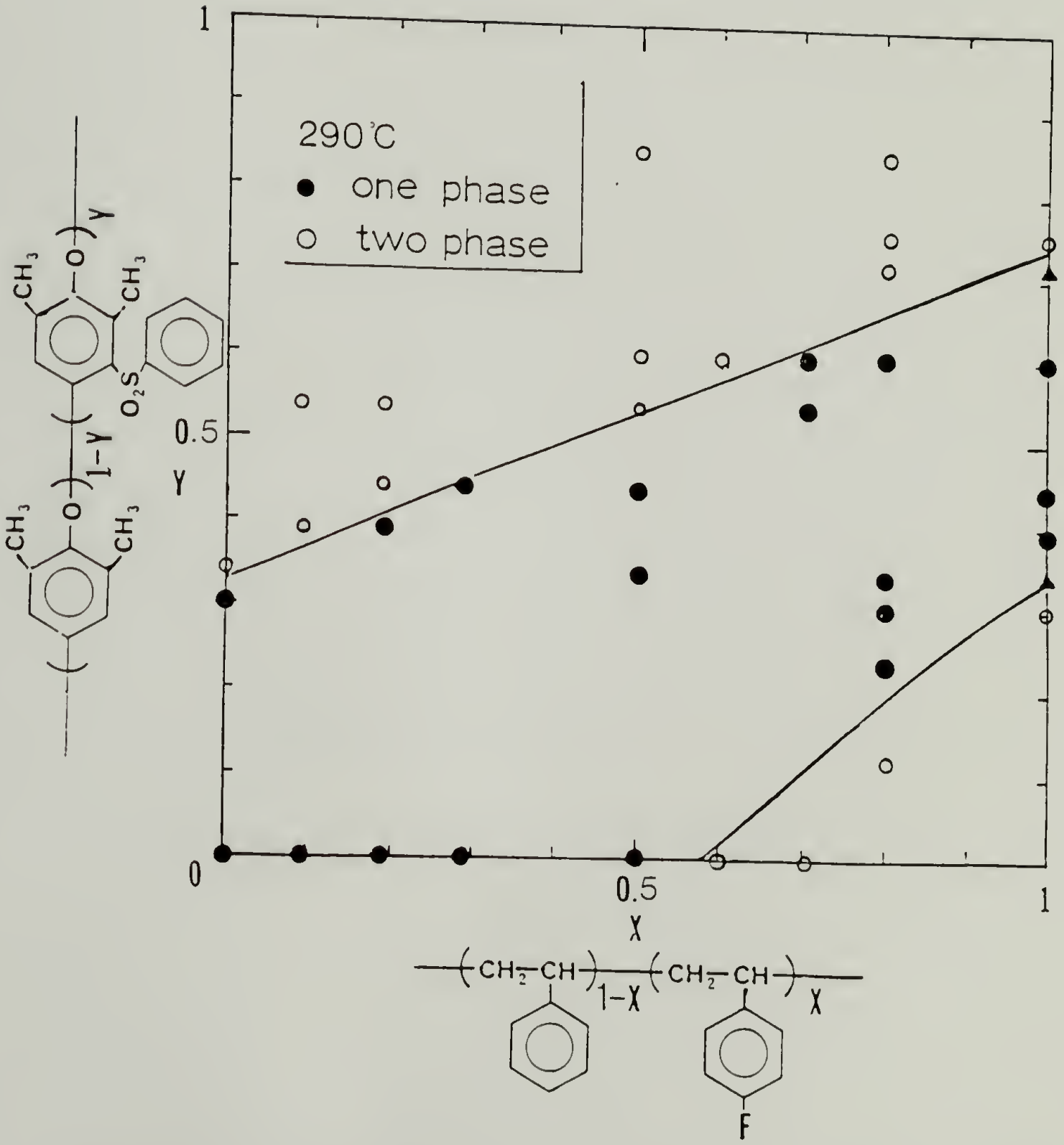

Figure 6.4. Miscibility domain for 50/50 wt% blends of P(S-pFS)/ SPPO copolymers at 290°C

negative exchange interaction owing to "repulsion effects" without any specific interaction. Thus, a "window of miscibility" was observed for SPPO copolymers with a degree of sulfonylation between 33-73 wt%. Figure 6.5 shows the DSC thermograms illustrating the temperature induced phase separation associated with the existence of an LCST ; the results are collected in Figure 6.6. Figure 6.7 also shows the temperature induced phase separation in blends of poly(p-fluorostyrene) with SPPO 34.

In contrast to an argument presented by McMaster[4] that demixing of polymer-polymer mixtures at higher temperature must be expected when the nearest neighbor interaction parameter is negative, LCST phenomena were observed like in blends[5] of PPO/poly(p-chlorostyrene-co-o-chlorostyrene), even though all χ_{ij}'s are positive. The LCST behavior may be explained by unfavorable compressibility contributions outweighing the negative exchange interaction due to "repulsive interactions" at higher temperature.

As seen in Figure 6.6, the greatest miscibility in the blends of poly(p-fluorostyrene) homopolymer with SPPO copolymers can occur at a degree of sulfonylation of approximately 55 wt%. The function f(x,y) is defined by[6]

$$f(x,y) = \chi_{blend} - \chi_{blend}^{crit} \qquad (6.1)$$

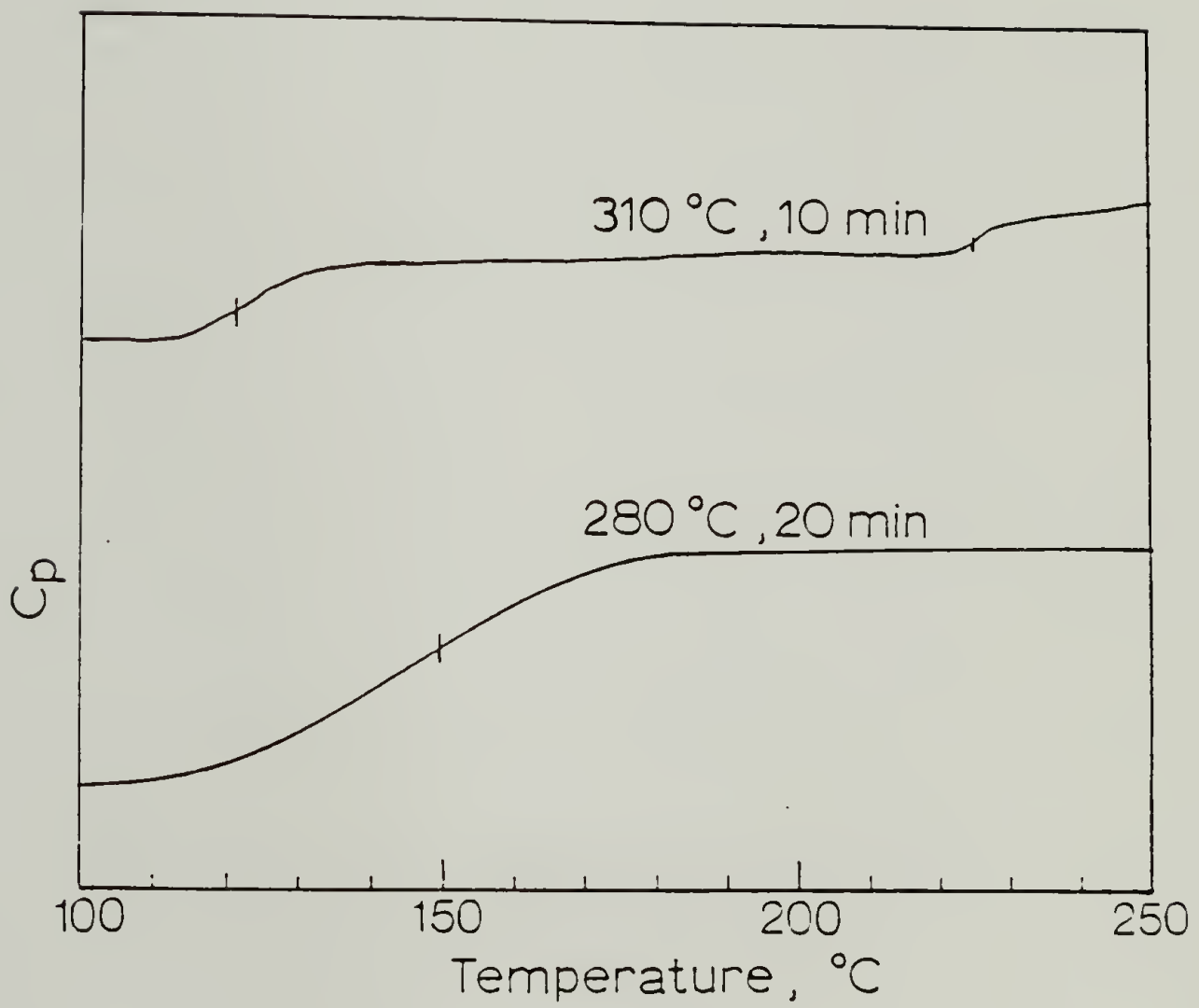

Figure 6.5. DSC thermograms for PpFS/SPPO 34 (50/50 wt% blend)

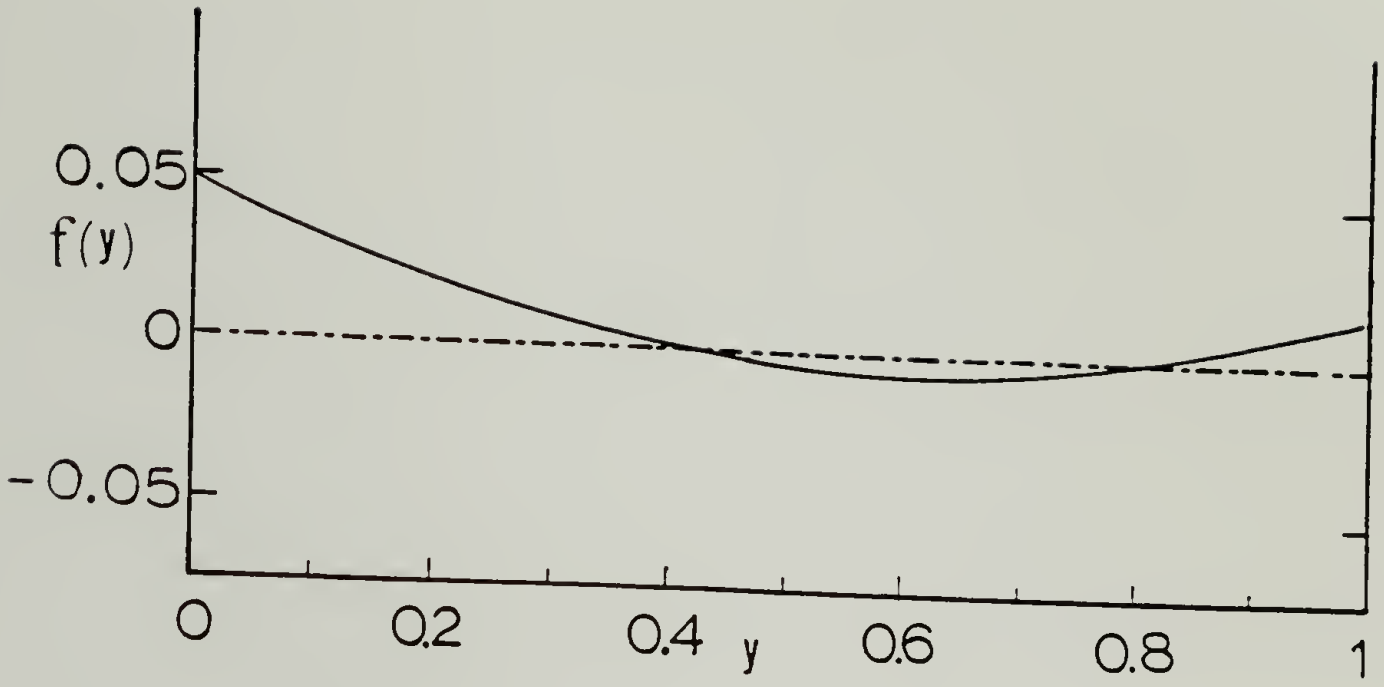

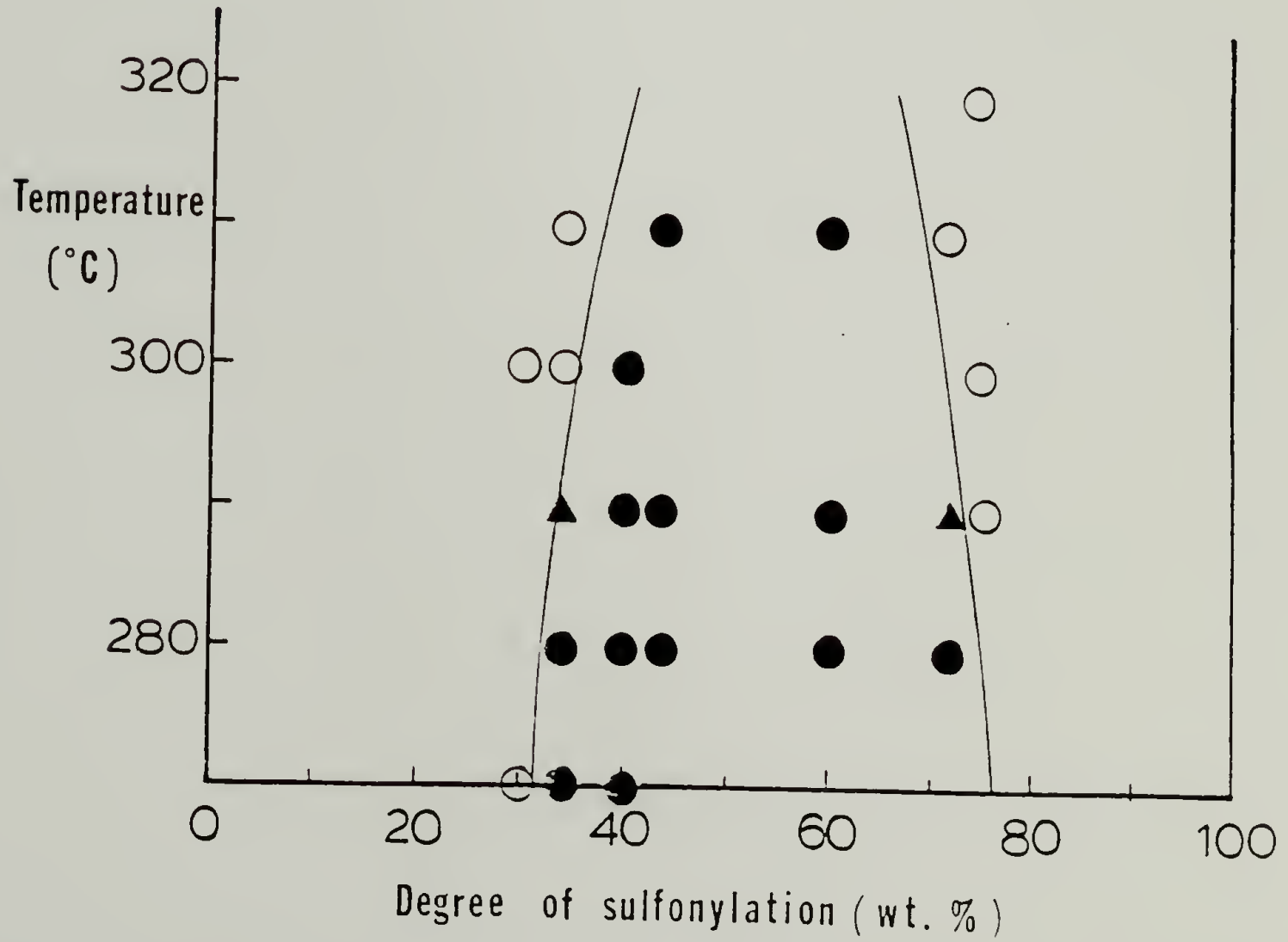

Figure 6.6. Miscibility of PpFS with SPPO copolymers. The insides of the curves represent the miscibility regions.

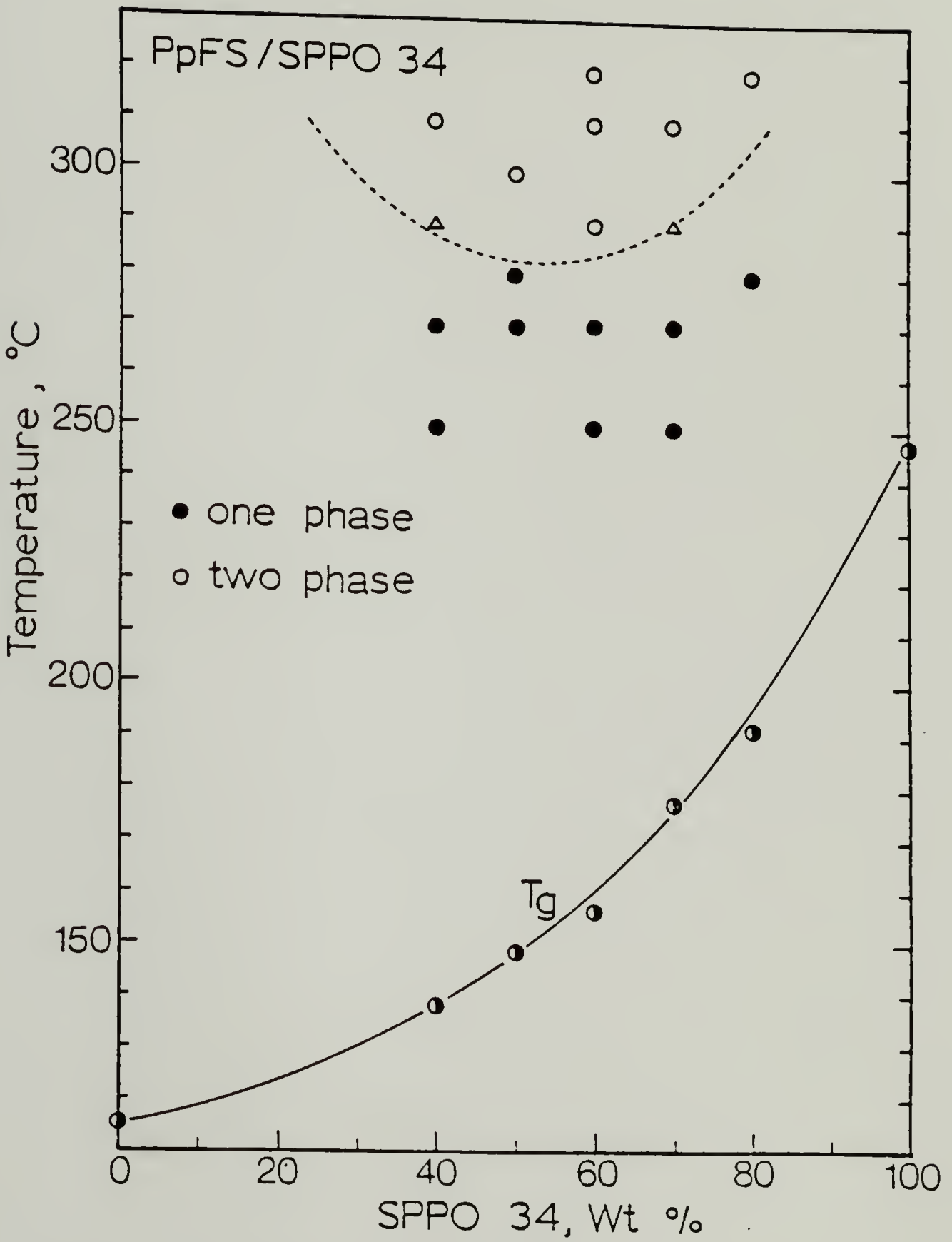

Figure 6.7. Phase diagram for blends of PpFS/SPPO 34

The sign of $f(x,y)$ will determine miscibility or immiscibility in the range of $0 \leq x,y \leq 1$; the region of miscibility will be found if $f(x,y)<0$ and that of immiscibility will be seen if $f(x,y)>0$. The boundary line i.e., the consolute point of the particular blend with a given copolymer composition x and y is represented by $f(x,y)=0$. In the case of the blends of poly(p-fluorostyrene) with SPPO copolymers, the quadratic function $f(y)$ is given by

$$f(y) = (1-y)\chi_{BC} + y\chi_{BD} - y(1-y)\chi_{CD} - \chi_{blend}^{crit}$$

$$= y^2\chi_{CD} + y(\chi_{BD} - \chi_{BC} - \chi_{CD}) + \chi_{BC} - \chi_{blend}^{crit} \qquad (6.2)$$

This function $f(y)$ is a convex function of y for a given temperature. By introducing all the corresponding values into Eqn. (6.2), one obtains

$$f(y) = 0.15y^2 - 0.185y + 0.051$$

$$= 0.15(y - 0.615)^2 - 0.0057 \qquad (6.3)$$

As seen in Figure 6.6, the minimum of $f(y)$ i.e., the maximum miscibility is predicted at $y = 0.62$. This prediction based on a mean field treatment is in reasonable agreement with the experimental findings. As stated earlier, the maximum in the miscibility window occurs at a degree of sulfonylation of 55 wt%.

ii). Blends of Poly(styrene-co-o-fluorostyrene) with SPPO Copolymers

These systems represent blends of the type $(A_{1-x}B_x)_{n_1}/(C_{1-y}D_y)_{n_2}$ in which A, B, C and D represent styrene, o-fluorostyrene, unsulfonylated phenylene oxide and sulfonylated phenylene oxide units, respectively.

Initially, the miscibility behavior of blends of poly(o-fluorostyrene) with PPO was reexamined. In contrast to the results of Vukovic's[1,2], these blends were found to be miscible using films cast from chloroform. It should be noted that Vukovic prepared the blend samples by coprecipitation into methanol from toluene solution. Discrepancies in the assessment of miscibility may be due to incomplete mixing. Figure 6.8 displays the composition dependence of T_g's of the blends. No change in either transition width or T_g could be observed even after annealing up to 310°C. Accordingly, these results imply that χ_{BC} is nearly equal to $\chi_{blend}^{crit} = 0.004$ and, hereafter, a value of $\chi_{BC} = 0.004$ will be adopted.

Figure 6.9 shows the composition dependence of the T_g's for the blends of poly(styrene-co-o-fluorostyrene, 80) with SPPO 12. Figure 6.10 shows the experimental composition-composition diagram demarcating the miscibility and immiscibility boundary. χ_{BD} was

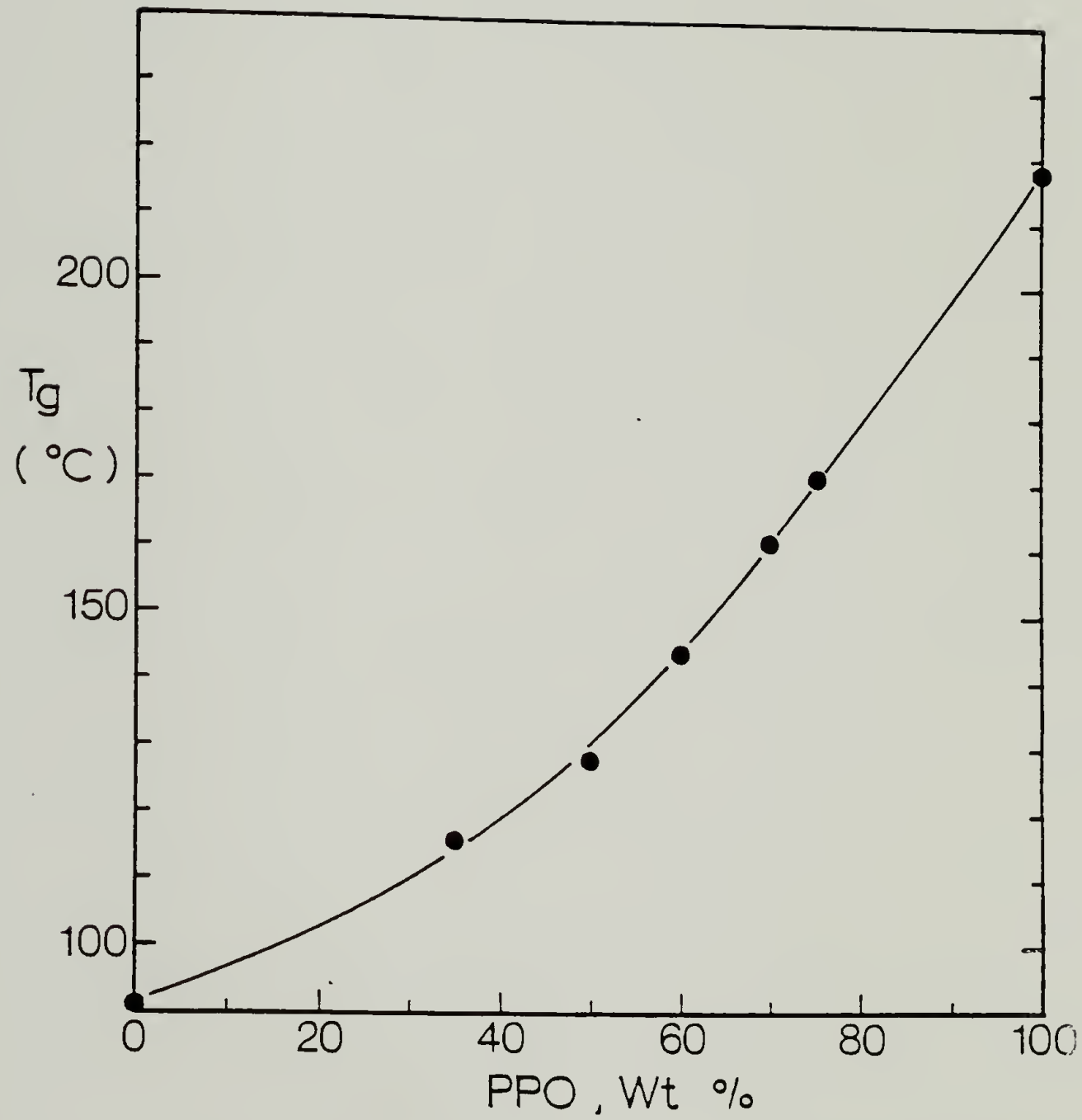

Figure 6.8. Composition dependences of T_g's for blends of PoFS/PPO

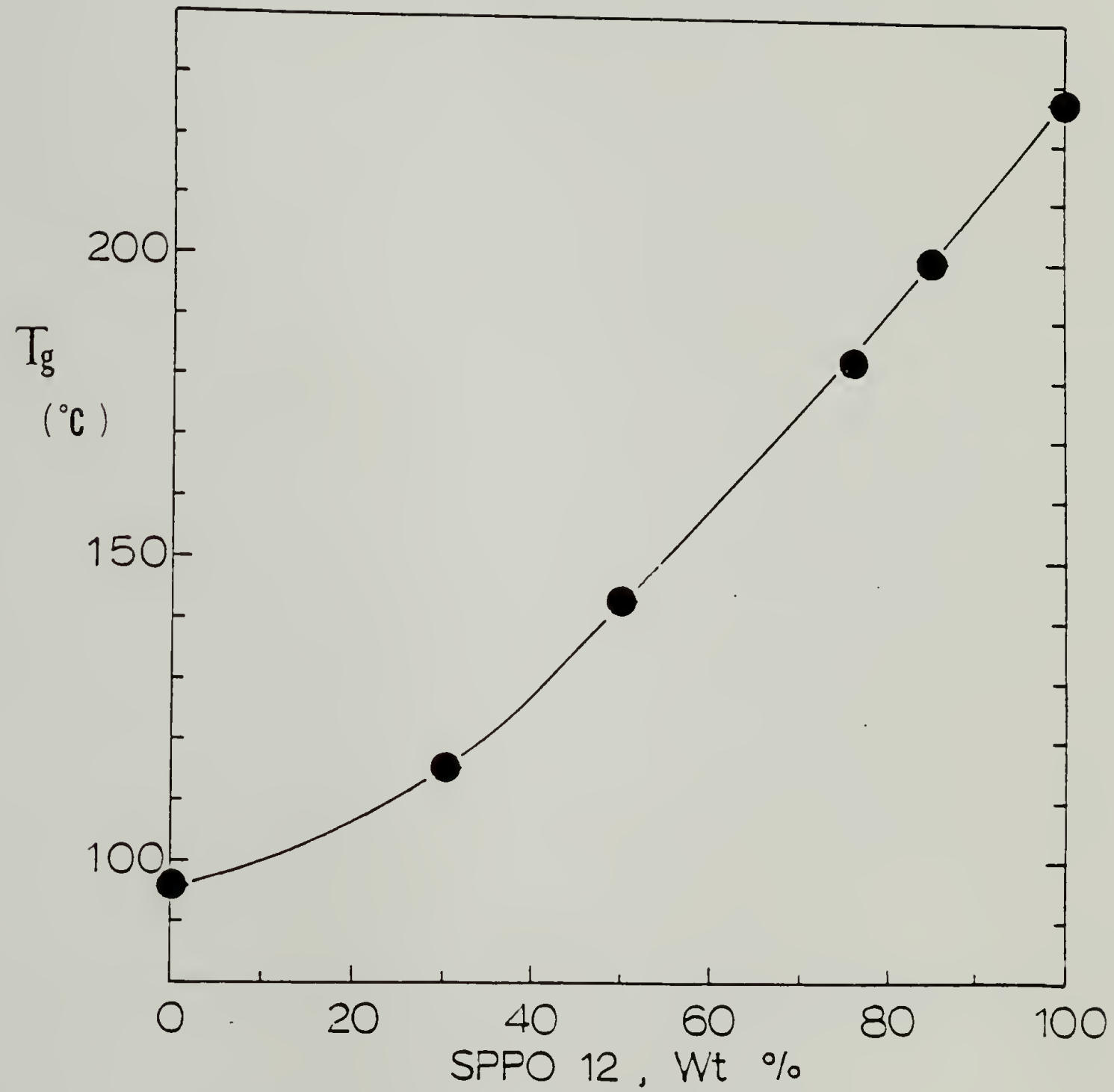

Figure 6.9. Composition dependences of T_g's for blends of P(S-oFS, 80)/SPPO 12

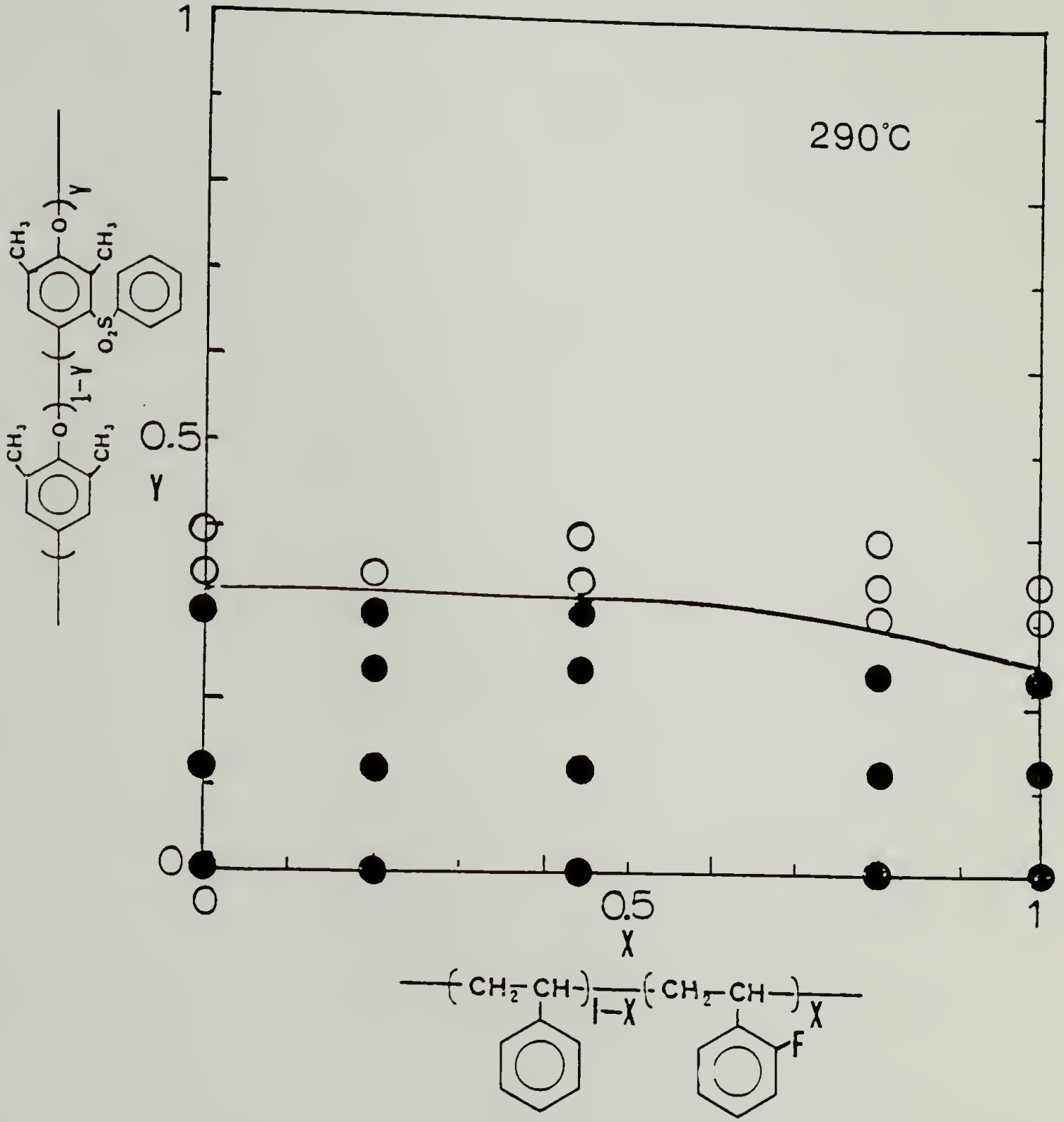

Figure 6.10. Miscibility domain for 50/50 wt% blends of P(S-oFS)/ SPPO copolymers at 290°C

determined to be 0.12 from the critical degree of sulfonylation in the far right abscissa of this diagram. It should be noted that χ_{BD}'s in the systems (I) and (II) are greatly different indicative of the isomeric effect of the fluorine atom. This may be due to polar and size effects of the substituents which affect the polymer-polymer miscibility[7]. From the comparison of miscibility behavior in blends of PPO with copolymers of styrene with various halogenated styrene, Ryan[7] found that p-fluoro substituent of polystyrene has greater power in inducing immiscibility with PPO than an o-fluoro substituent. However, in the current system, the poly(styrene-co-p-fluorostyrene) has a much wider miscibility regime with SPPO copolymers than poly(styrene-co-o-fluorostyrene), which is ascribed to the role of "repulsive interactions" found in the blends of poly(p-fluorostyrene) with SPPO copolymers.

iii). Blends of Poly(styrene-co-methyl acrylate) with SPPO Copolymers

These systems represent blends of the type $(A_{1-x}B_x)_{n_1}/(C_{1-y}D_y)_{n_2}$ in which A, B, C and D represent styrene, methyl acrylate, unsulfonylated phenylene oxide and sulfonylated phenylene oxide units, respectively. Figure 6.11 shows SMA copolymer versus feed composition. Although a series of copolymers over the whole composition range has not been prepared, the reactivity ratios of styrene (1) and methyl acrylate (2) have been evaluated according

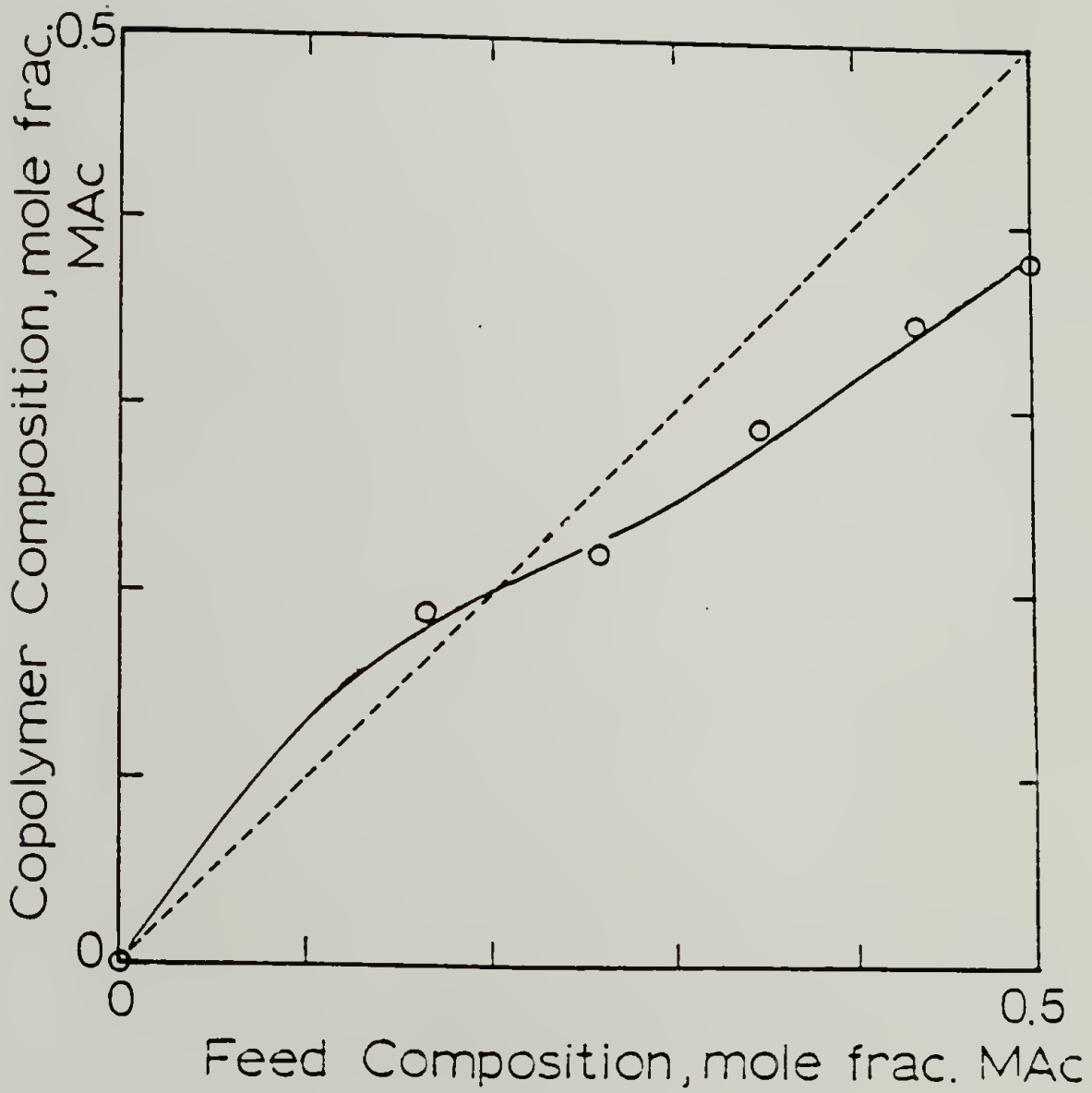

Figure 6.11. SMA copolymer vs. feed composition

to the methods of Fineman and Ross[8]. The reactivity ratios determined (r_1 = 0.95, r_2 = 0.20) are in reasonable agreement with the literature values (r_1 = 0.7, r_2 = 0.15)[9]. Figure 6.12 displays the T_g's of SMA copolymers and a comparison of the compositional variation of T_g to the Fox equation with k=1. The T_g of poly(methyl acrylate) was taken to be 6°C[10]. The calculated T_g values are in reasonable agreement with the experimental values.

To determine a segmental interaction parameter for styrene and methyl acrylate units (χ_{AB}), the miscibility behavior in blends of SMA copolymers which differ only in composition was studied. Figure 6.13 shows a DSC thermogram for 50/50 wt% blend of SMA 15/SMA 34, and indicates phase separation. These blends exhibited no change in phase stability i.e., homogenization of immiscible blends by annealing. On the basis of a series of DSC and optical microscopy studies a miscibility diagram for 50/50 wt% blends of SMA copolymers, as seen in Figure 6.14, could be constructed. The critical composition difference is seen to be 15 wt%. By employing Eqn. (3.2), χ_{AB} is then determined to be 0.13. Figure 6.15 shows the composition-composition diagram ("C-C plots") displaying the miscibility-immiscibility boundary for 50/50 wt% blends at 290°C. Figure 6.15 indicates that the critical methyl acrylate content for

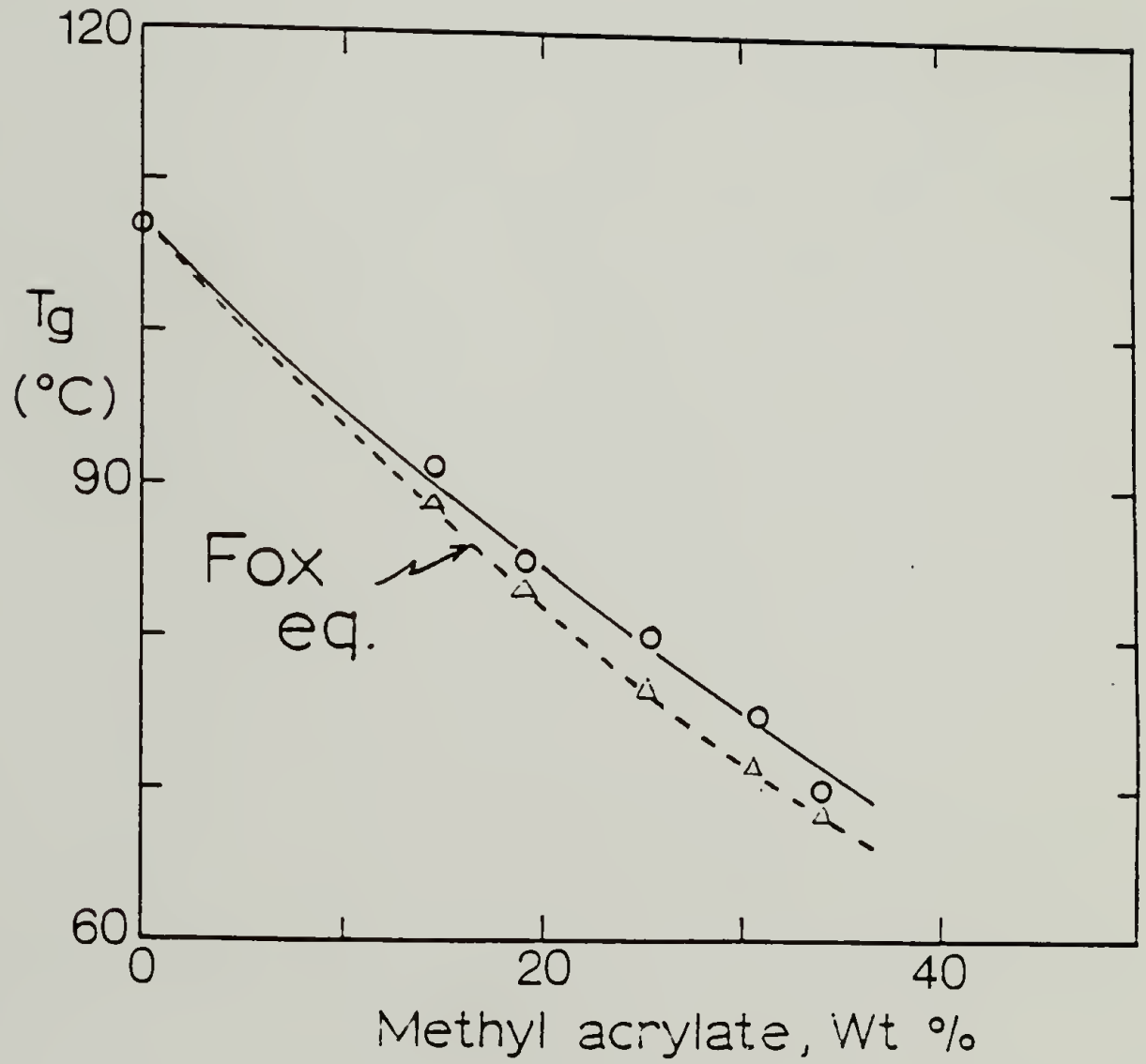

Figure 6.12. T_g's of SMA copolymers

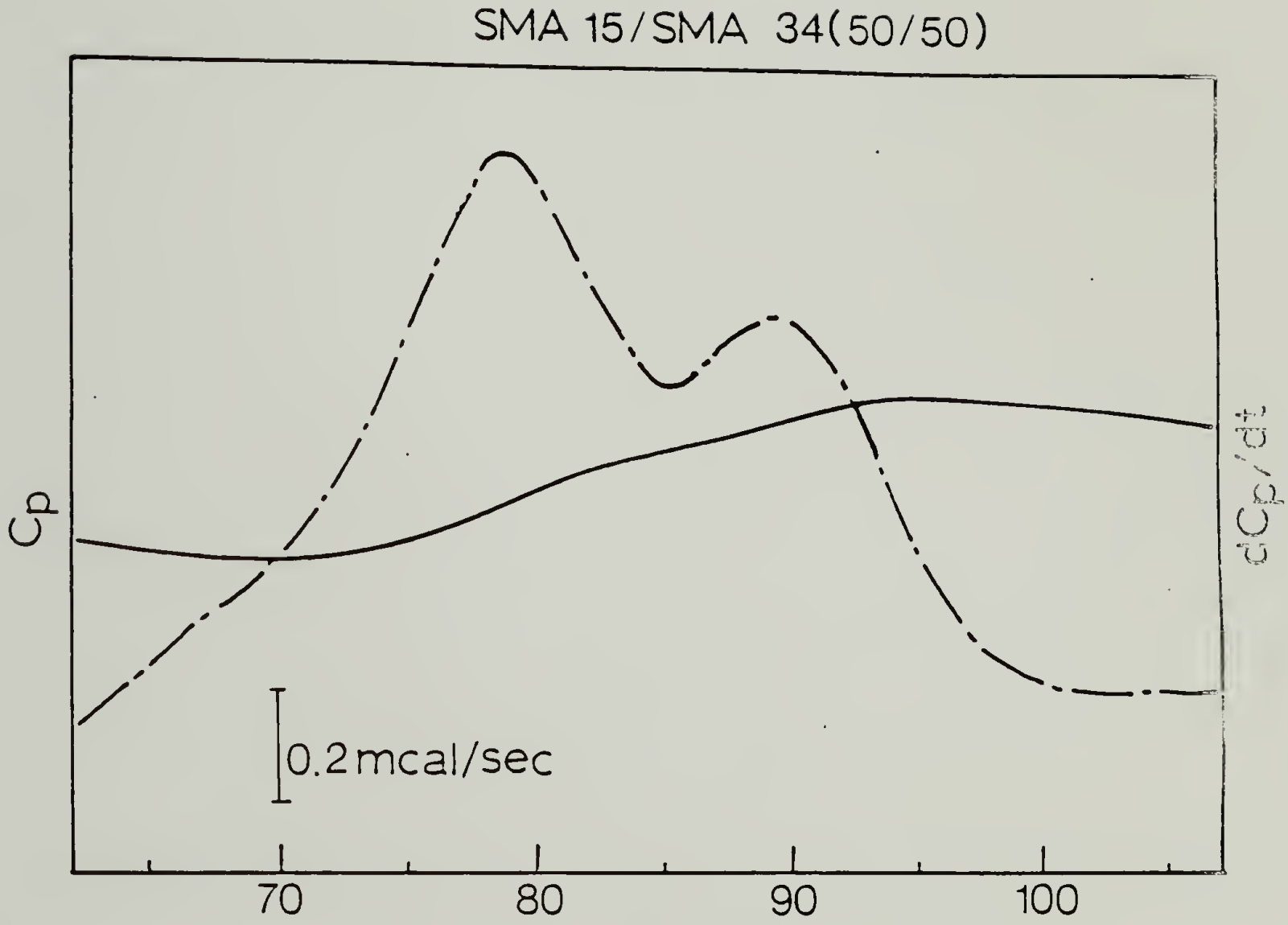

Figure 6.13. DSC thermogram for 50/50 wt% blend of SMA 15/SMA 34

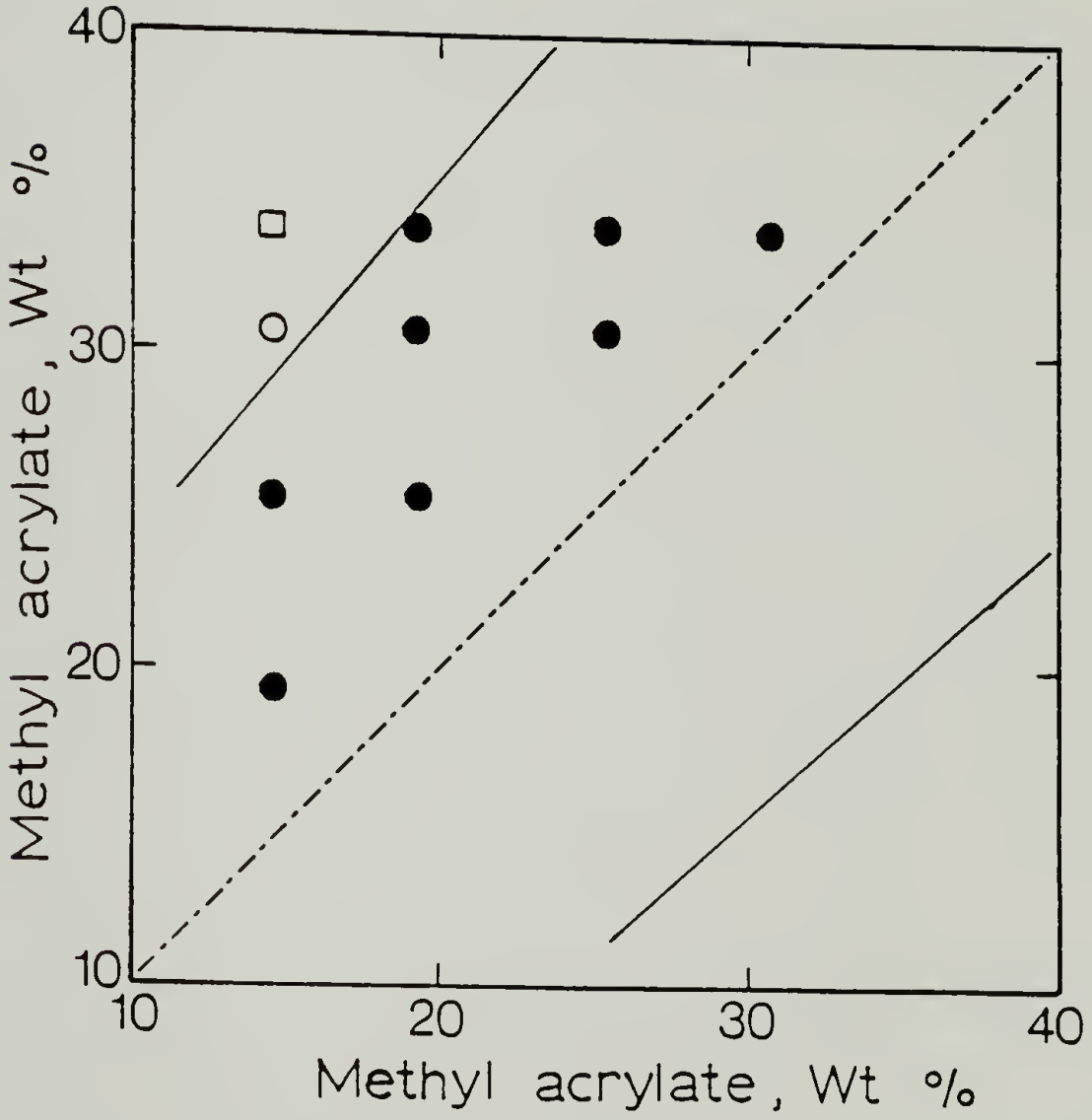

Figure 6.14. Miscibility diagram for 50/50 wt% blends of SMA copolymers

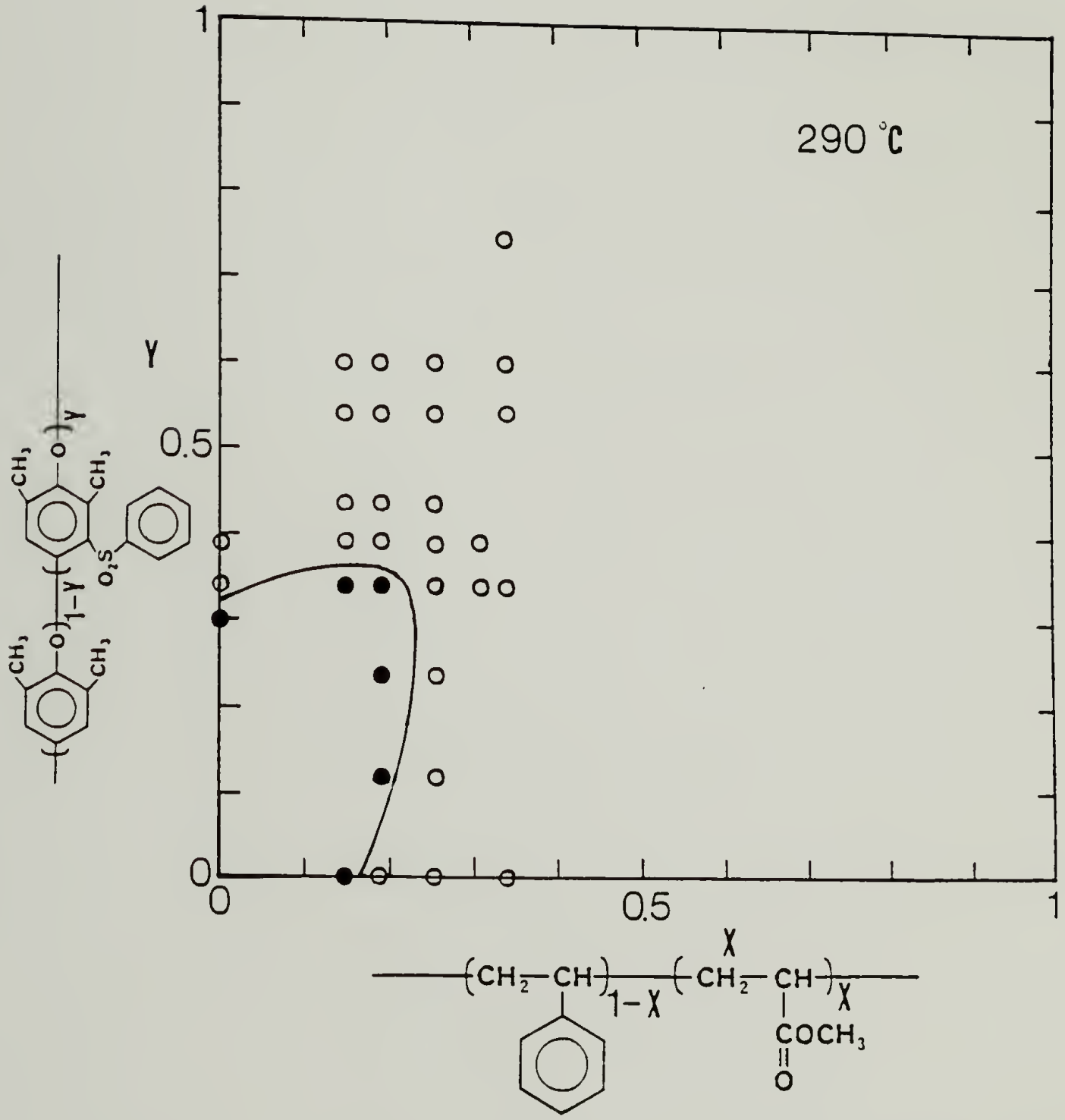

Figure 6.15. Miscibility domain for 50/50 wt% blends of SMA copolymers with SPPO copolymers at 290°C

miscibility in blends of SMA copolymers with PPO homopolymer is 18wt%. By employing Eqn. (5.2) χ_{BC} is determined to be 0.32.

REFERENCES

1. R. Vukovic, F.E. Karasz, W.J. MacKnight, J. Appl. Polym. Sci., 28, 219 (1983).
2. R. Vukovic, V. Kuresevic, F.E. Karasz, W.J. MacKnight, Thermochimica Acta, 54, 349 (1982).
3. P.R. Couchman, Macromolecules, 11, 6 (1978).
4. L.P. McMaster, Macromolecules, 6, 760 (1973).
5. P.S. Alexandrovich, F.E. Karasz, W.J. MacKnight, Polymer, 18, 1022 (1977).
6. T.Shiomi, F.E. Karasz, W.J. MacKnight, Macromolecules, 19, 2274 (1986).
7. C.L. Ryan, Ph.D. Thesis, University of Mass., 1979.
8. M. Fineman, S.D. Ross, J. Polym. Sci., 5, 756 (1956).
9. C.S. Marvel, R. Schwen, J. Amer. Chem. Soc., 79, 6003 (1957).
10. K.H. Illers, Kolloid Z. Z. Polym., 190, 16 (1963).

CHAPTER VII

CONCLUSIONS

A. Geometric Analysis of the Miscibility-Immiscibility Boundary

According to a mean field treatment, as described in Chapter I, from arrangement of Eqn. (1.14), χ_{blend} is given by

$$\chi_{blend} = \chi_{AB}x^2 + (\chi_{AC} - \chi_{BC} - \chi_{AD} + \chi_{BD})xy + \chi_{CD}y^2 + (\chi_{BC} - \chi_{AC} - \chi_{AB})x + (\chi_{AD} - \chi_{AC} - \chi_{CD})y + \chi_{AC} \qquad (7.1)$$

The function f(x,y) is defined by

$$f(x,y) = \chi_{blend} - \chi_{blend}^{crit} \qquad (7.2)$$

In a miscibility regime displayed in a Cartesian coordinate system in which the abscissa and ordinate represent the compositions of the respective copolymers, the boundary line demarcating the miscibility-immiscibility region is given by f(x,y) = 0. This function is a generalized form of the quadratic equation. Depending upon the set

of segmental interaction parameters this function can describe a straight line, circle, ellipse, parabola or hyperbola. Table 7.1 summarizes coefficients of x, y and the cross term, xy. x and y coefficients for all the systems except SMA copolymer systems are negligible compared with xy coefficients which are related to axial rotation . Figure 7.1 displays a comparison of the experimentally determined and calculated miscibility domains, employing values listed under each diagram and a computer program listed in the Appendix I. The calculated and experimental results are in reasonably good agreement and all the miscibility domains include x,y = 0 corresponding to the miscibility of the homopolymers A and C. A diagnostic test to determine the shapes of curves may be helpful. In the generalized form of equation

$$ax^2 + bxy + cy^2 + dx + ey + f = 0 \qquad (7.3)$$

if $(b^2 - 4ac) < 0$, then the curve will be an ellipse

$= 0$, a parabola

> 0, a hyperbola

Table 7.1 also includes values of $(b^2 - 4ac)$. From these values the miscibility and immiscibility boundaries for p(S-AN) and P(S-pFS) systems are considered to have forms of a pair of hyperbolas. The miscibility regions for p(S-oFS) and SMA systems are considered to be contained by ellipses.

Table 7.1

Coefficients of x, y and xy for Geometric Analysis

	x	y	xy	b^2-4ac
poly(styrene-co-acrylonitrile) system	0.088	0.093	-0.891	0.374
poly(styrene-co-p-fluorostyrene)	0.016	0.093	-0.274	0.027
poly(styrene-co-o-fluorostyrene)	0.007	0.093	-0.134	-0.006
poly(styrene-co-methyl acrylate)	0.183	0.093	-0.513	

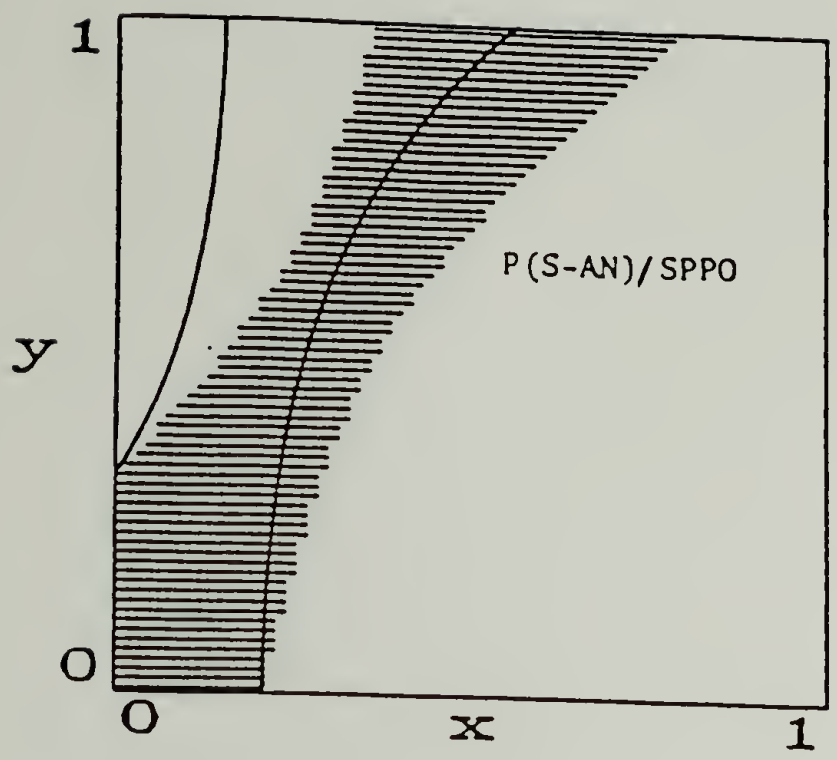

χ_{AB}= 0.700 χ_{AC}= -0.043 χ_{AD}= 0.200

χ_{BC}= 0.745 χ_{BD}= 0.097 χ_{CD}= 0.150

χ^{crit}_{blend}= 0.003

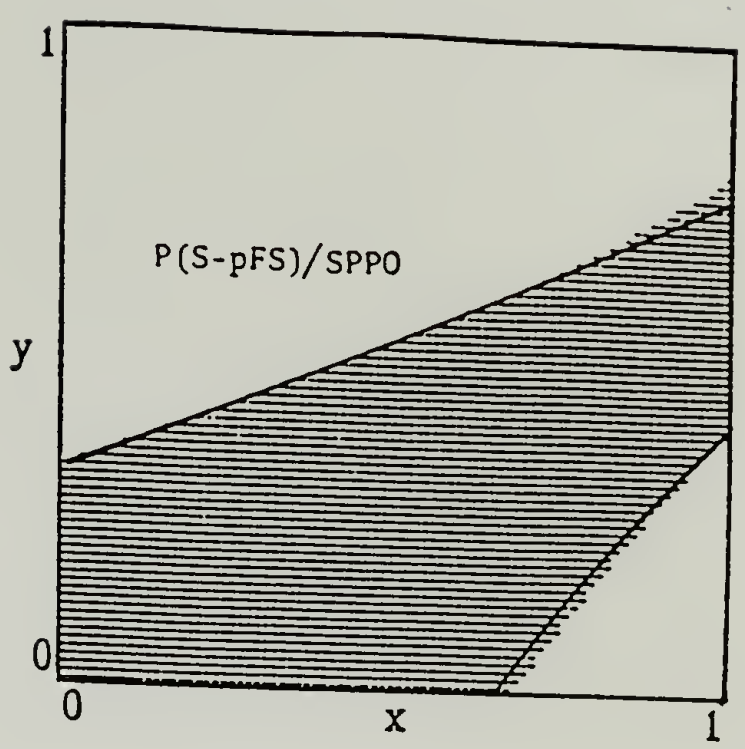

χ_{AB}= 0.080 χ_{AC}= -0.043 χ_{AD}= 0.200

χ_{BC}= 0.053 χ_{BD}= 0.022 χ_{CD}= 0.150

χ^{crit}_{blend}= 0.004

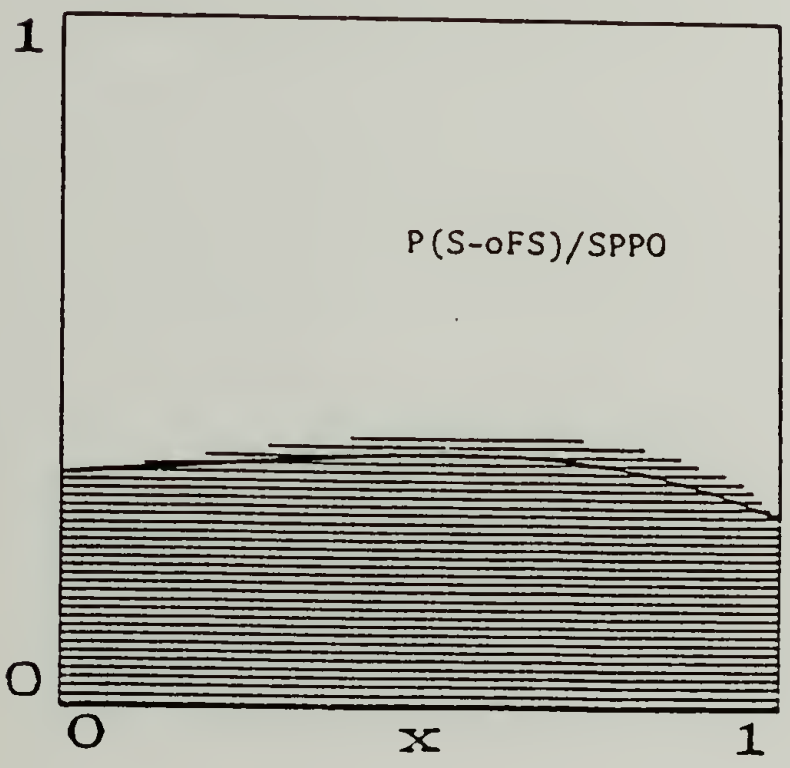

χ_{AB}= 0.040 χ_{AC}= -0.043 χ_{AD}= 0.200

χ_{BC}= 0.004 χ_{BD}= 0.113 χ_{CD}= 0.150

χ^{crit}_{blend}= 0.004

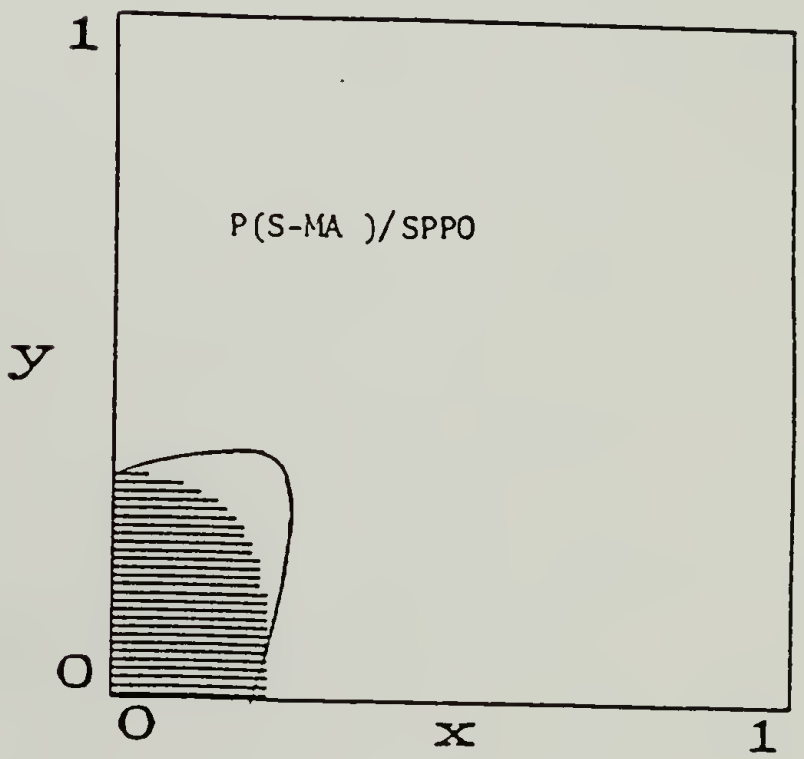

χ_{AB}= 0.150 χ_{AC}= -0.043 χ_{AD}= 0.200

χ_{BC}= 0.290 χ_{BD}= 0.020 χ_{CD}= 0.150

χ^{crit}_{blend}= 0.004

Figure 7.1. Comparison of calculated(shaded regions) and experimental (solid lines) miscibility domains

B. Summary of Results

A series of new thermally stable sulfonylated poly(2,6-dimethyl-1,4-phenylene oxide) (SPPO) copolymers has been prepared and characterized. These copolymers were mixed with the styrenic copolymers; poly(styrene-co-acrylonitrile), poly(styrene-co-p-fluorostyrene), poly(styrene-co-o-fluorostyrene) and poly(styrene-co-methyl acrylate). The monomer sequence distribution in poly(styrene-co-acrylonitrile) samples has also been investigated to confirm that they are of random nature.

The extent of miscibility and the phase stability above the glass transition temperature have been explored. Critical phenomena observed in this work are of an LCST type. The role of intramolecular interaction in inducing miscibility has been identified. A mean field treatment has been successfully applied to blends system of type "$(A_{1-x}B_x)_{n_1}/(C_{1-y}D_y)_{n_2}$" and the experimental miscibility-immiscibility boundaries are in reasonably good agreement with calculated boundaries.

C. Suggestions for Future Work

It might prove interesting to study the effect of blending on the low-temperature secondary relaxation of the component polymers, particularly in the blends of poly(styrene-co-acrylonitrile) with SPPO copolymers. These secondary relaxations are more sensitive to the small-scale local environment and such studies could provide valuable information. Many of the studies in this work involved only 50/50 wt% blends to the determine the miscibility domain. If one uses the blend compositions corresponding to the critical solution temperatures, then the estimation of the χ_{ij}'s will have much more significance. The employment of samples of lower polydispersity and lower T_g's might also clarify the phase behavior and allow study of the temperature dependence of the χ_{ij}'s.

The blends of poly(p-fluorostyrene) with SPPO copolymers have been found to be miscible for degree of sulfonylation ranging from 33 to 73 wt%, even though none of the homopolymer pairs is miscible. Accordingly, thermodynamic manifestations of the miscibility in these blends with other techniques such as vapor sorption measurements would make a rewarding study.

Finally, in the blends of polystyrene with SPPO copolymers, a comparison of the T_g transition width determined by DSC either with

direct morphological studies or with widths of dynamic loss spectra would be worthwhile.

BIBLIOGRAPHY

Alexandrovich P.R., Ph.D. Thesis, Univ. of Mass., 1978.

Alexandrovich P.R., Karasz F.E., MacKnight W.J., Polymer, 18, 1022 (1977).

Alexandrovich P.S., Karasz F.E., MacKnight W.J., Polymer, 21, 488 (1980).

Allen G., McAinsh J., Jeffs G.M., Polymer, 12, 85 (1971).

Attwood T.E., Dawson P.C., Freeman J.L., Hoy L.R.J., Rose J.B., Staniland P.A., ACS, Polymer Preprints, 20(1), 191 (1979).

Balazs A.C., Sanchez I.C., Epstein I.R., Karasz F.E., MacKnight W.J., Macromolecules, 18, 2188 (1985).

Bartenev G.M., Kongarov G.S., Rubber Chem. Technology, 36, 668 (1963).

Bondi A. , J. Phys. Chem., 68(2), 441 (1964).

Bopp R.C., Gaur U., Kambour R.P., Wunderlich B., J. Therm. Anal., 25(2), 243 (1982).

ten Brinke G., Karasz F.E., MacKnight W.J., Macromolecules, 16, 1827 (1983).

ten Brinke G., Rubinstein E., Karasz F.E., MacKnight W.J., Vukovic R.

J. Appl. Phys., 56(9), 2440 (1984).

ten Brinke G., Karasz F.E., Macromolecules, 17, 815 (1984).

Cabasso I., Jagur-Grodzinski J., Vofsi D., J. Appl. Polym. Sci., 18, 1969 (1974).

Callan J.E., Hess W.M., Scott C.E., Rubber Chem. Technol., 44, 814 (1971).

Chalk A.J., Hay A.S., J. Polym. Sci., A1(7), 691 (1968).

Chander K., Anand R.C., Varma I.K., J. Macromol. Sci. Chem., A20(7), 697 (1983).

Chander K., Anand R.C., Varma I.K., Angew. Makromol. Chem., 127, 137 (1984).

Chludzinski P.J., Austin J.F., Enos J.F., Office of Saline Water Research and Development Progress Report No. 697, General Electric Co., Lynn, Mass, 1971.

Cimmino S., Karasz F.E., MacKnight W.J., to be submitted.

Cook M., Williams G., Jones T.T., Polymer, 16(11), 835 (1975).

Couchman P.R., Macromolecules, 11, 6 (1978).

Dumais J.J., Cholli A.L., Jelinski L.W., Hedrick J.L., McGrath J.E., Macromolecules, 19, 1884 (1986).

Ehlers G.F.L., "Structure Stability Relationships of Polymers Based on Thermogravimetric Analysis Data, Pt. 1", AFML-TR-74-177.

Fineman M., Ross S.D., J. Polym. Sci., 5, 756 (1956).

Flory P.J., J. Chem. Phys., 9, 660 (1941).

Flory P.J., J. Chem. Phys., 10, 51 (1942).

Flory P.J., "Principles of Polymer Chemistry", Cornell University : Ithaca, NY, 1953.

Flory P.J., Orwell R., Vrij A., J. Amer. Chem. Soc., 86, 3507 (1964).

Flory P.J., J. Amer. Chem. Soc., 86, 1883 (1965).

Flory P.J., "Statistical Mechanics of Chain Molecules", Interscience, New York, 1969.

Flory P.J., Discuss. Faraday Soc., 49, 7 (1970).

Fox T.G., Bull. Amer. Phy. Soc., 1, 123 (1956).

Fried J.R., Ph.D. Thesis, University of Massachusetts, 1976.

Fried J.R., Karasz F.E., MacKnight W.J., Macromolecules, 11, 150 (1978).

Fried J.R., MacKnight W.J., Karasz F.E., J. Appl. Phys., 50(10), 6052 (1979).

Fried J.R., Hanna G.A., Polym. Eng. Sci., 22, 705 (1982).

Froslich H. , "Theory of Dielectrics", Oxford University Press, London, 1958.

Gall W.G., McCrum N.G., J. Polym. Sci., 50, 489 (1961).

Gibbs J.H., Collected Works, Vol. I, Longmans, Green : New York, 1928.

Glarum S., J. Chem. Phys., 33, 639 (1960).

Gordon M., Taylor J.S., J. Appl. Chem., 2, 493 (1952).

Gupta A.K., Chand N., Singh R., Mansingh A., Europ. Polym. J., 15, 129 (1979).

Gupta M.K., Ripmeester J.A., Carlsson D.J., Wiles D.M., J. Polym. Sci., Polym. Lett. Ed., 21, 211 (1983).

Hall W.J., Cruse R.L., Mendelson R.A., Trementozzi Q.A., ACS Div. Org. Plast. Chem. Prep., 47, 298 (1982).

Hammer C.F., Macromolecules, 4, 69 (1971).

Hirooka, M., Kato T., J. Polym. Sci., Polym. Lett. Ed., 12(1), 31 (1974).

Huang R.Y.M., Kim J.J., J. Appl. Polym. Sci., 29(12), Pt. 1, 4017 (1984).

Huggins M.L., J. Chem. Phys., 9, 440 (1941).

Huggins M.L., J. Phys. Chem., 46, 151 (1942).

Huggins M.L., J. Phys. Chem., 74, 371 (1970); 75, 1255 (1971); 80, 1317 (1976).

Illers K.H., Kolloid Z. Z. Polym., 190, 16 (1963).

Jackson Jr. W.J., Caldwell J.R., Adv. Chem. Ser., 48, 185(1965).

Jauhiainen T.P., Angew. Makromol. Chem., 104, 117 (1982).

Jenckel E., Herwig H.U., Kolloid-Z., 148, 57 (1956).

Johnston N.W., J. Macromol. Sci-Rev. Macromol. Chem., C14(2), 215 (1976).

Kambour R.P., Bendler J.T., Bopp R.C., Macromolecules, 16, 753 (1983).

Karasz F.E., MacKnight W.J., Stoelting J., J. Appl. Phys., 41, 4357 (1970).

Kelley F.N., Bueche F., J. Polym. Sci., 50, 549 (1961).

Khanarian G., Cais R.E., Kometani J.M., Tonelli A.E., Macromolecules, 15(3), 866 (1982).

Kollinsky F., Markert G., Makromol. Chem., 121, 117 (1969).

Koningsveld R., Chem. Z., 26, 263(1972).

Koningsveld R., Kleintjens L., Macromolecules, 18, 243 (1985).

Koningsveld R., a lecture note on " Polymer Phase Diagram" held in Univ. of Mass., Amherst, September, 1985.

Kwei T.K., Nishi T., Roberts R.F., Macromolecules, 7, 667 (1974).

Lacombe R.H., Sanchez I.C., J. Phys. Chem., 80, 2352 (1976).

Lacombe R.H., I.C. Sanchez, J. Phys. Chem., 80, 2568, (1976).

Landi V., Rubber Chem. Technology, 45, 222 (1972).

Lim T., Frosini V., Zaleckas V., Morrow D., Sauer J.A., Polym. Eng. Sci., 13, 51 (1973).

Livingston D.I., Rongone R.L., Proc. Int. Rubber Conf., 5th, p. 337 (1968).

Maconnachie A., Kambour R.P., White D.M., Rostami S., Walsh D.J., Macromolecules, 17, 2645 (1984).

Mark J.E., J. Amer. Chem. Soc., 94, 6645 (1972).

Mark J.E., J. Chem. Phys., 56(1), 451 (1972).

Marsh P.A., Voet A., Price L.D., Mullens T.J., Rubber Chem. Technol., 41, 344 (1968).

Marvel C.S., Schwen R., J. Amer. Chem. Soc., 79, 6003 (1957).

McCammon R.D., Saba R.G., Work R.N., J. Polym. Sci., A7, 1721 (1969).

McCrum N.G., Read B.E., Williams G., "Anelastic and Dielectric Effects in Polymeric Solids", John Wiley and Sons, London, 1967.

McMaster L.P., Macromolecules, 6, 760 (1973).

McMaster L.P., Adv. Chem. Ser., No. 142, 43 (1975).

Molau G.E., J. Polym. Sci., Polym. Lett. Ed., 3, 1007 (1965).

Noel O.F., Carley J.F., Polym. Eng. Sci., 15, 117 (1975).

Olabishi O., Robeson L.M., Shaw M.T., "Polymer-Polymer Miscibility", Academic Press, New York, 1979.

Onsager L., J. Amer. Chem. Soc., 58, 1486 (1936).

Patterson D., Robard A., Macromolecules, 11(4), 690 (1978).

Paul D.R., Barlow J.W., Polymer, 25, 487 (1984).

Paul D.R., Newman S., eds., "Polymer Blends", Vol. 1, Academic Press, New York, 1978.

Percec V., Auman B.C., Makromol. Chem., 185(11), 2319 (1984).

Petris S.E.B., Moore R.S., Flick J.R., J. Appl. Phys., 43, 4318 (1972).

Prigogine I., Defay R., "Chemical Thermodynamics", Longmans, Green : London, 1952.

Prigogine I., "The Molecular Theory of Solutions", North-Holland Pub., Amsterdam, 1957.

Rose J.B., Polymer, 15, 456 (1974).

Ryan C.L., Ph.D. Thesis, Univ. of Mass., 1979.

Saiz E., Mark J.E., Flory P.J., Macromolecules, 10(5), 967 (1977).

Sanchez I.C., Lacombe R.H., J. Phys. Chem., 80, 2352 (1976).

Sanchez I.C., "Polymer Compatibility and Incompatibility, Principle and Practice", Solc K., Ed.; Harwood, New York, 1982; MMI Symp. Ser., Vol. 3.

Schaefer J., Stejskal E.O., Perchak D., Skolnick J., Yaris R., Macromolecules, 18, 368 (1985).

Schroeder J.A., Karasz F.E., MacKnight W.J., Polymer, 26, 1795 (1985).

Scott R.L., J. Polym. Sci., 9, 423 (1952).

Shiomi T., Karasz F.E., MacKnight W.J., Macromolecules, 19, 2274 (1986).

Shiomi T., Karasz F.E., MacKnight W.J., Macromolecules, 19, 2644

(1986).

Smyth C.P., "Dielectric Behavior and Structure", McGraw-Hill, New york, 1955.

Solc K. (ed.), "Polymer Compatibility and Incompatibility : Principles and Practice", MMI Press, 1982, p. 59.

Starkweather H.W., ACS Symp. Ser., No. 127, 433 (1980).

Stoelting J., Karasz F.E., MacKnight W.J., Polym. Eng. Sci., 10, 133 (1970).

Tompa H., "Polymer Solutions", Butterworth, London, 1956.

Tonelli A.E., Macromolecules, 6, 503 (1973).

Tonelli A.E., Macromolecules, 7(5), 632 (1974).

Tonelli A.E., Macromolecules, 10(1), 153 (1977).

Ueda H., Karasz F.E., Macromolecules, 18, 2719 (1985).

Vukovic R., Bogdanic G., Kuresevic V., Karasz F.E., MacKnight W.J., to be summitted.

Vukovic R., Karasz F.E., MacKnight W.J., J. Appl. Polym. Sci., 28, 219 (1983).

Vukovic R., Karasz F.E., MacKnight W.J., Polymer, 24, 529 (1983).

Vukovic R., Kuresevic V., Karasz F.E., MacKnight W.J., Thermochimica Acta, 54, 349 (1982).

Vukovic R., Kuresevic V., Karasz F.E. , MacKnight W.J., J. Appl. Polym. Sci., 30, 317 (1985).

Vukovic R., Kuresevic V., Karasz F.E., MacKnight W.J., Gajnos G.E., J. Polym. Alloys, in press.

Vukovic R., Kuresevic V., Ryan C.L., Karasz F.E., MacKnight W.J., Thermochemica Acta, 85, 383 (1985).

Vukovic R., Kuresevic V., Segudovic N., Karasz F.E., MacKnight, W.J. J. Appl. Polym. Sci., 28, 1379 (1983).

Vukovic R., Kuresevic V., Segudovic N., Karasz F.E., MacKnight W.J. , J. Appl. Polym. Sci., 28, 3079 (1983).

Walsh D.J., Higgins J.S., Maconnachie A., eds., "Polymer Blends and Mixtures", Martinus Nijhoff Publishers, Dordrecht, 1985.

Wetton R.E., MacKnight W.J., Fried J.R., Karasz F.E., Macromolecules, 11, 158 (1978).

Williams G., Watts D.C., Dev S.B., North A.M., Trans. Far. Soc., 67, 1323 (1971).

Wood L.A., J. Polym. Sci., 28, 319 (1958).

Xie S., MacKnight W.J., Karasz F.E., J. Appl. Polym. Sci., 29(8), 2679 (1984).

Yamafuji K., Ishida Y., Kolloid-Z., 183, 15 (1962).

Yang H., Shibayama M., Stein R., Shimizu N., Hashimoto T. Macromolecules, 19, 1667 (1986).

Yee A.F., Polym. Eng. Sci., 17, 213 (1977).

Zakrzewski G.A., Polymer, 14, 347 (1973).

APPENDIX I

MISCIBILITY DIAGRAM COMPUTER PROGRAM

```
605 '--- Introduction display
610 CLS:SCREEN 0:X$=STRING$(73,45)
620 PRINT X$
630 PRINT "These programs are of two types : scanning &
    plotting. Scanning programs"
640 PRINT "produce crude but fast displays of the sign of
    Xblend values for various"
650 PRINT "x-parameter values. They can be used to search
    for x-parameter values for"
660 PRINT "which the Xblend function is negative and posi-
    tive in region that you"
670 PRINT "specify. Plotting programs generate higher -
    quality graphs that can be"
680 PRINT "displayed at a terminal or on the printer. "
690 PRINT:PRINT "To run a program type one of the options
    given below. For example, the"
700 PRINT "following will allow you to scan Xblend func-
    tion of x and y."
710 PRINT:PRINT "Enter an option, or 'q' to quit : s (cr)"
790 DIM X(50),Y(50),F(50),CHI$(7),CHIOPT(7,5),CHIVAL(7,20),
    CHIS(50,7),P$(13,12)
830 CHI$(1)="(1)Xab":CHI$(2)="(2)Xac":CHI$(3)="(3)Xad":
    CHI$(4)="(4)Xbc":CHI$(5)="(5)Xbd":CHI$(6)="(6)Xcd":
    CHI$(7)="(7)Xcrit"
1070 '
1080 '
1090 PRINT:PRINT X$
1093 FOR I=1 TO 7
1095 CHIOPT(I,1)=1:CHIOPT(I,2)=4:CHIOPT(I,3)=-.1:
    CHIOPT(I,4)=.1
1097 NEXT I
1100 PRINT SPC(11) "Dependent  Number of"
1110 PRINT "  Options  Variables  X-para      Source
1120 PRINT X$
1130 PRINT "  S or P      x,y" SPC(8) "7" SPC(8) "Kang"
1140 PRINT X$:PRINT
1150 INPUT "Enter an option, or 'q' to quit : ",A$
1160 IF A$<>"S" AND A$<>"s" AND A$<>"P" AND A$<>"p" AND
    A$<>"Q" AND A$<>"q" THEN GOTO 1150
1170 IF A$="S' OR A$="s" THEN GOTO 1300 ELSE IF A$="P" OR
    A$="p" THEN GOTO 4000 ELSE STOP
1290 '
1300 REM --- Scanning menu display
1310 PRINT:PRINT X$:PRINT "Do you want to:"
```

```
1320 PRINT "       (f) change the type of function to search
     for,"
1330 PRINT "       (c) change the chi values to use during
     the search,"
1340 PRINT "       (s) do the search, or"
1350 PRINT "       (q) quit?":PRINT X$
1360 INPUT "Enter f,c,s or q : ",A$
1370 IF A$<>"F" AND A$<>"f" AND A$<>"C" AND A$<>"c" AND
     A$<>"S" AND A$<>"s" AND A$<>"Q" AND A$<>"q" THEN
     GOTO 1360
1380 IF A$="F" OR A$="f" THEN GOTO 1500 ELSE IF A$="C" OR
     A$="c" THEN GOTO 1800 ELSE IF A$="S" OR A$="s" THEN
     GOTO 2500 ELSE GOTO 1090
1390 STOP
1490 '
1500 REM ---- function option
1510 PRINT X$:PRINT "      Option 'function' chosen.":PRINT
1520 PRINT "Specify the type of function you are looking
     for by entering"
1530 PRINT "For example : .2,.2,-1"
1540 PRINT "              .2,.8,1"
1550 PRINT "              .8,.8,1"
1560 PRINT "              .8,.2,1"
1580 PRINT "Would search for X values producing a negative
     region in near"
1590 PRINT "the origin of the graph.":PRINT X$:PRINT
1600 NF=0
1610 NF=NF+1:INPUT "Enter next x and y and 1 or -1  ",X(NF),
     Y(NF),F(NF)
1615 IF X(NF) < 0 OR X(NF) > 1 OR Y(NF) < 0 OR Y(NF) >1 OR
     (F(NF) <> 1 AND F(NF) <> -1) THEN GOTO 1618 ELSE
     GOTO 1620
1618 PRINT "Your input is not correct.":NF=NF-1:GOTO 1610
1620 INPUT "Do you want to enter another set of data? Type
     (y)es or (n)o ",A$
1625 IF A$<>"Y" AND A$<>"y" AND A$<>"N" AND A$<>"n" THEN
     GOTO 1620
1630 IF A$="Y" OR A$="y" THEN GOTO 1610 ELSE GOTO 1300
1790 '
1800 REM ---- chi option
1801 'chiopt[i,1] (1-original, 2-random ,3-specific, 4-
     range)
1802 'chiopt[i,2] :number of value
1803 'chiopt[i,3] :minimum , chiopt[i,4] : max. ,
     chiopt[i,5] : step
1810 PRINT "      Option 'chi' chosen.":PRINT
1820 'chiopt[i,2] :number of value
1825 PRINT
```

```
1830 FOR I=1 TO 7
1840 ON CHIOPT(I,1) GOSUB 1900,1930,1960,2100
1850 NEXT I
1860 GOTO 2200
1890 '
1900 REM---- original
1910 PRINT CHI$(I) " 4 values chosen randomly between
     -0.100 and 0.100."
1920 RETURN
1930 REM--- random
1940 PRINT CHI$(I) CHIOPT(I,2) "values chosen randomly
     between "; ' CHIOPT(I,3) " and " CHIOPT(I,4)" ."
1945 PRINT USING "+##.###\    \+##.###\\";CHIOPT(I,3);" and
     ";CHIOPT(I,4);"."
1950 RETURN
1960 REM ---- specific
1970 PRINT CHI$(I) CHIOPT(I,2) "values ";
1980 FOR J=1 TO CHIOPT(I,2)-1
1990 PRINT USING "+##.###";CHIVAL(I,J);
2000 NEXT J
2010 PRINT USING "+##.###\\";CHIVAL(I,CHIOPT(I,2));"."
2020 RETURN
2090 '
2100 REM ---- range
2110 PRINT CHI$(I) CHIOPT(I,2) "values from "; ' CHIOPT(I,3)
     " and " CHIOPT(I,4) " in steps of " CHIOPT(I,5) " ."
2115 PRINT USING "+##.###\    \+##.###\              \+##.###\\";
     CHIOPT(I,3);" and ";CHIOPT(I,4);" in steps of ";
     CHIOPT(I,5);"."
2120 RETURN
2180 '
2190 REM ---- chi value changing
2200 PRINT:INPUT "Which do you want to change(1 to 7) or
     (b)ack";A$
2205 IF A$<>"1" AND A$<>"2" AND A$<>"3" AND A$<>"4" AND
     A$<>"5" AND A$<>"6" AND A$<>"7" AND A$<>"B" AND A$<>"b"
     THEN GOTO 2200
2210 IF A$="B" OR A$="b" THEN GOTO 1300 ELSE S=VAL(A$)
2220 PRINT "      Option " CHI$(S) " chosen.":PRINT
2230 PRINT CHI$(S) ": Do you want "
2240 PRINT "      (r) random"
2250 PRINT "      (s) specific values or"
2260 PRINT "      (g) range of values?"
2270 INPUT"Enter r,s or g: ",A$
2280 IF A$<>"R" AND A$<>"r" AND A$<>"S" AND A$<>"s" AND
     A$<>"G" AND A$<>"g" THEN GOTO 2270
2290 IF A$<>"r" AND A$<>"R" THEN GOTO 2320
2300 PRINT "      Option 'random' chosen.":CHIOPT(S,1)=2
```

```
2310 GOTO 2400
2320 IF A$<>"S" AND A$<>"s" THEN GOTO 2350
2330 PRINT "      Option 'Specific' chosen.":CHIOPT(S,1)=3
2340 GOTO 2400
2350 PRINT "      Option 'Range' chosen.":CHIOPT(S,1)=4
2400 PRINT:INPUT "How many values?  ",CHIOPT(S,2)
2405 IF CHIOPT(S,2)-INT(CHIOPT(S,2))<>0 THEN GOTO 2400
2410 IF A$<>"S" AND A$<>"s" THEN INPUT "Enter a minimum
     and a maximum value. ",CHIOPT(S,3),CHIOPT(S,4)
2420 IF CHIOPT(S,4)-CHIOPT(S,3) <= 0 THEN 2410
2430 SEED=INT((CHIOPT(S,4)-CHIOPT(S,3))*100)
2440 IF A$="G" OR A$="g" THEN CHIOPT(S,5)=(CHIOPT(S,4)-
     CHIOPT(S,3))/(CHIOPT(S,2)-1)
2450 IF A$<>"S" AND A$<>"s" THEN GOTO 1825
2460 FOR I=1 TO CHIOPT(S,2)
2470 INPUT "What is it? ",CHIVAL(S,I)
2480 NEXT I
2490 GOTO 1825
2495 '
2500 REM --- Search option
2510 PRINT "      Option 'search' chosen.":PRINT
2520 IF SEED > 30000 OR SEED < -30000 THEN SEED=1987
2530 RANDOMIZE SEED
2540 FOR I=1 TO 7
2550 IF CHIOPT(I,1) >2 THEN GOTO 2600
2560 PRINT "The random value for " CHI$(I) " have been re-
     generated."
2570 FOR J=1 TO CHIOPT(I,2)
2580 CHIVAL(I,J)=RND*(CHIOPT(I,4)-CHIOPT(I,3))+CHIOPT(I,3)
2590 NEXT J
2600 IF CHIOPT(I,1) < 4 GOTO 2660
2610 REM --- range data setup
2620 CHIVAL(I,1)=CHIOPT(I,3):CHIVAL(I,CHIOPT(I,2))=
     CHIOPT(I,4)
2630 FOR J=2 TO CHIOPT(I,2)-1
2640 CHIVAL(I,J)=CHIVAL(I,J-1)+CHIOPT(I,5)
2650 NEXT J
2660 NEXT I
2690 '
2700 REM --- search
2710 COUNT=0:SN=0
2720 FOR AB=1 TO CHIOPT(1,2)
2730 FOR AC=1 TO CHIOPT(2,2)
2740 FOR AD=1 TO CHIOPT(3,2)
2750 FOR BC=1 TO CHIOPT(4,2)
2760 FOR BD=1 TO CHIOPT(5,2)
2770 FOR CD=1 TO CHIOPT(6,2)
2780 FOR CRIT=1 TO CHIOPT(7,2)
```

```
2800 REM --- function check
2810 COUNT=COUNT+1
2820 FOR I=1 TO NF
2830 X=X(I):Y=Y(I)
2840 IF (1-X)*(1-Y)*CHIVAL(2,AC)+(1-X)*Y*CHIVAL(3,AD)+X*
     (1-Y)*CHIVAL(4,BC)+X*Y*CHIVAL(5,BD)-X*(1-X)*CHIVAL(1,
     AB)-Y*(1-Y)*CHIVAL(6,CD)-CHIVAL(7,CRIT)>0 THEN D=1
     ELSE D=-1
2850 IF D<> F(I) THEN GOTO 3320
2860 NEXT I
2890 '
2900 REM --- drawing
2910 FOR YINC=0 TO 10
2920 Y=YINC*.1
2930 FOR XINC=0 TO 10
2940 X=XINC*.1
2950 IF (1-X)*(1-Y)*CHIVAL(2,AC)+(1-X)*Y*CHIVAL(3,AD)
     +X*(1-Y)*CHIVAL(4,BC)+X*Y*CHIVAL(5,BD)
     -X*(1-X)*CHIVAL(1,AB)-Y*(1-Y)*CHIVAL(6,CD)
     -CHIVAL(7,CRIT) > 0 THEN P$(XINC+2,YINC+2)="+ " ELSE
     P$(XINC+2,YINC+2)="- "
2980 NEXT XINC
2990 NEXT YINC
3000 FOR Y=1 TO 12
3010 P$(1,Y)="   "
3020 NEXT Y
3030 FOR X=1 TO 12
3040 P$(X,1)="   "
3050 NEXT X
3060 P$(1,12)="1 ":P$(1,7)="y ":P$(1,2)="0 "
3070 P$(2,1)="0 ":P$(7,1)="x ":P$(12,1)="1 ":PRINT
3080 FOR Y=12 TO 1 STEP -1
3090 PRINT SPC(10);
3100 FOR X=1 TO 11
3110 PRINT P$(X,Y);
3120 NEXT X
3130 PRINT P$(12,Y)
3140 NEXT Y
3190 '
3200 REM --- chi value printing
3210 PRINT:PRINT USING"\    \+##.###\      \+##.###\      \
     +##.###\      \+##.###\      \+##.###\      \+##.###";
     "Xab= ";CHIVAL(1,AB);" Xac= ";CHIVAL(2,AC);" Xad= ";
     CHIVAL(3,AD);" Xbc= ";CHIVAL(4,BC);" Xbd= ";
     CHIVAL(5,BD);" Xcd= ";CHIVAL(6,CD)
3220 PRINT USING "\      \+##.###";"Xcrit= ";CHIVAL(7,CRIT)
3230 PRINT:INPUT "Do you want to save this chi values? Type
     (y)es or (n)o. ",A$
```

```
3235 IF A$<>"Y" AND A$<>"y" AND A$<>"N" AND A$<>"n" THEN
     GOTO 3230
3240 IF A$<>"Y" AND A$<>"y" THEN GOTO 3290
3250 SN=SN+1
3260 CHIS(SN,1)=CHIVAL(1,AB):CHIS(SN,2)=CHIVAL(2,AC):
     CHIS(SN,3)=CHIVAL(3,AD)
3270 CHIS(SN,4)=CHIVAL(4,BC):CHIS(SN,5)=CHIVAL(5,BD):
     CHIS(SN,6)=CHIVAL(6,CD)
3280 CHIS(SN,7)=CHIVAL(7,CRIT)
3290 PRINT:INPUT "(c)ontinue or (b)ack to main menu? ",A$
3295 IF A$<>"C" AND A$<>"c" AND A$<>"B" AND A$<>"b" THEN
     GOTO 3290
3300 IF A$="B" OR A$="b" THEN GOTO 1300
3310 PRINT "      Option 'continue' chosen."
3320 IF COUNT=5000 OR COUNT=10000 OR COUNT=15000 THEN
     PRINT COUNT "sets of X values have been tested so far."
3400 NEXT CRIT
3410 NEXT CD
3420 NEXT BD
3430 NEXT BC
3440 NEXT AD
3450 NEXT AC
3460 NEXT AB
3500 PRINT "The search is complete."
3510 PRINT "      " COUNT " sets of X values were tested."
3520 GOTO 1300
3980 '
3990 '
4000 REM --- plot option
4005 HOR=1:XSAMP=20:YSAMP=20:P=1:KEY OFF:SCREEN 0
4010 SCREEN 0:PRINT:PRINT X$:PRINT "Main menu -- Do you
     want to:"
4020 PRINT "            (c) change chi values"
4030 PRINT "            (g) change the way of graph look"
4040 PRINT "            (s) see the graphs on your terminal"
4055 PRINT "               * When drawing is finished"
4056 PRINT "                  if you want to print it, type
     both `shift` and `prtsc' key.".
4057 PRINT "                     After the printing, type
     'return' key."
4058 PRINT "                  if not type `return` key."
4060 PRINT "            (q) or quit":PRINT X$
4070 INPUT "Type c,g,s,p or q : ",A$
4080 IF A$<>"C" AND A$<>"c" AND A$<>"G" AND A$<>"g" AND
     A$<>"S" AND A$<>"s" AND A$<>"P" AND A$<>"p" AND
     A$<>"Q" AND A$<>"q" THEN GOTO 4070
4090 IF A$="C" OR A$="c" THEN GOTO 4100 ELSE IF A$="G" OR
     A$="g" THEN GOTO 4300 ELSE IF A$="S" OR A$="s" THEN
     GOTO 4600
```

```
4095 SN=0:GOTO 1090
4098 '
4100 REM --- change option
4110 PRINT "       Option 'chis' chosen."
4120 PRINT:PRINT "Number of different settings of X's = "
     SN:PRINT
4130 FOR I=1 TO SN
4140 PRINT USING"##\     \+##.###\     \+##.###\     \+##.###
     \     \+##.###\     \+##.###\     \+##.###
     " Xab= ";CHIS(I,1);" Xac= ";CHIS(I,2);" Xad= ";
     CHIS(I,3);" Xbc= ";CHIS(I,4);" Xbd= ";CHIS(I,5);
     " Xcd= ";CHIS(I,6)
4150 PRINT USING"\       \+##.###";"    Xcrit= ";CHIS(I,7)
4160 NEXT I
4170 INPUT "Do you want to enter more values to plot? (y)es
     or (n)o. ",A$
4175 IF A$<>"Y" AND A$<>"y" AND A$<>"N" AND A$<>"n" THEN
     GOTO 4170
4180 IF A$="N" OR A$="n" THEN GOTO 4000
4190 SN=SN+1
4200 INPUT "Enter new Xab, Xac, Xad, Xbc, Xbd, Xcd and
     Xcrit : ",CHIS(SN,1),CHIS
4210 GOTO 4120
4300 REM --- graph option
4310 PRINT X$:PRINT "       Option 'graph' chosen.":PRINT
4320 PRINT:PRINT "Do you want to change the"
4330 PRINT "  (g) number of graphs horizontally : currently
     " HOR
4340 PRINT "  (s) number of x and y samples : currently "
     XSAMP " and " YSAMP
4350 PRINT "  (b) go back to the main menu":PRINT X$
4360 INPUT "Type g,s or b. : ", A$
4370 IF A$<>"G" AND A$<>"g" AND A$<>"S" AND A$<>"s" AND
     A$<>"B" AND A$<>"b" THEN GOTO 4360
4380 IF A$="G" OR A$="g" THEN GOTO 4500 ELSE IF A$="s" OR
     A$="S" THEN GOTO 4550 ELSE GOTO 4010
4500 REM --- number of graphs
4510 PRINT"       Option 'graphs per page' chosen.":PRINT
4520 INPUT "How many graphs horizontally on a page do you
     want? ",HOR
4530 GOTO 4320
4550 REM --- x,y samples
4560 PRINT "       Option 'samples of x and y' chosen.":PRINT
4570 INPUT "How many samples of x and of y would you like?
     ", XSAMP,YSAMP
4580 GOTO 4320
4590 '
4600 REM --- see graph
```

```
4615 PRINT
4620 PGNUM=INT(SN/HOR)+1:XSTEP=1/XSAMP:YSTEP=1/YSAMP:
     SCREEN 2
4640 FOR I=1 TO PGNUM
4650 CLS:ON HOR GOTO 4660,4700,4800
4660 X1=220:X2=420:Y1=110:Y2=23
4670 XGAP=200/XSAMP:XGO=XGAP*.6:YGAP=87/YSAMP
4680 GOSUB 5000:P=P+1:GOTO 4970
4700 REM --- hor 2
4710 XGAP=200/XSAMP:XGO=XGAP*.6:YGAP=87/YSAMP
4720 Y1=110:Y2=23
4730 X1=380:X2=580:GOSUB 5000
4740 P=P+1:IF P > SN GOTO 4970
4745 X1=60:X2=260:GOSUB 5000
4750 P=P+1:GOTO 4970
4800 REM --- hor 3
4810 XGAP=170/XSAMP:XGO=XGAP*.6:YGAP=75/YSAMP:Y1=110:Y2=35
4820 X1=435:X2=605:GOSUB 5000
4830 P=P+1:IF P > SN GOTO 4970
4835 X1=225:X2=395:GOSUB 5000
4840 P=P+1:IF P > SN THEN GOTO 4970
4845 X1=15:X2=185:GOSUB 5000
4850 P=P+1
4970 LOCATE 24,1:INPUT " ",A$
4980 LOCATE 25,1:PRINT:INPUT "Do you want to (c)ontinue or
     (b)ack to main menu? ",A$
4985 IF A$<>"C" AND A$<>"c" AND A$<>"B" AND A$<>"b" THEN
     GOTO 4980
4990 IF A$="B" OR A$="b" THEN GOTO 4010
4995 NEXT I
4998 '
4999 '
5000 IF P > SN THEN GOTO 4005:REM --- drawing
5010 LINE(X1,Y1)-(X2+XGAP,Y2),,B
5020 XPOS=X1-XGAP
5030 FOR XD=0 TO XSAMP
5040 X=XD*XSTEP:XPOS=XPOS+XGAP:YPOS=Y1+YGAP
5050 FOR YD=0 TO YSAMP
5060 Y=YD*YSTEP:YPOS=YPOS-YGAP
5070 IF (1-X)*(1-Y)*CHIS(P,2)+(1-X)*Y*CHIS(P,3)
     +X*(1-Y)*CHIS(P,4)+X*Y*CHIS(P,5)-X*(1-X)*CHIS(P,1)
     -Y*(1-Y)*CHIS(P,6)-CHIS(P,7) <= 0 THEN
     LINE(XPOS,YPOS)-(XPOS+XGO,YPOS)
5080 NEXT YD
5090 NEXT XD
5200 XLEFT=INT((X1-7)/8):YHALF=INT((Y1+Y2)/2):YUP=INT(Y2/8):
     LOCATE YUP+1,XLEFT:PRINT "1"
```

```
5210 LOCATE YHALF/8,XLEFT:PRINT "y":LINE(X1,YHALF)
     -(X1+XGO*.5,YHALF)
5220 LOCATE INT(Y1/8)+1,1:PRINT TAB(XLEFT) "0"
5230 XCENT=(X1+X2)/16:YLOW=INT((Y1+15)/8):LOCATE YLOW,
     INT(X1/8)+2:PRINT "0":LOCATE YLOW,XCENT+1:PRINT "x":
     LOCATE YLOW,INT(X2/8)+2:PRINT "1"
5310 LINE(XCENT*8,Y1)-(XCENT*8,Y1-XGO*.5)
5320 LOCATE YLOW+2,XLEFT+1:PRINT USING"\     \+##.###\     \
     +##.###";" Xab= ";CHIS(P,1);" Xac= ";CHIS(P,2)
5330 LOCATE YLOW+3,XLEFT+1:PRINT USING"\     \+##.###\     \
     +##.###";" Xad= ";CHIS(P,3);" Xbc= ";CHIS(P,4)
5340 LOCATE YLOW+4,XLEFT+1:PRINT USING"\     \+##.###\     \
     +##.###";" Xbd= ";CHIS(P,5);" Xcd= ";CHIS(P,6)
5350 LOCATE YLOW+5,XLEFT+1:PRINT USING"\       \+##.###";
     " Xcrit= ";CHIS(P,7)
5360 RETURN
```